Novel Dry Powder Preparations of Whole Inactivated Influenza Virus for Nasal Vaccination

Robert Joseph Garmise

A dissertation submitted to the faculty of the University of North Carolina at Chapel Hill in partial fulfillment of the requirements for the degree of Doctor of Philosophy in the Department of Molecular Pharmaceutics.

Chapel Hill
2007

Approved by,

Dr. Anthony J. Hickey

Dr. Moo Cho

Dr. Herman Staats

Dr. Vince Sullivan

Dr. Dhiren Thakker

Dr. Roland Tisch

ABSTRACT

Robert J. Garmise

Novel Dry Powder Preparations of Whole Inactivated Influenza Virus for Nasal Vaccination

(Under the direction of Dr. Anthony J. Hickey, Ph.D., D.Sc.)

Nasal dry powder vaccines may provide safe, effective, stable, and affordable alternatives to currently available influenza vaccines. It was proposed that maximal mucosal and systemic antibody production would be elicited by a whole inactivated influenza virus dry powder nasal vaccine formulation in response to increased local residence time. Full factorial designed experiments examining freezing rate, solute concentration, and annealing (freeze-drying) and solution feed rate, atomization airflow rate, and solute concentration (spray-freeze-drying (SFD)) were used to produce particles suitable for nasal delivery. Freeze-drying followed by milling and sieving produced heterogeneous-shaped particles below the targeted particle size, which weren't ideal for blending with mucoadhesive compounds (MA). Optimized SFD runs produced particles for human (D_{50}=38.5μm) and rat (D_{50}=26.9μm) delivery which were characterized for flow and thermal properties, surface area, true density, moisture content, and impact energy separation and demonstrated improved storage stability than liquid formulations. A modified cascade impactor was calibrated to characterize particles in the 10-20μm size range.

Wettability, dissolution rate, and swelling indices were obtained as potential predictors of the effects MA may have on the residence time. Gamma scintigraphy allowed for visual imaging of nasal clearance, while residence time studies quantified mucociliary clearance rates. *In vitro* and *in vivo* experiments indicated that sodium alginate (SA) and carboxymethylcellulose (CMC HMW) powder formulations had the greatest effect on increasing residence time in Brown Norway rats.

A dose-response curve determined that a 2μg dose was appropriate to quantify potential differences in antibody responses of formulations. IM delivery provided equivalent serum antibody titers to IN powder without MA, CMC HMW, SA, and hydroxypropyl methylcellulose (HPMC HMW) after initial dosing and IN liquid and IN powder without MA, CMC HMW, SA, and HPMC HMW after boosting. IN liquid vaccine provided equivalent serum antibody titers to IN powder without MA, CMC HMW, SA, chitosan, and HPMC HMW after the initial vaccination. IN liquid provided significantly greater serum antibody titers than IN powder with chitosan after boosting. While no significant differences between powder and liquid formulations were observed, trends are consistent with residence time studies with respect to eliciting an immune response. Maximal serum and mucosal antibodies were elicited following administration of IN powder with SA.

ACKNOWLEDGEMENTS

First and foremost, I would like to acknowledge the love and support of my family. My parents, Louise and Bob, and my two brothers, Mark and Steven, have all played an instrumental role in everything that I have been able to accomplish in my life – thank you. My extended family, including my grandparents, Joe and Rose, uncles, aunts, cousins, and the Thorpe family have given me tremendous support that I will never forget.

I would like to take the time to thank the very large number of individuals who helped contribute to this project. Vince Sullivan and his group at Becton Dickinson Technologies have been a tremendous help, not just with funding, but also with technical assistance. Matt Ferriter, Kevin Mar, Brandi Ford, C. Robin Hwang, Harry Sugg, Juan Huang, John Mitzka, and Rob Campbell have all taken time to educate me on equipment and techniques not readily available at the University.

I am forever indebted to Herman Staats, who has provided guidance and encouragement. The time spent discussing my project with him was invaluable.

Each of my committee members has sacrificed their time, was always willing to answer my questions and provided guidance. Their input was greatly appreciated.

I would like to thank Richard Kowalsky for instruction and use of radiolabel for the residence time studies, Mike Foster who provided expertise (and the gamma camera) for imaging studies, John Sheehan for use and instruction on the cone and plate viscometer, Hal Kohn for use of the tablet press, Dave Wargo and John Kirsch of Mylan Pharmaceuticals for donating the tablet tooling, Sridhar Desikan of Bristol-Myers Squibb for use and instruction on the helium pyncnometer, and Wallace Ambrose for use on the scanning electron microscope.

I would like to acknowledge a number of my current and former colleagues in the School of Pharmacy for their friendship and advice. Amber Allen, John An, Dave Bourdet, Christine Conwell, Lee Daub, Murali Duvvuri, Kathryn Fiscelli, David Gaul, Boka Hadzija, Jarrett Mitchell, Emily Olson, Sherrie Settle, Phil Smith, Phyllis Smith, and all other graduate students, professors, and staff have helped me a great deal in my time at UNC.

I would also like to thank the current and former members of the Dispersed Systems Laboratory. Lucila Garcia-Contreras, Dan Cooney, Timm Crowder, Masha Kazantseva, Margaret Louey, Dongmei Lu, Heidi Mansour, Pavan Muttil, Danielle Padilla, Matt Robinson, Vasu Sethuraman, Hugh Smyth, Martin Telko, Chenchen Wang, Sheena Wang, and Zhen Xu have been a tremendous help to me and have all contributed to this project.

I wouldn’t be where I am today without the guidance of my advisor, Tony Hickey, who has not only been a mentor, but a friend to me and my family. His perspective, intelligence, humility, and willingness to teach will forever influence the way I handle myself in my professional career.

Finally, I would like to thank my wife, Jennifer, for her undying love and support, and for putting up with me through thick and thin to help me accomplish my goals. I could not have done it without you.

TABLE OF CONTENTS

LIST OF TABLES

LIST OF FIGURES

LIST OF ABBREVIATIONS AND SYMBOL

ANOVA	analysis of variance
APC	antigen presenting cell
C_c	Cunningham correction factor
Chit	chitosan
CMC	carboxymethylcellulose sodium
D_{10}	diameter which 10% of particles are smaller than
d_{50}	cut-off diameter of a stage of a cascade impactor
D_{50}	diameter which 50% of particles are smaller than
D_{90}	diameter which 90% of particles are smaller than
da	aerodynamic diameter
D_j	diameter of the jet
dp	projected area diameter
DSC	differential scanning calorimetry
FD	freeze-drying
g	acceleration due to gravity
GSD	geometric standard deviation
H	hemagglutinin
HA	hemagglutination
HAI	hemagglutination inhibition
HMW	high molecular weight
HPMC	hydroxypropyl methylcellulose
Ig	immunoglobulin

IgA	immunoglobulin A
IgD	immunoglobulin D
IgE	immunoglobulin E
IgG	immunoglobulin G
IgM	immunoglobulin M
IM	intramuscular
IN	intranasal
LMW	low molecular weight
MA	mucoadhesive compound
MTR	mucociliary transport rate
N	neuraminidase
NALT	nasal-associated lymphoid tissue
NI	neuraminidase inhibitor
η	viscosity
ρ_g	density of the gas
ρ_p	density of the particle
ρ_0	unit density
PSA	purified surface antigen
Q	flow rate of the air
Re	Reynold's number
SA	sodium alginate
SEM	scanning electron microscopy
SFD	spray-freeze-drying

STK_{50}	Stoke's number
v	velocity of the air
V_{TS}	terminal settling velocity
WHO	World Health Organization
WIIV	whole inactivated influenza virus
χ	shape factor

1 INTRODUCTION

1.1 General Introduction

The nasal route of administration is becoming more widely used for the delivery of pharmaceutical and biological compounds (Ikechukwu Ugwoke, Sam et al. 1999; Kendall and Latter 2003). All currently approved nasal preparations are liquid formulations which could be improved, specifically pertaining to the fraction of the dose reaching its intended site of action and residence time in the nasal cavity. Optimized dry powder formulations may overcome these shortcomings. Several factors, including the anatomical and physical characteristics of the nasal cavity, the nature of the dry powder formulation, and the use of mucoadhesive compounds, play a role in effective nasal drug delivery.

1.1.1 Physiology of the Nasal Cavity

1.1.1.1 Functions of the nasal cavity

The nasal cavity has three main functions: filtration, conditioning of air, and olfaction (Proctor and Andersen 1982). The structure of the nasal cavity allows for the removal of large particles preventing entry to the lower respiratory tract. Inspired air is rapidly warmed and humidified by the warm, moist nasal mucosa, to near pulmonary airway conditions (within 1°C of body temperature, 97-98% relative humidity) (Guyton and Hall 1996). Olfactory nerves are located in the nasal cavity and distinguish odors.

1.1.1.2 Structure of the human nasal cavity

The human nasal cavity is located between the floor of the cranium and the roof of the mouth (Figure 1) (Taber and Thomas 2001). It is divided bilaterally by the nasal septum, with each half having a volume of about 7.5 mL (Mygind and Dahl 1998). The air enters through the anterior nares of the nostrils. In the posterior portion of the nostrils, the airways narrow to a cross-sectional area of about 0.3 cm^2 on each side at a constriction known as the nasal valve (Newman, Pitcairn et al. 2004). The region, which is the most constricted section of the upper respiratory tract, accounts for up to 80% of nasal resistance and almost half of the total respiratory resistance (Proctor and Lundqvist 1973). After the nasal valve, the airway bends at a right angle into the opening of the skull and then widens where air comes in contact with turbinates or conchae (respiratory region). There are three distinct turbinates designated superior, middle, and inferior. These structures increase the total surface area to approximately 150 cm^2 (Proctor and Andersen 1982). Finally, air passes through the posterior nares into the nasopharynx. The nasal cavity is enclosed by four groups of air-filled paranasal sinuses (Jones 2001). The olfactory region is located in the superior portion of the nasal cavity in an area of approximately 370 mm^2, lying partly on the septum and partly on the superior and middle turbinates (Jones 2001).

The anterior portion of the nasal cavity is lined with squamous epithelial cells which gradually change to pseudostratified columnar epithelial cells in the respiratory region (Illum 1999). Approximately 15% to 20% of these cells in the respiratory region are ciliated (Figure 2) (Ugwoke, Verbeke et al. 2001). Dispersed between the columnar cells are the mucus-producing, goblet cells (Quraishi, Jones et al. 1998). Below the columnar epithelium are "replacement" basal cells, which differentiate into the other cell types (Illum 1999).

1.1.1.3 Structure of the rat nasal cavity

The rat is an obligate nose breather due to the close proximity of the epiglottis to the soft palate (Krinke 2000). The nasal cavity has a total volume of about 0.25 mL and a surface area of approximately 13 cm^2 (Gross, Swenberg et al. 1982). The olfactory epithelium is located on the middle and superior nasal turbinates (ethmoturbinates) and constitutes approximately 50% of the total surface area, while the remaining regions are lined with respiratory epithelium (Gross, Swenberg et al. 1982). Among all laboratory animals, the rat presents the smallest deviation in the nasopharynx which has a bend angle of 15° (Schreider and Raabe 1981).

1.1.1.4 Mucus and mucociliary clearance

The secretions covering the nasal epithelium form two layers (Figure 3): the gel (or mucus) layer (0.5-2.0 μm thick) and the periciliary aqueous layer (7-10 μm thick). The gel layer is composed of 95% water, 2-3% glycoproteins, 1% lipid, 1% salts, and 0.02% DNA, which is exposed to the inspired air, is highly viscous, has non-Newtonian viscoelastic properties, and entraps inhaled particulates (Quraishi, Jones et al. 1998). In humans the mucus sheet in the nasal cavity is completely replaced approximately every 15 minutes. The periciliary layer is a low viscosity fluid with Newtonian properties which permits ciliary beating. The ciliary beat has two components: the effective stroke and the recovery stroke (Stannard and O'Callaghan 2006). In the effective stroke, the tip of the cilia penetrates the gel layer and the stroke pushes the mucus towards the posterior region of the nasal cavity. In the recovery stroke, the cilia move through the low viscosity periciliary fluid to the start position for the next stroke. The beat frequency is normally 15-20 Hz or approximately 1000 beats per minute (Mygind and Dahl 1998). Particles that deposit on the anterior portion of the nasal

cavity are cleared by mucus through the posterior region. In humans, the average rate of mucociliary clearance is 5 mm/min, though there is wide variation in mucociliary clearance between individuals (Proctor and Lundqvist 1973).

The range of published mucociliary clearance rates in rats, of 1.1-5.9 mm/min on the respiratory epithelium and 0.9 mm/min on the olfactory epithelium, overlaps that of humans (Morgan, Patterson et al. 1986).

1.1.1.5 Nasal-associated lymphoid tissue

Most infectious diseases are caused by pathogens invading the host through mucosal surfaces, which represent a considerably greater surface area of body than the skin surface (Mestecky, Moldoveanu et al. 1997). Mucosal immunity, the first line of defense against pathogens, is of major importance in preventing infectious diseases. The nasal-associated lymphoid tissue (NALT) is the principle mucosal lymphoid tissue in the upper respiratory tract (Kuper, Koornstra et al. 1992). The NALT is situated just under the nasal epithelium and consists of a reticular network filled with various types of lymphoid and non-lymphoid tissue (Roitt and Delves 2001). Particulate antigens may be removed from the nasal mucosa by the mucociliary system. However, if the antigen comes in contact with the nasal epithelium, it can be taken up by specialized epithelial cells called the microfold (M) cells. Alternately, the antigen can be engulfed by a phagocytic cell: the dendritic cell (Tamura and Kurata 2004). Portions of the antigen are displayed on the surface following phagocytosis of the antigen. M cells and dendritic cells are known as antigen presenting cells (APC). This stimulates the recruitment of helper T cells which signal to recruit B cells that evolve into plasma cells. The plasma cells, existing in lymphoid tissue, secrete antibodies in great amounts. The B cells which do not evolve into plasma cells circulate as memory cells. There

are five classes or isotypes of antibodies (also called immunoglobulins (Ig)): IgM, IgG, IgA, IgD and IgE (Leffell, Donnenberg et al. 1997). When characterizing an immune response elicited by a vaccine, IgG and IgA are good descriptors of a systemic and local mucosal immune response, respectively. IgE should be monitored as an indicator of a possible hypersensitivity reaction.

In rats, the NALT is located in the anterior portion of the nasal cavity (Spit, Hendriksen et al. 1989; Kuper, Hameleers et al. 1990; Kuper, Koornstra et al. 1992). In humans, the NALT is generally described as the Waldeyer's ring and consists of the adenoid (nasopharyngeal tonsil), the bilateral pharyngeal lymphoid bands, the bilateral tubal and facial (palatine tonsils), and the bilateral lingual tonsils (Kuper, Koornstra et al. 1992). Studies in infants have demonstrated that lymphoid tissue is disseminated in the whole nasal mucosa (Debertin, Tschernig et al. 2003). This is significant for the targeting of the antigen. A vaccine must come in contact with the NALT, wherever it is located, to elicit an immune response. The potential for the NALT to exist throughout the nasal cavity, in human infants, increases the probability of antigen reaching the target, resulting in a greater immune response to intranasal vaccination (Nordqvist 2006).

1.1.2 Particle Deposition in the Nasal Cavity

Nearly all particles greater than 50 μm and about half of the particles in the 2-4 μm size range are deposited in the nasal cavity (Proctor and Andersen 1982). All particles less than 2 μm pass through the human nasal cavity into the lower airways. The predominant factor in deposition in the nose is inertial impaction. After passing through the initial bend angle, of 90° in humans, the air enters the main region of the nasal cavity, which widens with consequent reduction in linear velocity. In the posterior region, prior to the nasopharynx, the

airway path bends, resulting in narrowing and an increase in airflow linear velocity in the area around the adenoid tissue. This increase in velocity results in higher particle inertia and local deposition. In rats, most of the particles larger than 0.5 μm or smaller than 0.05 μm deposit in the nasal airways, with the remaining fraction being deposited in the alveolar region (Krinke 2000). Ultrafine particle deposition increases with decreasing particle size, primarily because of Brownian diffusion, and coarse-particle deposition increases with increasing particle size and therefore inertia primarily because of inertial impaction (Kelly, Bobbitt et al. 2001).

1.1.3 Delivery of Drug to the Nasal Cavity

The nasal route of administration has been utilized for centuries to deliver non-therapeutic agents and drugs of abuse, for example tobacco or cocaine. The ancient Chinese were the first to utilize the nasal route to vaccinate people to prevent small pox infection (Voltaire 1961). However, it wasn't until the second half of the 20th century that the nasal delivery of pharmaceuticals and biologicals was widely considered. Early products focused on the use of locally acting pharmaceutical agents for chronic sinusitis. In the past 20 years, greater emphasis has been placed on the use of nasal delivery for systemic agents (Table 1). Delivery to the nasal cavity has advantages compared to conventional oral ingestion of systemically acting agents. Compounds, delivered orally, may have poor or unpredictable absorption or bioavailability (Illum, Jenkins et al. 1999). The onset of action for substances delivered intranasally is significantly shorter than that of oral delivery. Nasal delivery circumvents the first pass liver and gastrointestinal metabolism associated with oral ingestion.

1.1.4 Delivery of Vaccines to the Nasal Cavity

The nasal mucosa represents a promising route for the delivery of vaccines due to its: ease of accessibility; extent of vascularization; relatively large surface area; and the ability to induce both local and systemic immune responses. Moreover, immune responses elicited in the nasal cavity may induce responses in distant mucosal sites. The phenomenon of integration of responses from discrete mucosal sites is known as the "common mucosal immune system" (Roitt and Delves 2001). Delivery of vaccines and therapeutic drugs to the nasal and pulmonary systems has been studied extensively (Gonda 2000; Singh, Briones et al. 2001; Illum 2002; Groneberg, Witt et al. 2003; Roth, Chapnik et al. 2003). These approaches represent non-invasive alternatives to needle-based delivery. The nasal route facilitates vaccination of large groups of people, without employing large numbers of syringes and needles that are viewed as hazardous waste, requiring appropriate and expensive disposal (Partidos 2000).

Recently, a live, attenuated, cold-adapted trivalent intranasal (IN) influenza vaccine, FluMist^{TM}, was approved by the FDA. This vaccine was shown to be safe and well-tolerated in certain healthy pediatric and adult populations (Belshe, Mendelman et al. 1998; Nichol, Mendelman et al. 1999; Treanor, Kotloff et al. 1999), thus providing a non-invasive alternative to needle-based injection of influenza vaccines. However, to maintain potency, the product must be stored as a frozen liquid and thawed immediately before use. In addition, there have been safety concerns related to the use of a live virus vaccine in populations such as children under age 5, the elderly, and the immunocompromised (FluMist Package Insert 2003).

In addition to influenza, vaccination strategies have been developed for a number of diseases, including HIV, hepatitis B, measles, anthrax, plague, diphtheria, pertusis, tetanus, bacterial meningitis, respiratory syncytial virus and rotavirus (Hirabayashi, Kurata et al. 1990; Russell, Moldoveanu et al. 1996; Bergquist, Johansson et al. 1997; Muszkat, Friedman et al. 2000; Davis 2001; Boyaka, Tafaro et al. 2003). Liquid formulations of these vaccines, delivered IN, have been shown to elicit increased local and systemic responses compared to parenteral administration. While dry powder vaccines have the potential to overcome the costly and limiting cold chain requirements of liquid vaccines, there have been very few reported studies of their use in IN delivery systems. Anderson et al. showed that a powder form of rinderpest virus elicits protective immune responses in cattle (Anderson, Fishbourne et al. 2000). In addition, Illum et al. reported increased serum IgG and nasal IgA titers following IN delivery of a pertusis/chitosan powder vaccine to guinea pigs (Illum, Jabbal-Gill et al. 2001) However, control experiments comparing the results to standard parenteral routes were not conducted and the powders employed were not fully characterized (Huang, Garmise et al. 2004).

1.1.5 Mucoadhesive Compounds

Most IN vaccines do not elicit immune responses without co-administration with adjuvant. Concerns about toxicity limit the use of antigens in humans. Therefore, alternative strategies to enhance antigenicity are desirable, one of which is increasing the local residence time of antigen at the mucosal surface.

Enterotoxin-based adjuvants, such as cholera toxin or *Esherichia coli* heat-labile enterotoxin, are used commonly as mucosal adjuvants in animal studies. However, their potential toxicity in humans is a major concern with respect to their clinical application.

Nanoparticles, microspheres, synthetic lipopeptides, cytokines, and CpG-containing oligonucleotides have also been studied as potential adjuvants (Hunter, Andracki et al. 2001; Staats, Bradney et al. 2001; Debin, Kravtzoff et al. 2002; Mariotti, Teloni et al. 2002; Rharbaoui, Drabner et al. 2002). Bioadhesives are compounds that adhere to a biological surface. Where the biological surface is mucosal, the compound is referred to as a mucoadhesive compound (MA). MAs can interact with the mucus in a number of ways. Chitosan, a widely studied cationic polymer, interacts with the negatively charged sialic acid group of the mucin glycoprotein (Illum, Jabbal-Gill et al. 2001). Other mechanisms of mucoadhesion are hydrophobic interactions, hydrogen bonding, and van der Waal's interactions, depending on the polymer and the pH (Gu, Robinson et al. 1988). Another proposed mechanism of mucoadhesion is based on the local dehydration of the mucus; namely the water movement to the polymer causes the mucoadhesive interaction (Illum 1999). Carbopol's (polyacrylic acid) mucoadhesive properties are thought to be due to the entanglement of the chains of the Carbopol and mucin, thus decreasing mucociliary clearance. The mucoadhesive function of polymers, such as Carbopol and chitosan, may be useful in eliciting mucosal immunity to dry powder influenza vaccine formulations delivered IN.

MAs are used to increase local residence time in the nasal cavity. There is evidence that chitosan, a biocompatible and biodegradable polymer from crustacean shell, may be used as a mucoadhesive for IN delivery and will boost the mucosal immune response (Jabbal-Gill, Fisher et al. 1998; Illum, Jabbal-Gill et al. 2001; van der Lubben, Verhoef et al. 2001; Westerink, Smithson et al. 2001; van der Lubben, Kersten et al. 2003). Carbopol, has been used to demonstrate enhanced insulin bioavailability in rabbits (Callens and Remon 2000).

MAs have been studied in liquid IN influenza vaccine formulations, using purified surface antigens (PSA) (Bacon, Makin et al. 2000). Chitosan and gellan (bacterial polysaccharide) formulations were administered IN to mice and compared to IN or subcutaneous PSA alone. Each group of animals received three sequential doses (vaccination and two boosts at the same concentrations). The chitosan formulation elicited significantly higher IgG titers than IN PSA after three doses, and significantly higher IgG titers than the gellan formulation after the last two doses. Also, the chitosan formulation elicited equivalent hemagglutination inhibition (HI) to subcutaneous dosing, while IN PSA alone did not generate any HI titers. This is an important observation because the HI assay measures functional activity of the antibody and is recognized as a reliable measure of protective antibody titer against influenza vaccine (Glueck 2001).

The effect of chitosan on the mucociliary transport rate (MTR) in human nasal turbinates *ex vivo* has been evaluated (Aspden, Mason et al. 1997). Chitosans of varying salts (glutamate and hydrogen chloride) and molecular weights (< 50, 205, and 340 KDa) were delivered in a nasal spray. A significant decrease in MTR occurred for each of the three chitosans when compared to control. The two highest molecular weight chitosans delivered in nasal drops resulted in a significant decrease in the MTR when compared to a nasal spray. Thus, chitosan may decrease the MTR through the nasal cavity and increase the residence time of a co-administered antigen on the nasal mucosa, potentially increasing its immunogenicity.

The mucoadhesive effects of chitosan have also been evaluated as a function of formulation (Soane, Hinchcliffe et al. 2001). Chitosan microspheres and solutions were compared with saline control for effects on mucociliary clearance in sheep. Clearance half-

life (time to clear 50% of a radiolabeled marker, ^{99m}Tc) increased by more than 7-fold for the chitosan microsphere formulations compared to ~3-fold for chitosan solutions, indicating that chitosan powders could effectively increase residence time on the nasal mucosa compared to solutions or controls.

The use of MA in nasal delivery, has been widely described and recently reviewed comprehensively (Ugwoke, Agu et al. 2005; Illum 2006).

1.1.6 Influenza Virus

Influenza infections occur when the virus invades the host through the thin and permeable mucosal surface in the upper respiratory tract (Lamb and Krug 1996). The virus is primarily transmitted person to person in liquid droplets generated by talking, coughing or sneezing (Dimmock, Easton et al. 2001). Influenza is a highly contagious disease that causes high morbidity and mortality worldwide each year (WHO 2006). Although difficult to assess, these annual epidemics are thought to result globally in three to five million cases of severe illness and between 250,000 and 500,000 deaths. Most deaths ascribed to influenza in industrialized countries occur among the elderly, individuals over 65 years of age (WHO 2006).

The currently circulating influenza viruses associated with human disease are divided into two groups (A and B). Influenza viruses are defined by two different antigens on their surface. They are apparently spike-like features identified as hemagglutinin (H) and neuraminidase (N) (Lamb and Krug 1996). Hemagglutinin has 16 subtypes (H1 through H16), but only the first three, H1, H2, and H3, routinely infect humans (Nicholson, Webster et al. 1998). Neuraminidase has 9 subtypes (N1 through N9), but only the first two, N1 and N2, routinely infect humans. Influenza A has two subtypes which can infect humans:

A(H3N2) and A(H1N1), of which the former is currently associated with most deaths (WHO 2006).

Avian influenza, influenza A, is of great global interest due to the potential to mutate to a form capable of transmission to humans. Of the hundreds of strains of avian influenza A viruses, only four are known to have caused human infections: H5N1, H7N3, H7N7, and H9N2. H5N1 virus is of greatest public health concern (WHO 2006). Between 2003 and the first half of 2006, the H5N1 virus was responsible for a reported 202 cases, with 113 of these resulting in death (WHO 2006). The virus is not yet capable of efficient infection and transmission between humans. This may be the only reason that avian influenza has not resulted in pandemic disease (Aldhous and Tomlin 2005). From an epidemiological perspective it appears inevitable that H5N1, or one of the other strains, will eventually be capable of causing worldwide disease. A vaccination strategy that is quick and effective will be necessary to prevent such a global pandemic.

Hemagglutinin has been the subject of considerable study because of its role as the major antigen against which a protective immune response is directed (Tsurudome, Glueck et al. 1992). Hemagglutinin, which is distributed evenly on the surface of the virus particles, is the target for an immune response that results in host protection (Glueck 2001). It is H that allows the virus to attach to specific sialic acid receptors on the cell surface and causes endosomal fusion of the virion and cell membranes. The surface H units are trimers of H_1-H_2 units. The H_1 monomer has a globular membrane-distal domain of anti-parallel beta sheets, which contain the sialic acid containing receptor-binding site (Tsurudome, Glueck et al. 1992). Neuraminidase, the other major protein component of the influenza virus, cleaves sialic acid from receptors, allowing the replicated virus to bud from the host cell (Nicholson,

Webster et al. 1998). Another important physical feature of the influenza virus crucial for replication is the M2-proton channel. The proton channel mediates an influx of H^+ ions into the infecting virion early in the viral replication cycle. This cycle facilitates the dissociation of the ribonucleoproteins from the virion interior and allows them to be released into the cytoplasm and transported into the cell nucleus (Hayden 2006). Neuraminidase and M2-proton channel have been drug targets but are not considered as part of a vaccine strategy.

1.1.7 Influenza Treatment

There are currently several marketed drug products for prophylaxis and treatment of the signs and symptoms of influenza. These medications fall into two classes: the M2 ion-channel inhibitors (adamantanes) and the neuraminidase inhibitors (NI). The adamantanes, amantadine (Symmetrel®) and rimantidine (Flumadine®), are active against influenza A viruses, but not influenza B viruses.(Keitel and Piedra 1998). The NI, zanamivir (Relenza®) and oseltamivir (Tamiflu®), are active against both influenza A and B viruses. The adamantanes can reduce the duration of uncomplicated influenza A illness, and the NI can reduce the duration of uncomplicated influenza A and B illness by approximately one day when administered within two days of the onset of illness to otherwise healthy adults.(Smith, Bresee et al. 2006) Amantadine, rimantadine, and oseltamivir are administered orally. Zanamivir is available as a dry powder for pulmonary delivery using the Diskhaler® inhalation device. Oseltamivir and zanamivir are not a substitute for vaccination, although they can be critical adjuncts in preventing and controlling influenza (Smith, Bresee et al. 2006). It has recently been suggested that neither amantadine nor rimantadine should be used for the treatment or chemoprophylaxis of influenza A in the United States because of recent data indicating widespread resistance of this virus to these medications (Bright, Shay et al.

2006). The resistant virus has a single amino acid mutation which prevents the adamantanes from binding to the M2 ion-channel and exerting its effect.(Hayden 2006)

1.1.8 Influenza Vaccination

Vaccination has a major impact on disease prevention and containment of epidemics. It is recommended by the World Health Organization (WHO) that the elderly and those of any age who are considered high risk (i.e. immunocompromised patients, healthcare workers, pregnant women) for influenza-related complications, due to underlying health conditions, should be vaccinated (WHO 2006). Among the elderly, vaccination is thought to reduce influenza-related morbidity by 60% and influenza-related mortality by 70-80%. Among healthy adults, vaccination is effective (70-90%) in reducing influenza morbidity, and has substantial health-related and economic benefits (WHO 2006). In addition, vaccination reduces both health-care costs and productivity losses associated with influenza illness.

The strains of influenza virus are designated according to a formula which describes their full pedigree. A strain is named by type, sub-type, geographical location of first isolation, a laboratory identification number and the year of isolation (Keitel and Piedra 1998). The strains of influenza utilized for the 2005-06 season were A/California/7/2004 (H3N2)-like, A/New Caledonia/20/99 (H1N1)-like, and B/Shanghai/361/2002-like antigens. For the A/California/7/2004 (H3N2)-like antigen, manufacturers were able to use the antigenically equivalent A/New York/55/2004 (H3N2) virus, and for the B/Shanghai/361/2002-like antigen, manufacturers were able to use the antigenically equivalent B/Jilin/20/2003 virus or B/Jiangsu/10/2003 virus (Smith, Bresee et al. 2006). These virus strains were chosen for their growth properties, and also because they were representative of the influenza virus strains likely to circulate in the United States during the

2005-2006 season. Circulating influenza A (H1N2) viruses are a reassortment of influenza A (H1N1) and (H3N2) viruses. Therefore, antibodies directed against influenza A, (H1N1) and (H3N2), vaccine strains provide protection against circulating influenza A (H1N2) viruses (Smith, Bresee et al. 2006).

Inactivated influenza vaccines are made by inoculating fertilized chicken eggs with virus, harvesting the fluid, and then extensively purifying it. Thus, vaccines contain small amounts of residual egg protein which can potentially cause an allergic reaction in certain individuals. New technology focuses on the use of MDCK cell lines for virus production, which eliminates this side effect, and allows rapid production of large amounts of vaccine (Audsley and Tannock 2004).

Influenza vaccines currently present antigen in four forms: (1) whole inactivated influenza virus (WIIV); (2) subunit vaccine; (3) split vaccine; and (4) live attenuated virus. The first three forms require chemical inactivation of the virus, usually with formaldehyde (Keitel and Piedra 1998). The WIIV utilizes the whole virion. In a subunit vaccine (also referred to as PSA), the H and N proteins of the influenza virus are extensively purified, by procedures such as zonal centrifugation, so that the vaccine consists predominantly of only these proteins. Split vaccines require that the lipid envelope of the influenza virion is digested by detergents, freeing the soluble H and N proteins and internal proteins from the whole virus particle which can then be used as the vaccine. The split vaccine was originally developed to reduce the side effects caused by the lipid envelope (Keitel and Piedra 1998). Early split and subunit vaccines displayed reduced immunogenicity with respect to the WIIV, due to the removal of adjuvant associated with the lipid envelope. However, modern versions of these vaccines utilize adjuvants such as aluminum phosphate, making the immunogenicity

comparable to that of the WIIV. Similarly, modern WIIV vaccines are extensively purified so that the incidence of side effects is not significantly different to that of the subunit or split vaccines. The advantage of utilization of a live attenuated virus is the induction of mucosal and systemic immune responses that more closely resemble those provided by the natural infection (Keitel and Piedra 1998).

1.1.9 Rationale for a Dry Powder Influenza Vaccine

Current efforts to control influenza are based on the use of neuraminidase inhibitors, adamantanes, or annual vaccines. The drug compounds are costly prescription medications that must be taken prior to infection and are not effective if symptoms have lasted for more than two days. The need for vaccination is of increasing importance with the development of resistance to the adamantanes. There are currently four different commercial trivalent vaccine formulations: three intramuscular (IM) injections and an intranasal (IN) solution. The IM vaccines contain inactivated influenza virus. They must be administered invasively by a health care professional, stored refrigerated, kept sterile, and containers, needles and syringes must be disposed of as biological waste. The IN vaccine, FluMist®, provides a non-invasive alternative to needle-based injection of influenza vaccines and delivers live, attenuated, and cold-adapted virus. However, in order to maintain potency, the vaccine must be stored frozen and thawed immediately before use. The IN vaccine elicits a systemic immune response (IgG production), but, unlike IM administration, the IN vaccine also elicits a local mucosal response (IgA production). However, the IN vaccine hasn't been approved for use in select populations such as children, the elderly and the immunocompromised, which are most commonly affected by the virus.

One option, which is being widely considered to overcome the shortcomings of the currently approved products, is the use of nasal dry powder vaccines. There is growing interest in the development of stable powder vaccine formulations and delivery technologies to overcome refrigerated storage and distribution (i.e., "cold chain") requirements, associated with liquid based vaccine stability and delivery. Dry powder formulations are potentially superior to liquid formulations in their sterility and stability, eliminating the necessity of the cold chain, thereby facilitating mass vaccination particularly in the developing world (LiCalsi, Christensen et al. 1999; Anderson, Fishbourne et al. 2000; Illum, Jabbal-Gill et al. 2001; LiCalsi, Maniaci et al. 2001; Smith, Bot et al. 2003). There is an urgent need not only to overcome cold chain requirements (for improved stability), but also to provide single-use, non-refillable delivery technologies that require minimal training. This route of administration offers protection from influenza, since the virus uses the nasal route of entry into the host and IN vaccine elicits both a local and systemic immune response. This approach may ultimately provide a safe and an effective alternative to the currently available influenza vaccines.

A dry powder influenza vaccine system containing WIIV and a high-molecular-weight ionic polysaccharide extracted and purified from *Aloe vera* has been studied for intranasal delivery (Ni and Yates 2004). The system is capable of *in situ* gelation, greatly increasing the residence time in the nasal cavity. Preclinical studies showed that the vaccine induced a strong protective immune response at a low antigen dose after a single nasal immunization and a strong boosting effect following a second immunization (Ni, Tian et al. 2005). A human Phase I safety study showed that this powder system (without an antigen) was safe and well tolerated (Yates 2006).

Practical considerations for the manufacture of a dry powder IN influenza vaccine must be addressed. Powder manufacture and characterization, dispersion properties, and methods to assess deposition, clearance and immune response elicited are important considerations in determining optimal vaccine characteristics (Figure 1.4). Powder systems require hydration/dissolution to occur for the system to be effective (Figure 1.5). Release of the active component from a powder to the nasal mucosa must take into account the water uptake and dissolution rates and the interaction between the mucoadhesive and mucus (Medi, Tian et al. 2006).

1.1.10 Formulation of Nasal Dry Powders

The advantages of local mucosal immunity and stability of powder formulations, have led to increasing interest in this form of vaccine delivery to the respiratory tract (LiCalsi, Christensen et al. 1999; Anderson, Fishbourne et al. 2000; Illum, Jabbal-Gill et al. 2001; LiCalsi, Maniaci et al. 2001; Smith, Bot et al. 2003). Processing methods are available for producing powder forms of vaccines tailored specifically for delivery to either the nasal cavity or lungs. LiCalsi et al. have developed a pulmonary powder delivery device and characterized powder formulations of the measles vaccine (LiCalsi, Christensen et al. 1999; LiCalsi, Maniaci et al. 2001). However, the vaccine was developed specifically for pulmonary rather than IN delivery and *in vivo* protection or immunogenicity data for such formulations have not been published.

Historically, two methods for the manufacture of multi-component dry powder formulations have been employed, spray-drying and freeze-drying. Spray-drying involves the transformation of liquid feed through an atomizing nozzle into a dried form by spraying the feed into a hot drying medium (Masters 1976). However, the high drying temperature

necessary during the process of spray-drying can result in the denaturation of the vaccine protein components which is undesirable since this leads to inactivity and therapeutic ineffectiveness. Lyophilization and spray-freeze-drying are, arguably, more appropriate methods for the manufacture of dry powder particles suitable for nasal delivery, since little denaturation is anticipated.

1.1.10.1 Lyophilization

Lyophilization (or freeze-drying) occurs when a solution or suspension is crystallized at a low temperature, followed by solvent removal from the solid-state through the process of sublimation (Gennaro and Remington 1995). The freeze-drying (FD) process is divided into two steps as its name suggests. Freezing is most critical to product quality and is influenced by a number of factors (Oetjen and Haseley 2004). These factors include freezing rate, number and geometry of foreign particles (nuclei), the degree of sub cooling, the rate and growth of ice crystals, the presence and amount of unfrozen water, and the crystallization of the dissolved substances. These factors are interdependent. For example, the degree of sub cooling is strongly influenced by the freezing rate and the number and geometry of foreign particles. Both the rate and growth of ice crystals and the crystallization of the dissolved substances are influenced by the temperature and the viscosity of the solution (Oetjen and Haseley 2004).

The addition of cryoprotective agents, such as lactose, sucrose, mannitol, or trehalose influences the cooling, solidification process and adds to the solid mass of the solution, significantly decreasing molecular mobility and, thereby, preventing hydrolytic degradation of a protein or peptide (Rey and May 2004). Furthermore, cryoprotectants maintain the peptide or protein in its active conformation in the solid state by maintaining favorable H-

bonding interactions as water is removed. A number of excipients have been studied for their cryoprotective properties in maintaining the activity of enzymes (Carpenter, Arakawa et al. 1992). Lactose, sucrose, and trehalose maintained high levels of enzyme activity after freeze-drying. Although lactose can maintain protein activity during lyophilization, it is a reducing sugar and can degrade proteins by the Maillard reaction during storage, hence, it is not considered the cryoprotectant of choice for this category of macromolecules (Hageman 1992).

1.1.10.2 Spray-freeze-drying

A new manufacturing method, spray-freeze-drying (SFD) which combines the methods of spray-drying and freeze-drying has been developed recently (Table 1.2) (Gombotz, Healy et al.; Maa, Nguyen et al. 1999; Costantino, Firouzabadian et al. 2000; Carrasquillo, Carro et al. 2001; Carrasquillo, Stanley et al. 2001; Costantino, Firouzabadian et al. 2002). This process is initiated by spraying a liquid feed into liquid nitrogen, thus freezing the droplets. The frozen particles are lyophilized at a low temperature and pressure, eliminating the possibility of heat damaging or destroying the solute. SFD frequently produces large porous particles with different aerodynamic properties than spray-dried particles (Maa, Nguyen et al. 1999). Ideally, spray-freeze-dried particles are spherical and in a narrow particle size range. They rarely require further particle size reduction (if required this is limited to deaggregation), minimizing the potential loss of activity, and rendering them suitable for blending with an added mucoadhesive compound.

1.1.11 Particle size characterization of dry powders

Quantitative descriptors of particle size are as numerous as the specific properties from which they are derived. The projected area diameter (d_p) is obtained from two dimensional images of particles and represents the diameter of a disc with the same projected area as the particle being examined (Martin and Bustamante 1993). The equivalent volume diameter (d_e) is the diameter of a sphere of the same volume to the particle. While these diameters are readily measured by microscopy or laser diffraction techniques, respectively, they have limited application to particles deposited in the respiratory tract. The aerodynamic diameter (d_a) is the dimension used to represent airborne particle size. The d_a of a particle is the diameter of a unit density sphere that has the same terminal settling velocity in air as the actual particle (Hinds 1999):

$$V_{TS} = \frac{\rho_0 d_a{}^2 g}{18\eta} = \frac{\rho_p d_e{}^2 g}{18\eta\chi} \qquad (1.01)$$

where V_{TS} is the terminal settling velocity of the unit density sphere, ρ_0 is unit density, ρ_p is the particle density, g is the acceleration of gravity, η is the air viscosity, and χ is a factor based on the particle shape (χ=1 for spherical particles). This equation states that as the particle diameter increases but density is uniform, the terminal settling velocity increases, and the larger particle is more likely to deposit by inertial impaction than a small one. However, if density can vary, a larger, low density particle can have the same terminal settling velocity as a smaller high density particle. This is important because spray-freeze-drying generally produces porous particles (low-density) which may result in a significant difference between the directly observable, geometric diameter and the aerodynamic diameter.

Powders consisting of particles of similar size (i.e. monodisperse) can be described by a single parameter, the diameter. However, most powders consist of a range of particle sizes (i.e. polydisperse) that affect their flow and dispersion, and the entire distribution of particle sizes must be characterized (Hinds 1999). A particle size distribution can be represented in several ways (Figure 1.6). A frequency distribution is the proportion of the particles of a specific size plotted with respect to particle diameter. A plot of the frequency against the logarithm of particle size results in a normal or Gaussian distribution, termed lognormal. A lognormal distribution can also be plotted on a logarithmic scale against the cumulative fraction of particles below that size, termed a cumulative distribution plot. A log-probability plot is a linear plot that results from the percent undersize on a logarithmic scale plotted against the logarithm of particle size. Finally, a probit frequency scale, a linearized function of variance, is employed to plot data with respect to the logarithm of particle size. The median diameter, d_{50}, is by definition the geometric mean and is assigned a probit value of five, consistent with its function of dividing the distribution into two equal halves, at the fiftieth percentile. The diameters at the 16^{th} and 84^{th} percentiles are one standard deviation below and above the median and are given values of four and six, respectively. A probit plot of a lognormal distribution is linear. Distributions which may not be fitted by a log-normal mathematical approximation, e.g. multimodal distributions, will deviate from linearity on a log-probability plot.

The median diameter is used to represent the 50^{th} percentile of the distribution and geometric standard deviation is used to represent the breadth of the particle size distribution. The median of a size distribution can be based on the count, mass, or volume and are termed count median diameter (CMD), mass median diameter (MMD) and volume median diameter

(VMD), respectively. The geometric standard deviation (GSD) for a normal distribution can be calculated from the following equation (Hinds 1999):

$$GSD = \frac{D_{84\%}}{D_{50\%}} = \frac{D_{50\%}}{D_{16\%}} = \left[\frac{D_{84\%}}{D_{16\%}}\right]^{1/2} \quad (1.02)$$

where D_{84} and D_{16} represent the diameters at the cumulative percentiles of 84% and 16%, respectively, and the median diameter of the distribution is represented by D_{50}. Particle distributions with a higher GSD are more polydisperse and represent a greater range of deposition characteristics. For an aerodynamic size distribution, the median is identified as the mass median aerodynamic diameter (MMAD).

The span is an alternative measure of the breadth and uniformity of a distribution, which is commonly used to describe nasal formulations where laser diffraction technique has been used to collect equivalent volume diameter data (Newman, Pitcairn et al. 2004):

$$Span = \frac{D_{90\%} - D_{10\%}}{D_{50\%}} \quad (1.03)$$

where $D_{90\%}$ and $D_{10\%}$ represent the diameters at the cumulative percentiles of 90% and 10%, respectively. Both GSD and span are dimensionless parameters.

1.1.12 Physico-chemical characterization of dry powders

The flow properties of a powder reflect the cohesive forces of a powder (Carstensen 1993; Martin and Bustamante 1993). The ability of a powder to flow is a factor that affects the mixing of different materials to form a blend (Martin and Bustamante 1993). This may be important for the blending of the virus particle preparation and excipient to achieve a dry powder formulation. Nasal delivery also requires fluidization of the powder bed, where the flow properties of powders would be anticipated to affect the emitted dose from the device

and subsequent deposition in the nasal cavity. Static methods, reflecting particle interactions, may be used to predict the potential flow properties of a powder and include bulk/tapped density and static angle of repose (Gennaro and Remington 1995).

The surface area of particles influences particle interactions in a powder due to the number of contact points available for these interactions to occur. Surface area for a single spherical particle is equivalent to πd^2 and, therefore, increases as the diameter, d, of the particle increases. However, in a defined mass of powder there are many more small particles than large ones. On a population basis, the sum of the surface area of small particles is greater than that of large particles in any particular powder.

Where particles are irregularly shaped their surface area to volume ratios are substantially different, and potentially variable across a population, from those of a spherical particle hence the estimates of particle diameter based on equivalent spherical sizes may be quite different when based on different physical dimensions (e.g. surface and volume). These differences may be employed to derive shape factors (Martin and Bustamante 1993). The dominant effect of shape is on surface area. The surface area is most commonly measured by gas adsorption at the surface of a known mass of powder (Crowder 2003).

Particles consist of organized structures of molecules the dimensions of which dictate the crystal system. The appearance of the each particle is dictated to large extent by the nature of the particle manufacturing process and the nature of the growth phenomenon which gives rise to a particular crystal habit. Pharmaceutically the underlying molecular structure contributes to the stability of the powder system. Thermal analysis is one means of studying this structure. The principle underlying thermal analysis is to apply energy, in the form of heat, that can be absorbed by the solid and may contribute to a re-ordering of the system into

another form (solid, liquid or gas) or result in dissociation of important elements of the stucture (e.g.water). Differential scanning calorimetry (DSC) is the method most frequently employed to study these phenomena.

DSC measures differences in the amount of heat required to increase the temperature of a sample with respect to a reference (Craig, Royall et al. 1999). When the sample undergoes a physical transformation, such as in phase transitions (thermodynamic or kinetic), there will be a difference in heat needed to flow to it than the reference to maintain both at the same temperature. Whether more or less heat must flow to the sample depends on whether the process is exothermic or endothermic. DSC may be used to measure denaturation and unfolding events in peptides and proteins. DSC may also be used to measure kinetic phase transitions, such as glass transitions.

The forces of attraction that can exist between particles include van der Waals forces, electrostatic forces, and capillary forces. There are numerous ways to characterize the forces of interaction between particles and/or surfaces. Experimental measurements of adhesive forces are made by determining the force required to separate a particle from a surface. Limited data are available on the adhesion force between micron sized particles and solid surfaces (Staniforth 1994). Methods used to evaluate the adhesive force include the variation of the slope of a surface, pendulum (Otsuka, Iida et al. 1983), microbalance method, centrifuge (Kulvanich and Stewart 1987), aerodynamic or hydrodynamic (Visser 1970), and the vibration method (Mullins, Michaels et al. 1992). The only methods applicable to particles in the 0.1-50 μm size range are the centrifugal, aerodynamic, and vibrational methods. An impact energy apparatus has previously been developed (Concessio 1997; Concessio, Van Oort et al. 1998) to enable characterization of particles as small as 1 μm. The

purpose of the device was to determine the force required to detach particles from solid surfaces. With this apparatus, the detachment of nasal powder from a surface can be studied.

In addition, the hygroscopicity, capacity to take on moisture, and the ambient relative humidity of powders in a dry powder formulation can influence their flow and dispersion. Powders with higher moisture contents are more likely to aggregate due to surface tension effects and capillary forces, and hygroscopicity can increase the probability of these effects occurring (Hickey and Ganderton 2001). A high ambient relative humidity (between 65 and 100%) presents water to the surfaces (adsorption) of particles leading to large capillary forces (Kulvanich and Stewart 1988). Low relative humidity can lead to low equilibrium moisture content that results in an increase in electrostatic forces in non-conducting solids. It is important to know the capacity of a powder for moisture uptake over a range of relative humidities to assess the potential for particle aggregation (Hickey and Ganderton 2001). Moisture content is determined by difference, measuring the change in weight of a powder before and after heating.

The cascade impactor is used to separate airborne particles into aerodynamic size classes (Lodge and Chan 1986). Cascade impactors operate on the basis of inertial impaction (Hinds 1999). These devices consist of a series of stages with orifices that decrease in size with each succeeding stage (Figure 1.7). A vacuum drawn at the base of the impactor by a pump is adjusted to generate a predesignated volumetric airflow rate. Particles are drawn into the impactor on the conveying air stream. Collection surfaces serve to obstruct the path of the airflow. Since the orifice size decreases with succeeding stages, the linear velocity of air increases at each successive stage. Therefore, the inertia and stopping distance of the particles increases at each stage increasing their probability of deposition (Baron and Willeke

2001). This allows particles with a range of aerodynamic diameters to be deposited on each collection surface with particles having a higher aerodynamic diameter depositing on the upper stages. Additionally, the amount of powder dispersed from the delivery device can be quantified and an emitted dose can be calculated.

Cascade impactors must be calibrated or mensurated before operation. Calibration is typically performed with aerosols containing particles of the same diameter, monodisperse aerosols (Mercer 1963). Impactor efficiency curves can be generated for each stage of the impactor during the calibration. The aerodynamic diameter of the particles at which 50% of the mass from the air stream impacts on the collection surface, d_{50}, is the effective cut-off diameter for that impactor stage. Since the cut-off diameter for each successive stage decreases, the aerodynamic diameters of particles that deposit on each successive stage also decrease. This allows for the measurement of the aerodynamic diameter distribution of the particles after they have been dispersed. Therefore, the size distribution obtained is an indication of the particle dispersion. Mensuration involves assumptions regarding manufacturing tolerances. A single impactor is calibrated as described above. Other impactors are manufactured according to documented specifications, their functional dimensions (jet diameters, numbers, and distance to impaction surfaces) are measured accurately and sensitive pressure drop measurements are conducted for comparison to the calibrated device. These uncalibrated impactors are assigned the same collection efficiency curves as the calibrated device, if their measured dimensions are within manufacturers' specifications (USP 2006).

Mucociliary clearance has been evaluated *in vivo* (Puchelle, Aug et al. 1981; Ugwoke, Exaud et al. 1999; Ugwoke, Agu et al. 2000). Gamma scintigraphy is a non-

invasive method for studying the deposition and clearance of particles associated with radiolabeled materials that have been administered to animals and humans. It allows both quantitative and direct visual imaging of distribution and clearance of the radiolabeled vaccine formulation. To perform scintigraphic imaging, a γ-radiation emitting tracer, usually a form of ^{99m}Tc associated with the substance of interest, is placed under a camera and imaged using a detector array. Analysis of nasal delivery requires the presence of radiolabeled particles in the nasal cavity and acquisition of gamma camera images of the lateral side of the head taken at various time points. There are limitations to this approach. Imaging of nasal deposition in rodents is difficult to achieve and clearance studies as a function of time pose imaging sensitivity questions (Liversidge, Wilson et al. 1988). Nasal lavage is a technique that has been used to collect and quantify markers of inflammation in the nasal cavity (Foy and Schatz 2004; Wilfong and Dey 2005). Nasal imaging studies allow the disposition of labeled formulations to be followed as a function of time following administration. However, nasal lavage may be employed to wash the radiolabeled particles from the nasal cavity and subsequent scintillation counting of the collected lavage fluid allows estimation of residual materials.

1.2 Problem Statement

Current efforts to control influenza are based on the use of NI, adamantanes, or annual vaccines. NI prevent the budding of replicated influenza from the host cell, thus limiting the ability of the influenza virus to proliferate. NI must be taken just prior to infection, are not effective if symptoms have lasted for more than 2 days, are prescription medications, and are costly. There are currently four different commercial vaccine preparations: three IM injections and an IN solution. The IM vaccines contain whole,

inactivated influenza virus (WIIV). They require invasive delivery monitored by a health care professional, frozen storage, sterility, and their delivery systems (containers, needles and syringes) must be disposed of as biological waste. The IN vaccine is a live, attenuated, cold-adapted trivalent influenza. The IN vaccine provides a non-invasive alternative to needle-based injection of influenza vaccines. However, to maintain potency, the vaccine must be stored frozen and thawed immediately before use. The IN vaccine elicits a systemic immune response (IgG production), but, unlike IM delivery, the IN vaccine also elicits a local mucosal response (IgA production). However, there have been safety concerns related to the use of a live virus vaccine in select populations such as children, the elderly and the immunocompromised.

1.3 Hypothesis and Specific Aims

A novel integrated approach to the preparation and evaluation of WIIV vaccines is desirable. The delivery of nasal dry powder vaccines may ultimately provide a safe, effective, stable, and affordable alternative to currently available influenza vaccines. It is proposed that maximal mucosal and systemic antibody production will be elicited by a dry powder nasal vaccine formulation containing whole inactivated influenza virus in response to increased local residence time. This hypothesis was addressed by the following series of specific aims:

1. <u>To prepare particles containing whole inactivated influenza virions and to evaluate the powder properties for nasal delivery.</u>

Particle Manufacture- Dry powders of suitable size for nasal delivery of WIIV and excipients were prepared by FD followed by milling or SFD. Desirable properties for the manufactured particles included: a) aerodynamic particle size > 20 μm with a median diameter of 30-60 μm; b) suitable for dispersion (good flow properties). (Chapter 2)

Powder Characterization- Each manufactured powder was characterized for particle size and size distribution, particle morphology, thermal properties (crystallinity, polymorphism), moisture content/uptake, bulk/tapped density, static angle of repose, surface area, and electrostatic properties. Several delivery devices were employed and the dispersion properties of the formulations were examined. Functional stability of the dry powder preparation after shelf storage at room temperature was determined using a hemagglutination assay. (Chapter 3)

Novel Methods/Applications- a) Impact force detachment was used to evaluate the dispersion properties of heterogeneous particles. b) A modified Andersen cascade impactor method was employed to characterize particles with aerodynamic diameters < 20 μm. Development of this method allowed accurate estimation of quantities of powder that might potentially enter the lungs, an undesirable characteristic as it may be associated with adverse effects. Cut-off diameters of stages of the cascade impactor at a reduced flow rate were calibrated using a vibrating orifice monodisperse aerosol generator. (Chapter 3)

Effects of Mucoadhesive Compounds- a) Mucoadhesive compounds exhibiting a range of structural and charge properties were evaluated with respect to swelling and viscosity factors consistent with retention on the nasal mucosa. Representative compounds were selected following designed experiments to identify desirable physico-chemical properties. b) Site of deposition was evaluated using scintigraphic imaging. The effect of mucoadhesive compounds on the residence time on the nasal mucosa was evaluated by nasal lavage of radiolabeled powder preparations. (Chapter 4)

2. <u>To demonstrate the effectiveness of the powder vaccine delivered intranasally in eliciting a local IgA and systemic IgG immune response *in vivo*.</u> Dry powder vaccine was

delivered to the nasal cavity of rats to determine the magnitude of the immune response compared to positive and negative controls, a nasal solution and an IM injection. Production of local and systemic antibodies in a rat model was measured after dosing of vaccine formulation by conducting nasal lavage and taking blood samples. (Chapter 5)

Figure 1.8 depicts the specific aims and the manner in which they will be addressed in the dissertation.

1.4 Summary

Drug delivery to the nasal cavity has been achieved using a variety of delivery systems. Influenza affects a large number of people annually and invades the host through the mucosal membranes in the upper respiratory tract. An intranasal influenza vaccine can elicit both a local and systemic immune response. Dry powder vaccines offer the advantages of thermal and physical stability over liquid formulations. Freeze-drying followed by milling and spray-freeze-drying are manufacturing processes used to formulate dry powder vaccines. Particle size is the most important physico-chemical property of nasal delivery dictating the site of deposition in the nasal cavity. Mucoadhesive compounds, such as chitosan and gellan, extend the residence time for powder formulations in the nasal cavity, increasing the elicited immune response.

With respect to: (specific aim 1) the manufacture and size characterization of particles suitable for the formulation of a WIIV dry powder intranasal vaccine are discussed in the following chapter.

Table 1.1– Nasal drug products approved currently in the United States.

INGREDIENT NAME	TRADENAME	DOSE	UNIT	DOSAGE FORM	FIRM NAME
AZELASTINE HYDROCHLORIDE	ASTELIN NASAL SPRAY	137	MCG	SPRAY	ALLSCRIPTS HEALTHCARE SOLUTIONS, PHYSICIANS TOTAL CARE INC, MEDPOINTE PHARMACEUTICALS
BECLOMETHASONE DIPROPIONATE	VANCENASE INHALER NASAL	42	MCG	SPRAY	DRX PHARMACEUTICAL CONSULTANTS
	BECONASE AQ NASAL SPRAY	42	MCG	SPRAY	DRX PHARMACEUTICAL CONSULTANTS INC, GLAXOSMITHKLINE CORP, PHYSICIANS TOTAL CARE
BUDESONIDE	RHINOCORT AQUA NASAL SPRAY	32	MCG	SPRAY	PHYSICIANS TOTAL CARE INC, ALLSCRIPTS HEALTHCARE SOLUTIONS, ASTRA ZENECA
CALCITONIN	MIACALCIN NASAL SPRAY	200	UNT	SPRAY	NOVARTIS PHARMACEUTICALS CORP, SANDOZ INC, UNIGENE LABORATORY, UPSHER SMITH LABORATORIES
CROMOLYN SODIUM	NASALCROM	40	MG	SPRAY	PHARMACIA, PHARMEDIX
CYANOCOBALAMIN	NASCOBAL GEL	0.5	%WV	GEL	SCHWARZ PHARMA, NASTECH PHARMACEUTICAL
DESMOPRESSIN ACETATE	DDAVP SPRAY NASAL	0.1	MG/ML	SPRAY	AVENTIS PHARMACEUTICAL PRODUCTS INC, FERRING PHARMACEUTICALS, ARCOLA LABORATORIES, BAUSCH AND LOMB, APOTEX, SUN PHARMACEUTICAL
	MINIRIN NASAL SPRAY	0.1	MG/ML	SPRAY	FERRING PHARMACEUTICALS
	STIMATE NASAL SPRAY	1.5	MG	SPRAY	ZLB BEHRING, FERRING PHARMACEUTICALS
DIHYDROERGOTAMINE MESYLATE	MIGRANAL NASAL SPRAY	0.5	MG	SPRAY	NOVARTIS PHARMA AG, VALEANT PHARMACEUTICALS
EPINEPHRINE	ADRENALIN CHLORIDE SOLUTION	1	MG	SPRAY	MONARCH PHARMACEUTICALS, PARKEDALE PHARMACEUTICALS
FLUNISOLIDE	FLUNISOLIDE NASAL SOLUTION	0.3	MG	SPRAY, METERED	BAUSCH AND LOMB
FLUTICASONE PROPIONATE	NASALIDE SOLUTION	0.3	MG	AEROSOL, SPRAY	DRX PHARMACEUTICAL CONSULTANTS, OREAD
	NASAREL SOLUTION NASAL	0.3	MG	SOLUTION	ELAN BIOPHARMACEUTICALS, PATHEON, IVAX LABORATORIES
	FLONASE NASAL SPRAY	0.1	%WW	SUSPENSION	PHYSICIANS TOTAL CARE, GLAXOSMITHKLINE INC, PAR PHARMACEUTICAL
IPRATROPIUM BROMIDE	ATROVENT NASAL SPRAY	21, 42	MCG	SPRAY, METERED	BOEHRINGER INGELHEIM PHARMACEUTICALS, ROXANE LABORATORIES, APOTEX CORP
	IPRATROPIUM BROMIDE	0.1	%WW	SOLUTION	APOTEX CORP, BAUSCH AND LOMB, PHYSICIANS TOTAL CARE, ROXANE LABORATORIES, NOVEX PHARMA
MOMETASONE FUROATE	NASONEX NASAL SPRAY	50	MCG	SPRAY, METERED	SCHERING-PLOUGH CORP, PHYSICIANS TOTAL CARE
MIPIROCIN CALCIUM	BACTROBAN NASAL OINTMENT	21.5	MG	OINTMENT	PHYSICIANS TOTAL CARE
NAFARELIN ACETATE	SYNAREL SOLUTION NASAL	2	MG	SOLUTION	GD SEARLE LLC, OREAD
NICOTINE	NICOTROL NS SPRAY	10	MG	LIQUID	ECR PHARMACEUTICALS, PFIZER CONSUMER HEALTHCARE, PHARMACIA AND UPJOHN
PIRBUTEROL ACETATE	MAXAIR INHALER	0.2	MG	AEROSOL	3M PHARMACEUTICALS, PHARMEDIX
SUMATRIPTAN	IMITREX NASAL SPRAY	5, 20	MG	SPRAY	ALLSCRIPTS HEALTHCARE SOLUTIONS, GLAXOSMITHKLINE
TETRAHYDROZOLINE HYDROCHLORIDE	TYZINE NASAL SOLUTION	0.5, 1	MG	SOLUTION	DENISON PHARMACEUTICALS, BRADLEY PHARMACEUTICALS
TRIAMCINOLONE ACETONIDE	NASACORT INHALER NASAL	55	MCG	SPRAY, METERED	ARMSTRONG PHARMACEUTICALS, AVENTIS, GROUP HEALTH
ZOLMITRIPTAN	ZOMIG NASAL SPRAY	5	MG	SPRAY	ASTRAZENECA PHARMACEUTICALS , MEDPOINTE PHARMACEUTICALS

Table 1.2– Literature review of therapeutic powders manufactured utilizing a spray-freeze-drying (SFD) process.

ACTIVE INGREDIENT	EXCIPIENT(S)	NOZZLE TYPE	SOLUTION FEED RATE	ATOMIZATION AIR FLOW	SOLUTION CONC	PARTICLE SIZE	REF
Bovine pancreas trypsinogen	Mannitol, trehalose, dextran 37500, polysorbate 80	Ultrasonic	3 mL/min	Not Available	20%	20-90 µm	(SONNER, MAA ET AL. 2002)
Bovine serum albumin	Poly (lactide-co-glycolide), Zn	Two fluid	33-857 L/min	20-331 L/min	20-25 mg/mL	0.2-12.6 µm	(COSTANTINO, FIROUZABADIAN ET AL. 2000)
	Poly (lactide-co-glycolide), Zn	Two fluid	33-857 L/min	20-331 L/min	20 mg/mL	0.2 µm	(COSTANTINO, FIROUZABADIAN ET AL. 2002)
	Poly (lactide-co-glycolide), poloxamer 188 (Pluronic F68), trehalose	Two fluid	33-857 L/min	20-331 L/min	20-25 mg/mL	Not Available	(CARRASQUILLO, STANLEY ET AL. 2001)
	Trehalose	Two fluid	10-15 psi	20-331 L/min	10 mg/mL	Not Available	(CARRASQUILLO, CARRO ET AL. 2001)
Cetrorelix acetate	Lactose	Two fluid (d=0.5mm)	Not Available	800 L/hr	Not Available	2.13-2.32 µm	(ZIJLSTRA, HINRICHS ET AL. 2004)
Darbopoetin alfa	Trehalose dihydrate, sodium phosphate	Ultrasonic (2 W)	3 mL/min	Not Available	0.2 µm	3.2-5.2 µm	(NGUYEN, HERBERGER ET AL. 2004)
	Trehalose dihydrate, poly (lactide-co-glycolide) 50:50	Ultrasonic (2 W)	1.5 mL/min	Not Available	0.2 µm	29 µm	(BURKE, KLUMB ET AL. 2004)
Diphtheria toxoid, tetanus toxoid, hepatitis B surface antigen	Dextran, mannitol, trehalose dihydrate, glycine, aluminum phosphate, AlOH	Ultrasonic	2 mL/min	Not Available	Not Available	38-53 µm	(MAA, ZHAO ET AL. 2003)
Goat anti-human IgG, goat anti-human IgG peroxidase	Poly (DL-lactide-co-glycolide) 50/50, PVA, Tween 80, mannitol, trehalose, Zn	Ultrasonic	5 ml/min	Not Available	8.3%	110-190 µm	(WANG, CHUA ET AL. 2004)
Influenza subunit or split-virion	Dextran, mannitol, poloxamer 188 (Pluronic F68), polysorbate 20, trehalose dihydrate	Ultrasonic	1.5 mL/min	Not Available	20-35%	30-60 µm	(MAA, AMERI ET AL. 2004)
Recombinant hemoglobin	PEG 3350, dextran T500, trehalose, mannitol, sucrose. All solutions are in 5 m*M* potassium phosphate, 150 m*M* NaCl (pH 7.4).	Ultrasonic (120 kHz, 2 W)	Not Available	Not Available	Not Available	Not Available	(HELLER, CARPENTER ET AL. 1999)
Recombinant human growth hormone	Poly (lactide-co-glycolide), Zn	Two fluid	217-480 mL/min	24-121 L/min	5 or 20 mg/mL	0.2-4.5 µm	(Costantino, Johnson et al. 2004)
Recombinant human nerve growth factor	Histidine, sodium bicarb, Zn, trehalose, sucrose, mannitol, lactose, pluronic	Ultrasonic	5 mL/min	Not Available	Not Available	Not Available	(Lam, Duenas et al. 2001)
Recombinant-derived humanized anti-IgE monoclonal antibody, recombinant human deoxyribonuclease	Mannitol, trehalose, sucrose	a) Ultrasonic b) Two fluid	a) 5 mL/min b) 15 mL/min	a) Not Available b) 1050 L/hr	Not Available	3.3-32 µm	(Maa, Nguyen et al. 1999)

Figure 1.1– Schematic diagram of the nasal cavity showing the location of: A) nostril; B) nasal valve; C) olfactory region; D) superior turbinate; E) middle turbinate; F) inferior turbinate; and G) adenoids and tonsils.

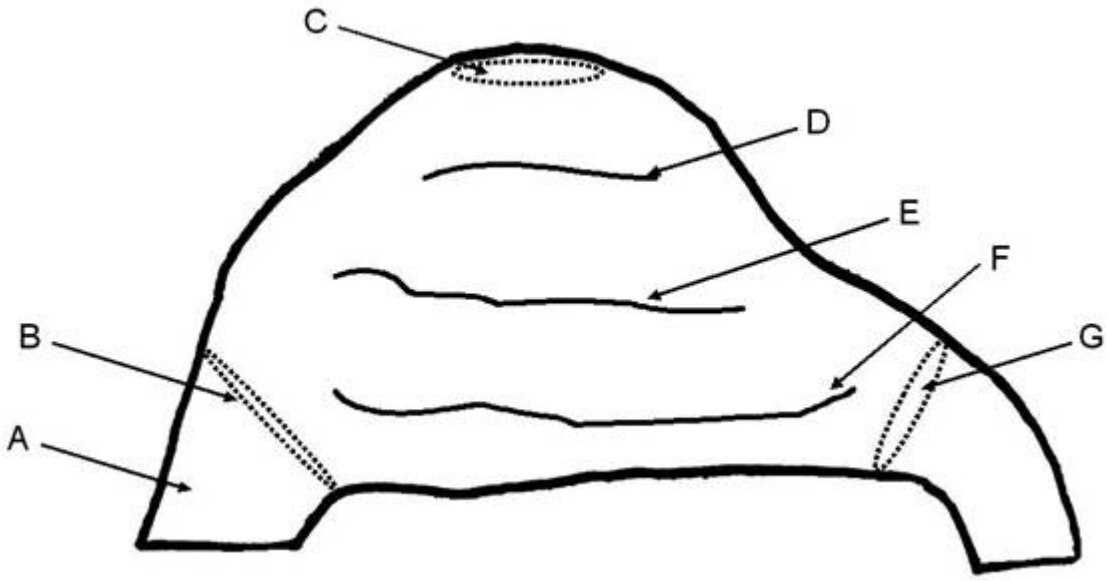

Figure 1.2– Schematic diagram of the nasal epithelium showing location and features of: A) ciliated cell; B) non-ciliated cell; C) goblet cell; D) mucus layer; E) periciliary layer; F) basal cell; and G) basement membrane. Adapted from (Ugwoke, Verbeke et al. 2001).

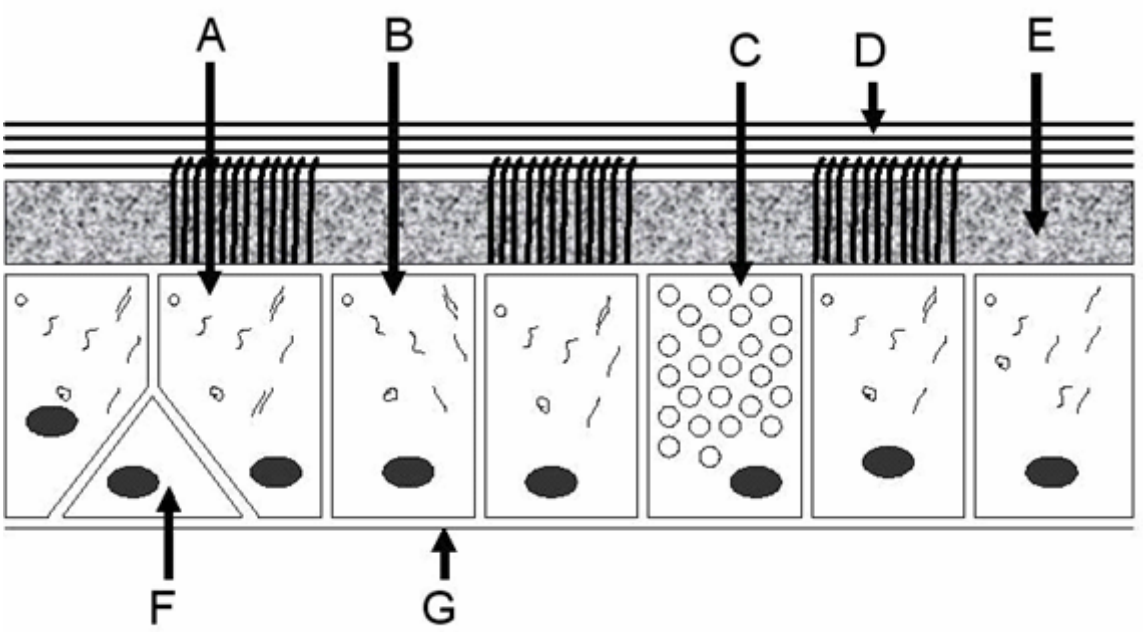

Figure 1.3– Schematic diagram depicting mucus and periciliary fluid forming a double layer. Adapted from (Quraishi, Jones et al. 1998).

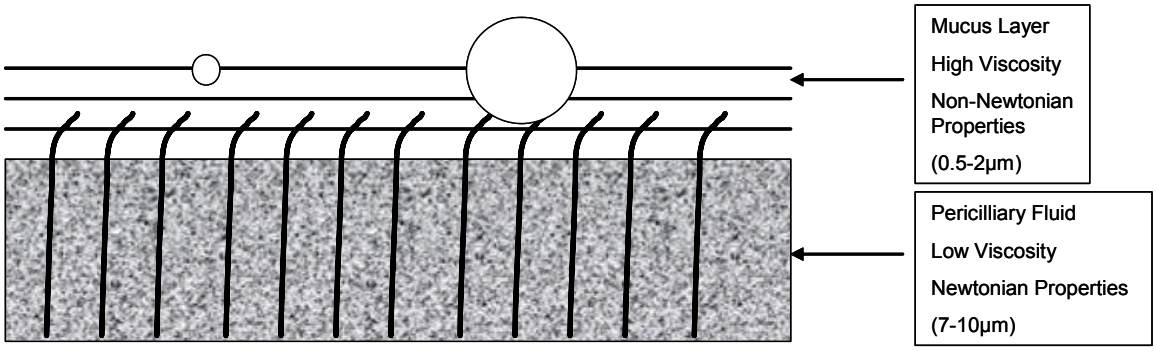

Figure 1.4– Formulation, droplet/particle and biological factors that affect nasal delivery.

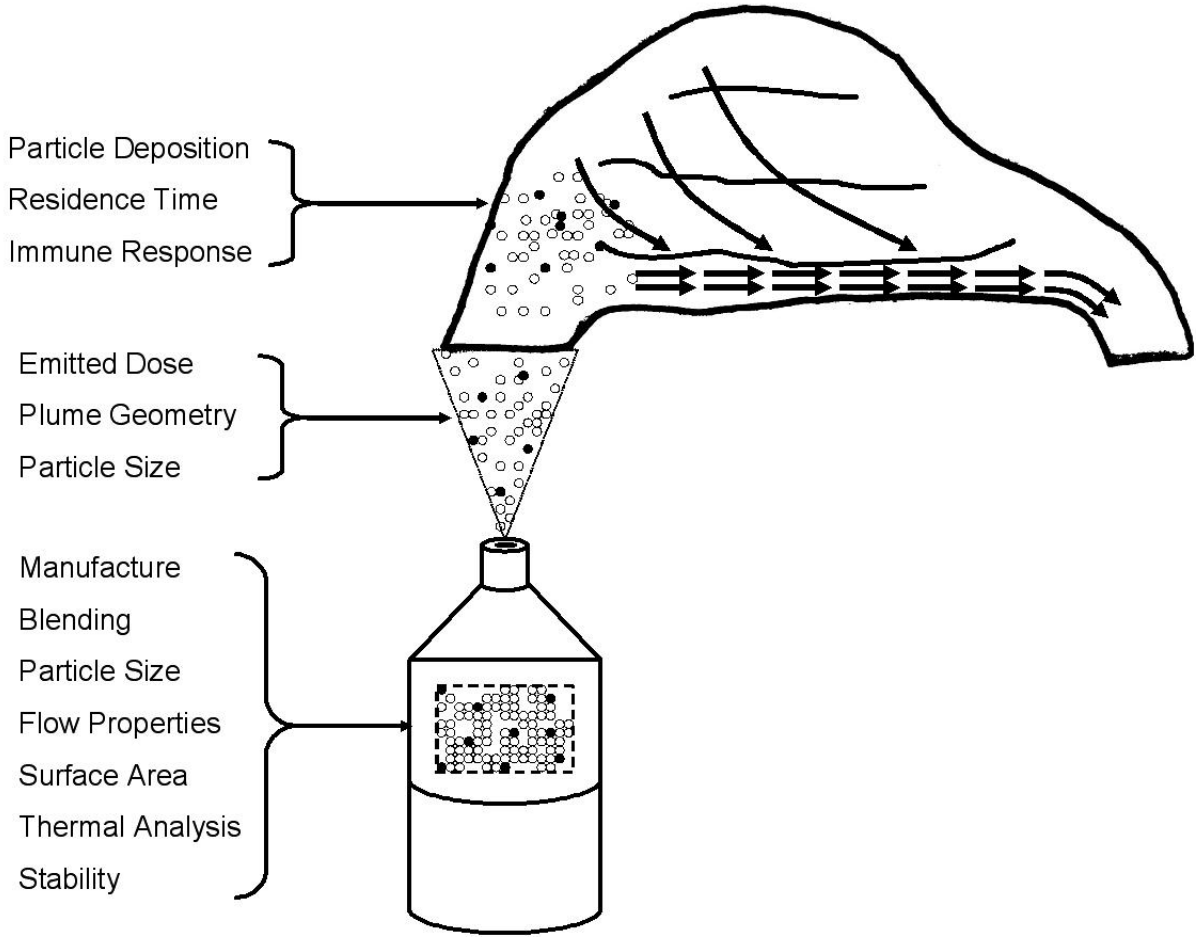

Figure 1.5– Factors that affect powder interaction with the nasal mucosa.

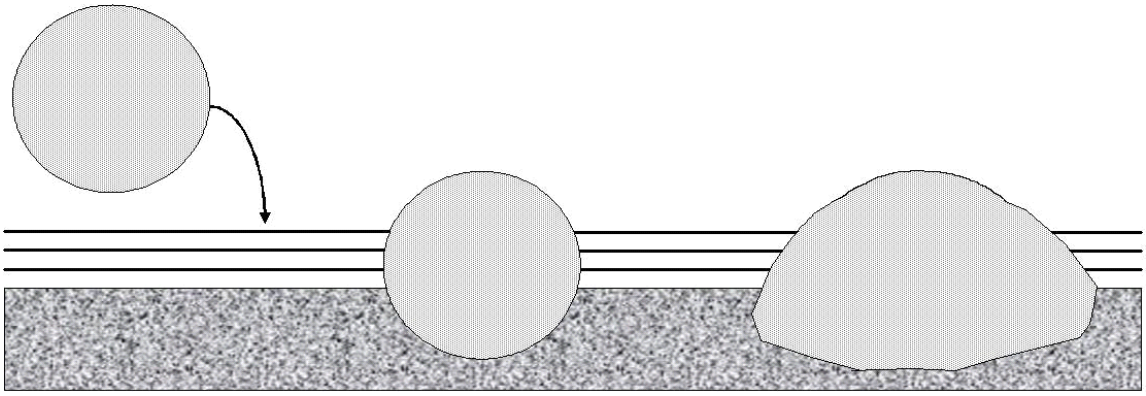

Solubility	→	Amorphous v. Crystalline, Contact Angle
Hydration	→	Dissolution Rate
Viscosity	→	Viscosity
Swelling	→	Swelling Time
Hindrance	→	?????

Figure 1.6– Particle size distributions shown as: a) frequency with respect to particle size, b) frequency with respect to the logarithm of particle size, c) probability with respect to the logarithm of particle size, and d) probits with respect to the logarithm of particle size. These figures illustrate transformations that may be employed to derive statistical descriptors of particle size and distribution.

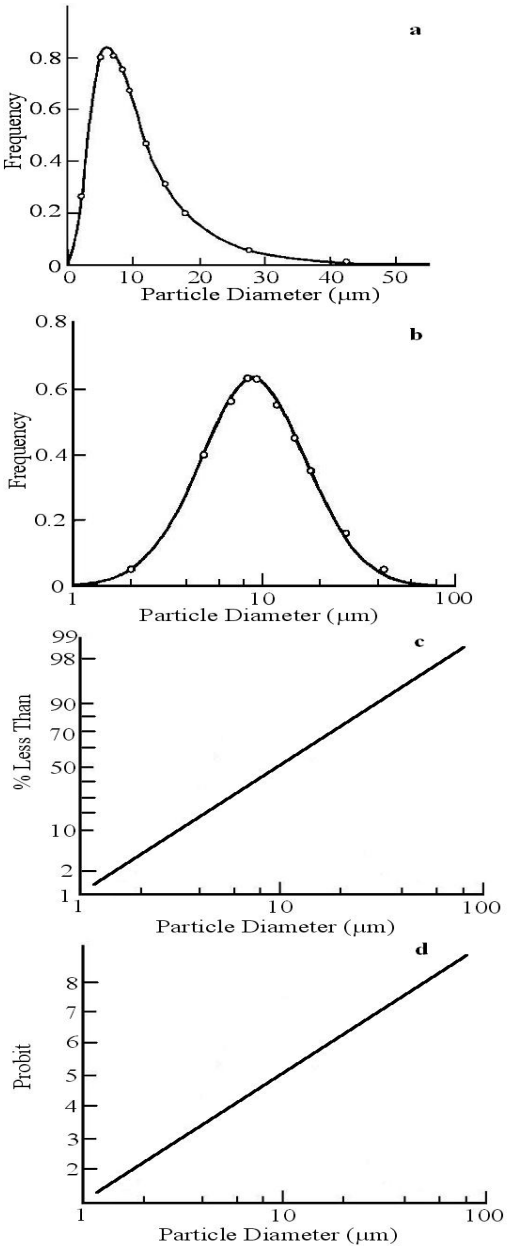

Figure 1.7– Schematic diagrams of a) the Andersen eight stage non-viable cascade impactor and b) streamline airflow (indicated by arrows) through an orifice impinging on a collection surface.

a)

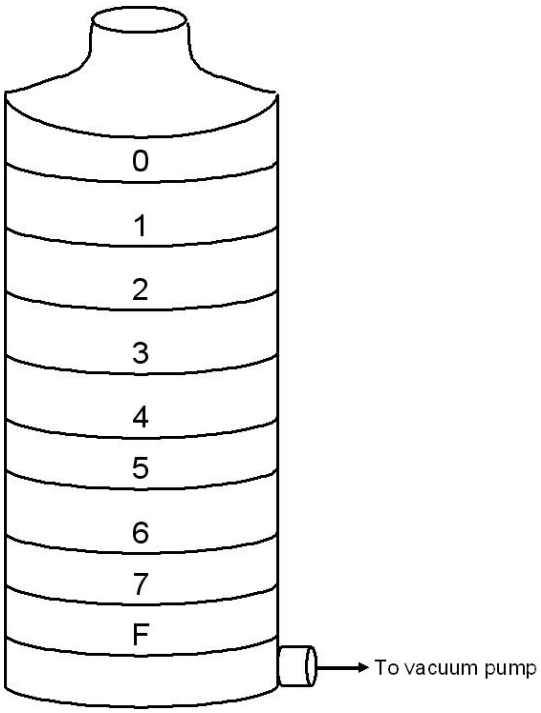

b)

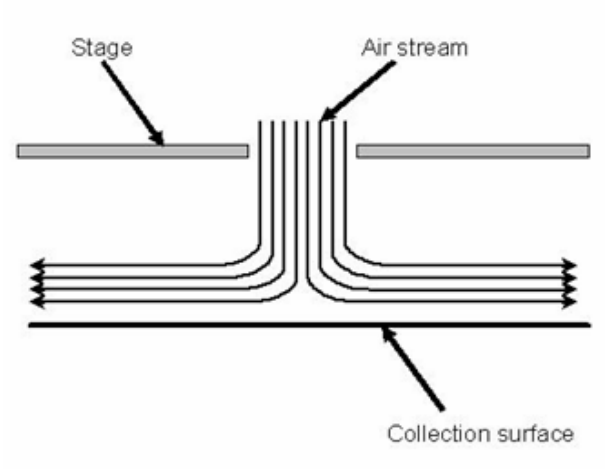

Figure 1.8– Flow diagram of specific aims and their presentation in the dissertation.

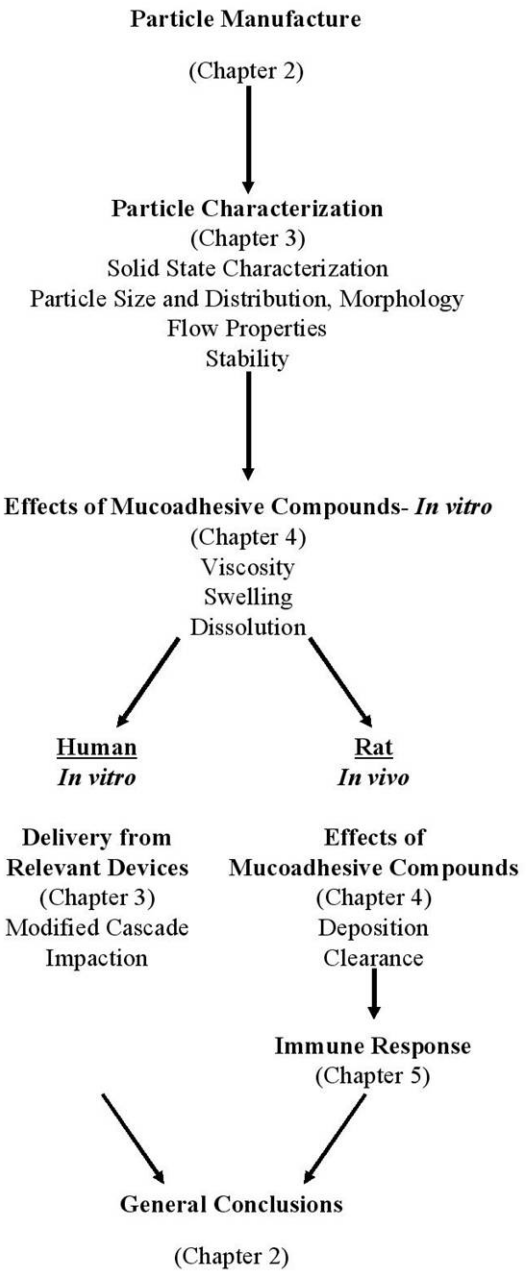

2 PARTICLE MANUFACTURE

2.1 Introduction

In order to deliver antigen to the nasal mucosa in the form of dry particles, specific manufacturing and characterization approaches must be selected. The importance of these methods is that they: (a) achieve the desired particle size for nasal delivery; (b) avoid particle penetration into the deep lung; (c) result in measurable and reproducible properties, most significantly of morphology (shape and surface roughness), size and distribution, and stability. To prepare powder for nasal delivery several techniques may be considered. Freeze-drying (lyophilization), a conventional method for the production of dry powders containing materials of biological origin, has been used for the preparation of vaccines for parenteral delivery. Spray-freeze-drying (SFD) is a new and, as yet, commercially unproven technique for pharmaceutical particle manufacture. The following sections describe each of these methods in general and indicate the nature of their adoption for the following experimental sections.

Lyophilization requires two sequential processes to occur, freezing of components in solution that will become elements of the final solid product and drying to remove the solvent. As mentioned in Section 1.1.10.1, the freezing process greatly affects the outcome of the final lyophilized product. A variety of factors that influence the final product characteristics can be noted. The effect of freezing rate on a solution has been reported (Dawson and Hockley 1992). These studies demonstrated that a solution frozen too slowly develops a concentrate that can cause the surface to collapse, and thus, reduce the drying

speed. In addition to collapsing, rapid freezing causes the sample to be amorphous and fibrous. Solute concentration also affects drying time. At higher solute concentration (i.e., >10 % solids in solution), the dry product has smaller specific area, and it is more difficult to remove the water. Thus, longer times and/or higher temperatures are needed to finish secondary drying , which can adversely affect protein stability (Tang and Pikal 2004). Annealing has been used to elicit a phase transition in water from amorphous to crystalline as a means of controlling the final product morphology (Gatlin 1992). It entails the freezing of a solution at a low temperature below the Tg', or glass transition temperature if all freezable water crystallized, followed by slow temperature elevation to just below the melting point and holding for a period of time (Oetjen and Haseley 2004). Lyophilization was the first manufacturing technique used, in the experiments described in this chapter, to produce dry powder particles suitable for nasal delivery. Factors of freezing rate, annealing and solute concentration were evaluated in the experimental design.

Ball milling of powders is a common size reduction method in which particles are fractured by the repetitive collision with stainless-steel or ceramic balls or cylinders (milling media) (Gennaro and Remington 1995). Total milling time, speed, powder mass, size of mill, and number of milling media elements are all important variables for milling and must be determined separately for each formulation (Hickey and Ganderton 2001). A faster milling speed corresponds to rapid particle size reduction. Typically, the degree of milling reaches a plateau and then may decrease due to the creation of aggregates (Hickey and Ganderton 2001). Milling occurs more slowly for a higher proportion of powder with respect to milling media. The media experiences reduced freedom of motion which reduces the energy expended in the milling process. The combined effect of milling time and powder load also

may be explained by speed of milling since more time is required to mill a larger load of powder. Freeze dried powders were milled to produce particles suitable for nasal delivery and optimal milling conditions, of time, mass of powder and quantity of milling media, were assessed.

Sieving is a method of obtaining particles of a desired size range from a powder with a wide range of particle sizes (Fonner, Banker et al. 1966). Sieves may be used to remove smaller particles (<25 um) that may impact negatively the performance of the powder (i.e. results in poor flow and mixing properties). It is also used in the separation of large excipient particles in designated size ranges that have a variety of flow properties, where larger particle size fractions flow well due to decreased particle interactions. In the context of nasal delivery, the removal of small particles prevents entry and deposition of particles in the lower respiratory tract. Sieving was used to select particles of antigen preparation and excipient in sizes suitable for dispersion and deposition in the nose.

The SFD process requires atomization of droplets which can be achieved by forcing a liquid through a nozzle. The liquid and accompanying air pressures, along with the nozzle geometry, causes the liquid stream to break into ligaments, which are then further broken down into droplets. The size of the droplets formed depends on the liquid flow rate, air pressure, spray angle, and liquid properties (surface tension and viscosity). Low liquid or high airflow rates and smaller nozzle dimensions generally result in the production of small droplets and particles (Masters 1976). SFD was employed in the present studies and each of the above factors was studied.

Effectiveness of particle manufacture is assessed by measuring important characteristics of the powder product. Techniques that may be employed include microscopy

and optical methods for specifying morphology, particle size and distribution. Moreover, these methods can be designated as endpoint measures (responses) in statistically controlled experimental designs to allow optimization of the factors in the manufacturing process. Methods of representing data from such experiments (half-normal probability plots, ANOVA, residual, interaction and cube plots) are described below.

Scanning electron microscopy (SEM) is a technique capable of producing high-resolution images of a sample (Martin and Bustamante 1993). SEM images have a characteristic three-dimensional appearance and are useful for judging the surface structure of particles. SEM can also be utilized to show morphological differences between FD cakes manufactured under various conditions (Dawson and Hockley 1992).

Laser diffraction is one of the most commonly used light scattering methods of particle sizing. Particles are passed through a laser (frequently Helium-Neon, 682.3 nm) creating a diffraction pattern on a detector array. An algorithm can be used to calculate the particle size distribution from this diffraction pattern (Ranucci 1992). It is notable that the geometry of the detector array and the algorithm for data presentation vary for each instrument manufacturer. The algorithms themselves, which are based on Fraunhofer or Mie theory, are considered proprietary.

The design of experiments is commonly used in the pharmaceutical industry for a wide range of applications including the development of solid dosage forms and dispersed systems (Gohel and Amin 1998; Deaton, Jones et al. 2002; Smyth, Brace et al. 2006). Factorial designs are among the most frequently utilized statistical designs in industry. A general factorial design is performed by selecting a fixed number of levels for each of the variables (or factors) and running experiments to determine responses for all possible

combinations of factors (Box, Hunter et al. 2005). A response is a variable which is measured during an experiment and is dependent on the factors in the study. A full or complete factorial design, in which the factors are examined in all possible combinations, are best suited for studies where the number of factors is not too large. Full factorial designs at two levels are the most commonly used designs in the pharmaceutical literature (Box, Hunter et al. 2005).

The target particle morphology, size, and distribution for dry powders for potential delivery of whole inactivated influenza virus to humans was spherical (or regular polygonal) 40μm median diameter with limited quantities of powder below 10 μm (See 1.1.2). The target properties for powders to deliver to rats were 25 μm median diameter spherical particles. The size was smaller than that for humans because of delivery device limitations. Two manufacturing processes were evaluated for their potential to produce particles of suitable size and morphology for nasal delivery. The factors affecting freeze-drying (freezing rate, solute concentration, and annealing) and spray-freeze-drying (solution feed rate, airflow rate, and solute concentration) were optimized using designed experiments. The morphology of manufactured cakes and powders and mucoadhesive compounds (MA) were observed using scanning electron microscopy and particle size analysis was performed using laser diffraction (Figure 2.1).

Selection of Materials

Whole inactivated Influenza virus (WIIV) of the H1N1 strain, A/PR/8/34, purchased from Charles River SPAFAS (North Franklin, Connecticut; Lot#4PRI000901, 2 mg/ml), was used as a liquid preparation as provided by the vendor or prepared as a powder. WIIV was

propagated in the allantoic fluid of chicken eggs, purified from a sucrose gradient, inactivated by buffered formalin, and re-suspended in HEPES saline.

D-(+)-trehalose dihydrate (referred to as trehalose, Sigma Chemical Co., St. Louis, MO) was used as a cryoprotective agent. Trehalose is a non-reducing sugar formed from two glucose units joined by a 1-1 alpha bond. This bonding makes trehalose very resistant to acid hydrolysis, and, therefore, stable in solution at high temperatures even under acidic conditions. The bonding also keeps non-reducing sugars in closed-ring form, such that the aldehyde or ketone end-groups do not bind to the lysine or arginine residues of proteins, known as glycation.

Hydroxypropyl methylcellulose (MW= 10 kD, HPMC LMW or MW= 90 kD, HPMC HMW, Sigma), is a cellulose ether as shown in Figure 2.2A. The functional properties of HPMC depend on the degree of substitution of the cellulose structure, and on the chain length of the cellulose backbone. HPMC is used as an emulsifier, thickening agent, stabilizer, and suspending agent. It is a white to off-white fibrous powder which swells in water to produce a viscous colloidal solution, non-ionic. HPMC dissolves slowly in cold water and is insoluble in hot water.

Carboxymethylcellulose sodium (MW= 90 kD, CMC LMW or MW= 700 kD, CMC HMW, Sigma) is a cellulose derivative with carboxymethyl groups bound to some of the hydroxyl groups of the glucopyranose monomers that make up the cellulose backbone as shown in Figure 2.2B. The polar carboxyl groups enhance the solubility of the cellulose and contribute to chemical reactivity. The functional properties of CMC depend on the degree of substitution of the cellulose structure, and on the chain length of the cellulose backbone. CMC is used in food science as a viscosity modifier (thickener) and to stabilize emulsions.

Sodium alginate (SA, Sigma, 200-400 cps) is the sodium salt of alginic acid (Gennaro and Remington 1995) as shown in Figure 2.2C. It is an extract of seaweed and is used as a thickener in the food industry and as a gelling agent and emulsifier.

Chitosan (MW= 161 kD, degree of deacetylation= 92%, donated by Vansen) is a linear polysaccharide composed of randomly distributed β-(1-4)-linked D-glucosamine (deacetylated unit) and N-acetyl-D-glucosamine (acetylated unit) as shown in Figure 2.2D. Chitosan is produced commercially by deacetylation of chitin, which is the structural element in the exoskeleton of crustaceans (crabs, shrimp, etc.). The amino group in chitosan has a pKa value of ~6.5, thus, chitosan is positively charged and soluble in acidic to neutral solution with a charge density dependent on pH and the degree of deacetylation. Chitosan is bioadhesive and readily binds to negatively charged surfaces such as mucosal membranes. Chitosan enhances the transport of polar compounds across epithelial membranes by opening of tight junctions (Artursson, Lindmark et al. 1994) and is biocompatible and biodegradable.

2.2 Methods

2.2.1 Particle Manufacture and Powder Preparation

2.2.1.1 Freeze-Drying Followed By Milling

Freeze-drying. The factors affecting the FD process were examined using the principles of statistical factorial design. Changes in the concentration of the solution (1 and 10%), the freezing rate of the solution (slow and fast), and thermal treatment (yes or no) were all optimized for the formulation used. Effective initial designed experiments examine a very broad range of factors, ensuring capture of the desired response (Wu and Hamada 2000). With this in mind, the concentration range was dictated by the upper limit, as previously

stated, of 10% solids. The lower limit was set one order of magnitude lower than the upper limit. Solutions of the designated concentrations of trehalose in water were prepared. Five milliliters of each solution was placed in a 20 mL lyophilization vial. Freezing rates were determined by exposing the solutions to different low-temperature conditions. Liquid nitrogen was chosen because of its low boiling point (~ -180°C), while the lower limit of freezing rate was determined by freezing a solution below its Tg', which for trehalose is -30°C. For fast freezing, the lyophilization vials were placed in a tray of liquid nitrogen and then transferred to a freeze-dryer (Dura-Stop/Dura-Dry, FTS Systems, Stonebridge, NY) pre-cooled to -40°C shelf temperature. For the slow freezing, the vials were located on the pre-cooled shelf for 2 hours. Empty vials were placed around the edge of the shelf and aluminum foil was placed over the glass door to reduce thermal effects by radiant energy and heat transfer from chamber walls. Annealed samples were prepared by gradually elevating the shelf temperature over 6 h to -10°C. Samples underwent a lyophilization cycle in which drying was performed at -10°C shelf temperature for 6 h, 0°C shelf temperature for 6 h, 10°C shelf temperature for 6 h, 15°C shelf temperature for 6 h, and 20°C for 24 h. The vials were stoppered under dry nitrogen at atmospheric pressure, to reduce the potential for oxidation or hydrolysis that might impact product stability.

Particle size reduction. A micro-ball mill (SPEX Certiprep #3117 Metuchen, NJ) was used to reduce particle size for small quantities of powder (<300 mg). The mill consists of a stainless steel vessel containing a 1/4" steel ball. Optimization of the milling process was performed previously (Garmise, Mar et al. 2006). A milling time of 30 minutes with a powder load of 150 mg was used. The mini-mill was sealed and mounted on an oscillating motor (Variable Speed Jig Saw, Black & Decker Inc., Towson, MD) to provide agitation at

200 rpms. To minimize moisture effects, work was completed in a dry box (<20% RH, 22.0 ± 2°C).

Sieving. Milled powders were sieved with sieve mesh sizes of 45, 75, 125, 180, and 300 μm using a 3-inch sieve shaker (Model No. SS-5, Gilson Company Inc., Worthington, OH). The sieves were arranged in descending order of mesh size with the 300 μm sieve on top and the 45 μm sieve on the bottom. A mass ≤10 g of powder was placed on the top sieve and the sieve shaker was operated in the tap mode for two hours. Milled FD and bulk MA powders were sieved and particles in the 45-125 μm size range were collected. Similar to milling, relative humidity was controlled during the sieving runs (<20% RH, 22.0 ± 2°C).

2.2.1.2 Spray-Freeze-Drying

The factors affecting the SFD process were examined using the principles of factorial design, similar to those employed to develop the FD process. The concentration of the solution, the flow rate of the solution, and the atomizing airflow rate were all optimized to achieve the desired properties. Similar to FD experiments, the upper limit for solute concentration was 10%, while the lower limit was 1%. The maximum rate of solution flow for this system was 25 mL/min. The lower level was set at 3 mL/min. Powders produced by SFD in the literature were produced utilizing two-fluid nozzles with high airflow rates (~1000 L/hr), while producing particles < 10 μm (Costantino, Firouzabadian et al. 2002; Costantino, Johnson et al. 2004). The upper limit of the experimental design was set at 500 L/hr, while the lower limit was set at 250 L/hr to produce larger particles. Aqueous solutions containing trehalose were prepared and passed through a spray nozzle (7 mm diameter) from a bench top spray-dryer (Büchi Mini Spray-Dryer, B-191, Switzerland) at the desired flow rate. Atomizing nitrogen gas, with a fixed back pressure of 1 atm was used to deliver the

suspension. When spraying was complete, the frozen droplets in the liquid nitrogen were transferred to a glass container to be lyophilized at a fixed manifold temperature (-55°C) and pressure (25 mtorr) for 72 hours.

2.2.2 Particle Morphology of Powders

Scanning electron microscopy. The powders were adhered to double-sided adhesive carbon tabs (Ted Pella Inc., Redding, CA) on aluminum stubs (Ernest F. Fullam, Inc., Latham, NY) scanning electron microscopy (SEM). A Polaron sputter coater (model E-5200, Electron Beam Services (EBS), Agawan, MA) was used to coat the samples with gold-palladium. A scanning electron microscope (JEOL 6300, JEOL Corp., Peabody, MA) was used with an electron beam at an acceleration voltage of 15 kV and a working distance of ~25 mm. Representative areas of the stub were photographed (n=3).

2.2.3 Particle Size and Size Distribution of Powders

Laser diffraction. Each powder was subjected to laser diffraction (Malvern 2600 Series, Worcestershire, UK) particle size analysis by a suspension method using a small liquid dispersion sample cell. The sample cell has an integral stir bar and a volume of ~15 ml. The cuvette was filled with 1% w/w Span 80 (Sigma) in light, white mineral oil (Sigma). Powder samples of ~10 mg were dispersed in 2 ml of 1% w/w Span 80 in light, white mineral oil, sonicated for five minutes and then placed into the sample cell one drop at a time until a laser obscuration between 2 and 30% was achieved (n=3), as recommended by the manufacturer for optimal data collection.

2.2.4 Experimental Design

Factorial designs maximize the information gained while minimizing the resources used and offer the advantage of exhibiting a high degree of "hidden" replication. Factorial designs also provide estimates of possible interactions between each of the factors. With a factorial approach, the effects of a single factor are examined for every possible combination of the other factors included in the experiment. This effectively maximizes the information regarding the influence of various factors in the design and their inter-relationships on the designated response(s).

Normal and half-normal plots are graphical tools for determining effects in the model that are significant. These graphical techniques are not used alone in deciding significant effects, but rather are used in conjunction with analysis of variance. A sigmoidal cumulative normal curve is generated for a normal distribution by plotting P versus X (an effect), where P represents the percentage probability of the occurrence of X (Box, Hunter et al. 2005). Plotting the same data on normal probability paper yields a straight line. Data that may be explained by random variation around a mean (a near normal distribution) falls on a straight line when plotted on a normal probability scale. Points that do not fall on the straight line are effects that are not easily explained as chance occurrences, and are considered significant. The half-normal plot is employed to make decisions regarding of the observed effects. Plotting the cumulative distribution of the set of effects from a 2 factorial experiment on a half-normal plot assists in the interpretation of the data by highlighting outliers, heteroscedasticity (different variances), dependence of the variance on mean and defective randomization with a greater degree of accuracy than a normal plot. In a half-normal plot the points of the modified distribution fall on a straight line that passes through the origin. Points

that fall off the line are considered large, and their effects distinguished from the rest as significant.

Data from experimental designs employ an analysis of variance (ANOVA). The variance associated with a specific independent variable or interactions between independent variables is compared with the variance associated with the random error occurring in the experiment (Box, Hunter et al. 2005). A variable is considered to have a statistically significant effect on the measured response if a difference exists between the treatment and error variance. For these experiments, the criterion for significance was $P<0.05$.

Plots of residuals (the difference between the observed value and the predicted value for the model used) versus predicted values should appear as points randomly scattered around a horizontal line, provided the residuals have a mean zero, a constant variance, are independent and normally distributed (Box, Hunter et al. 2005). An inadequate model or variances that are not constant lead to abnormalities in the scatter pattern, which may be corrected by transforming the independent or dependent variable, or by adding additional terms to the model.

Interactions graphs reveal trends in the measured response as the factor varies from the lower level to the higher. These graphs plot individual responses as a function of factors that have a statistically significant effect on the specified measured response.

Cuboidal plots are utilized to reveal trends in the data by comparing the lower level and higher level factors simultaneously. Factors are plotted on an axis in the x, y, or z direction. These plots facilitate data interpretation in identifying significant factors in designed experiments.

The specific experimental designs for each manufacturing method are shown in Tables 2.1 and 2.2. A full 2^3 factorial design was employed for each of the two methods, FD followed by milling and sieving, and SFD. Three replicate batches for each of the conditions were prepared. The latter replicates were performed to account for inherent variability.

2.3 Results and Discussion

2.3.1 Particle Manufacture and Powder Preparation

2.3.1.1 Lyophilization Followed by Milling and Sieving

The freeze-dried material formed white, porous cakes showing slight shrinkage (detachment from container walls), but no large-scale collapse was observed.

2.3.1.2 Spray-freeze-drying

The spray-freeze-dried material formed a white, low density, porous powder that seemed to flow very easily.

2.3.2 Particle Morphology of Powders

Scanning electron micrographs (SEMs) of bulk trehalose fractions are shown at various magnifications (Figure 2.3). Bulk trehalose particles are orthorhombic crystals that are heterogeneous in size and cuboidal or needle-like in shape. SEMs of 45-75 μm sieved trehalose fractions are shown at various magnifications (Figure 2.4). The sieved trehalose particles are polyhedral crystals, rhomboidal in shape, that exhibit a fairly narrow size distribution.

SEMs of mucoadhesive compounds were taken at 60X (Figure 2.5) and 150X (Figure 2.6) of sieved fractions of HPMC LMW, HPMC HMW, CMC LMW, CMC HMW, chitosan

(all 45-75 μm), and SA (45-125 μm). HPMC LMW is a white to off-white powder consisting of a mixture of fibrous and granular particles that are heterogeneous in size and shape. HPMC HMW, CMC LMW, and CMC HMW are white to off-white powders with fibrous-shaped particles. Chitosan is an off-white colored powder with granular and needle-like particles. SA is a yellow-brown powder consisting of granular particles. Because of the low yield of SA particles in the 45-75 μm size range, 45-125 μm sieved fractions were used.

SEM of lyophilized cakes of 10% trehalose in deionized water are shown at 40X (Figure 2.7) and 100X (Figure 2.8) magnification. The pore sizes of the channels through which water was removed appear to be larger in the cakes prepared at a slower freezing rate than those frozen rapidly. This is consistent with the literature (Thijssen 1969). The freezing rate determines the size of the ice crystals. When the temperature of a solution is decreasing at a slow rate, ice crystals will grow first, effectively concentrating the dissolved solute in a small volume of solvent. This is termed the freeze concentrate. The size of the ice crystals can be estimated from the size of the pores in the dried cake. As the freezing rate is increased, a decrease in the mean pore diameter occurs (Thijssen 1969). This is an important phenomenon because the pore size dictates the drying rate of the frozen product. When large ice crystals are sublimed, the resultant pores in the cake are necessarily large.

Factors such as concentration of the solution and freezing rate give rise to a highly viscous concentrate on freezing. The consequent lowering of the freezing point hinders the transition causing an amorphous state representing disorder between the water and the solids (Dawson and Hockley 1992). Rapidly frozen samples did not appear to exhibit this phenomenon on visual inspection. If a product is frozen too quickly, the concentrated liquid is located at the center of the mass, forming an uneven surface and causing a partially

collapsed channel during drying. Visual inspection has also verified that the drying time of 48 hours was sufficient for all of the freeze-dried cakes.

SEMs of trehalose powder after milling and sieving are shown at 60X (Figure 2.9), 150X (Figure 2.10), and 600X (Figure 2.11) magnifications of four different FD runs. FD followed by milling and sieving produced polydisperse, irregularly shaped particles. These particles tended to aggregate after milling. Milling methods generally result in non-spherical solid particles with a wider size distribution than spray-drying (Hickey and Ganderton 2001). The stability of the points of contact between the particles, which depends on the shape of the particles, will influence the blending and dispersion (Podczeck, Newton et al. 1997). Elongated particles, such as trehalose, have larger areas of contact and will flow poorly. In addition, surface irregularities may increase the amount of mechanical interlocking between particles making dispersion more difficult. Frictional heating during the milling must also be controlled as it can potentially cause a reduction in the activity of the thermolabile materials such as macromolecules or structural components of micro-organisms present in vaccines. A slow milling speed was used to minimize the potential for milling to reduce vaccine potency (Garmise, Mar et al. 2006).

SEMs of trehalose powder after SFD are shown at 60X (Figure 2.12) and 150X (Figure 2.13) magnifications for four different SFD runs. Particles are spherical and fairly homogeneous in size and shape for powders produced by the slower solution feed rate. However, the faster solution feed rate produced particles of heterogeneous size and shape. Some of the particles were spherical while others were fibrous. As the shape of the particles becomes more irregular, the ability of a powder to flow decreases due to increased particle-

particle interactions correlated with large planar surfaces and increased specific surface areas (Ridgway and Rupp 1969).

2.3.3 Particle Size and Size Distribution of Powders

Mucoadhesive Compounds

Particle sizes of bulk and sieved 45-125 μm sieved fractions of HPMC, CMC, chitosan, and SA are shown (Figure 2.14). A sieving step was utilized to remove very large (>125 μm) and fine particles (<45 μm) to prevent potential deposition in the lower respiratory and enable blending with the manufactured trehalose particles. The bulk HPMC powders were composed of predominantly large particles and bulk CMC and SA powders contained significant fine particles content that was removed by sieving (Table 2.3).

Freeze-Drying

A designed experiment was utilized to evaluate the effect of three selected factors: freezing rate; concentration; and annealing on the production of particles of suitable size for nasal delivery. The four responses measured, by laser diffraction, were median diameter (D_{50}), 90% diameter (D_{90}), 10% diameter (D_{10}), and span ((D_{90}-D_{10})/D_{50}). The matrix of the three factors evaluated, each at two levels with three replicates, is shown (Table 2.1). Values of D_{50} ranged from 10.70 to 28.65 μm, D_{90} ranged from 22.97 to 89.94 μm, D_{10} ranged from 0.97 to 6.95 μm, and span ranged from 1.77 to 3.94 of milled, sieved powders. Particle sizes of powders grouped by manufacturing parameters are shown (Table 2.4).

a) Median Diameter

The half normal % probability as a function of effect for the D_{50} of particles produced by FD followed by milling and sieving is shown (Figure 2.15). The effects of primary variables of freezing rate (A), concentration (B), annealing (C), freezing rate-concentration

interaction (AB), and confounded variables of freezing rate-annealing interaction (AC), concentration-annealing interaction (BC), and freezing rate-concentration-annealing interaction (ABC) had a significant effect on D_{50}, as indicated by points deviating from the straight line.

ANOVA confirmed the conclusions drawn from the half normal plots. All of the above factors had a statistically significant effect ($P<0.05$) on D_{50}, with p-values listed below (ANOVA tables in Appendix A).

Factor	A	B	C	AB	AC	BC	ABC
p-value	<0.0001	0.0482	<0.0001	<0.0001	<0.0001	<0.0001	<0.0001

The residuals plotted versus predicted values for the model describing the effect of various factors on median diameter (D_{50}) of powders manufactured by FD followed by milling and sieving were randomly distributed (Figure 2.16). The model exhibited a good fit with an R^2 of 0.99.

Interaction graphs indicating the effects of a) solute concentration (B-=1%, B+=10%) and freezing rate (A-=Slow, A+=Fast), and b) annealing (C-=No, C+=Yes) and freezing rate (A-=Slow, A+=Fast) on median diameter (D_{50}) of particles produced by FD followed by milling and sieving are shown (Figure 2.17). The effect of solute concentration was dependent on freezing rate. At slower freezing rates, a lower concentration of solute produced larger median diameters, while at faster freezing rates, a higher concentration of solute produced larger median diameters (Figure 2.17a). In the absence of annealing, larger median diameters were produced compared to annealed samples, regardless of the freezing rate. However, larger particles were produced with a lower freezing rate (Figure 2.17b). Interaction graphs indicating the effects of annealing and solute concentration on D_{50} of

particles produced by FD followed by milling and sieving show that without annealing particles with larger median diameters were produced compared to annealed samples, regardless of the concentration. However, larger particles were produced with a lower concentration (Figure 2.18).

A cuboidal plot indicating the effects of freezing rate, solute concentration, and annealing on D_{50} of particles produced by FD followed by milling and sieving is shown (Figure 2.19). This plot indicates that to maximize the median diameter within the conditions of the experiment, a 1% trehalose solution should be frozen at a slow freezing rate with no annealing.

b) 90% Diameter

The half normal % probability as a function of effect for the D_{90} of particles produced by FD followed by milling and sieving is shown (Figure 2.20). The effects of freezing rate, concentration, annealing, and concentration-annealing interaction had a significant effect on D_{90}.

ANOVA confirmed the conclusions drawn from the half normal plots. All of the above factors had a statistically significant effect ($P<0.05$) on D_{90}, except concentration with p-values listed below (ANOVA tables in Appendix A). Concentration was treated as a significant effect because it was a factor in an interaction.

Factor	A	B	C	BC
p-value	<0.0001	0.9486	<0.0001	<0.0001

The residuals plotted versus predicted values for the model describing the effect of various factors on D_{90} of powders manufactured by FD followed by milling and sieving were randomly distributed (Figure 2.21). The model exhibited a reasonable fit with an R^2 of 0.90.

The interaction graph exhibiting the effects of annealing and solute concentration on D_{90} of particles produced by FD followed by milling and sieving show that annealing produced smaller D_{90} compared to samples that are not annealed, regardless of the concentration, but smaller D_{90} were produced with a lower concentration (Figure 2.22).

A cuboidal plot indicating the effects of freezing rate, solute concentration, and annealing on D_{90} of particles produced by FD followed by milling and sieving is shown (Figure 2.23). To minimize the 90% diameter within the conditions of the experiment, a 1% trehalose solution should be frozen at a slow freezing rate with annealing.

c) 10% Diameter

The half normal % probability as a function of effect for the D_{10} of particles produced by FD followed by milling and sieving is shown (Figure 2.24). The effects of freezing rate, concentration, annealing, freezing rate-concentration interaction(AB), freezing rate-annealing interaction (AC), concentration-annealing interaction (BC), and freezing rate-concentration-annealing interaction (ABC) had a significant effect on D_{10}.

ANOVA confirmed the conclusions drawn from the half normal plots. All of the above factors had a statistically significant effect ($P<0.05$) on D_{50}, with p-values listed below (ANOVA tables in Appendix A).

Factor	A	B	C	AB	AC	BC	ABC
p-value	0.0213	0.0435	<0.0001	<0.0001	<0.0001	0.0026	<0.0001

The residuals plotted versus predicted values for the model describing the effect of various factors on D_{10} of powders manufactured by FD followed by milling and sieving were randomly distributed (Figure 2.25). The model exhibited a good fit with an R^2 of 0.96.

Interaction graphs indicating the effects of a) solute concentration and freezing rate and b) annealing and freezing rate on D_{10} of particles produced by FD followed by milling and sieving are shown (Figure 2.26). The effects of solute concentration was dependent on freezing rate. At slower freezing rates, a lower concentration of solute produced a larger D_{10}, while at faster freezing rates, a higher concentration of solute produced a larger D_{10} (Figure 2.26a). Annealing produced larger D_{10} compared to unannealed samples, regardless of the freezing rate. However, larger particles were produced with a lower freezing rate (Figure 2.26b). Interaction graphs indicating the effects of annealing and solute concentration on D_{10} of particles produced by FD followed by milling and sieving show that no annealing produced larger median diameters compared to annealed samples, regardless of the concentration (Figure 2.27).

A cuboidal plot indicating the effects of freezing rate, solute concentration, and annealing on D_{10} of particles produced by FD followed by milling and sieving is shown (Figure 2.28). To maximize the 10% diameter within the conditions of the experiment, a 1% trehalose solution should be frozen at a slow freezing rate without annealing.

d) Span

The half normal % probability as a function of effect for the span of particles produced by FD followed by milling and sieving is shown (Figure 2.29). The effects of freezing rate (A), concentration (B), annealing (C), freezing rate-concentration interaction (AB), freezing rate-annealing interaction (AC), concentration-annealing interaction (BC), and freezing rate-concentration-annealing interaction (ABC) had a significant effect on span.

ANOVA confirmed the conclusions drawn from the half normal plots. All of the above factors, except concentration, annealing, and concentration-annealing interaction had a

statistically significant effect ($P<0.05$) on span, with p-values listed below (ANOVA tables in Appendix A). Because concentration, annealing, and concentration-annealing interaction were involved in other interations, they were treated as significant effects.

Factor	A	B	C	AB	AC	BC	ABC
p-value	<0.0001	0.4560	0.2080	<0.0001	0.0055	0.3831	<0.0001

The residuals plotted versus predicted values for the model describing the effect of various factors on span of powders manufactured by FD followed by milling and sieving were randomly distributed (Figure 2.30). The model exhibited a reasonable fit with an R^2 of 0.92.

Interaction graphs indicating the effects of a) solute concentration and freezing rate and b) annealing and freezing rate on span of particles produced by FD followed by milling and sieving are shown (Figure 2.31). The effect of solute concentration is dependent on freezing rate. While a higher concentration of solute doesn't change the span at different freezing rates, a lower concentration of solute produces a smaller span at slower freezing rates (Figure 2.31a). The effect of annealing is dependent on freezing rate. No annealing produced smaller spans compared to annealed samples at the lower freezing rate. However, smaller spans were produced with annealing at a faster freezing rate (Figure 2.31b). An interaction graph indicating the effects of annealing and solute concentration on the span of particles produced by FD followed by milling and sieving show that annealing and concentration do not affect each other (Figure 2.32).

A cuboidal plot indicating the effects of freezing rate, solute concentration, and annealing on D_{50} of particles produced by FD followed by milling and sieving is shown

(Figure 2.33). To maximize the span within the conditions of the experiment, a 1% trehalose solution should be frozen at a slow freezing rate with annealing.

Optimization

The SEM images of the freeze-dried and milled particles indicate that they are not spherical. While some are have multiple planes of symmetry (may be considered regular polygonal) many are elongated and exhibit surface asperities.

The target median diameter of a human formulation was 40 μm. However, based on the factors examined in these experiments and the milling method previously optimized, the D_{50} ranged from 10.70 to 28.65 μm, which is well below the targeted particle size. Also, the D_{10} ranged from 0.97 to 6.95 μm, which is well below 10 μm, indicating that a significant percentage of the powder could potentially deposit in the lower respiratory tract. Additionally, the heterogeneous shape of the milled particles is unsuitable for blending with MA.

The factors that must be taken into account for the FD process are shown (Figure 2.34). The correlation coefficients of the $D_{50,}$ $D_{90,}$ $D_{10,}$ and span were all above 0.90, indicating at least a reasonable fit, with the D_{50} and D_{10} exhibiting a very good fit. This is indicative that all factors were taken into account in the production of these particles. Because the process space is limited by the categorical variables (freezing rate and annealing) and the continuous variable has been maximized to prevent protein degradation, it would not be practical to produce nasal particles, with the defined specification above, for delivery to humans by this method.

From the known deposition characteristics for particles in the rat nasal cavity the particles were required to be larger than 5 μm. It is important that little or none of the powder

is smaller than 5 μm, since lung deposition might be possible. It is known that particles smaller than 10 μm tend to aggregate which results in poor flow and non-uniform dispersion (Hickey 2003). Consequently, to take advantage of the opportunity to deposit smaller particles in the nose of rats than would be suitable for humans the target range is 10 – 40 μm. Therefore, the target median diameter of a powder for delivery to rats was 25 μm. Based on the factors examined in these experiments, the optimized run conditions to produce the target particles was 10% trehalose solution, frozen at the slow freezing rate, without annealing, lyophilized, milled at 200 rpms for 30 minutes, and sieved in tap mode for 2 hours.

Spray-Freeze-Drying

A designed experiment was utilized to evaluate the effect of three selected factors defined as, solution flow rate, atomization airflow rate, and solute concentration on the production of particles of suitable size for nasal delivery. The four responses measured were D_{50}, D_{90}, D_{10}, and span. These sizes were determined by laser diffraction. The matrix of the three factors evaluated, each at two levels with three replicates, is shown in Table 2.2. Values of D_{50} ranged from 15.76 to 50.92 μm, D_{90} ranged from 24.42 to 181.67 μm, D_{10} ranged from 4.13 to 13.63 μm, and span ranged from 1.28 to 3.39 of milled, sieved powders. Particle sizes of powders grouped by run parameters are shown (Table 2.5). The D_{50}, D_{90}, and D_{10} are directly proportional to the solution feed rate. This is consistent with the literature (Masters 1976). An increase in the flow rate of the liquid through the nozzle will increase the droplet size produced. An increase in spraying pressure will reduce droplet size. An increase in the spray angle will reduce droplet size. Greater energy is required to break up high viscosity and surface tension liquids, resulting in the formation of a larger droplet size.

a) Median Diameter

The half normal % probability as a function of effect for the D_{50} of particles produced by SFD is shown (Figure 2.35). The effects of solution feed rate (A) and airflow (B) had a significant effect on D_{50} as indicated by points deviating from the straight line.

ANOVA confirmed the conclusions drawn from the half normal plots. All of the above factors had a statistically significant effect ($P<0.05$) on D_{50}, with p-values listed below (ANOVA tables in Appendix A).

Factor	A	B
p-value	<0.0001	0.0100

The residuals plotted versus predicted values for the model describing the effect of various factors on D_{50} of powders manufactured by SFD were randomly distributed (Figure 2.36). The model exhibited a fit of R^2 of 0.85.

A cuboidal plot indicating the effects of solution feed rate (A-=3 mL/min, A+=25 mL/min), airflow rate (B-=250 L/hr, B+=500 L/hr), and solute concentration (C-=1%, C+=10%) on D_{50} of particles produced by SFD is shown (Figure 2.37). To maximize the median diameter within the conditions of the experiment, a solution should be pumped at a high solution feed rate and atomized with a low airflow.

b) 90% Diameter

The half normal % probability as a function of effect for the D_{90} of particles produced by SFD is shown (Figure 2.38). The effects of solution feed rate (A) and airflow (B) had a significant effect on D_{90}.

ANOVA confirmed the conclusions drawn from the half normal plots. All of the above factors had a statistically significant effect ($P<0.05$) on D_{90}, with p-values listed below (ANOVA tables in Appendix A).

Factor	A	B
p-value	<0.0001	0.0036

The residuals plotted versus predicted values for the model describing the effect of various factors on D_{90} of powders manufactured by SFD were randomly distributed (Figure 2.39). The model exhibited a fit of $R^2=0.78$.

A cuboidal plot indicating the effects of solution feed rate, airflow rate, and solute concentration on D_{90} of particles produced by SFD is shown (Figure 2.40). To minimize D_{90} within the conditions of this experiment, use a 10% solution of trehalose at 3 mL/min with an airflow rate of 500 L/hr.

c) 10% Diameter

The half normal % probability as a function of effect for the D_{10} of particles produced by SFD is shown (Figure 2.41). The effects of solution feed rate (A), airflow (B), solute concentration (C), and the solution feed rate-airflow interaction (AB) had a significant effect on D_{10}.

ANOVA confirmed the conclusions drawn from the half normal plots. All of the above factors had a statistically significant effect ($P<0.05$) on D_{10}, with p-values listed below (ANOVA tables in Appendix A).

Factor	A	B	C	AB
p-value	<0.0001	0.4560	0.2080	<0.0001

The residuals plotted versus predicted values for the model describing the effect of various factors on D_{10} of powders manufactured by SFD were randomly distributed (Figure 2.42). The model exhibited a fit of R^2 of 0.81.

An interaction graph indicating the effect of solute concentration and freezing rate on D_{10} of particles produced by SFD is shown (Figure 2.43). Both the lower and higher solute concentrations produce larger D_{10} at the faster solution feed rate than the slower solution feed rate, but the D_{10} of the higher solute concentration is larger.

A cuboidal plot indicating the effects of solution feed rate, airflow rate, and solute concentration on D_{10} of particles produced by SFD is shown (Figure 2.44). To maximize D_{10} within the conditions of this experiment, use a 10% solution of trehalose at 25 mL/min with an airflow rate of 500 L/hr.

d) Span

The half normal % probability as a function of effect for the span of particles produced by SFD is shown (Figure 2.45). The effects of solution feed rate (A), airflow (B), solute concentration (C), and the solution feed rate-airflow interaction (AB) had a significant effect on span.

ANOVA confirmed the conclusions drawn from the half normal plots. All of the above factors had a statistically significant effect ($P<0.05$) on span, with p-values listed below (ANOVA tables in Appendix A).

Factor	A	B	C	AB
p-value	<0.0001	<0.0001	0.0002	0.0078

The residuals plotted versus predicted values for the model describing the effect of various factors on span of powders manufactured by SFD were randomly distributed (Figure 2.46). The model exhibited a fit of R^2 of 0.84.

An interaction graph indicating the effects of solute concentration and freezing rate on the span of particles produced by SFD is shown (Figure 2.47). Both the lower and higher solute concentrations produce a smaller span at the slower solution feed rate than the faster solution feed rate, but there is no difference at the lower flow rate between the two solute concentrations.

A cuboidal plot indication the effects of solution feed rate, airflow rate, and solute concentration on the span of particles produced by SFD is shown (Figure 2.48). To minimize span within the conditions of this experiment, use a 10% solution of trehalose at 3 mL/min with an airflow rate of 500 L/hr.

Optimization

The target D_{50}, of 40 μm particles for human application, falls within the limits determined by these experiments, the factors needed to produce the target powder can be determined statistically. Based on the factors examined in these experiments, the optimized run conditions to produce the target particles is a 4.96% trehalose solution, pumped at 20.60 mL/min, with an atomization airflow rate of 296.29 L/hr, and lyophilized (Figure 2.49). Because the solute concentration did not have a significant effect on D_{50}, 10% solute concentration was used to maximize the cryoprotective properties of trehalose. Also, because of the lack of sensitivity of the equipment, a 20 mL/min solution feed rate and an atomization airflow rate of 300 L/hr were used. The predicted responses of these conditions and the actual data from three separate runs performed under these conditions are shown (Table 2.6a).

There is good agreement between the predicted and actual parameters. SEMs of the 40 μm SFD for human use formulation at 60X, 150X, and 600X magnification are shown (Figure 2.50). Spherical, porous particles were produced. The 40 μm SFD trehalose particles had regions of porosity and surface coating. The surface coating is a result of solvent evaporation during the atomization process and removal of solvent during the lyophilization process. Small particles can be seen on the surfaces of the larger particles that could potentially enter the lower respiratory tract, if inhaled. A particle size distribution, plotted as the relative frequency as a function of particle size is shown (Figure 2.51). A mode is present at ~40 μm. This plot also indicates the presence of particles <10 μm. Particles with a low density, such as porous particles, are more easily fluidized than solid particles of the same diameter (Dunbar, Hickey et al. 1998). Therefore, porous particles with geometric diameters suitable for nasal delivery may, with suitably low density, enter the lungs. A sieving step may be necessary to remove these particles for clinical purposes.

SEMs of SFD particles show that spherical, porous particles were produced (Figure 2.52). Similar to the 40 μm SFD trehalose particles, the 25 μm SFD trehalose particles exhibited areas of surface coating. The optimized run conditions to produce the target particle size, of 25 μm for delivery to rats, was a 6.05% trehalose solution, pumped at 8.33 mL/min, with an atomization airflow rate of 485.58 L/hr, and lyophilized (Figure 2.53). Ten percent solute concentration was used to maximize the cryoprotective properties of trehalose because the solute concentration did not have a significant effect on D_{50}. Also, because of the lack of sensitivity of the equipment, a 10 mL/min solution feed rate and an atomization airflow rate of 500 L/hr were used. The predicted responses of these conditions and the actual data from three separate batches performed under these conditions are shown (Table 2.6b). There is

good agreement between the predicted and actual parameters. A particle size distribution, plotted as the relative frequency as a function of particle size is shown (Figure 2.54). Modes are present at about 4, 10, 20, and 40 μm.

Powders containing WIIV were produced under the conditions for the 25 μm SFD powders for use in rats. Particle size analysis, performed by laser diffraction, was performed to determine if the addition of the WIIV had an effect on the size of the particles. The particle size of the 25 μm SFD powder was 24.92 μm, with a standard deviation of 3.24 μm. This was not significantly different than the particles produced under the same conditions with trehalose alone.

One area of concern is the values and range of the coefficient of variations (R^2, ~0.78 – 0.85) for the SFD designed experiments. These modest fits suggest that not all variables were taken into account when describing the process space of the system (Figure 2.55). Some variables were not addressed in these experiments as they were presumed to be constant. They include: tubing used in the peristaltic pump, pump rate, nozzle diameter, height of nozzle above liquid nitrogen, freeze-drying and ambient conditions. While the nozzle diameter was not altered (and might be assumed constant under ambient conditions), there were limitations on accuracy and precision associated with holding other variables constant. For example, since the tubing diameter of the peristaltic pump is fixed, variable flow rate is achieved by increasing the linear velocity of the fluid which requires variable rotation speed of the pump. It is not clear that the efficiency of the pump is consistent at all flow rates due to potential responses of changes in tubing properties and pump characteristics under different conditions. The nozzle height was determined based on its proximity to the liquid nitrogen avoiding freezing solution and blocking the nozzle. At heights higher than the one utilized,

the loss of material was substantial. Clearly, this qualitative estimate of height to the surface is subject to variability. The FD conditions are controlled but will be susceptible to some variability based on actual control and accuracy and precision of temperature gauges (manufacturer's specification unavailable). Ambient conditions were monitored (T= 23 ± 2°C, 40 ± 5%RH) but not controlled.

2.4 Summary

Designed experiments examining three factors (freezing rate, solute concentration, and annealing for freeze-drying and solution feed rate, atomization airflow rate, and solute concentration for spray-freeze-drying) in a full 2^3 factorial design were used to produce particles suitable for nasal delivery. The four responses measured, by laser diffraction, were median diameter (D_{50}), 90% diameter (D_{90}), 10% diameter (D_{10}), and span. The goal of these experiments was the production of particles for potential human use (target D_{50}=40 μm, all particles greater than 10 μm) and particles to be used in rat studies (target D_{50}=25 μm).

Freeze-drying followed by milling and sieving produced particles below the targeted particle size for human delivery. Also, a significant percentage of the powder was in a size range that could potentially deposit in the lower respiratory tract. The heterogeneous shape of the milled particles was not ideal for blending. Subsequent blending with MA particles was intended. Particles prepared for delivery to rats, were produced with appropriate size characteristics under conditions of 10% trehalose solution, freezing at the slow freezing rate, without annealing, lyophilized, milled at 200 rpms for 30 minutes, and sieved in tap mode for two hours. However, the irregular shape and likelihood of poor blending properties resulted in this method being discarded in favor of the SFD method.

An optimized SFD run of 10% trehalose, a 20 mL/min solution feed rate and an atomization airflow rate of 300 L/hr was used to produce particles for human delivery with a D_{50}=38.5 μm. Also, an optimized spray-freeze-drying run of 10% trehalose, a 10 mL/min solution feed rate and an atomization airflow rate of 500 L/hr was used to produce particles for rat delivery with a D_{50}=26.9 μm. These powders were further characterized with respect to: (specific aim 1) *in vitro*, physico-chemical and dispersion properties (Chapter 3); (specific aim 1) the physico-chemical properties of MA and their influence on residence time in the nasal cavity of the rat (Chapter 4) and; (specific aim 2) immunogenicity of a dry powder whole inactivated influenza virus (WIIV) vaccine following nasal delivery to rats (Chapter 5).

Table 2.1– Median diameter (D_{50}), 90% diameter (D_{90}), 10% diameter (D_{10}), and span values obtained by laser diffraction for each freeze-drying (FD) run evaluating the effects of three factors: freeze rate, solute concentration, and annealing.

Std Order	Run Order	Freeze Rate	Solute Concen. (g/100mL)	Annealing	D_{50} (μm)	D_{90} (μm)	D_{10} (μm)	Span
10	1	Fast	10.00	No	19.84	59.73	5.78	2.72
23	2	Fast	10.00	Yes	22.95	59.15	6.49	2.29
6	3	Fast	1.00	No	23.35	87.42	5.67	3.50
9	4	Slow	10.00	No	19.92	47.00	6.00	2.06
1	5	Slow	1.00	No	27.78	66.74	6.66	2.16
15	6	Slow	1.00	Yes	10.67	22.97	3.97	1.78
20	7	Slow	10.00	Yes	11.01	38.68	0.97	3.24
18	8	Fast	1.00	Yes	10.74	45.12	2.76	3.94
24	9	Fast	10.00	Yes	23.46	56.24	6.38	2.39
4	10	Fast	1.00	No	22.29	75.13	5.54	3.27
8	11	Slow	10.00	No	19.69	44.89	5.86	1.98
19	12	Slow	10.00	Yes	11.06	40.36	2.94	3.28
16	13	Fast	1.00	Yes	12.06	48.91	2.81	3.82
11	14	Fast	10.00	No	20.49	63.23	5.90	3.86
2	15	Slow	1.00	No	28.49	65.57	6.95	2.06
12	16	Fast	10.00	No	21.79	89.94	5.83	2.80
13	17	Slow	1.00	Yes	10.81	23.24	4.05	1.77
7	18	Slow	10.00	No	19.92	45.89	5.92	2.01
17	19	Fast	1.00	Yes	10.97	42.18	2.73	3.60
21	20	Slow	10.00	Yes	11.04	39.15	2.94	3.38
14	21	Slow	1.00	Yes	10.70	22.97	4.06	1.77
3	22	Slow	1.00	No	28.65	70.28	6.38	2.23
5	23	Fast	1.00	No	21.67	78.41	5.49	3.21
22	24	Fast	10.00	Yes	22.91	62.59	6.56	2.18

Table 2.2– Median diameter (D_{50}), 90% diameter (D_{90}), 10% diameter (D_{10}), and span ((D_{90} D_{10})/D_{50}) values obtained by laser diffraction for each spray-freeze-drying (SFD) run evaluating the effects of three factors: solution feed rate, airflow, and solute concentration.

Std Order	Run Order	Solution Feed Rate (mL/min)	Atomiz. Flow (L/hr)	Solute Concen (g/100 mL)	D_{50} (μm)	D_{90} (μm)	D_{10} (μm)	Span
7	1	3.00	500.00	1.00	15.82	33.55	4.13	1.85
10	2	25.00	500.00	1.00	39.72	90.08	10.8	2.00
2	3	3.00	250.00	1.00	21.60	46.37	4.96	1.92
22	4	25.00	500.00	10.00	38.63	85.29	13.63	1.85
3	5	3.00	250.00	1.00	20.72	43.44	4.99	1.86
4	6	25.00	250.00	1.00	44.97	115.37	8.34	2.38
1	7	3.00	250.00	1.00	20.63	44.01	4.85	1.90
12	8	25.00	500.00	1.00	39.43	90.84	10.71	2.03
14	9	3.00	250.00	10.00	20.80	37.91	5.21	1.57
16	10	25.00	250.00	10.00	42.79	102.73	9.51	2.18
9	11	3.00	500.00	1.00	16.95	34.46	4.47	1.78
23	12	25.00	500.00	10.00	38.62	80.65	13.47	1.74
17	13	25.00	250.00	10.00	42.22	98.50	9.05	2.12
5	14	25.00	250.00	1.00	50.92	181.67	9.10	3.39
13	15	3.00	250.00	10.00	37.78	72.04	9.83	1.65
6	16	25.00	250.00	1.00	50.44	158.58	9.23	2.96
15	17	3.00	250.00	10.00	26.39	48.94	9.08	1.51
11	18	25.00	500.00	1.00	40.19	89.36	10.81	1.95
20	19	3.00	500.00	10.00	22.12	39.99	8.95	1.40
19	20	3.00	500.00	10.00	15.76	24.42	4.26	1.28
18	21	25.00	250.00	10.00	43.54	115.55	9.74	2.43
21	22	3.00	500.00	10.00	29.26	53.10	10.05	1.47
8	23	3.00	500.00	1.00	22.46	40.25	5.71	1.55
24	24	25.00	500.00	10.00	39.22	82.46	13.52	1.76

Table 2.3– Particle sizes of bulk and sieved 45-125 µm sieved fractions of hydroxypropyl methylcellulose (HPMC), carboxymethylcellulose sodium (CMC), sodium alginate (SA), and chitosan (Mean (SD), n=3).

Powder		D_{50} (µm)	D_{90} (µm)	D_{10} (µm)	Span
HPMC LMW	Bulk	69.66 (1.53)	149.27 (1.93)	15.54 (0.23)	1.92 (0.06)
	Sieved	61.63 (0.73)	137.48 (6.43)	14.57 (0.24)	1.99 (0.08)
HPMC HMW	Bulk	78.82 (3.97)	184.60 (15.13)	17.57 (0.88)	2.12 (0.08)
	Sieved	63.82 (1.37)	146.09 (8.07)	15.13 (0.20)	2.05 (0.09)
CMC LMW	Bulk	39.01 (0.28)	63.28 (2.04)	8.59 (0.12)	1.40 (0.04)
	Sieved	60.87 (2.71)	152.31 (73.58)	20.72 (0.83)	2.13 (1.07)
CMC HMW	Bulk	23.31 (2.11)	36.75 (3.47)	5.29 (0.20)	1.35 (0.03)
	Sieved	63.94 (2.49)	185.34 (6.30)	19.96 (0.31)	2.59 (0.11)
SA	Bulk	32.90 (1.10)	50.01 (4.07)	5.61 (1.47)	1.29 (0.05)
	Sieved	124.25 (6.35)	214.76 (7.77)	53.69 (1.90)	1.30 (0.15)
Chitosan	Bulk	62.60 (1.37)	104.64 (0.69)	19.94 (0.29)	1.36 (0.02)
	Sieved	108.24 (2.03)	198.92 (15.24)	35.39 (0.31)	1.51 (0.14)

Table 2.4– Particle sizes of milled and sieved freeze-dried (FD) trehalose by laser diffraction (Mean (SD), n=3).

Freezing Rate	Annealing	Solute Concen. (g/100mL)	D_{50} (μm)	D_{90} (μm)	D_{10} (μm)	Span
Slow	No	10	19.84 (0.13)	45.93 (1.06)	5.93 (0.07)	2.02 (0.04)
Slow	Yes	1	10.73 (0.07)	23.06 (0.16)	4.03 (0.05)	1.77 (0.01)
Slow	No	1	28.31 (0.46)	67.53 (2.45)	6.66 (0.29)	2.15 (0.09)
Slow	Yes	10	11.04 (0.03)	39.40 (0.87)	2.28 (1.14)	3.30 (0.07)
Fast	No	1	22.44 (0.85)	80.32 (6.36)	5.57 (0.09)	3.33 (0.15)
Fast	Yes	10	23.11 (0.31)	59.33 (3.18)	6.48 (0.09)	2.29 (0.11)
Fast	No	10	20.71 (0.99)	70.97(16.52)	5.84 (0.06)	3.13 (0.64)
Fast	Yes	1	11.26 (0.71)	45.40 (3.37)	2.77 (0.04)	3.79 (0.17)

Table 2.5– Particle sizes of spray-freeze-dried (SFD) trehalose by laser diffraction (Mean (SD), n=3).

Flow Rate (mL/min)	Atomization Flow Rate (L/hr)	Solute Conc. (g/100 mL)	D_{50} (μm)	D_{90} (μm)	D_{10} (μm)	Span
3	250	1	21.41 (2.46)	44.56 (5.57)	5.44 (1.01)	1.83 (0.06)
3	250	10	28.32 (8.66)	52.96 (17.42)	8.04 (2.48)	1.58 (0.07)
3	500	1	18.41 (3.55)	36.09 (3.64)	4.77 (0.83)	1.72 (0.16)
3	500	10	22.38 (6.75)	39.17 (14.36)	7.75 (3.07)	1.38 (0.10)
25	250	1	48.78 (3.31)	151.87 (33.65)	8.89 (0.48)	2.91 (0.51)
25	250	10	42.85 (0.66)	105.59 (8.88)	9.43 (0.35)	2.24 (0.16)
25	500	1	39.78 (0.38)	90.09 (0.74)	10.77 (0.06)	1.99 (0.04)
25	500	10	38.82 (0.34)	82.80 (2.34)	13.54 (0.08)	1.78 (0.06)

Table 2.6– Comparison of predicted parameters and data (n=3) of a) human formulation (target D_{50}= 45 µm) and b) rat formulation (target D_{50}= 25 µm) using conditions determined by design of experiment software.

a) Predicted formulation for human use parameters

Factor	Name	Level
A	Sol.Feed Rate	20.00
B	Airflow	300.00
C	Sol. Conc	10.00

Parameter	Predicted Value	Actual Value (Mean)	Actual Value (Std. Dev)
D_{50}	39.62	38.5	2.3
D_{90}	100.97	93.7	11.5
D_{10}	10.18	10.7	0.8
Span	2.08	2.2	0.20

b) Predicted formulation for rat use parameters

Factor	Name	Level
A	Sol. Feed	10.00
B	Airflow	500.00
C	Sol. Conc.	10.00

Parameter	Predicted Value	Actual Value (Mean)	Actual Value (Std. Dev)
D_{50}	26.21	26.9	2.9
D_{90}	50.33	44.5	2.1
D_{10}	9.31	11.1	2.2
Span	1.47	1.3	0.16

Figure 2.1– The process flow for the manufacture of freeze-dried (FD) and spray-freeze-dried (SFD) powders.

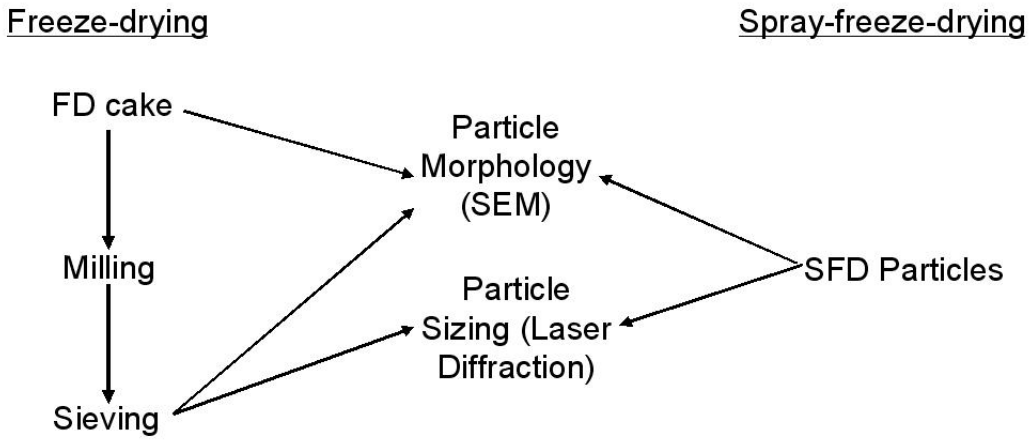

Figure 2.2– The structures of A) hydroxypropyl methylcellulose (HPMC), B) carboxymethylcellulose sodium (CMC), C) chitosan (Chit), and D) sodium alginate (SA).

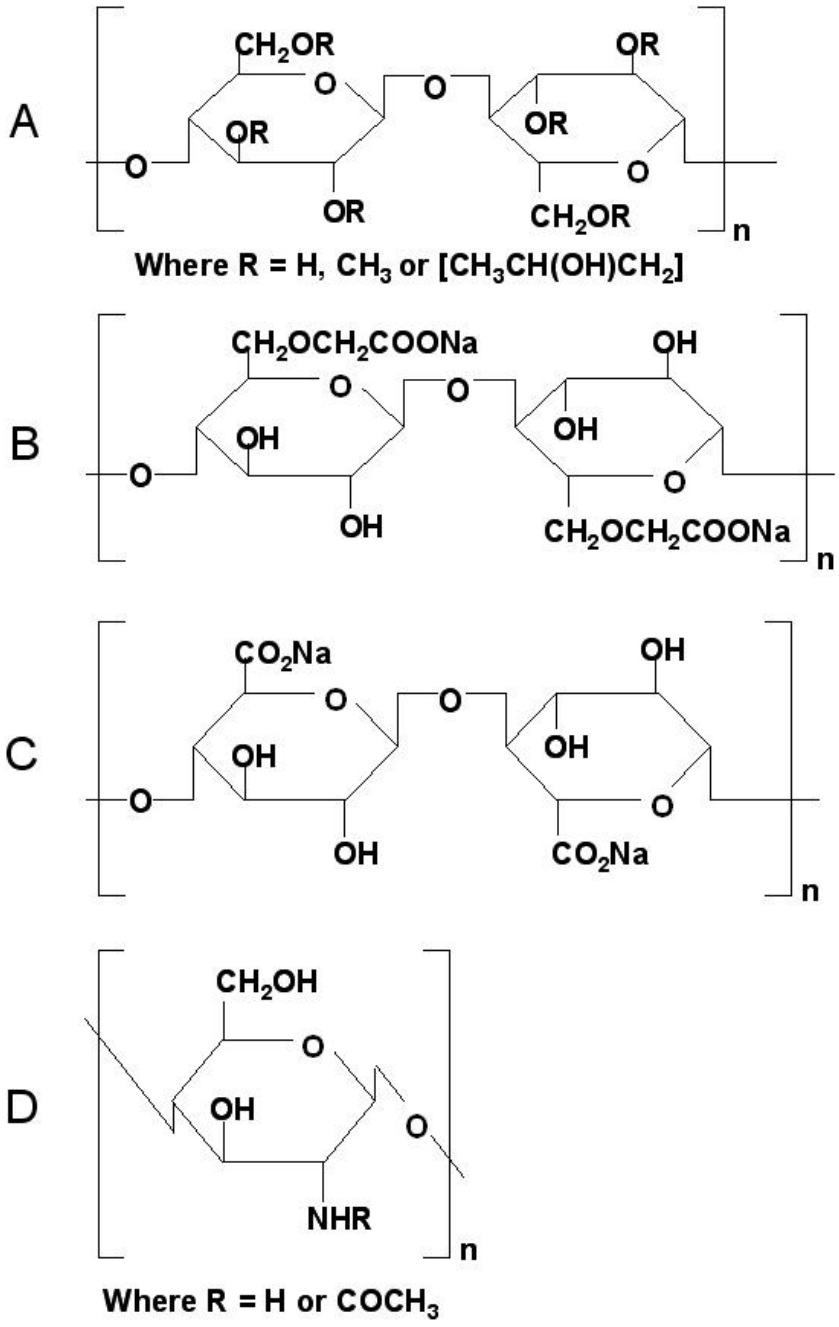

Figure 2.3– Scanning electron micrographs of bulk trehalose at A) 60X magnification, B) 150X magnification, C) 600X magnification, and D) 1500X magnification.

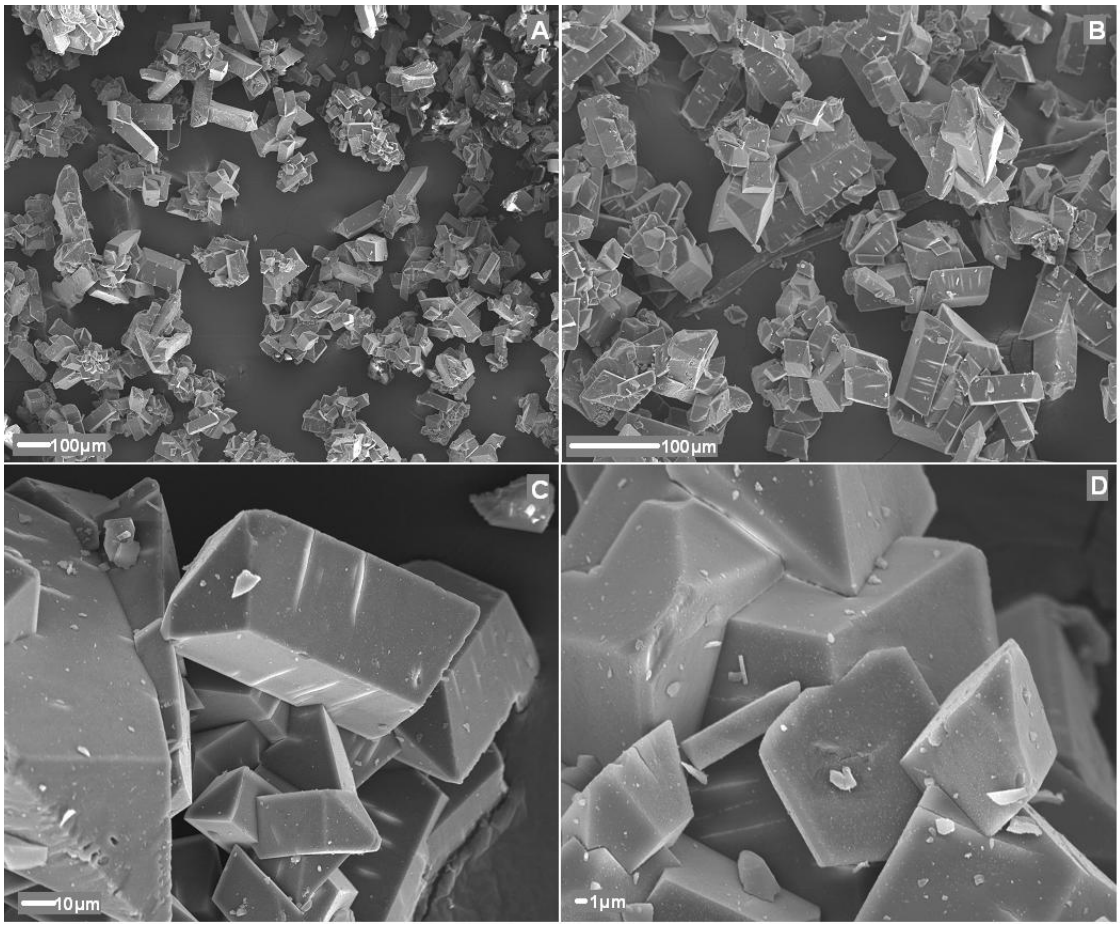

Figure 2.4– Scanning electron micrographs of 45-75 μm sieved trehalose at A) 60X magnification, B) 150X magnification, C) 600X magnification, and D) 1500X magnification.

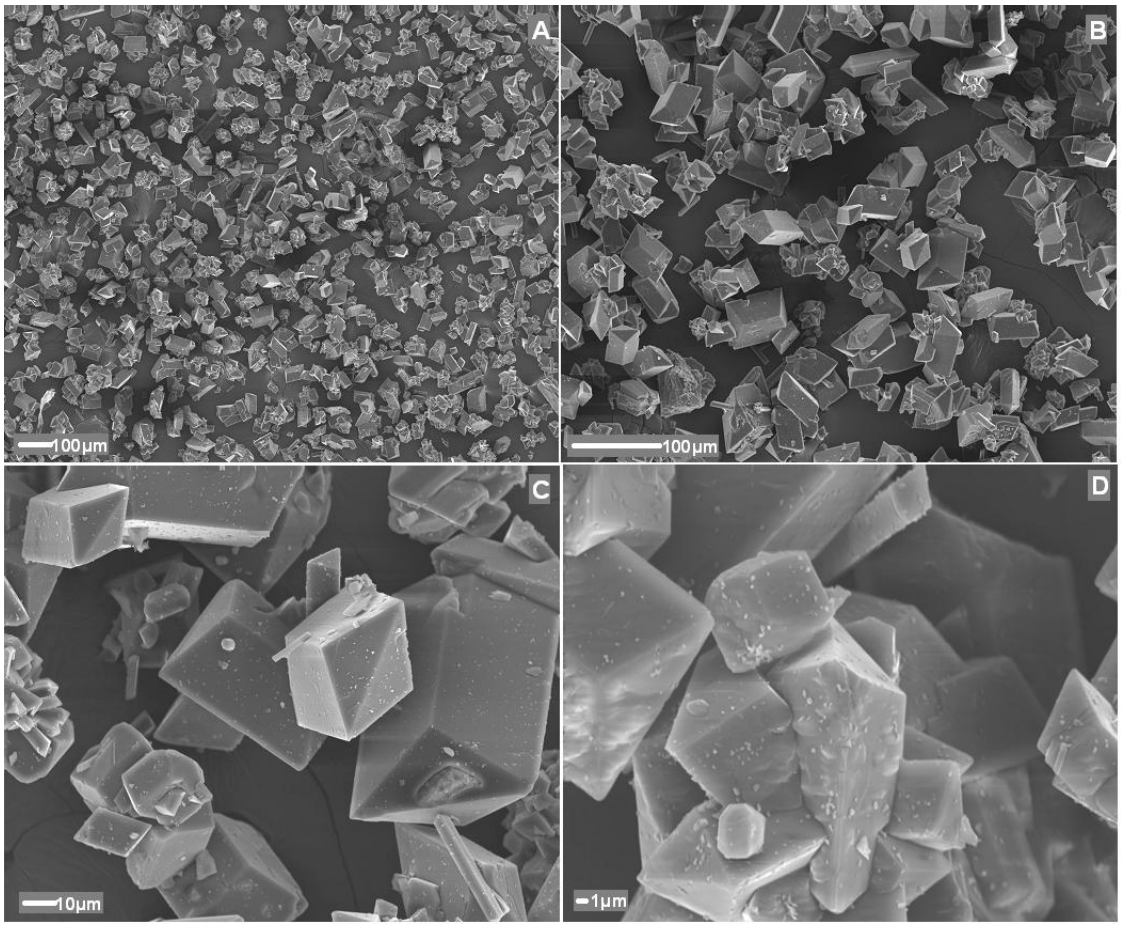

Figure 2.5– Scanning electron micrographs (60X magnification) of 45-75 µm sieved fractions of A) HPMC LMW, B) HPMC HMW, C) CMC LMW, D) CMC HMW, and E) Chit and 45-125 µm sieved fraction of F) SA.

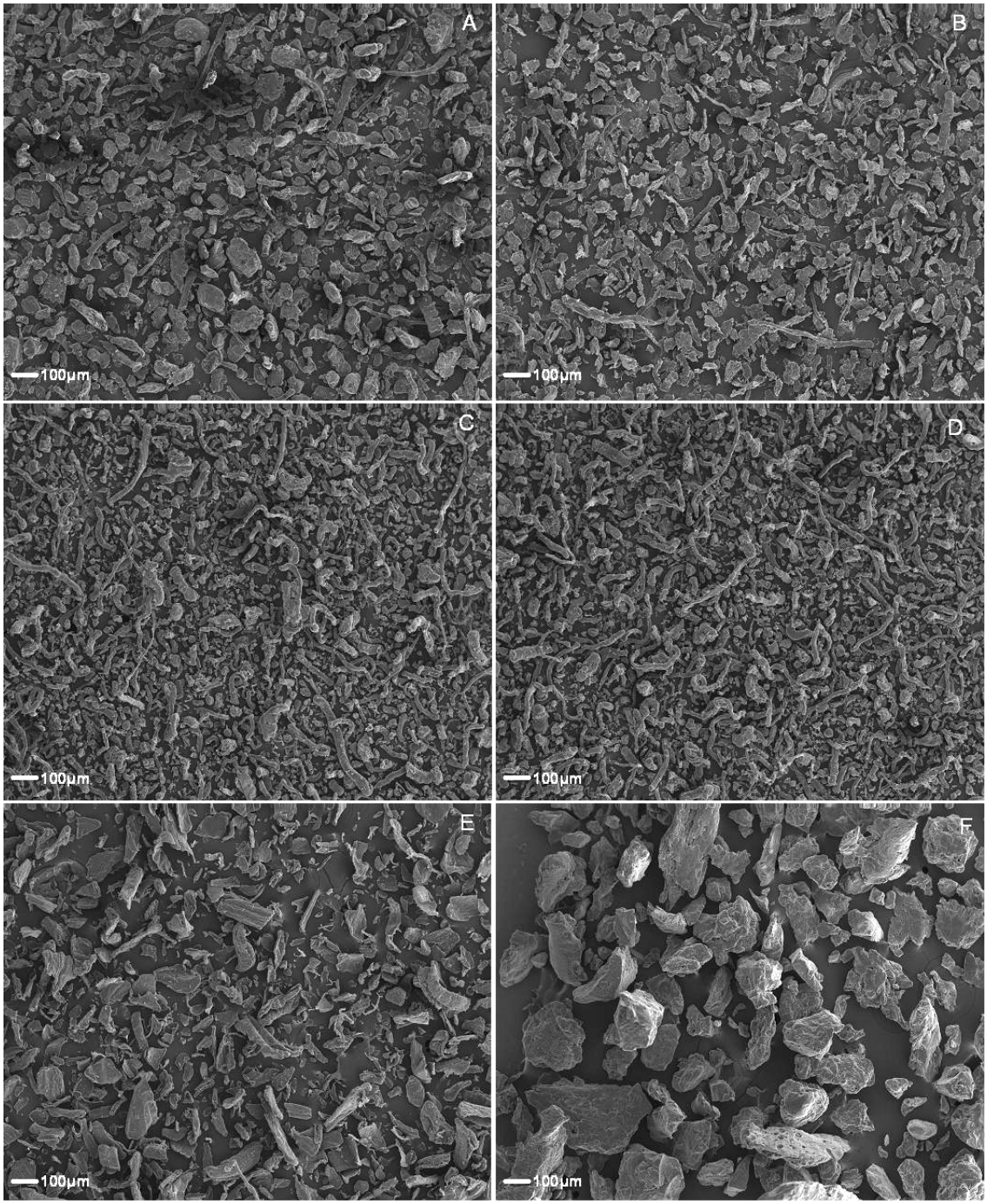

Figure 2.6– Scanning electron micrographs (150X magnification) of 45-75 µm sieved fractions of A) HPMC LMW, B) HPMC HMW, C) CMC LMW, D) CMC HMW, and E) Chit and 45-125 µm sieved fraction of F) SA.

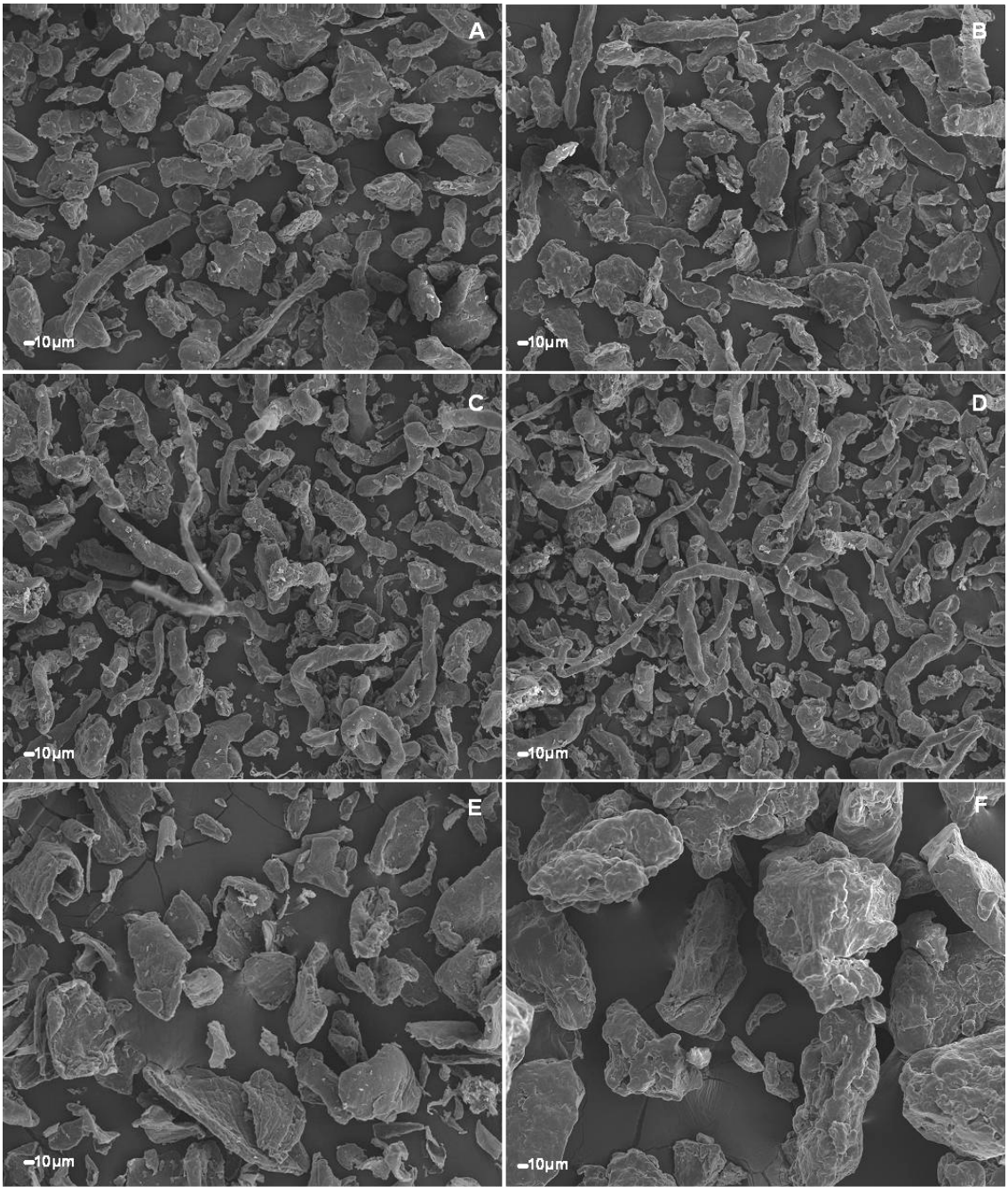

Figure 2.7– Scanning electron micrographs (40X magnification) of lyophilized cakes of 10% trehalose in deionized water by A) slow freeze, no annealing, B) fast freeze, annealing, C) fast freeze, no annealing, and D) slow freeze, annealing.

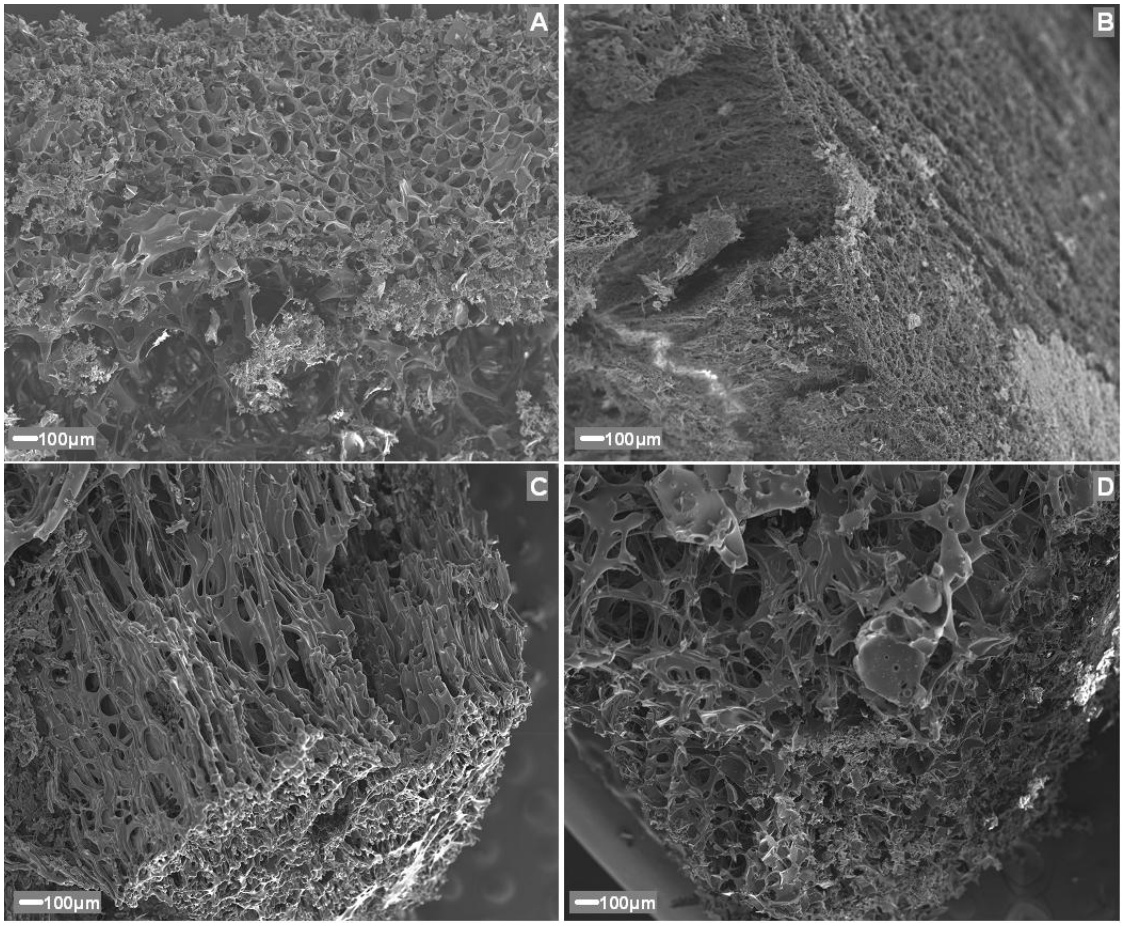

Figure 2.8– Scanning electron micrographs (100X magnification) of lyophilized cakes of 10% trehalose in deionized water by A) slow freeze, no annealing, B) fast freeze, annealing, C) fast freeze, no annealing, and D) slow freeze, annealing.

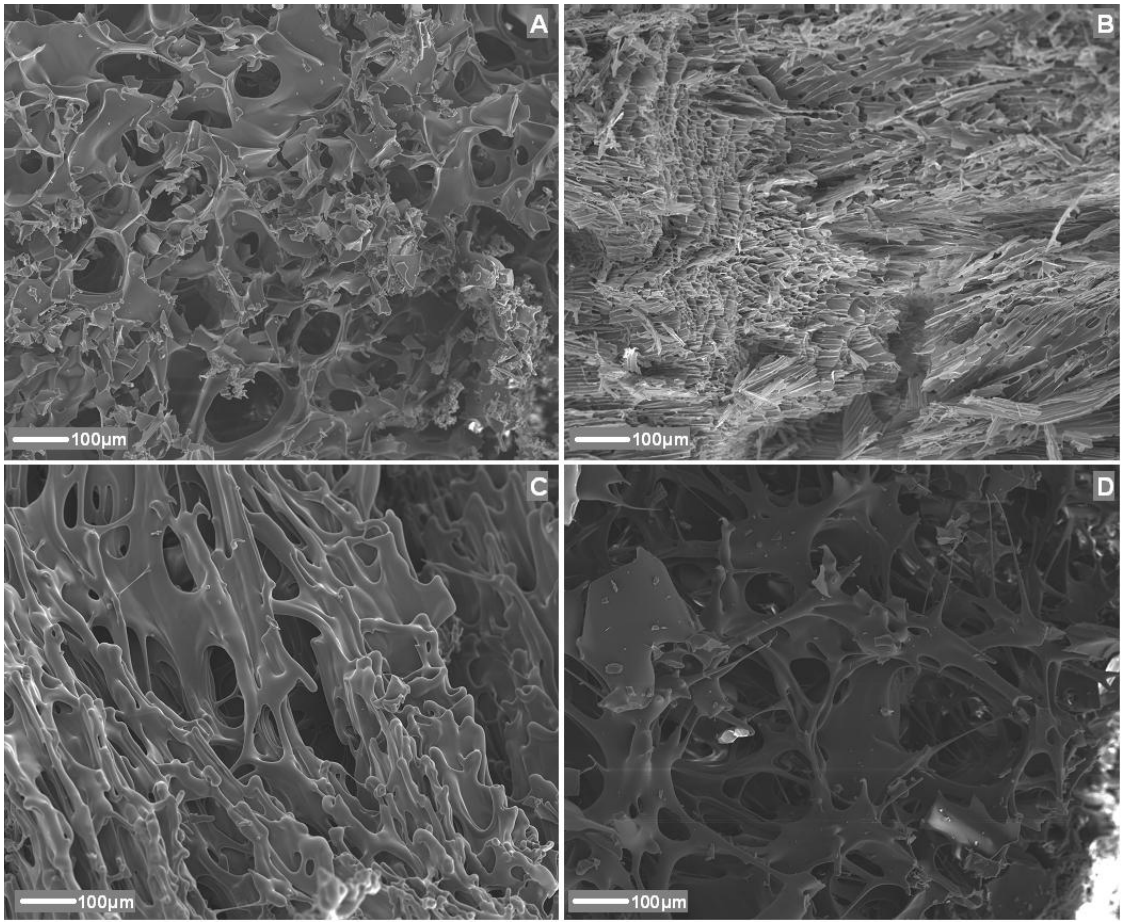

Figure 2.9– Scanning electron micrographs (60X magnification) of milled lyophilized cakes of A) 10% trehalose, slow freeze, no annealing, B) 1% trehalose, fast freeze, no annealing, C) 1% trehalose, slow freeze, annealing, and D) 10% trehalose, fast freeze, annealing.

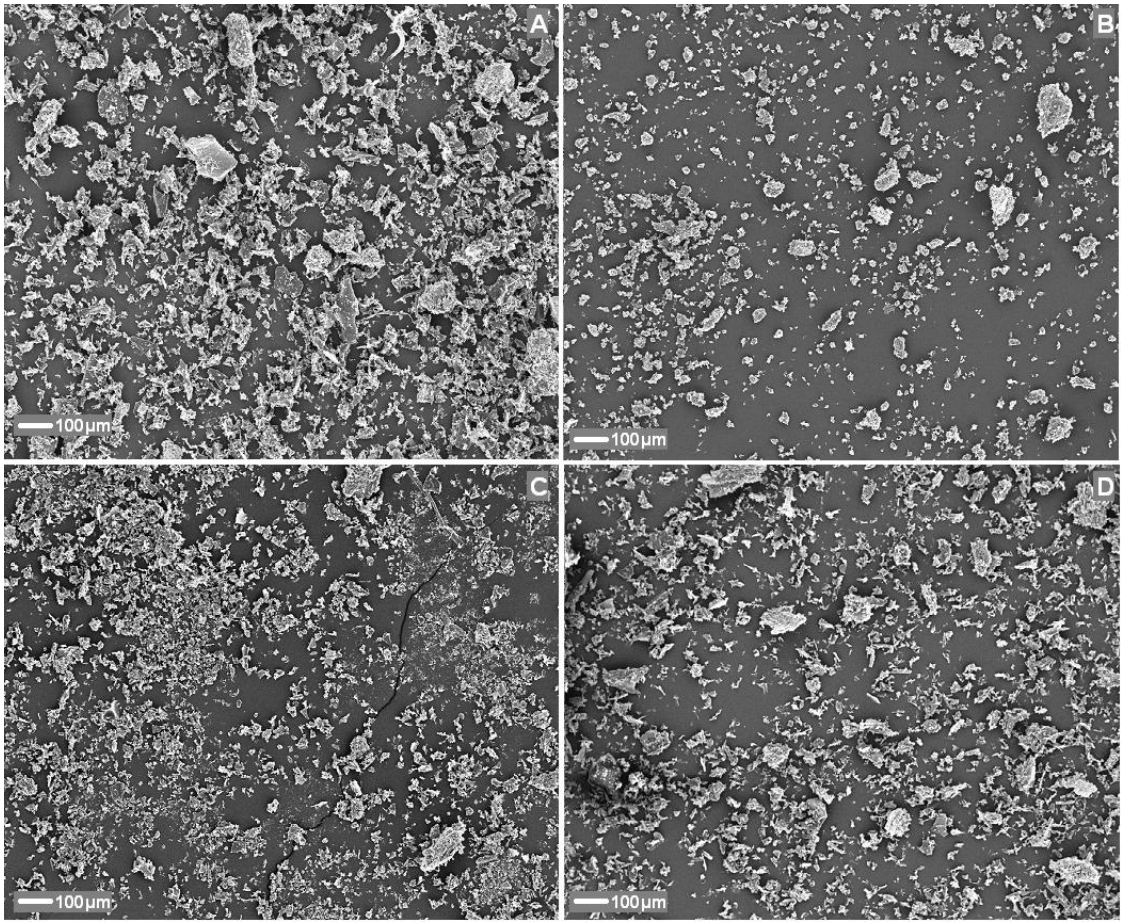

Figure 2.10– Scanning electron micrographs (150X magnification) of milled lyophilized cakes of A) 10% trehalose, slow freeze, no annealing, B) 1% trehalose, fast freeze, no annealing, C) 1% trehalose, slow freeze, annealing, and D) 10% trehalose, fast freeze, annealing.

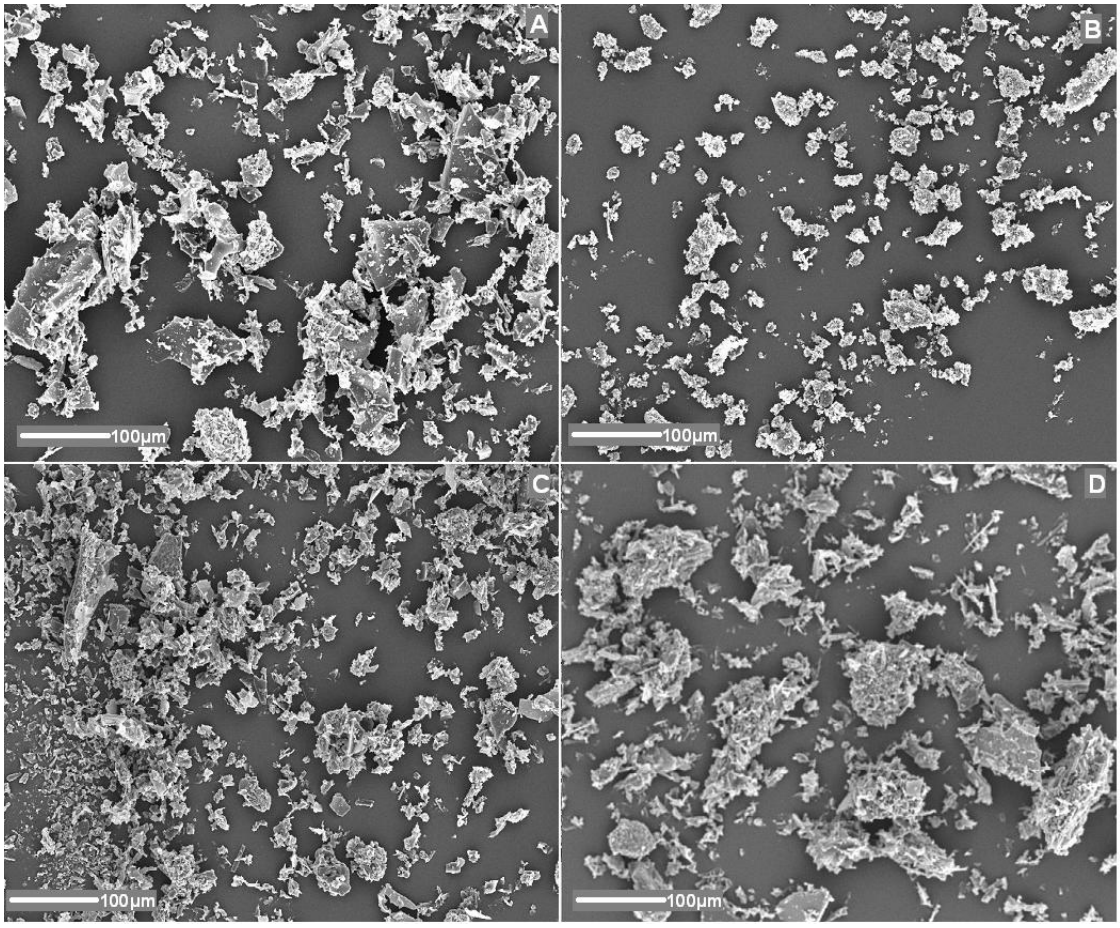

Figure 2.11– Scanning electron micrographs (600X magnification) of milled lyophilized cakes of A) 10% trehalose, slow freeze, no annealing, B) 1% trehalose, fast freeze, no annealing, C) 1% trehalose, slow freeze, annealing, and D) 10% trehalose, fast freeze, annealing.

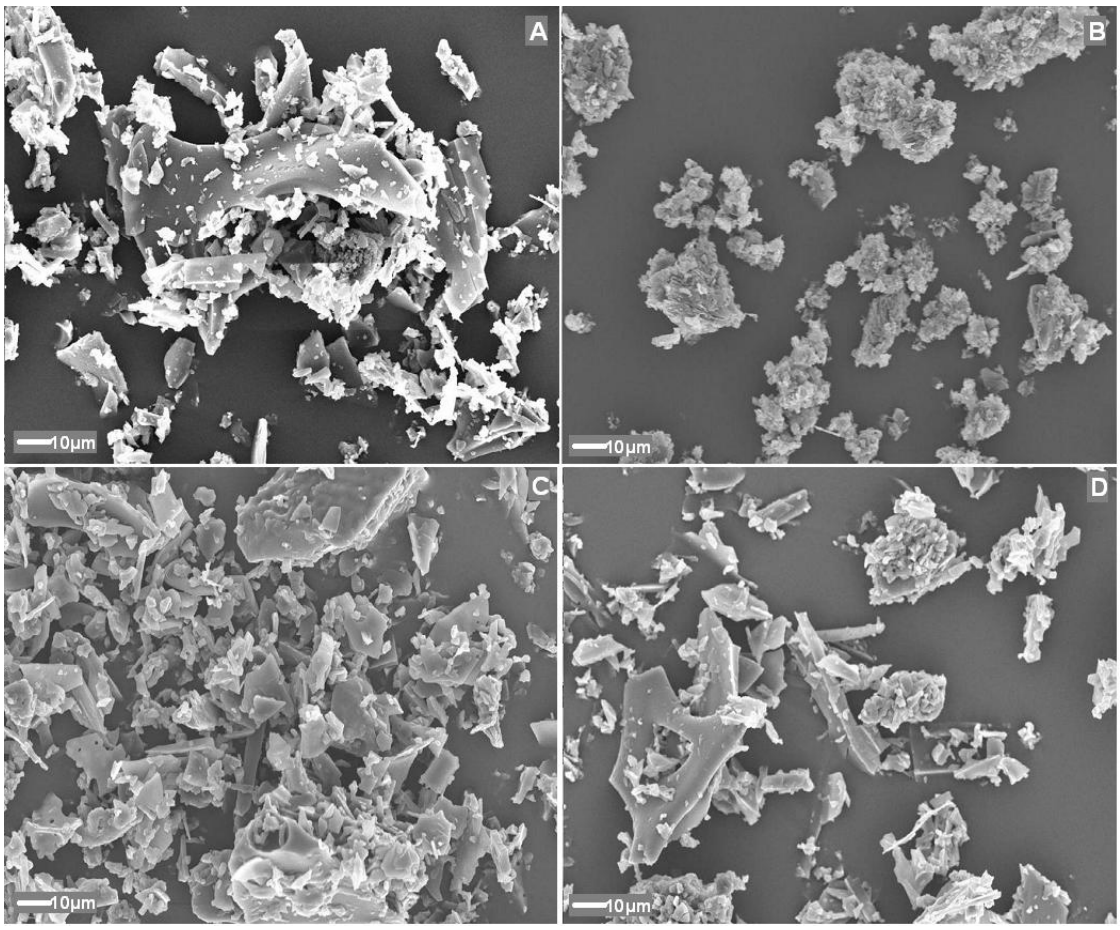

Figure 2.12– Scanning electron micrographs (60X magnification) of SFD particles of A) 10% trehalose, 500 L/hr, 25 mL/min, B) 10% trehalose, 500 L/hr, 3 mL/min, C) 1% trehalose, 500 L/hr, 3 mL/min, and D) 1% trehalose, 250 L/hr, 25 mL/min.

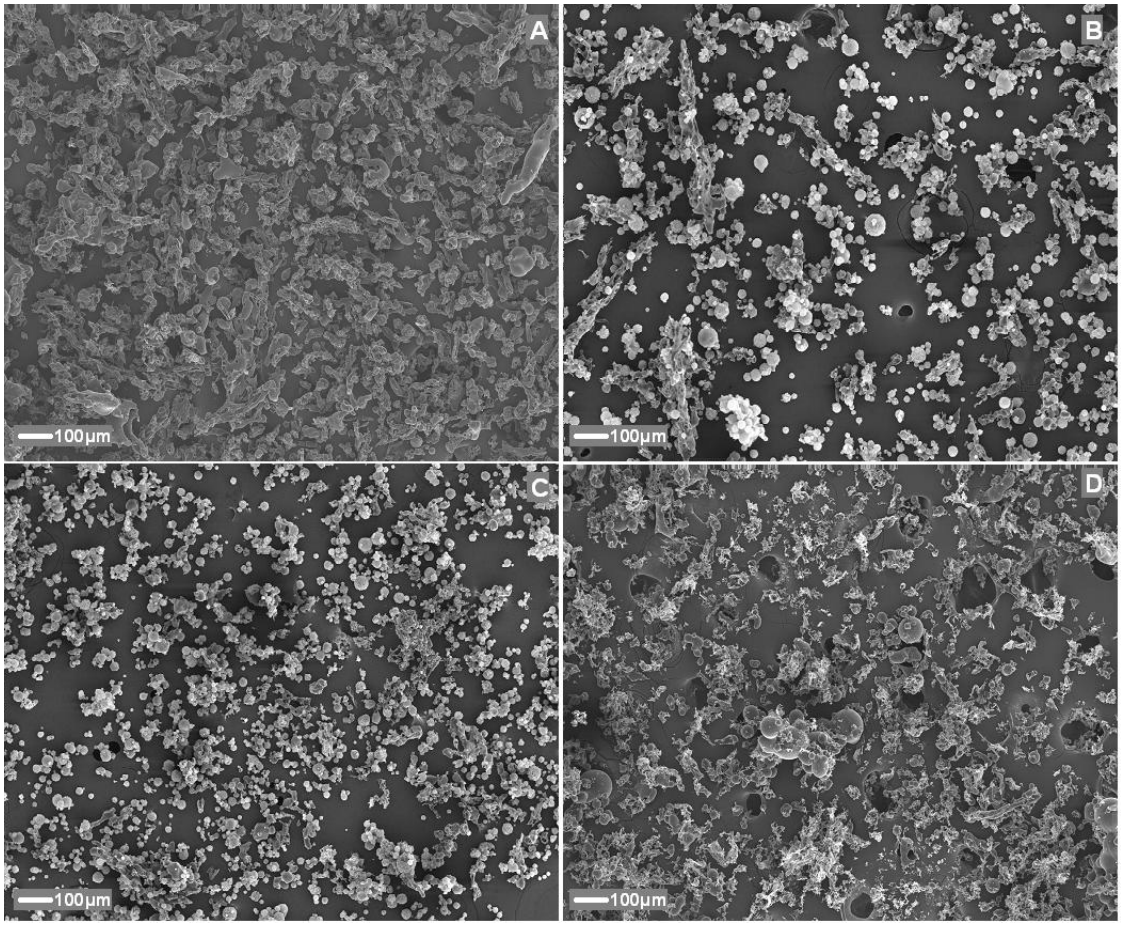

Figure 2.13– Scanning electron micrographs (150X magnification) of SFD particles of A) 10% trehalose, 500 L/hr, 25 mL/min, B) 10% trehalose, 500 L/hr, 3 mL/min, C) 1% trehalose, 500 L/hr, 3 mL/min, and D) 1% trehalose, 250 L/hr, 25 mL/min.

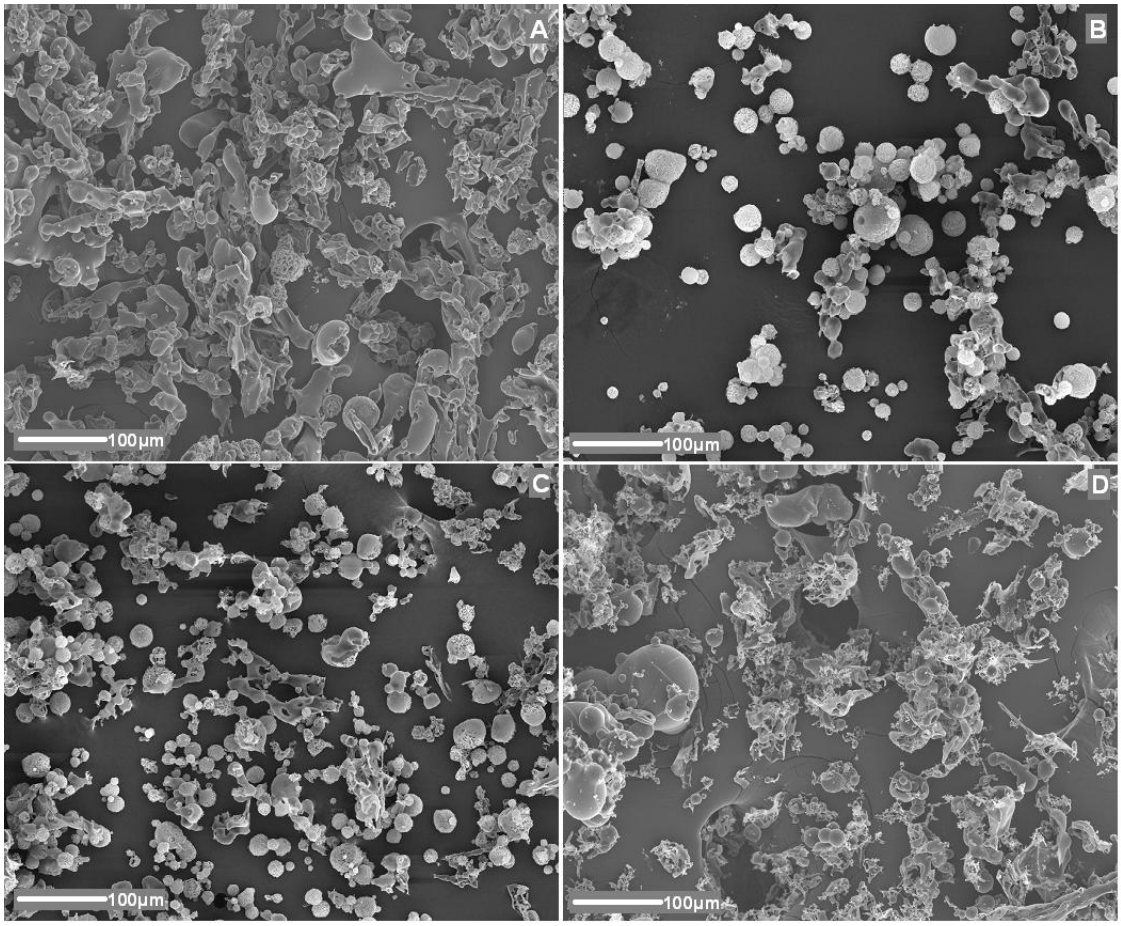

Figure 2.14– Particle size distributions of A) hydroxypropyl methylcellulose (HPMC LMW), B) HPMC HMW, C) carboxymethylcellulose (CMC LMW), D) CMC HMW, E) chitosan (Chit), and F) sodium alginate (SA).

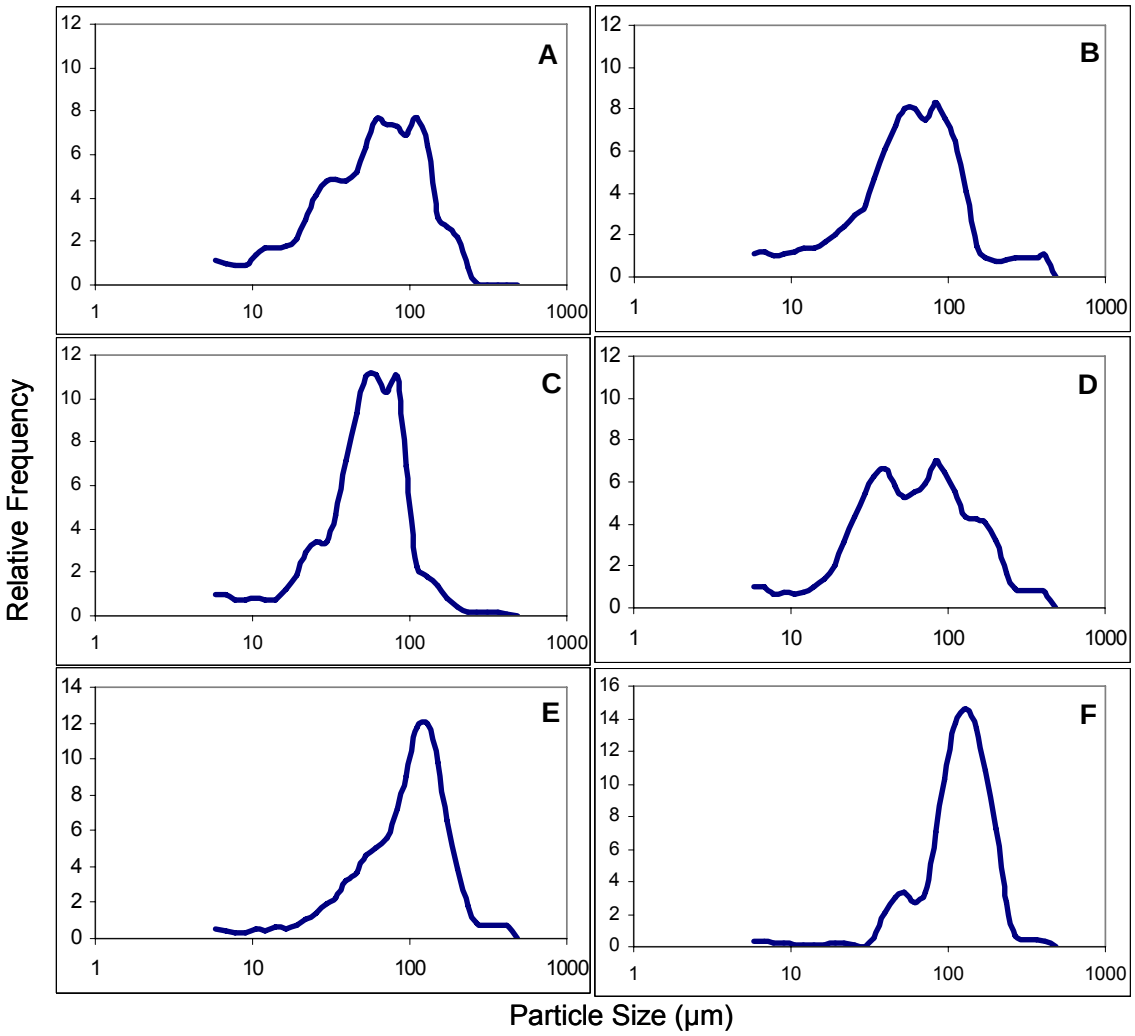

Figure 2.15– The half normal % probability as a function of effect for the median diameter (D_{50}) of particles produced by FD followed by milling and sieving.

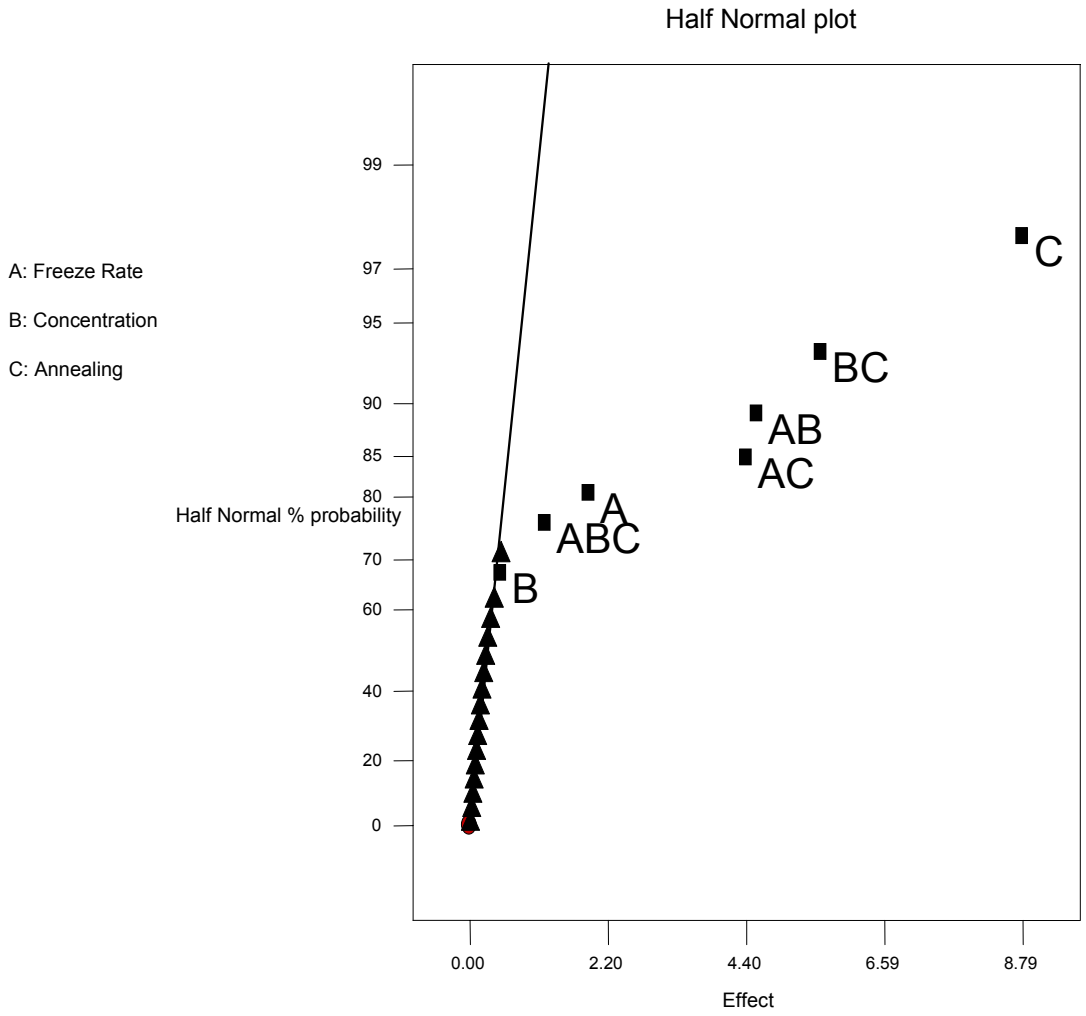

Figure 2.16– Cuboidal plot indicating the effects of freezing rate (A-=Slow, A+=Fast), solute concentration (B-=1%, B+=10%), and annealing (C-=No, C+=Yes) on median diameter (D_{50}) of particles produced by FD followed by milling and sieving.

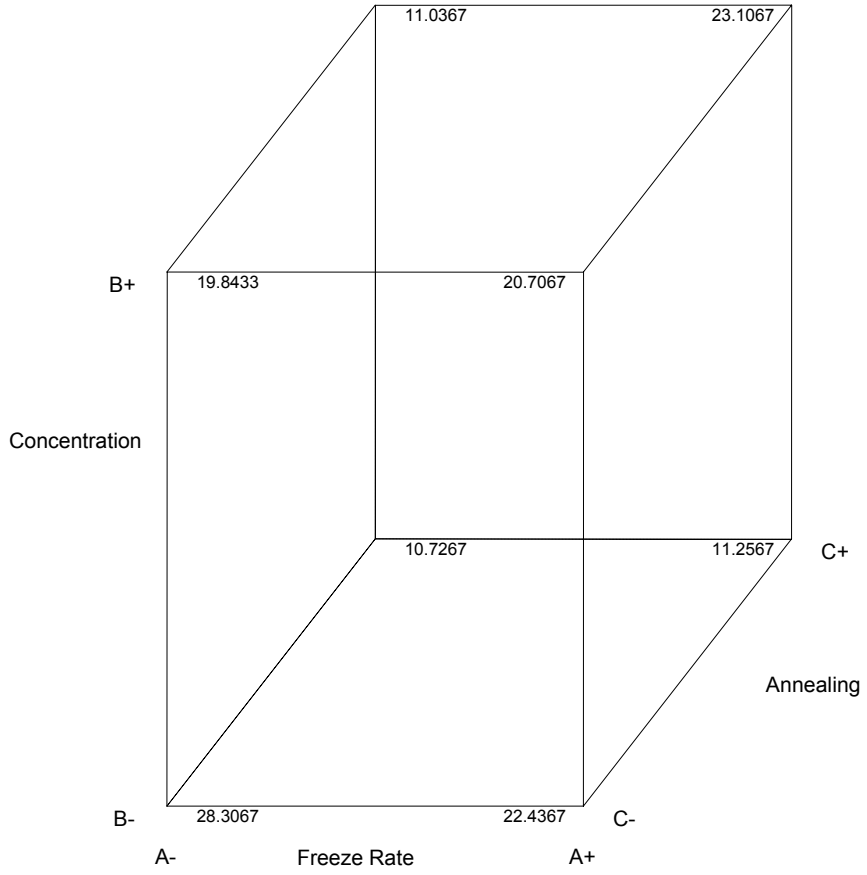

Figure 2.17– The half normal % probability as a function of effect for the 90% diameter (D_{90}) of particles produced by FD followed by milling and sieving.

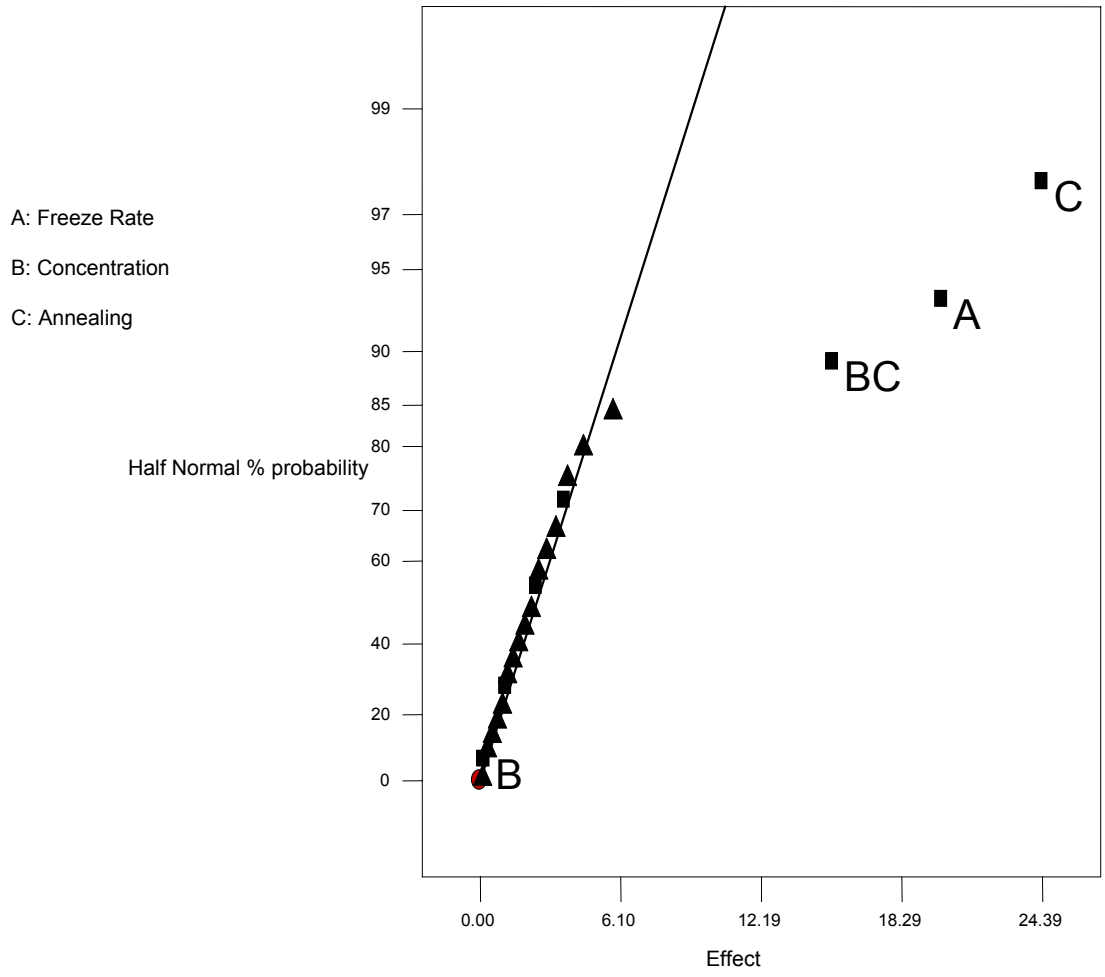

Figure 2.18– Cuboidal plot indicating the effects of freezing rate (A-=Slow, A+=Fast), solute concentration (B-=1%, B+=10%), and annealing (C-=No, C+=Yes) on 90% diameter (D_{90}) of particles produced by FD followed by milling and sieving.

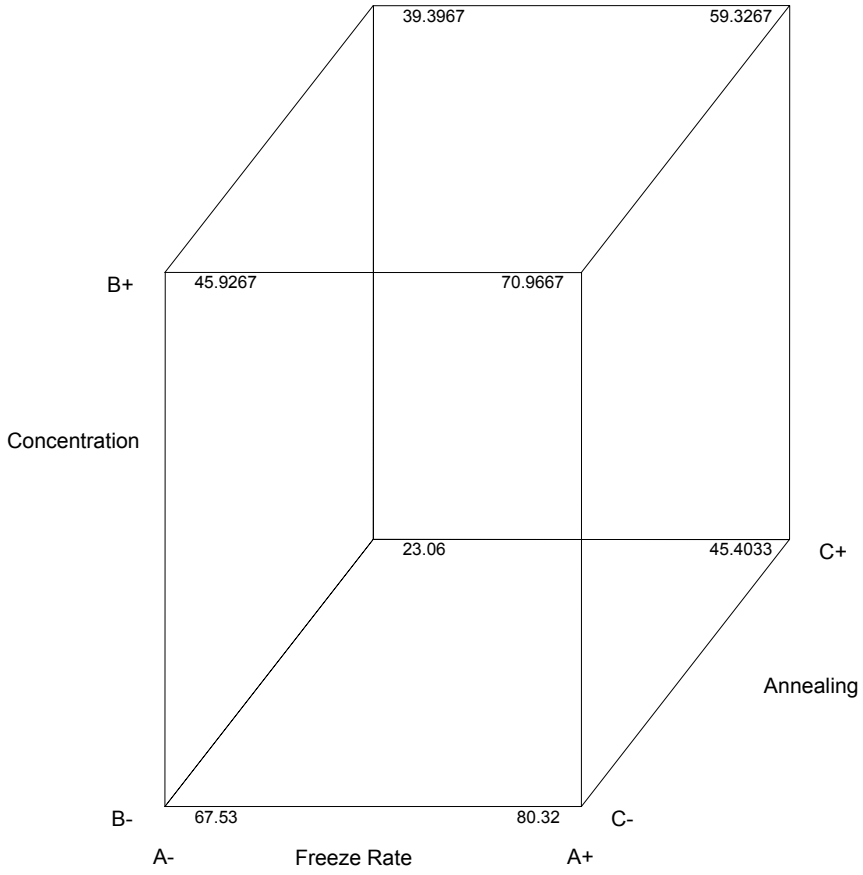

Figure 2.19– The half normal % probability as a function of effect for the 10% diameter (D_{10}) of particles produced by FD followed by milling and sieving.

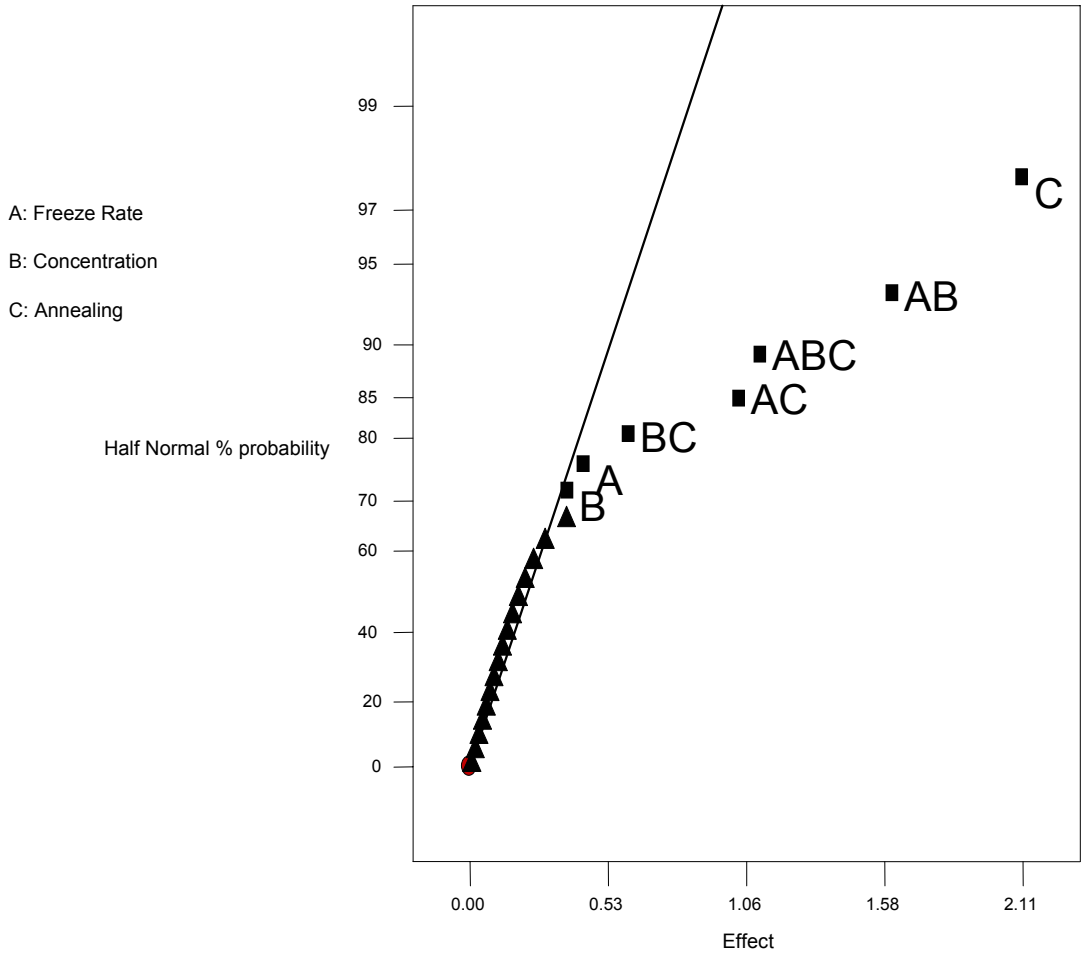

Figure 2.20– Cuboidal plot indicating the effects of freezing rate (A-=Slow, A+=Fast), solute concentration (B-=1%, B+=10%), and annealing (C-=No, C+=Yes) on 10% diameter (D_{10}) of particles produced by FD followed by milling and sieving.

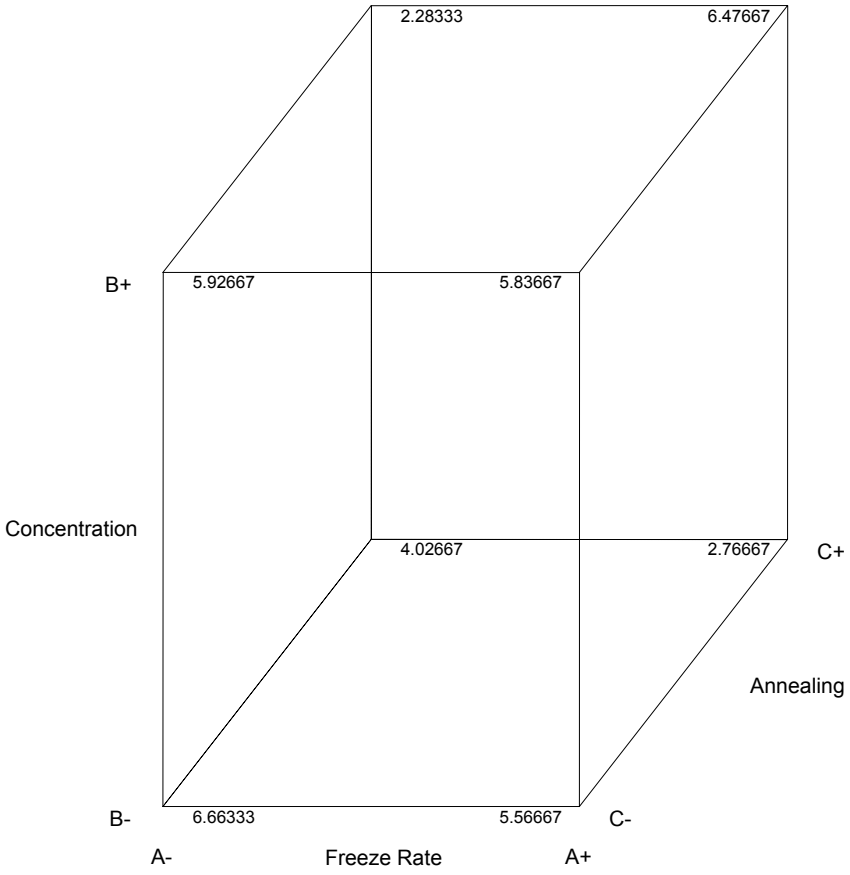

Figure 2.21– The half normal % probability as a function of effect for the span of particles produced by FD followed by milling and sieving.

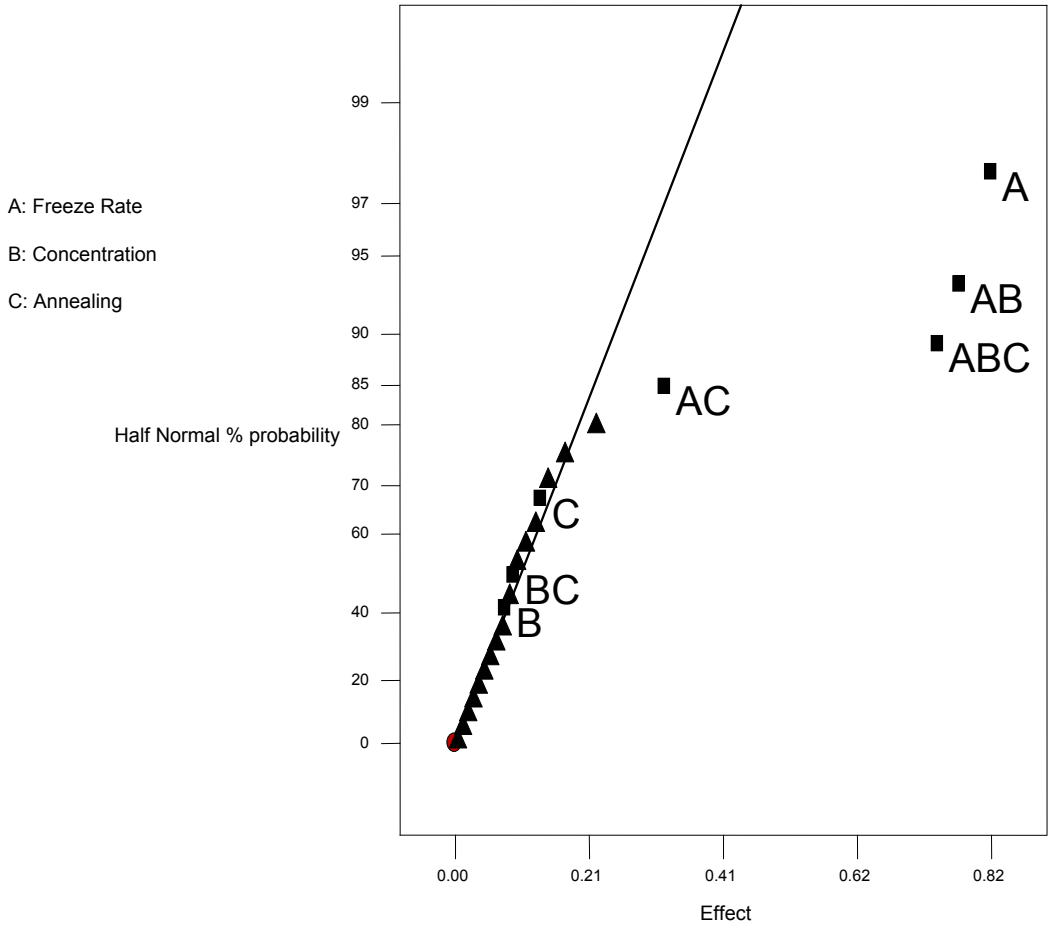

Figure 2.22– Cuboidal plot indicating the effects of freezing rate (A-=Slow, A+=Fast), solute concentration (B-=1%, B+=10%), and annealing (C-=No, C+=Yes) on span of particles produced by FD followed by milling and sieving.

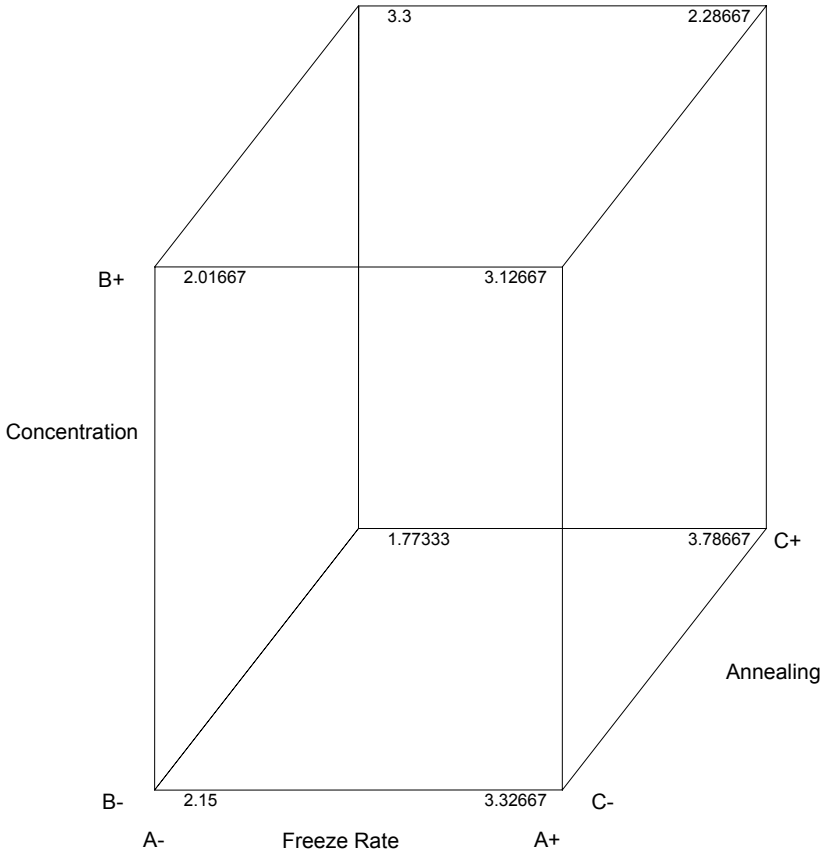

Figure 2.23– Diagram showing factors that must be taken into consideration for freeze-drying.

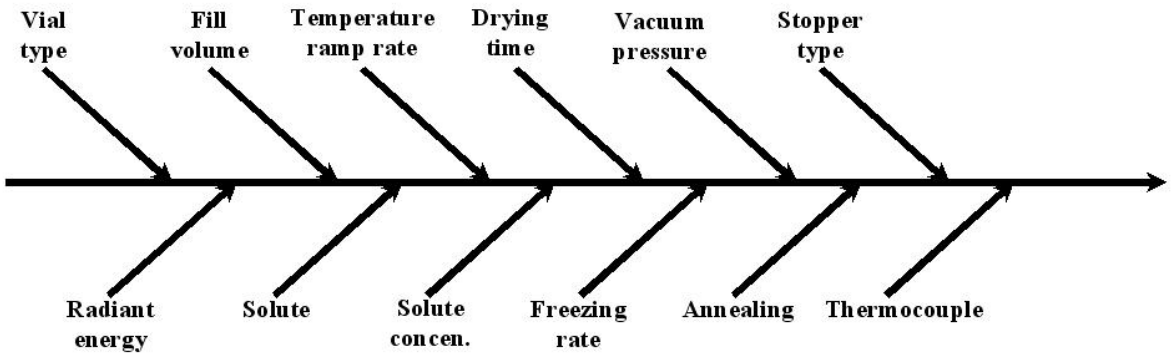

Figure 2.24– The half normal % probability as a function of effect for the median diameter (D_{50}) of particles produced by SFD.

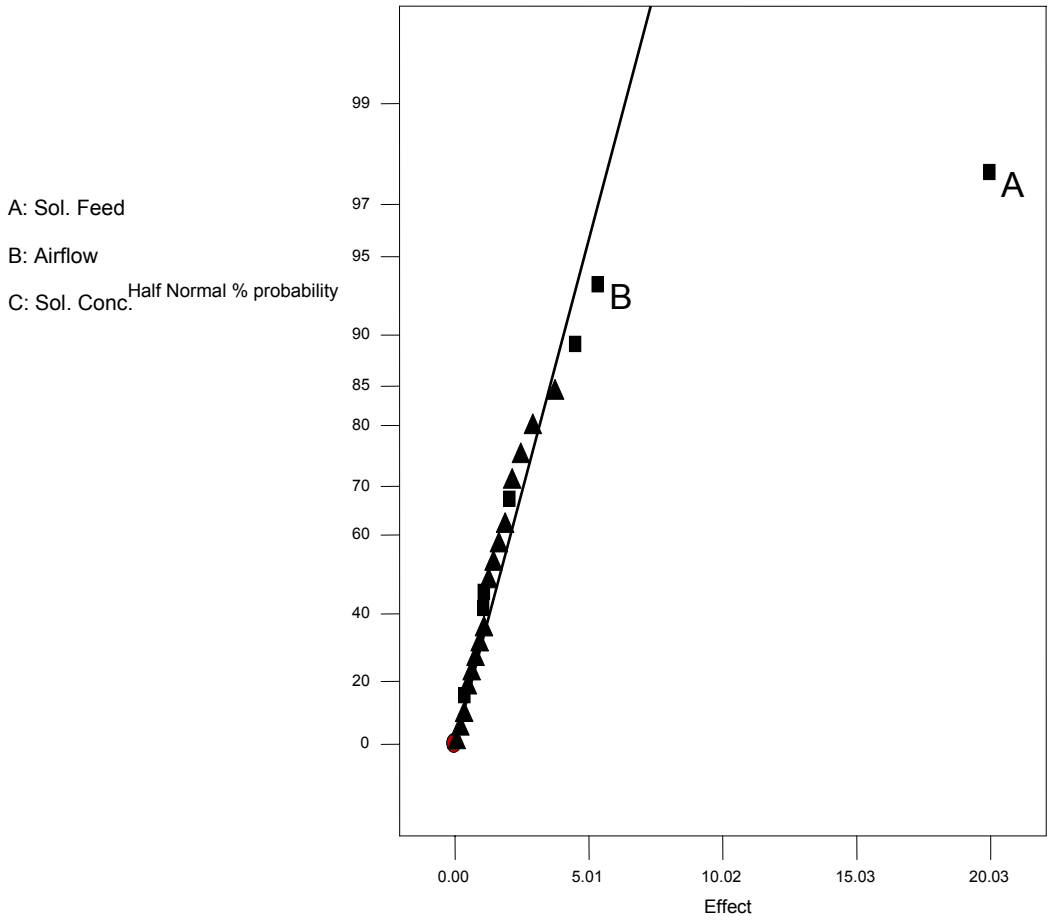

Figure 2.25– Cuboidal plot indicating the effects of solution feed rate rate (A-=3 mL/min, A+=25 mL/min), airflow rate (B-=250 L/hr, C+=500 L/hr), and solute concentration (C-=1%, C+=10%) on median diameter (D_{50}) of particles produced by SFD.

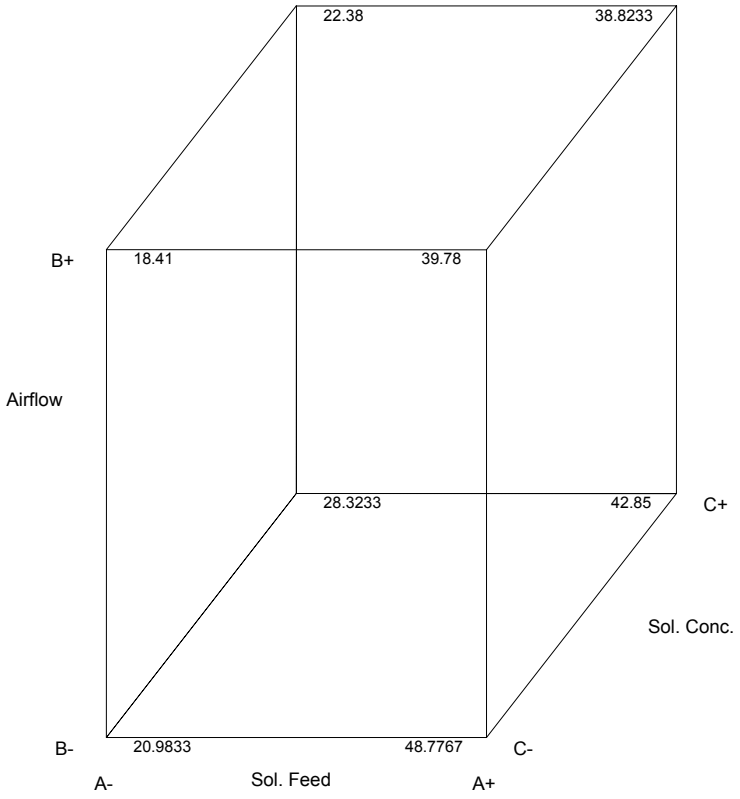

Figure 2.26– The half normal % probability as a function of effect for the 90% diameter (D_{90}) of particles produced by SFD.

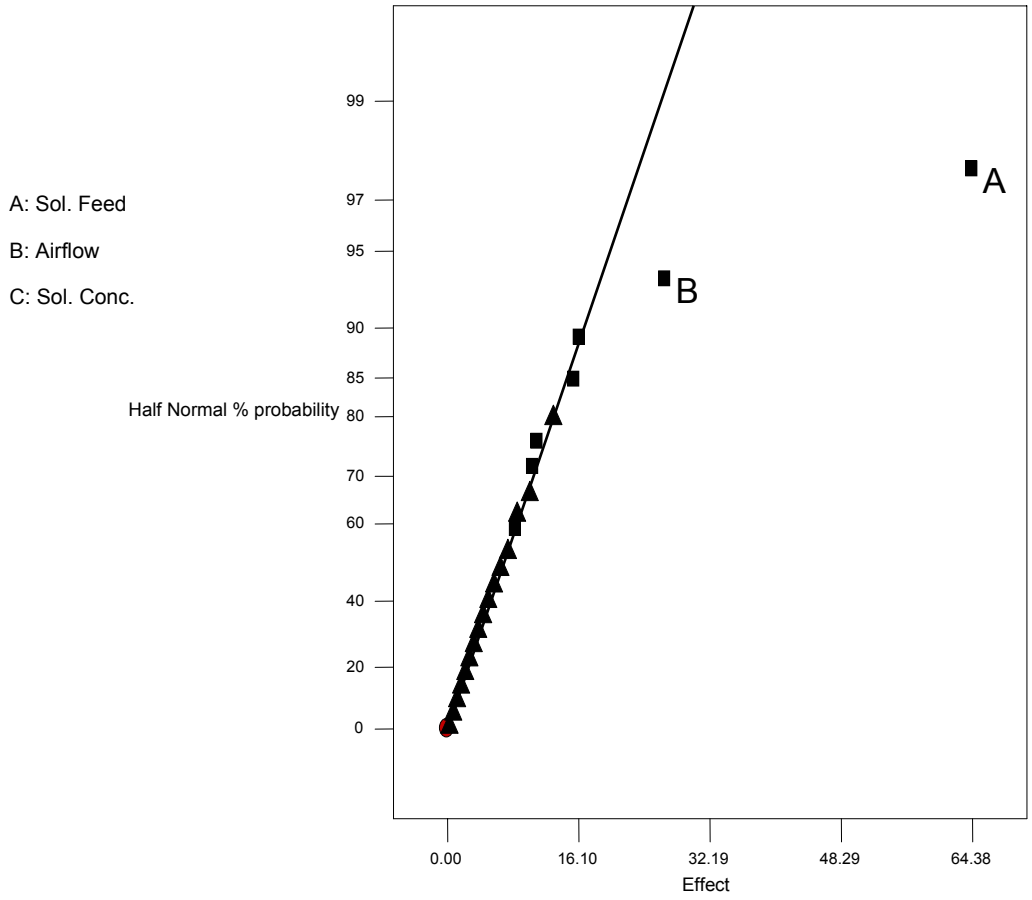

Figure 2.27– Cuboidal plot indicating the effects of solution feed rate (A-=3 mL/min, A+=25 mL/min), airflow rate (B-=250 L/hr, C+=500 L/hr), and solute concentration (C-=1%, C+=10%) on 90% diameter (D_{90}) of particles produced by SFD.

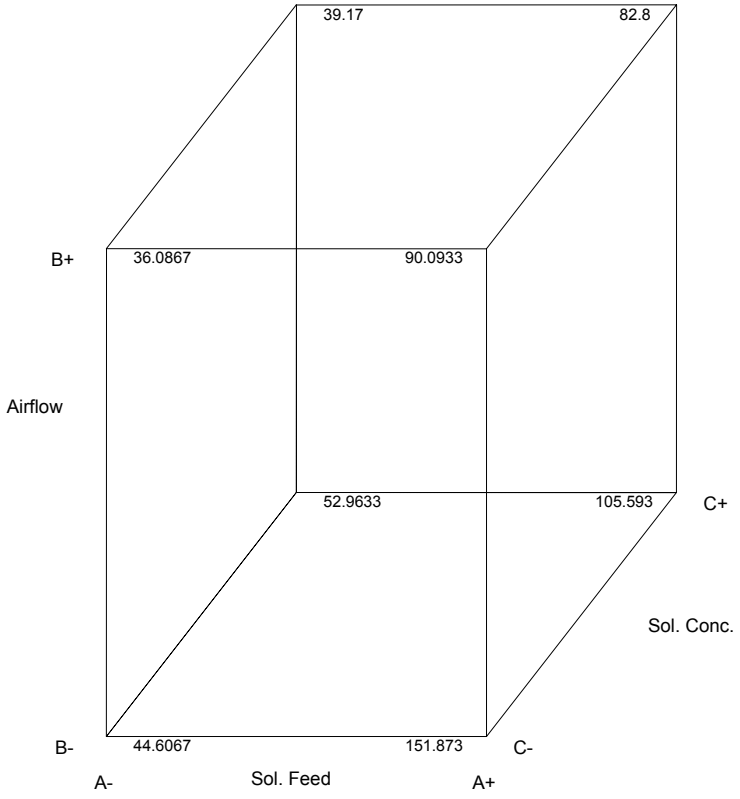

Figure 2.28– The half normal % probability as a function of effect for the 10% diameter (D_{10}) of particles produced by SFD.

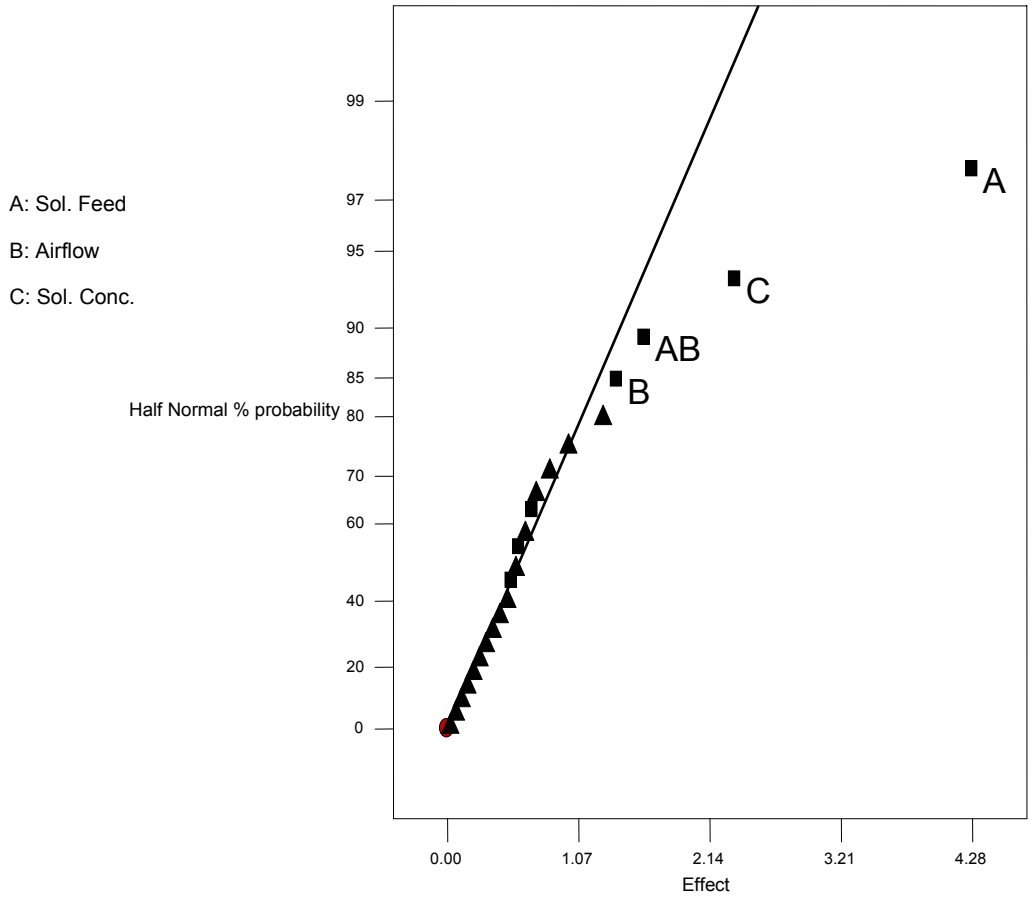

Figure 2.29– Cuboidal plot indicating the effects of solution feed rate (A-=3 mL/min, A+=25 mL/min), airflow rate (B-=250 L/hr, C+=500 L/hr), and solute concentration (C-=1%, C+=10%) on 10% diameter (D_{10}) of particles produced by SFD.

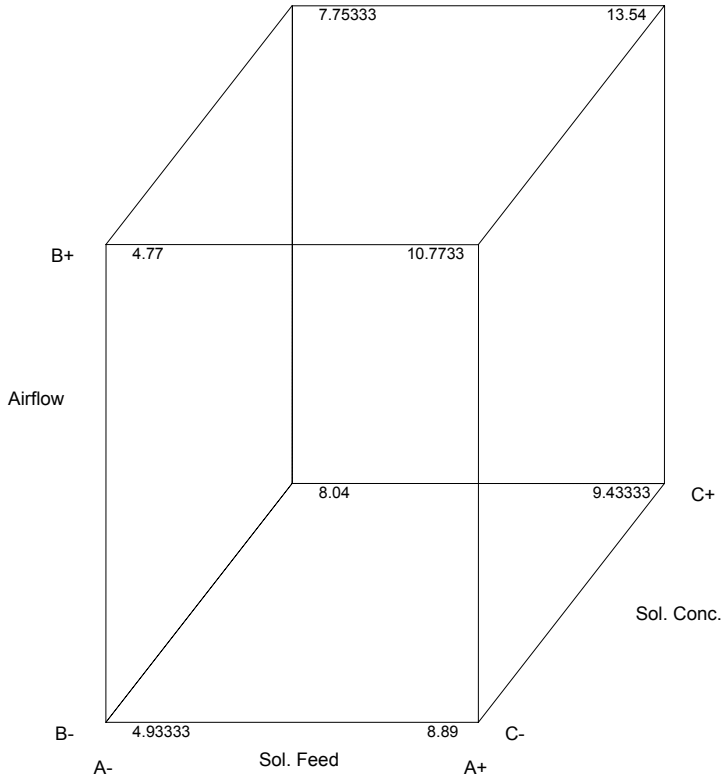

Figure 2.30– The half normal % probability as a function of effect for the span of particles produced by SFD.

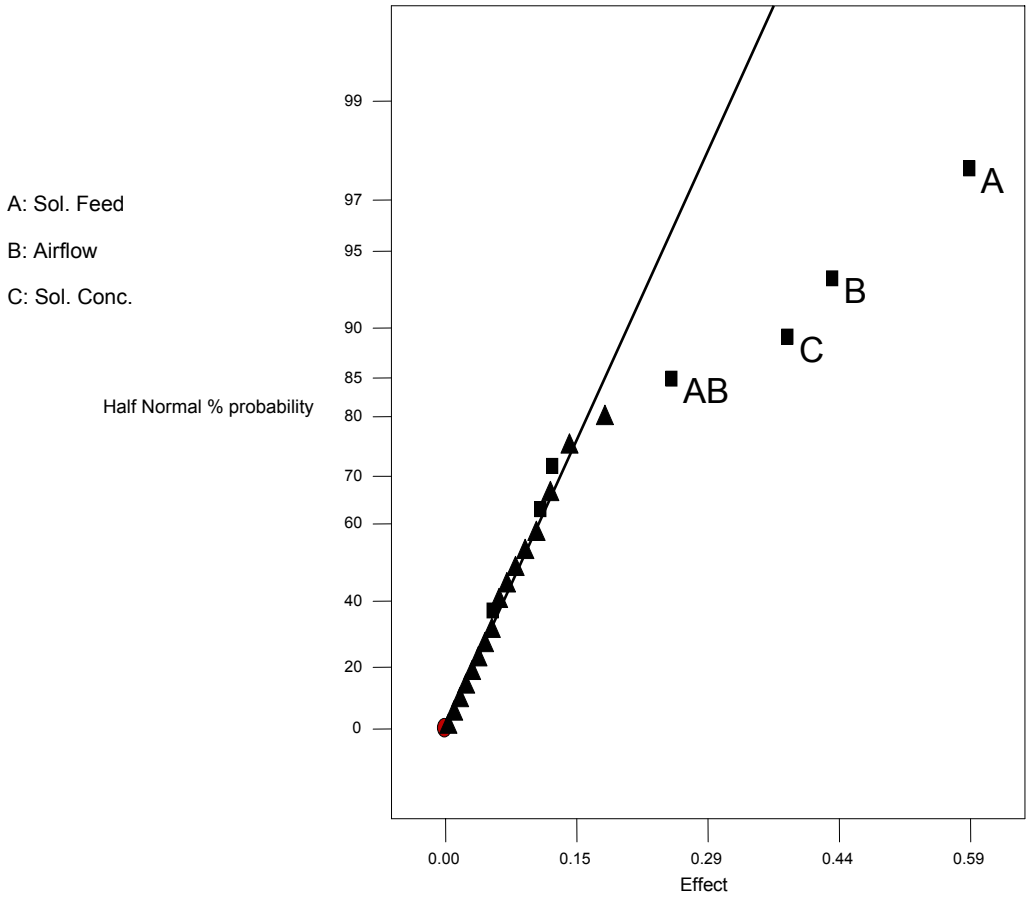

Figure 2.31– Cuboidal plot indicating the effects of solution feed rate (A-=3 mL/min, A+=25 mL/min), airflow rate (B-=250 L/hr, C+=500 L/hr), and solute concentration (C-=1%, C+=10%) on span of particles produced by SFD.

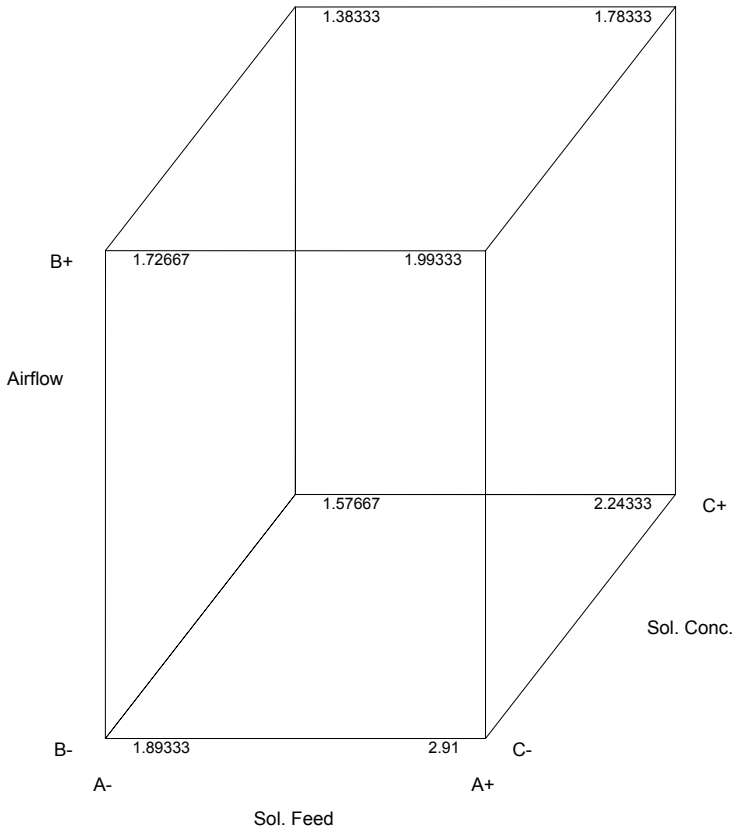

Figure 2.32– Plot of airflow versus solution feed rate to identify run conditions to produce formulation for human use (target D_{50}= 40 µm).

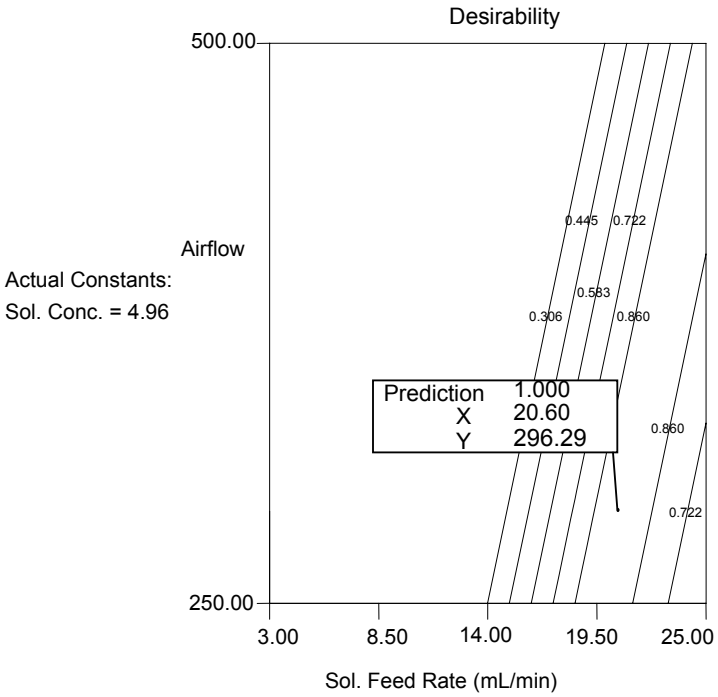

Figure 2.33– Scanning electron micrographs of spray-freeze-dried (SFD) formulation for human use at A) 60X magnification, B) 150X magnification, and C) 600X magnification.

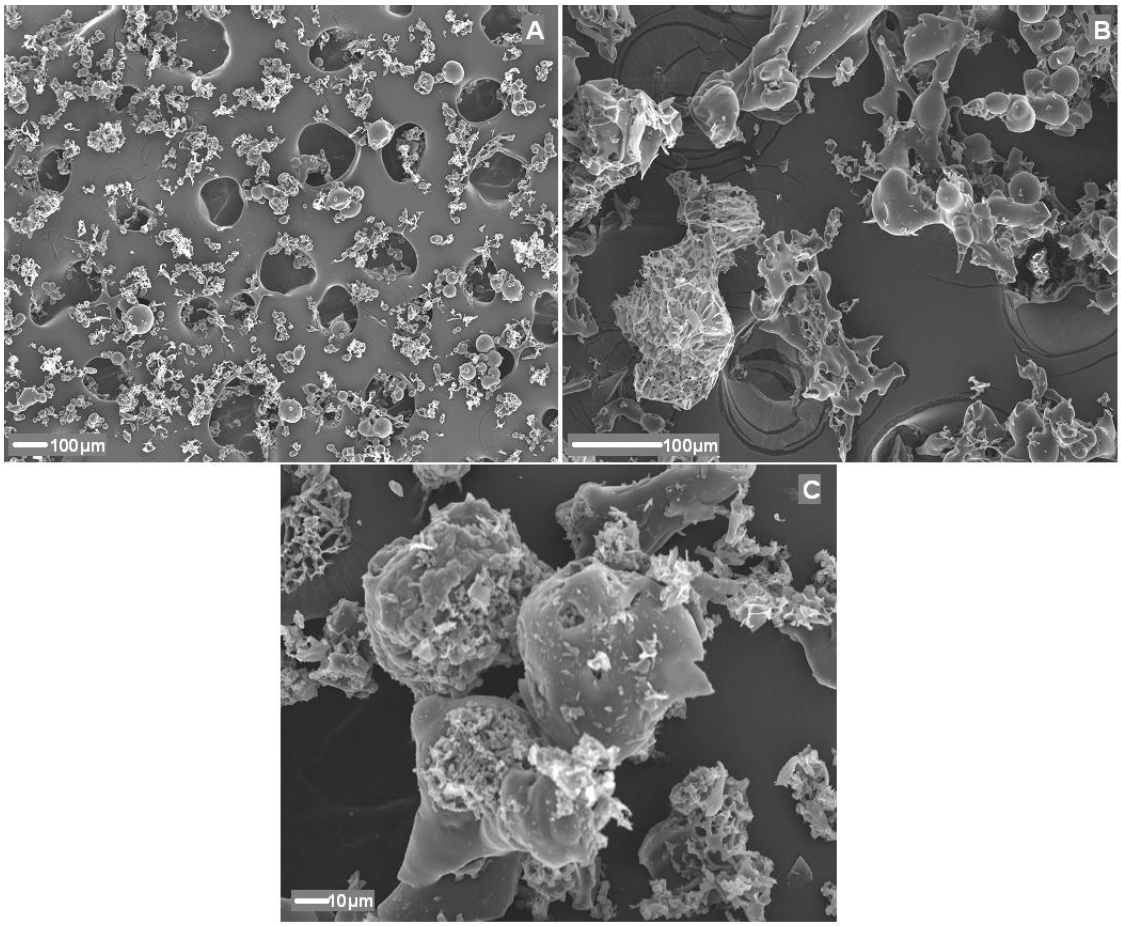

Figure 2.34– Particle size distribution of spray-freeze-dried (SFD) trehalose for human use.

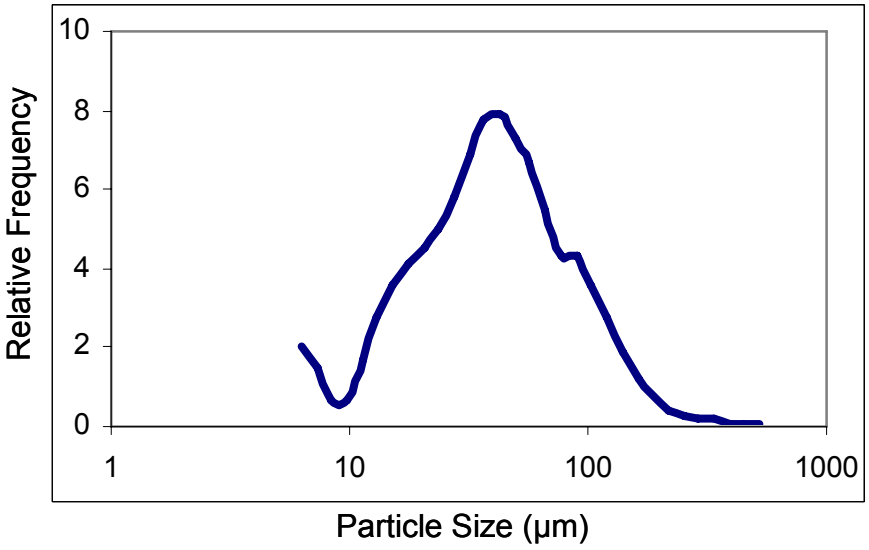

Figure 2.35– Scanning electron micrographs of SFD formulation for use in rats at A) 60X magnification, B) 150X magnification, C) 600X magnification, and D) 1500X magnification.

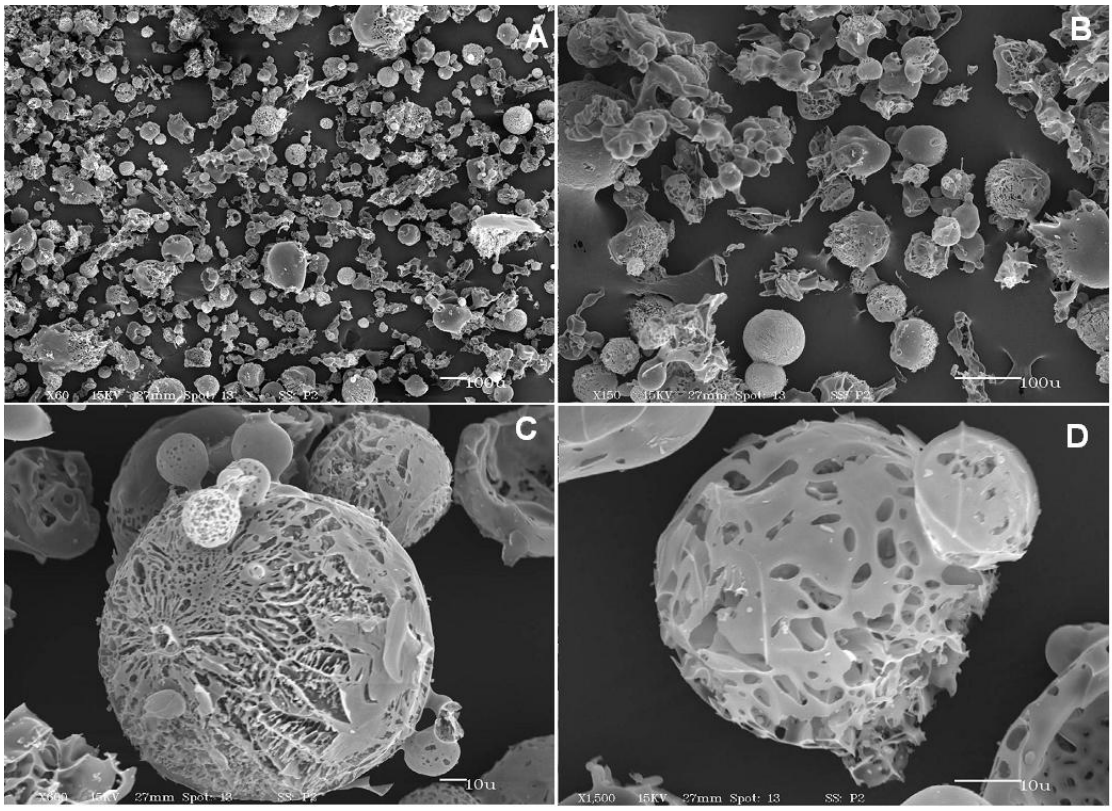

Figure 2.36– Plot of airflow versus solution feed rate to identify run conditions to produce formulation for use in rats (target D_{50}= 25 μm).

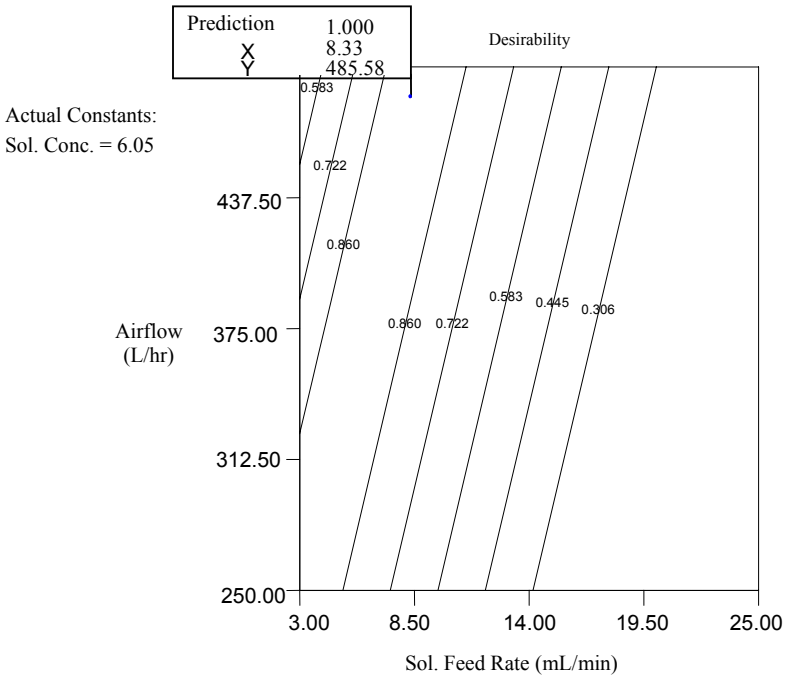

Figure 2.37– Particle size distribution of spray-freeze-dried (SFD) trehalose for use in rats.

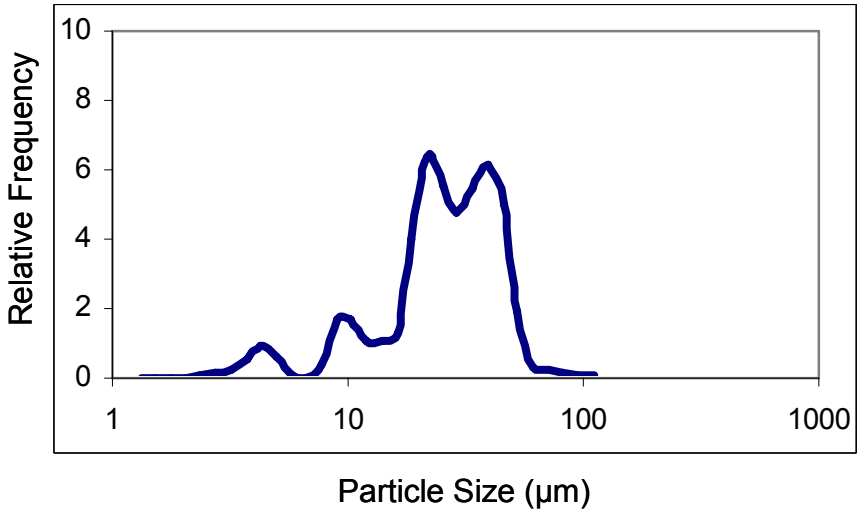

Figure 2.38– Diagram showing factors that must be taken into consideration for spray-freeze-drying.

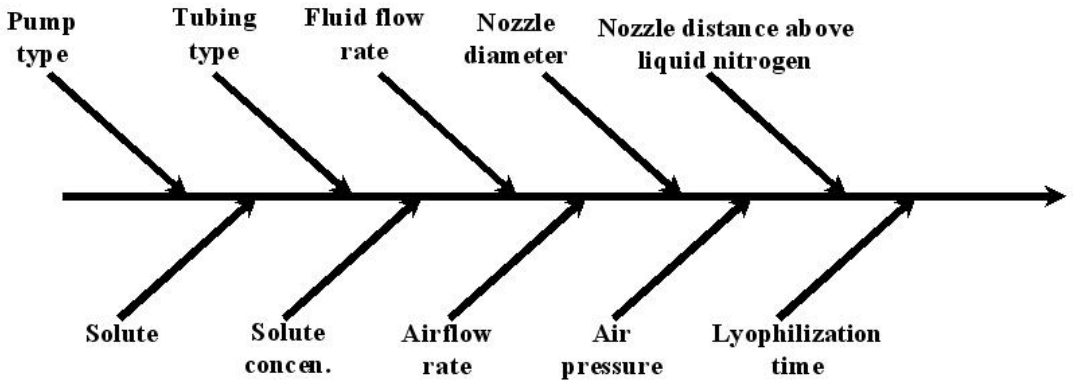

3 PHYSICO-CHEMICAL CHARACTERIZATION

3.1 Introduction

Nasal powders are best characterized in terms of particle morphology, size, and distribution as described in the previous chapter. There are, however, a number of other physico-chemical characteristics of a these particles that may be quantified. They include: flow properties to quantify particle-particle interactions; surface area of the particles a measure of porosity and factor in dissolution; solid-state characteristics of the particles; powder moisture content; temperature and humidity which influence the physical stability; and the dispersion properties of the vaccine formulation as it relates to efficient delivery.

One method to assess potential for powder flow is to measure the bulk and tapped densities. The bulk density is the mass of a powder divided by the volume prior to packing. The tapped density is equal to the mass divided by the volume of the powder after it has been tapped until no further decreases in volume occur (Carr 1965). The Carr's compressibility index (CCI) is parameter for quantifying the powder flow and is defined as (Carr 1965):

$$\text{CCI} = \left(\frac{\text{Tap Density} - \text{Bulk Density}}{\text{Tap Density}} \right) \text{x } 100\% \qquad (3.01)$$

As powder flow improves, the bulk density approaches the tap density and any further tapping will not cause a decrease in volume. Therefore, as the CCI decreases to 0%, powder flow improves as particle interactions decrease (Carstensen 1993).

When a powder is poured onto a surface from a fixed height, it forms a cone. The angle formed by the cone to the horizontal surface can be calculated and is known as the static angle of repose (Crowder 2003). This angle is another measure of the potential flow properties of a powder. As the static angle of repose increases, powder flow decreases. The static angle of repose has been stated to be an indirect measure of particle size, shape, porosity, cohesion, fluidity, surface area, and bulk (Carr 1965).

The surface area of a particle can be computed by direct calculation from the particle size distribution data or by measurement of the amount of a gas adsorbed onto a sample of powder to form a monolayer (Martin and Bustamante 1993). The latter technique is most accurate and relevant to further applications. When a mixture of nitrogen and helium (typically 30% nitrogen) are passed through a cell containing the powder, adsorption and desorption of nitrogen gas are measured with a thermal conductivity detector. At low pressures, the volume of nitrogen gas that adsorbs to a given mass of powder increases linearly until a monolayer of nitrogen is formed. The Brunauer-Emmett- Teller (BET) allows for the calculation of this volume and is described as:

$$\frac{P}{V(P_0 - P)} = \frac{1}{V_m C} + \frac{(C-1)}{V_m C}\left(\frac{P}{P_0}\right) \tag{3.02}$$

where V is the volume of nitrogen adsorbed, P is the pressure, P_0 is the saturation vapor pressure of liquid nitrogen, Vm is the volume of gas required to form a monolayer at normal temperature and pressure, and C is a constant related to the difference between the heat of vaporization of a monolayer and the heat of vaporization of liquid nitrogen (Crowder 2003). Vm and C can be determined graphically by the linear plot of $P/(V(P_0-P))$ against P/P_0. When C is large (i.e. the heat of adsorption is higher than the heat of vaporization), the slope of the plot is equal to 1/Vm. This allows for a single point measurement to determine surface area,

assuming that the gas forms a monolayer over the powder, which is not unreasonable for nitrogen (Brunauer, Emmett et al. 1938). The specific surface area is the surface area per gram of the sample (Martin and Bustamante 1993).

Differential scanning calorimetry (DSC) is a method of monitoring phase transitions that occur when the temperature of a material is increased (Martin and Bustamante 1993). The glass transition temperature (Tg) of a material is the temperature at which a supercooled noncrystalline liquid existing below its crystallization temperature (amorphous state) converts to a glass. The amorphous state and its glass are metastable and kinetically-dependent transitions. Tg is usually applicable to completely or partially amorphous powders, such as lyophilized powders. Above Tg, the material (eg. protein, polymer, phosholipid bilayer, sugars, inorganic molecules) becomes rubbery, lacking long-range order and capable of elastic or plastic deformation without fracture. To assure long-term stability of the virus in the dried solid formulation, the Tg of the lyophilized solid-state material must exceed the planned storage temperature, such that the solid-state material exists in the glassy state (having low molecular mobility) rather than in the amorphous state which has a higher molecular mobility, and hence, greater physical and chemical reactivity and instability (degradation) (Carpenter, Pikal et al. 1997).

Moisture content measurement involves monitoring the weight change of a material after heating. It is useful in the measurement of moisture content, since any water present in the material can result in loss of activity of proteins (loss of H-bonds which maintain the active conformation) or can affect the structural stability of the powder (Chang, Reeder et al. 1996). Water weight will be lost during heating allowing percent weight loss of the material

to be calculated. When used together, moisture content analysis and DSC allow for a determination of the stability of the materials in different temperature ranges (Brittain 1995).

Forces of interaction must be considered when developing dry powder formulations. Interparticulate forces can be influenced by particle properties and properties of the surrounding medium (Baron and Willeke 2001). As the size of the particles decreases, surface area increases and there may be greater contact between individual particles (Hickey and Ganderton 2001). Therefore, surface area plays a crucial role in the degree of particle interactions. The forces of attraction that can exist between particles include van der Waals forces, electrostatic forces, and capillary forces (Mullins, Michaels et al. 1992). The force necessary to detach a particle from a surface can be measured by subjecting particles to a centrifugal force perpendicular to the surface and determining the speed of rotation required to detach the particle (Clarke, Peart et al. 2002). In the aerodynamic method, the velocity of air required to remove a certain percentage of monodisperse particles from a surface is measured. An impact energy apparatus was previously developed to enable characterization of the amount of energy required to remove particles from a hard surface (Concessio 1997; Concessio, Van Oort et al. 1998). The process utilizes microscopy, for particles > 10μm in median diameter, to size the particles remaining on the surface after successive strikes with a hammer applied by rotation of a pendulum.

The use of cascade impactors for particle size characterization has been previously discussed (1.1.9). The flow rates of air through the impactor stages effectively characterize deposition of particles in the respiratory tract. Current methods to determine in vitro deposition of nasal sprays utilizing the cascade impactor involve using a “short stack” (stages 0, 1, 2, and filter, (Suman, Laube et al. 2002; Newman, Pitcairn et al. 2004)) with a 2L

expansion chamber. However, there is currently no well established method in place to characterize deposition of particles greater than about 10 μm. At aerodynamic diameters of up to 20 μm, as much as 10% of the particles could potentially enter the respiratory tract, leading to potential toxicity problems (Bates, Fish et al. 1966). Significant pulmonary deposition can occur for nasal preparations that have a large quantity of particles with small aerodynamic diameters (<5 μm). The Food and Drug Administration (FDA) requires proof that when a nasal preparation is delivered, it does not penetrate to the lungs (FDA 2003). However, *in vitro* approaches to characterizing respirable particles were limited and did not account for the full range of sizes that might potentially deposit in the lungs. Radionuclide imaging is commonly performed to satisfy this requirement by showing deposition in the nasal cavity, but none in the lung (Newman, Steed et al. 1995). This process can be very costly. An *in vitro* system would be ideal for predicting the potential for deposition of a nasal formulation in the pulmonary region. A modified Andersen Mk II non-viable cascade impactor was calibrated (Appendix A.3) and was used to characterize potential deposition into the lower respiratory tract.

In the following sections, powder physico-chemical properties of bulk/tapped density, angle of repose, thermal, surface area, moisture content analyses and dispersion characteristics with respect to bulk and spray-freeze-dried (SFD) trehalose and mucoadhesive compounds (MA) are described.

3.2 Methods

3.2.1 Bulk/tapped density

The bulk and tapped densities were determined for sieved fractions of trehalose, bulk and sieved MA, and SFD powders (n=3). Approximately 10 mL of powder was employed to

conduct each measurement by pouring into a graduated cylinder (Martin and Bustamante 1993).

3.2.2 Static angle of repose

Measurements of the static angle of repose were conducted for sieved fractions of trehalose, bulk and sieved MA, and SFD powders (n=3). Approximately 10 mL of powder was poured through a glass funnel (7cm diameter entry reducing, over a distance of 5 cm, to a 1.5 cm diameter vertical tube 3 cm in length) onto a flat collection surface where the angle to the horizontal was measured (Carstensen 1993).

3.2.3 Surface Area

Single-point surface area analysis was performed on sieved trehalose (1.5-1.75 g) and SFD (0.5-0.75 g) powders (Quantasorb Jr., Quantachrome Corp., Boynton Beach, FL). Accurately weighed samples were degassed under vacuum at 60°C for 5 hours with nitrogen followed by repetitive adsorption and desorption of the adsorbate, 30% nitrogen in helium gas.

3.2.4 Moisture Content

Moisture content determination was conducted (Mettler LJ16 Moisture Analyzer, Mettler-Toledo, Columbus, OH). Each sample was loaded onto an aluminum tray coating the bottom with a thin layer of powder. The initial powder weight was recorded. The powder was then heated to 150°C and the final weight of the powder was measured accurately and precisely, using a moisture balance (n=3). The difference between the final and initial powder weight was the water content in the sample and it was recorded as a percent of the total weight.

3.2.5 True Density

True density measurements were conducted with a helium pycnometer (Ultrapycnometer, Quantachrome Instruments, Boynton Beach, FL.) on bulk trehalose and SFD powders ((Martin and Bustamante 1993), n=3).

3.2.6 Thermal Analysis

Differential scanning calorimetry (Perkin Elmer DSC 6, Wellesley, MA) was performed on powder samples. Known quantities of powder were sealed in an aluminum pan and differences in heat flow were measured against an empty pan. SFD powders were pretreated at 60°C for 5 hours. Analysis was performed between 50 and 250°C at a ramp rate of 10°C per minute for bulk and SFD trehalose and between 50 and 220°C at a ramp rate of 5, 10, 20, and 40°C per minute for MA.

3.2.7 Physical Stability

WIIV of the H1N1 strain, A/PR/8/34 (Charles River SPAFAS, North Franklin, CT), was propagated in the allantoic cavity of SPF eggs, purified from sucrose gradient, inactivated by formaldehyde, and resuspended in Hepes-saline at a concentration of 2 mg H /mL. The hemagglutination assay (HA) titer for the WIIV, as provided by the manufacturer, was 1:131,072 for 0.05 mL. Liquid preparation of whole inactivated influenza virus from the vendor was diluted to 2 μg H/25 μL with sterile saline and sealed in 1.7 mL centrifuge tubes. About 5 mg total 25 μm SFD powder for rat use containing 5 μg H/5 mg trehalose was packed into each capsule and sealed in a vial. Vials containing liquid or powder samples were stored in the following conditions: 37°C and 80% RH, 23°C and 40% RH, 4°C and 50% RH. Samples were taken at different time points for determination of HA titers for up to

12 weeks. Two samples were taken from each storage condition at defined time points. Powder was reconstituted with saline to 1 mg influenza virus/mL, based on H content. The HA titers of each formulation at different time points were compared to the week 0 sample (without storage) of the same formulation and the percentage change in HA titer was taken as an indicator of sample stability. All samples were analyzed in duplicate. Fifty μL of double serial diluted inactivated influenza virus samples were added to wells containing 50 μL of 0.5% chicken red blood cells (Charles River SPAFAS) and incubated at RT for 1 hr for the HA assay. The endpoint HA titer was defined as the reciprocal of the highest influenza vaccine dilution showing complete hemagglutination of chicken red blood cells.

3.2.8 Impact Energy Separation

An impact force particle dispersion device was developed previously (Concessio 1997). The instrument was constructed of stainless steel, and consisted of a pendulum arranged with a hammer head at one end capable of impinging on a vertically mounted sapphire disc, 20mm in diameter and 2mm thick (Tech. Spec. sapphire windows, Edmund Scientific, Industrial Optics Div., Barrington, NJ). Three different hammer head weights of 35, 45, and 55g were utilized to increase the hammer load. The sieved trehalose or SFD powder to be evaluated was thinly coated on the sapphire disc which was tilted to pour off the excess powder. This resulted in a uniform coating of the sapphire disc. The coating was achieved by virtue of the adhesive forces exhibited by the particles. The disc was carefully placed into the slot and subjected to an impact by the pendulum hammer head. Photographs were taken after each impact by a digital camera (Nikon CoolPix 5000, Nikon, Corp., Japan) mounted onto a light microscope (Leica Corp., Ernst-Leitz-Strasse, Germany). Image

analysis software (ImageJ, U. S. National Institutes of Health, Bethesda, Maryland) was used to determine the median diameter of particles remaining on the surface.

3.2.9 Modified Cascade Impactor

Powder dispersion was performed by fluorescent labeling SFD human trehalose by preparing a 0.05% blend with micronized disodium fluorescein. A monodose insufflator (MDS, Miat Corp., Milan, Italy) and a specialized powder delivery device developed by BDT (Becton Dickinson Technologies, Research Triangle Park, NC), described in (Huang, Garmise et al. 2004), but with a modified nozzle for human delivery were characterized using a calibrated, modified Andersen MKII non-viable cascade impactor (Graseby Andersen, Smyrna, GA), described in Appendix 3, with a one-liter inlet port (Figure 3.1). Dispersion properties were studied at a flow rate of 15 L/min (n=5). The collection plates were coated with 1% silicon oil (Fisher Scientific, Fair Lawn, NJ) in hexane (Sigma-Aldrich, St Louis, MO). Glass fiber filters with a pore size of 0.22 μm (Graseby Andersen, Smyrna, GA) were used below the last stage of the impactor. Gelatin capsules (size 3, Capsugel Inc., Peapack, NJ) were filled with 5 mg of the blend. A vacuum pump was used to draw air through the impactor at 15 L/min. Following piercing of each capsule, sampling was continued for 10 seconds. The device and collection plates were washed with known quantities of phosphate buffer (pH 7.4). Samples were analyzed using a spectrofluorometer (Chameleon Plate Reader, Hidex Oy, Turku, Finland) operated at an excitation wavelength of 500 nm and emission wavelength of 550. A standard curve was prepared with disodium fluorescein concentrations ranging from 0-100 ng/mL in phosphate buffer.

3.3 Results and Discussion

3.3.1 Bulk/tapped density

Flow properties are a manifestation of the action of cohesive (and adhesive in mixtures) forces acting on a powder. In these experiments, manufacturing conditions were optimized for producing particles of the desired size (~40 μm for use in humans and ~25 μm for use in rats), not for flow properties. However, the flow properties do affect the performance of the final product. The bulk (0.1-0.2 g/mL) and tapped (0.1-0.3 g/mL) densities of the SFD powders were significantly lower than bulk trehalose (Table 3.1, 0.5 and 0.6 g/mL, respectively). The bulk and tap densities of the MA were similar to sieved trehalose (Table 3.2). The bulk and tap densities (0.7-0.9 g/mL and 0.9-1.0 g/mL, respectively) of SA were much larger than any of the other MA.

Large cohesive forces acting on a powder, result in poor flow properties and render it easily compressible (i.e. the higher the CCI). A free-flowing powder has a CCI less than ~20% to 21% (Carr 1965). The 40 μm SFD use and sieved trehalose (~20-23%) had lower CCIs than the SFD rat trehalose (~36%). Based on CCI, the 40 μm SFD powder was the only one considered free-flowing. Bulk and sieved fractions of SA and chitosan (~9, 16, 21, and 21, respectively) were the only MA to be considered free-flowing.

3.3.2 Static angle of repose

A large static angle of repose is indicative of large cohesive forces within the powder. As a guide, powders with static angles of repose less than 40° are considered to be free-flowing powders; with angles greater than 50°, the powders flow poorly or not at all (Carr 1965). Tables 3.1 and 3.2 show the angles of repose for each of the powders studied. The

static angle of repose of 25 µm SFD (~36°) was larger than the 40 µm SFD and sieved trehalose (~20-23°), but all three powders are regarded as free-flowing. All of the MA were considered free-flowing with the exception of sieved CMC HMW (~43°), bulk chitosan (~41°), and sieved chitosan (~40°).

The ability of a powder to flow is one of the factors that affect the mixing of different materials to form a powder blend and is influenced by particle size, size distribution, shape, surface texture, surface energy, chemical composition, moisture content, and other factors (Staniforth 2002). This may be important for the blending of the virus and excipient with the mucoadhesive compound. Also, because nasal delivery requires a fluidization of the powder bed, it is conceivable that flow properties of powders could affect the emitted dose from the device and delivery of the vaccine to the nasal cavity.

The CCI and static angles of repose of the powders did not always agree with regards to which powders had a better ability to flow. The CCI identified both the bulk and sieved fractions of chitosan as free-flowing, while the static angle of repose results differed. This has been seen in the literature (Li, Rudolph et al. 2004). One potential reason for this occurrence is the adhesive forces of the chitosan to the graduated cylinder are greater that the energy put into the system by tapping, making it seem as if there is little difference between the bulk and the tapped densities. A majority of the powders did not flow well based on CCI, but did flow well based on static angle of repose. This was seen in all of the powders with fibrous shapes seen in SEM. The shape of these particles could have played a role in the differences between the bulk and tapped densities. Bulk and sieved fractions of SA exhibited good flow in both methods. Particle shape may also play a role due to their proximity to being spherical. CMC HMW did not flow well in either method.

3.3.3 Surface Area

The specific surface area of the powders was measured using nitrogen adsorption (Table 3.1). The specific surface area of the SFD powders (~1.2-1.7 m^2/g) was significantly greater than the bulk, sieved trehalose (~0.5 m^2/g). This is consistent with the literature (Maa, Nguyen et al. 1999; Costantino, Firouzabadian et al. 2000; Yu, Johnston et al. 2006).Surprisingly, the specific surface area of the 40 μm SFD formulation was greater than the specific surface area of the 25 μm SFD formulation. One potential explanation for this is that the 25 μm SFD formulation had a large proportion of its particles spherical, while the 40 μm SFD, though a majority of the particles were spherical, a substantial number were opened spheres and irregularly shaped particles.

3.2.4 Moisture Content

The moisture contents of the trehalose powders are shown in Table 3.1. Moisture content was low in SFD powders because of the lyophilization process. Lyophilized powders generally have 3-5% moisture present. The sieved trehalose, as a dihydrate, has greater moisture content (~10%) than the SFD powders (2.5-5.5%). The moisture contents of HPMC LMW and HPMC HMW (3-5%) were significantly lower than the other MA (>10%, Table 3.2).

3.3.5 True Density

The true density of the powders was measured using helium pycnometry. The true density of 25 μm SFD, 40 μm SFD, bulk trehalose, SFD were 1.5237 ± 0.0560 , 1.5750 ± 0.2168, and 1.5381 ± 0.0151 g/mL, respectively. The SFD process did not alter the true density of the starting material.

3.3.6 Thermal Analysis

Thermal scans of SFD powders and bulk trehalose are shown in Figure 3.2. In order to establish the characteristic Tg associated with the SFD amorphous solids, the powder had to be treated to remove the moisture. Consequently, powders were held at 60°C for 5 hours. The peaks of interest of the SFD powder are the Tg at 117°C, a crystallization peak at 174°C, and a sharp melting peak at 214°C. The results obtained, and shown in Figure 3.2, are consistent with that in the literature (Surana, Pyne et al. 2004). Bulk trehalose dehydrate exhibited a sharp peak at 100°C, indicating the removal of surface moisture. At ~120°C, the bound water of crystallization was removed from the trehalose dihydrate. The melting peak can be seen at 214°C. These curves indicate the production of an amorphous powder by SFD. The relatively high Tg indicate that the trehalose should be stable under normal handling conditions.

Thermal scans of the HPMC LMW (Figure 3.3) and HPMC HMW (Figure 3.4) were completed and exhibited a glass transition at 170°C (very subtle in HMW). The HPMC LMW degrades at 275°C, while the HPMC HMW degrades at 330°C, which is expected due to the increase in the molecular weight. CMC LMW (Figure 3.5) and CMC HMW (Figure 3.6) were examined. They both underwent an exothermic reaction at 290°C and 315°C. This is believed to be a thermal gelling phenomenon followed by disintegration. SA (Figure 3.7) demonstrated removal of water at 100°C and degradation at 200°C. Chitosan (Figure 3.8) exhibited water loss at 100°C and degraded at 310°C. All MA appeared stable under the normal handling conditions of a dry powder nasal product.

3.3.7 Physical Stability

A functional stability test of the vaccine was conducted. Vials containing liquid or powder samples were stored under the following conditions: 4°C and 50% RH, 23°C and 40% RH, 37°C and 80% RH, which were as close to standard conditions of refrigeration, room and accelerated storage (5 ± 3°C, 25 ± 2°C and 60 ± 5% RH, 40 ± 2°C and 75 ± 5% RH, (FDA 2003)) as was possible with existing equipment. Samples were taken at different time points for determination of HA titers for up to 12 weeks. Experiments were run in duplicate to allow for more time points due to a limited amount of the high-cost WIIV. The HA titers of each formulation at different time points were compared to week 0 sample (without storage) of the same formulation and percentage change in HA titer was taken as an indicator of sample stability (Figure 3.9). At 4°C and 50% RH, powder vaccine retained 100% of HA activity for the duration of the 12 weeks. However, the HA activity of the liquid formulation under these conditions dropped to 75% after week 2. Similarly, at 23°C and 40% RH, the powder vaccine retained 100% of HA activity, whereas the HA activity of the liquid dropped to 50% at week 2 and was further reduced to 25% of pre-storage levels at week 8. The powder formulation showed a drop in stability over time under the accelerated storage conditions (37°C and 80% RH). Under these conditions HA activity was reduced to 75% of pre-storage levels by week 2 and 50% by week 4, decreasing to only 6.25% of activity remaining by week 12. Nonetheless, the powder formulation was still more stable than the corresponding liquid, which lost 100% of activity by week 8. These results demonstrate that the vaccine storage stability exhibited by the powder formulation is improved with respect to liquid.

The high Tg and low moisture content (< 3%) of the trehalose are two important factors in the increased stability of the powder formulation. To assure the long-term stability of a biological macromolecules, particularly proteins and peptides, as a dried solid, the Tg of the amorphous phase must exceed the planned storage temperature (Pikal 1994; Carpenter, Pikal et al. 1997). Since water is a plasticizer of the amorphous phase, low residual moisture is needed to ensure stability (Carpenter and Chang 1996). The Tg of ~117°C far exceeds the maximum storage temperature that a powder product would experience. The loss of activity seen under accelerated conditions may be explained by the large surface area of the SFD trehalose particles. Greater stability might be achieved by optimization, with control of surface area as an objective in a designed experiment.

3.3.8 Impact Energy Separation

Microscopy was utilized to characterize the size and distribution of particles detached from the impaction surface as a function of impact energy (Table 3.3). The size of which 84% of particles are less than (D_{84}) remaining on the sapphire disc following impact decreased with the logarithm of increasing impact energy, as shown in Figure 3.10. Smaller particles were detached by the heavier hammer weights, resulting in a smaller D_{84} for all of the powders up to impact energies of 20 mJ. At energies greater than that, the D_{84} increased, indicating the formation of aggregates and particles from areas above the field of view detaching but reattaching at a lower point. Similar trends were observed for all powders evaluated by microscopy. The sample to sample variability was much greater for the bulk sieved trehalose than either of the SFD powders after impacts greater than 20 mJ. This may be due to the needle-like shape of the bulk sieved trehalose compared to the spherical shape of the SFD powders. Particle geometry has been shown to have an effect on adhesion when

comparing cylindrical and spherical particles (Mullins, Michaels et al. 1992). The increased contact area could result in a greater probability of the particles reattaching to the sapphire disc after detachment.

Figure 3.11 shows the D_{84} of sieved trehalose, 25 μm SFD, and 40 μm SFD particles remaining on a sapphire disc as a function of impact energy applied by a pendulum for the first four strikes of the pendulum. At impact energies of 5.0 and 11.1 mJ, the D_{84} of particles remaining for 25 μm SFD was significantly greater than the sieved trehalose and 40 μm SFD particles ($P<0.05$). The slope of the best fit line of the sieved and 40 μm SFD trehalose particles were similar, while the slope of the 25 μm SFD was much steeper. This is in agreement with the other flow properties of these powders. The 25 μm SFD had a greater CCI and static angle of repose than the sieved and 40 μm SFD trehalose powders.

3.3.9 Modified Cascade Impactor

There is interest in needle-free approaches using small, convenient, unit-dose delivery systems to facilitate mass vaccination (Giudice and Campbel 2006). The development of devices for dry powder nasal vaccine formulations has recently been discussed in detail (Sullivan, Mikszta et al. 2006). Particle delivery systems require characterization by relevant sizing methods. An inertial impaction method, designed to sample and size particles dispersed in air, would be a valuable tool in determining potential for particles to deposit in the nasal cavity and the fraction of the powder, in various size ranges, that would pass through this region and enter the lungs. The latter component is undesirable as the lungs are not the intended route of administration and may be the site of potential toxicity. Inertial impactors, operated under conventional conditions, do not sample particles above 10 μm but it is known that substantial quantities of particles in the 10-20 μm size range can deposit in

the lungs when inhaled through the nose. Since the impactor arrangement (stages employed and operating flow rate) requires particles >10 μm but < 20 μm (Bates, Fish et al. 1966)) to be sampled the instrument required calibration under the new conditions. Extensive experiments, involving the delivery of monodisperse aerosols, (Vibrating Orifice Aerosol Generator, Model 3450, TSI, Inc., Shoreview, MN) were conducted to map the collection efficiency curve (≥9 particle sizes, n=3) for each of the three stages of the impactor under defined sampling airflow conditions (15 L/min). These experiments are described in Appendix 2.

The mass of particles entering the impactor should be equivalent to the total mass of particles from each collection surface. However, this is rarely the case because not all particles impact on the collection surfaces. Mass balance may not be achieved, as some particles will not be recovered. These particles are commonly referred to as wall or inter-stage losses (Vaughn 1989). If these losses exceed 5%, the USP recommends that they be included with the associated collection surfaces (USP 2006). Initial experiments completed using the modified cascade impactor yielded a recovery of ~70% of the entering mass. It was determined that the solid center portion of the Stage -2 orifice plate was collecting a significant number of particles. Experiments were repeated, but the center of that orifice plate was coated, using the same method as that for the collection plates and washed separately with a known volume of phosphate buffer (pH 7.4). Recovery then increased to 99.9 ± 7.2%.

The dispersion properties of the 40 μm SFD formulation from both the MDS and BDT devices are shown (Figure 3.12). There were no significant differences between the mass fractions of powder collected on any portion of the modified cascade impactor. Approximately 50% of powder was collected in the inlet device, while no other stage

collected greater than 20%. A significant amount of powder (~15%) was recovered from the orifice plate for Stage -2. Less than 10% of the powder was collected on Stage -2, Stage -0, or the filter.

The recovered mass was adjusted for the amount of powder that left the device (Figure 3.13). There were no significant differences between the emitted dose (ED) fractions of powder collected on any portion of the modified cascade impactor. Over 60% of powder was collected in the inlet device, while no other stage collected greater than 20%. A significant amount of powder (~20%) was recovered from the orifice plate for Stage -2. Approximately 10% of the powder was collected on each of Stage -2, and the filter, while < 10% was collected on Stage -0.

The ED and lung dose fraction (LDF) are shown in Table 3.4. The LDF is the mass fraction of powder collected below the Stage -2. It represents the mass that could potentially enter the lower respiratory tract. There were no significant differences between the ED and LDF when comparing the two devices. This indicates that the dispersion properties of these devices are similar.

The use of a blended fluorescent label assumes that the shear on the particles upon dispersion is insufficient to separate the micronized fluorescein from the SFD trehalose. Inspection of the data (Figure 2.48, Chapter 2) shows that the fraction of the 40 μm SFD trehalose in the micron size range (0.22-12μm, those particles collected on the filter), as determined by laser diffraction was ~11%. This is approximately the same percentage of particles collected by the MCI with the fluorescein particles. Dissociation of micronized fluorescein from the trehalose particle would result in larger filter deposition than would be predicted by laser diffraction.

3.4 Summary

Powders manufactured by SFD, bulk trehalose, and MA were characterized. Bulk and tap densities, and the static angle of repose were measured to quantify the powders' potential ability to flow, which may be important for blending the virus and excipient with the mucoadhesive compound and subsequent powder dispersion. The surface area of the SFD powders was measured to assess the available surface and the extent of porosity. True density measurements were performed on bulk and SFD trehalose to determine if any changes to material density occurred during the SFD process. The moisture content and thermal analysis was performed to indicate the temperature at which physical transformations occur. Liquid and SFD powder vaccine formulations were stored for 12 weeks under a variety of temperatures and relative humidities to assess the stability of the formulations. Two devices were utilized with a calibrated, modified cascade impactor to characterize the dispersion properties of the 40 μm SFD trehalose.

Sieved trehalose and 40 μm SFD had lower CCIs than the 40 μm SFD trehalose. Based on CCI, 40 μm SFD was the only powder to be considered free-flowing. Bulk and sieved fractions of SA and chitosan were the only MA to be considered free-flowing. The static angle of repose of SFD rat was larger than 25 μm SFD and bulk, sieved trehalose, but all three powders are regarded as free-flowing. All of the MA were considered free-flowing with the exception of sieved CMC HMW, bulk chitosan, and sieved chitosan.

The surface areas of the SFD formulations were significantly greater than bulk trehalose, while the true densities of the SFD formulations and bulk trehalose were the same, indicating that the SFD process produced porous particles. The moisture content of the SFD

powders was significantly less than the bulk trehalose and the MA. Additionally, the thermal analysis indicated that the SFD powders were amorphous.

At 4°C and 50% RH and 23°C and 40% RH, powder vaccine retained 100% of HA activity for the duration of the 12 weeks, while the liquid formulation decreased in activity. Even at the most aggressive storage conditions (37°C and 80% RH), the powder performed better than the liquid formulation. These results demonstrate the improved vaccine storage stability provided by the powder formulation.

Impact energy separation can be a useful tool in characterizing the adhesive and cohesive forces of powders. With each successive strike of a pendulum, the D_{84} of particles remaining on the sapphire disc decreased at energies up to 20 mJ. Trends seen after increasing impact energies were in agreement with the flow properties of the powders.

Current cascade impactor protocols do not completely rule out nasal preparations entering the lower respiratory tract. The modified cascade impactor will give a more complete picture of the deposition of particles in the 10 to 20 μm size range. This method is significant in evaluating the powder that could potentially enter the lungs, which is undesirable as it may be associated with adverse effects. There were no significant differences between the mass fractions of powder collected on any portion of the modified cascade impactor, regardless of device. For the 25 μm SFD trehalose, there were no significant differences between the ED and LDF when comparing the two devices. This indicates that the dispersion properties of these devices are similar. These powders were further characterized with respect to: (specific aim 1) the physico-chemical properties of MA and their influence on residence time in the nasal cavity of the rat (Chapter 4) and; (specific

aim 2) immunogenicity of a dry powder whole inactivated influenza virus (WIIV) vaccine following nasal delivery to rats (Chapter 5).

Table 3.1– The flow properties, specific surface area, and moisture content of 25 µm spray-freeze-dried (SFD) trehalose, 40 µm SFD trehalose- human formulation, and sieved trehalose (Mean (SD), n=3).

Powder	Bulk Density (g/mL)	Tap Density (g/mL)	Carr's Compress. Index (CCI)	Static Angle of Repose (°)	Specific Surface Area (m^2/g)	Moisture Content (%)
25 µm SFD	0.2 (0.01)	0.3 (0.01)	34.8 (0.9)	36.1 (2.1)	1.25	5.39 (0.52)
40 µm SFD	0.1 (0.00)	0.1 (0.00)	19.3 (1.0)	25.4 (0.4)	1.65	2.42 (0.52)
Sieved*	0.5 (0.01)	0.6 (0.01)	23.0 (1.3)	21.6 (1.5)	0.49	9.64 (0.06)

* Published in (Garmise, Mar et al. 2006).

Table 3.2– Flow properties and moisture content analysis of bulk or 45-75 μm sieved fractions of a) hyrdroxypropyl methylcellulose (HPMC LMW), b) HPMC HMW, c) carboxymethylcellulose sodium (CMC LMW), d) CMC HMW, e) chitosan (Chit) and f) 45-125 μm sieved fraction of sodium alginate (SA, Mean (SD), n=3).

Powder		Bulk Density (g/mL)	Tap Density (g/mL)	Carr's Compress. Index (CCI)	Static Angle of Repose (°)	Moisture Content (%)
HPMC LMW	Bulk	0.5 (0.01)	0.6 (0.00)	22.20 (1.92)	32.15 (0.35)	3.53 (0.14)
	Sieved	0.5 (0.01)	0.6 (0.01)	23.45 (1.99)	31.42 (0.31)	
HPMC HMW	Bulk	0.3 (0.01)	0.5 (0.01)	25.37 (1.22)	37.71 (0.61)	5.47 (0.15)
	Sieved	0.4 (0.06)	0.6 (0.09)	24.03 (3.35)	34.10 (0.36)	
CMC LMW	Bulk	0.5 (0.01)	0.7 (0.01)	23.82 (1.44)	32.62 (1.60)	13.40 (0.01)
	Sieved	0.5 (0.01)	0.7 (0.01)	29.14 (1.90)	36.59 (1.02)	
CMC HMW	Bulk	0.5 (0.01)	0.7 (0.01)	29.96 (2.17)	36.53 (2.78)	13.33 (1.09)
	Sieved	0.5 (0.00)	0.6 (0.01)	28.73 (0.83)	43.20 (0.84)	
SA	Bulk	0.9 (0.02)	0.9 (0.03)	8.94 (1.54)	20.29 (4.35)	11.21 (0.01)
	Sieved	0.7 (0.003)	0.9 (0.01)	16.05 (1.07)	29.29 (1.56)	
Chitosan	Bulk	0.2 (0.01)	0.3 (0.00)	21.02 (1.12)	41.41 (1.45)	10.85 (0.16)
	Sieved	0.2 (0.00)	0.3 (0.00)	20.71 (1.09)	40.04 (3.03)	

Table 3.3– The diameter which 84% of particles remaining (D_{84}) on the surface of a sapphire disc after repeated striking with increased energy by an impact energy separation device (Mean (SD), n=3).

Energy (mJ)	25 um SFD	40 um SFD	Trehalose (45-75 um)
0.98	52.5 (5.1)	30.6 (2.6)	31.1 (3.8)
4.99	44.4 (5.5)	29.0 (4.7)	22.4 (4.8)
11.10	37.0 (9.8)	28.6 (6.9)	21.5 (7.0)
19.38	18.0 (3.7)	18.5 (3.2)	18.0 (11.1)
41.42	29.0 (8.9)	27.1 (0.5)	12.8 (3.5)
64.43	32.0 (9.9)	23.8 (3.4)	25.0 (16.6)
83.67	17.3 (8.5)	8.9 (0.3)	21.9 (15.8)
101.25	16.6 (7.2)	8.5 (0.7)	19.5 (13.7)

Table 3.4– The emitted dose (ED) and lung dose fraction (LDF) of 0.05% fluorescein in 40 μm SFD trehalose from a monodose insufflator and a Becton Dickinson Technologies (BDT) device (Mean ± SD, n=5).

Device	ED (%)	LDF (%)
Monodisperse insufflator	85.3 ± 5.4	10.3 ± 1.9
BDT device	81.6 ± 6.7	11.8 ± 3.4

Figure 3.1– The modified three-stage Andersen cascade impactor, with FDA guidance document induction port, for nasal product characterization.

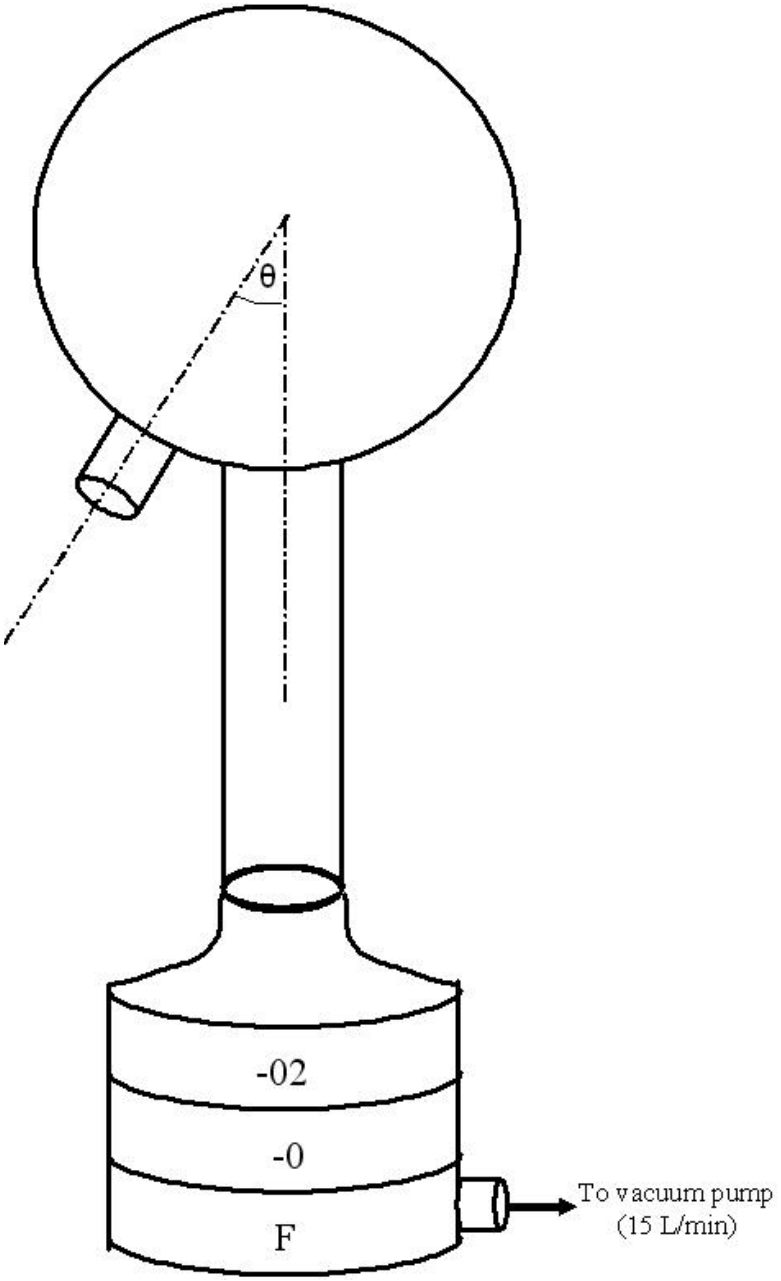

Figure 3.2– Differential scanning calorimetry (DSC) heating scans of: A) spray-freeze-dried (SFD) human and B) bulk trehalose. Following drying at 60°C for 5 hours, the 40 µm SFD trehalose samples were heated to 250°C at 10°C/min. The 40 µm SFD trehalose was also scanned at 40°C/min to better resolve the Tg at ~110°C. Bulk trehalose was not pre-treated and was heated from room temperature to 250°C at 10°C/min.

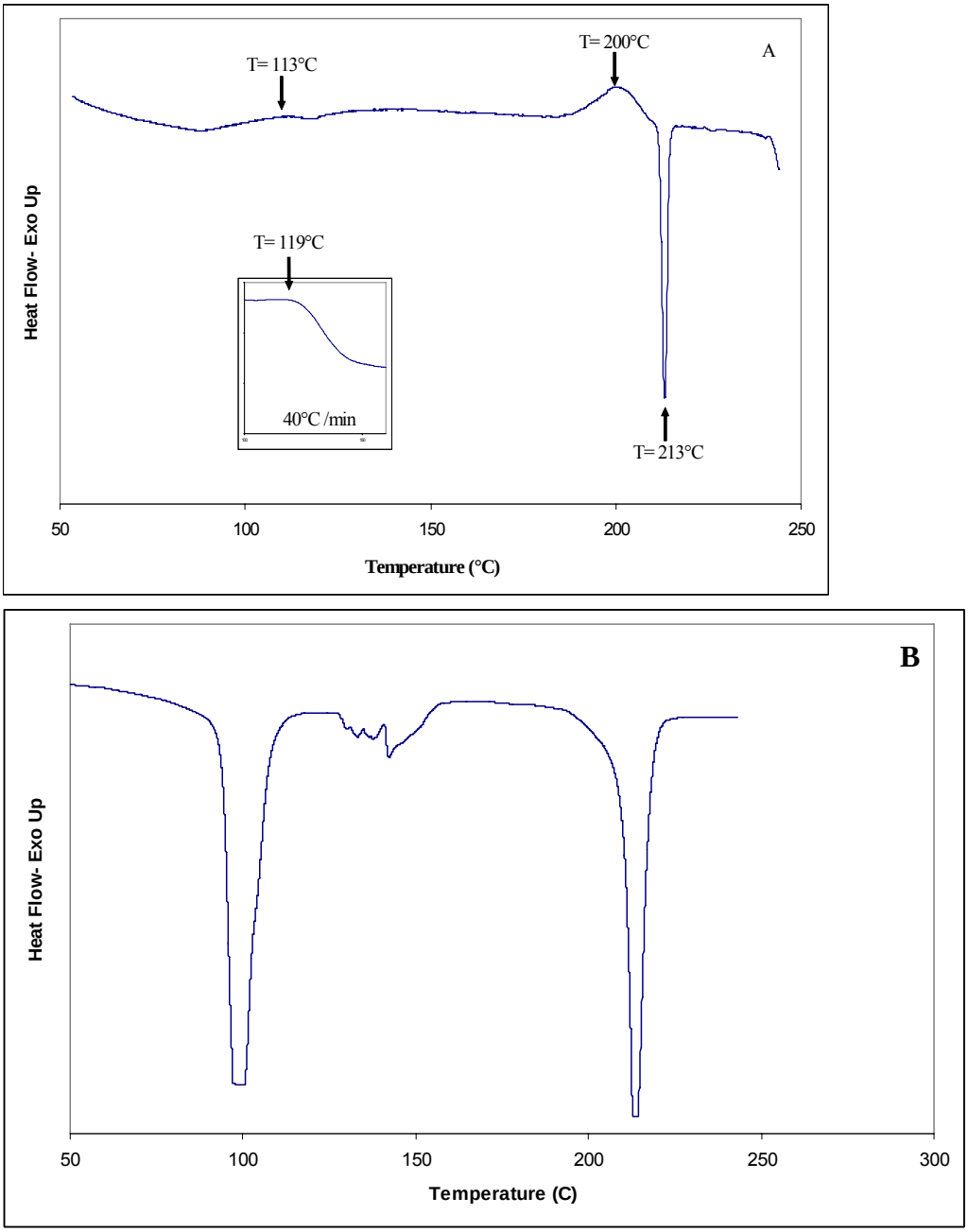

Figure 3.3– Differential scanning calorimetry (DSC) heating scans of hydroxypropyl methylcellulose (HPMC LMW) powder heated from 10°C to 250°C at different heating rates.

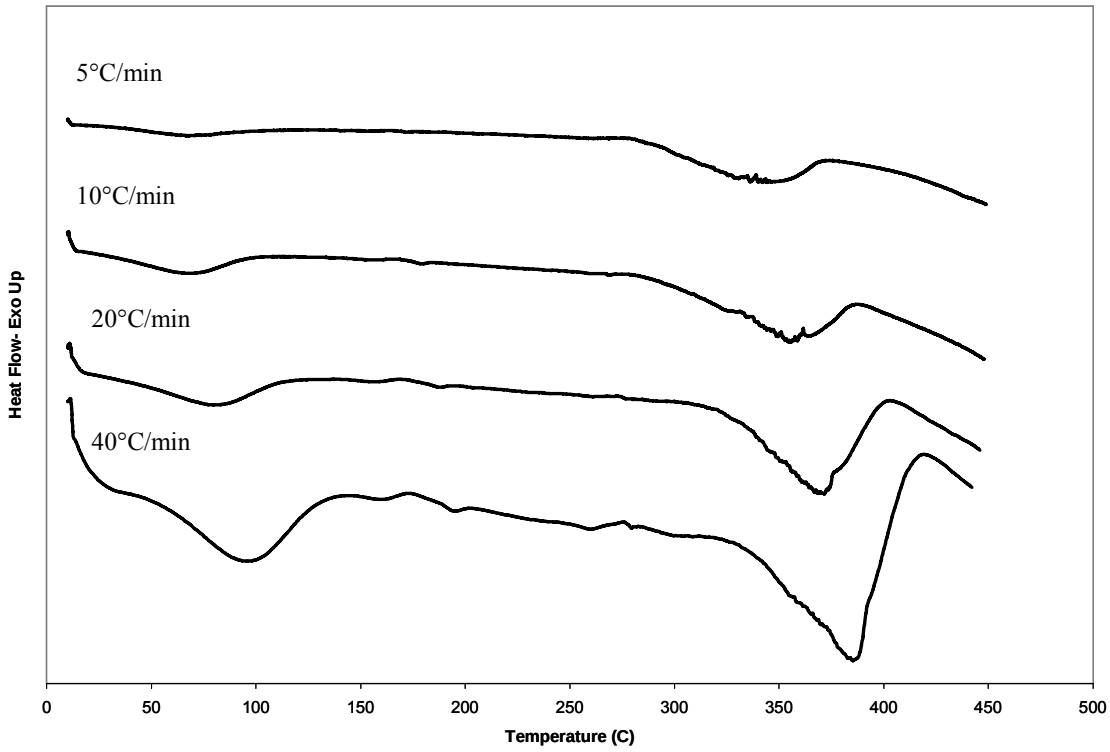

Figure 3.4– Differential scanning calorimetry (DSC) heating scans of hydroxypropyl methylcellulose (HPMC HMW) powder heated from 10°C to 450°C at different heating rates.

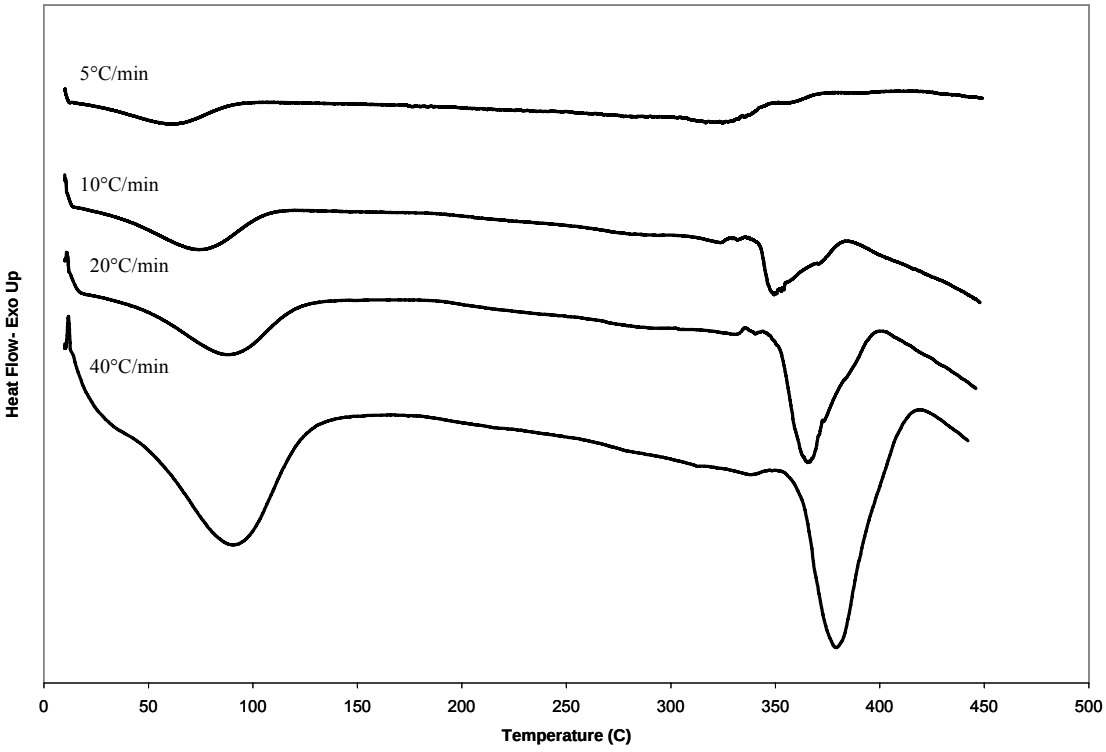

Figure 3.5– Differential scanning calorimetry (DSC) heating scans of carboxymethylcellulose sodium (CMC LMW) powder heated from 10°C to 450°C at different heating rates.

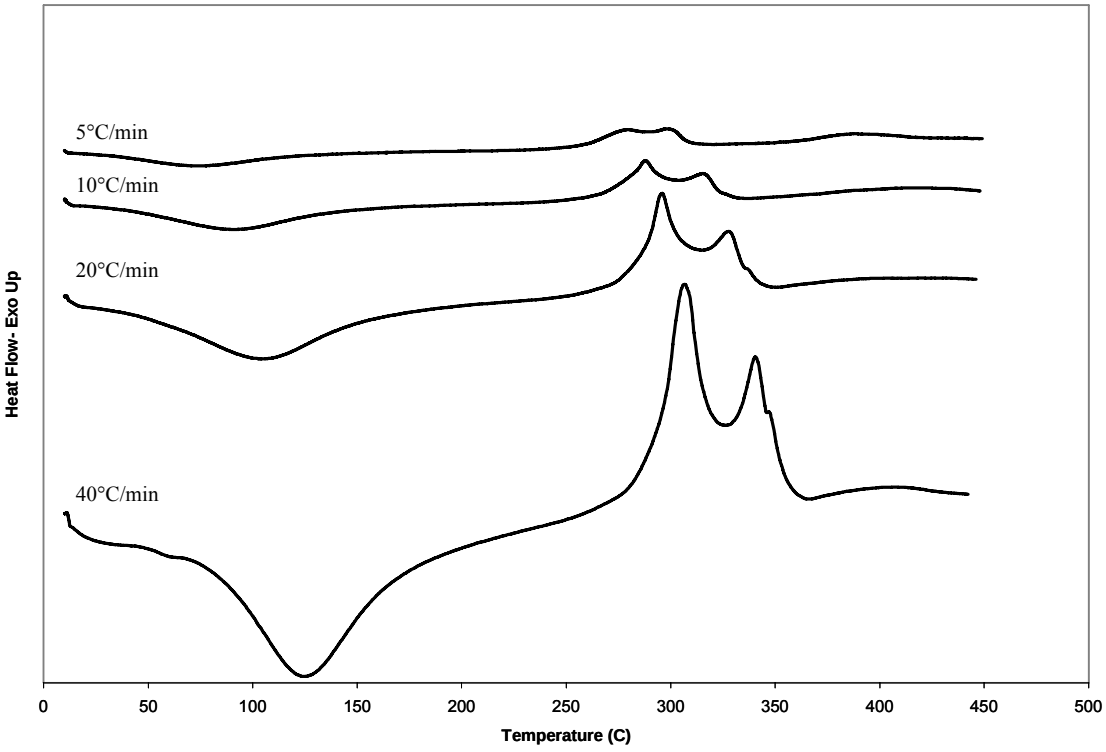

Figure 3.6– Differential scanning calorimetry (DSC) heating scans of carboxymethylcellulose sodium (CMC HMW) powder heated from 10°C to 400°C at different heating rates.

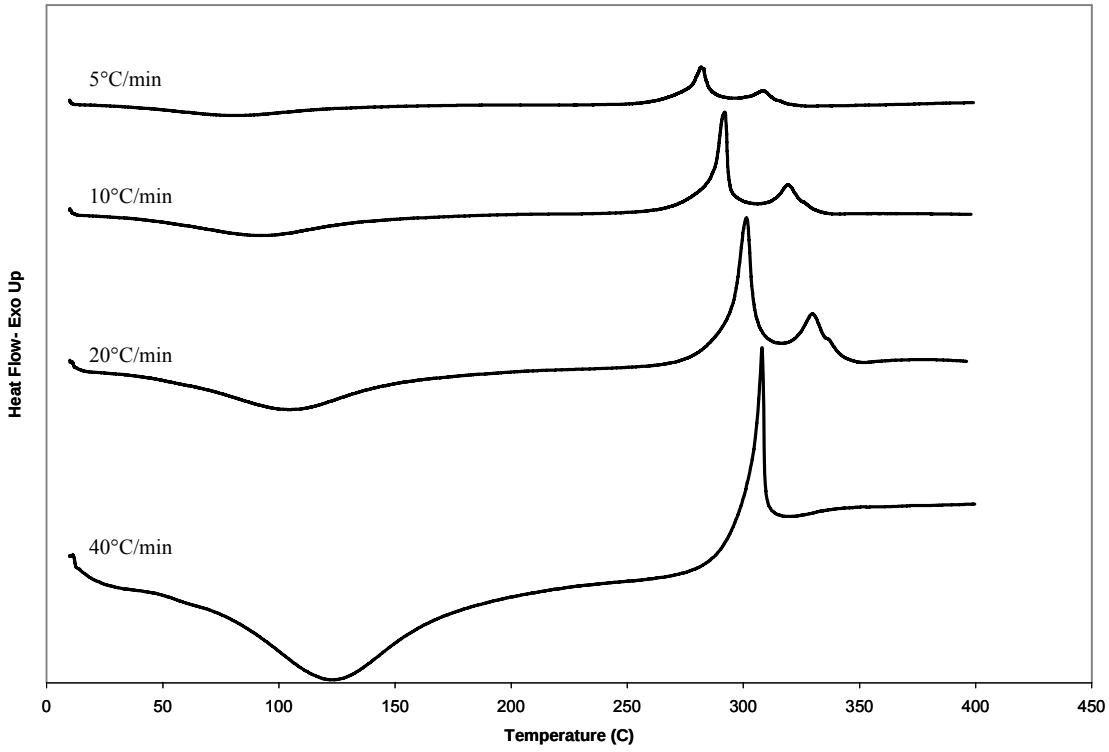

Figure 3.7– Differential scanning calorimetry (DSC) heating scans of sodium alginate (SA) powder heated from 10°C to 325°C at different heating rates.

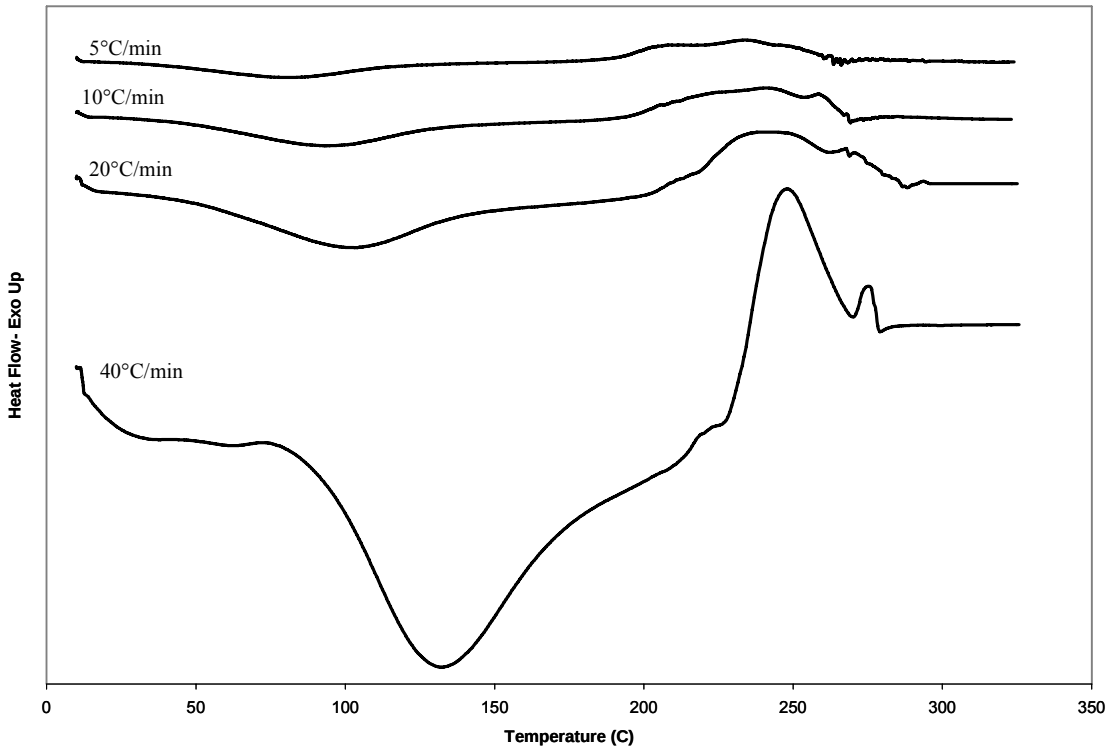

Figure 3.8– Differential scanning calorimetry (DSC) heating scans of chitosan powder heated from 10°C to 375°C at different heating rates.

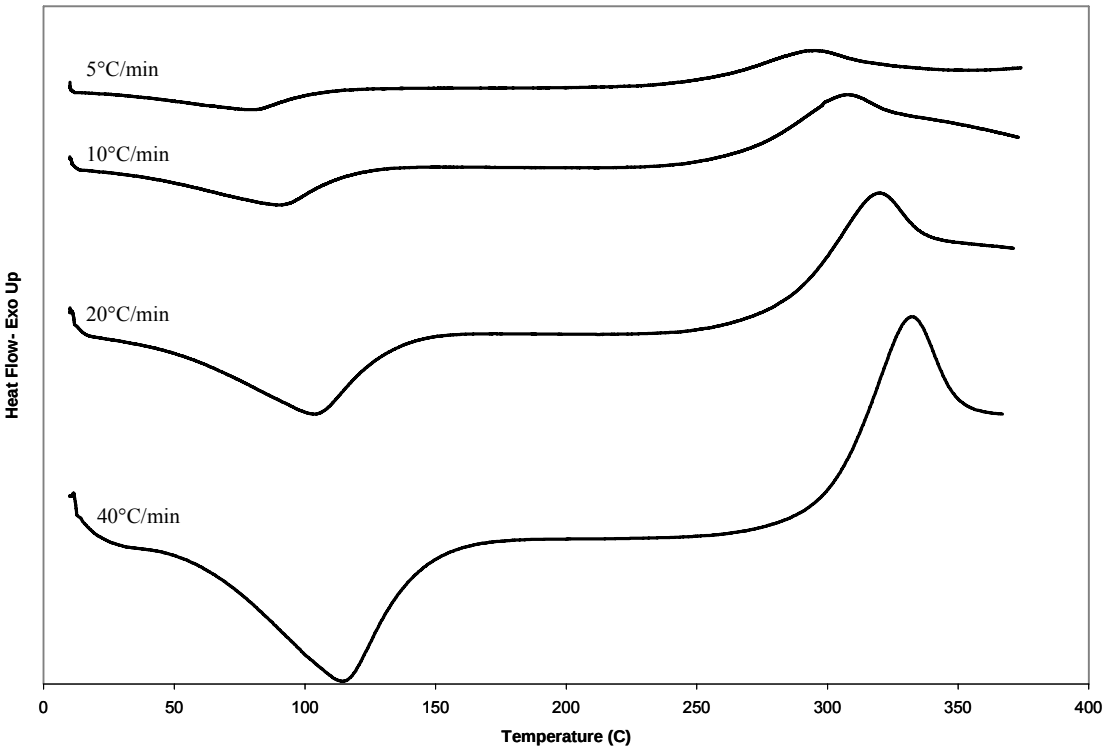

Figure 3.9– Vaccine stability study performed on liquid (open square) or powder (closed diamond) vaccine stored under the following conditions: A) 4°C, 50% RH, B) 25°C, 40% RH, and C) 37°C, 80% RH. The HA titers of each formulation at different time points were measured and compared to the week 0 sample (without storage) of the same formulation. Each data point represents the mean of duplicate samples.

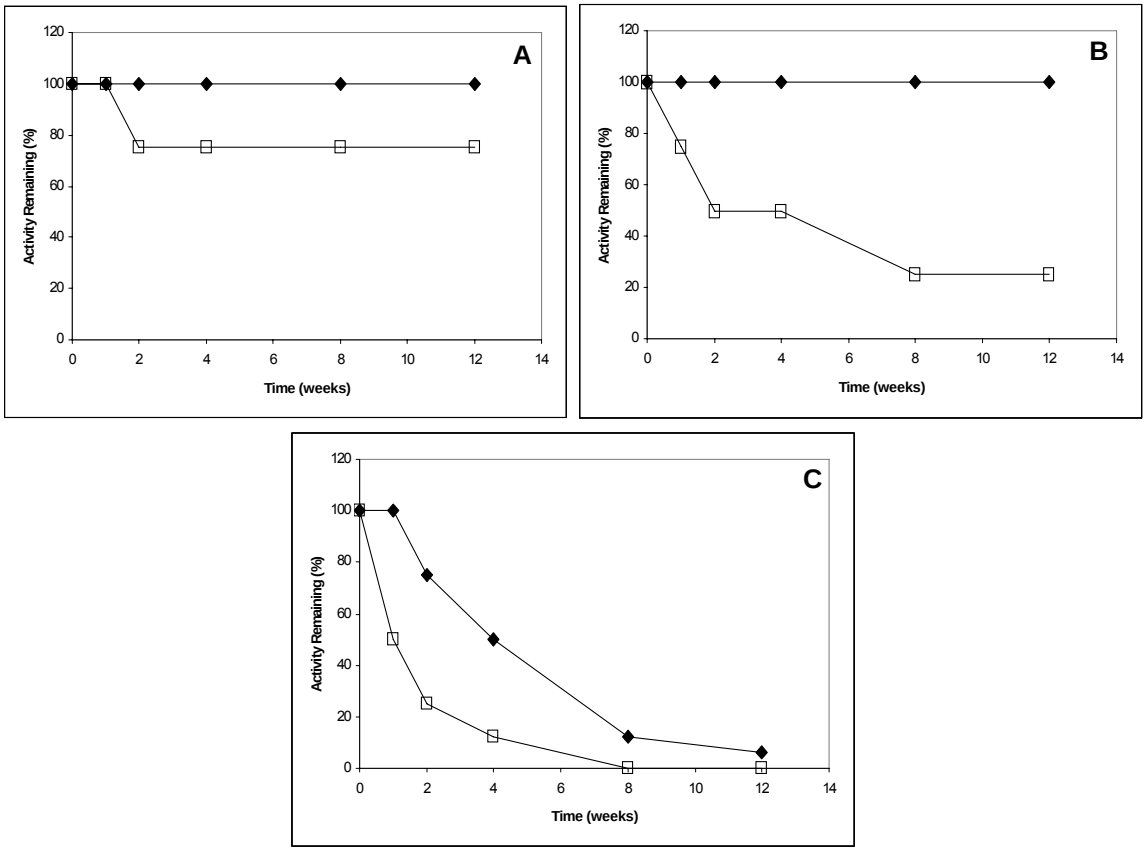

Figure 3.10– The diameter at which 84% of particles are less than (D84) of sieved trehalose, 25 µm spray-freeze-dried (SFD), and 40 µm SFD particles remaining on a sapphire disc as a function of the logarithm of impact energy applied by a pendulum (mean).

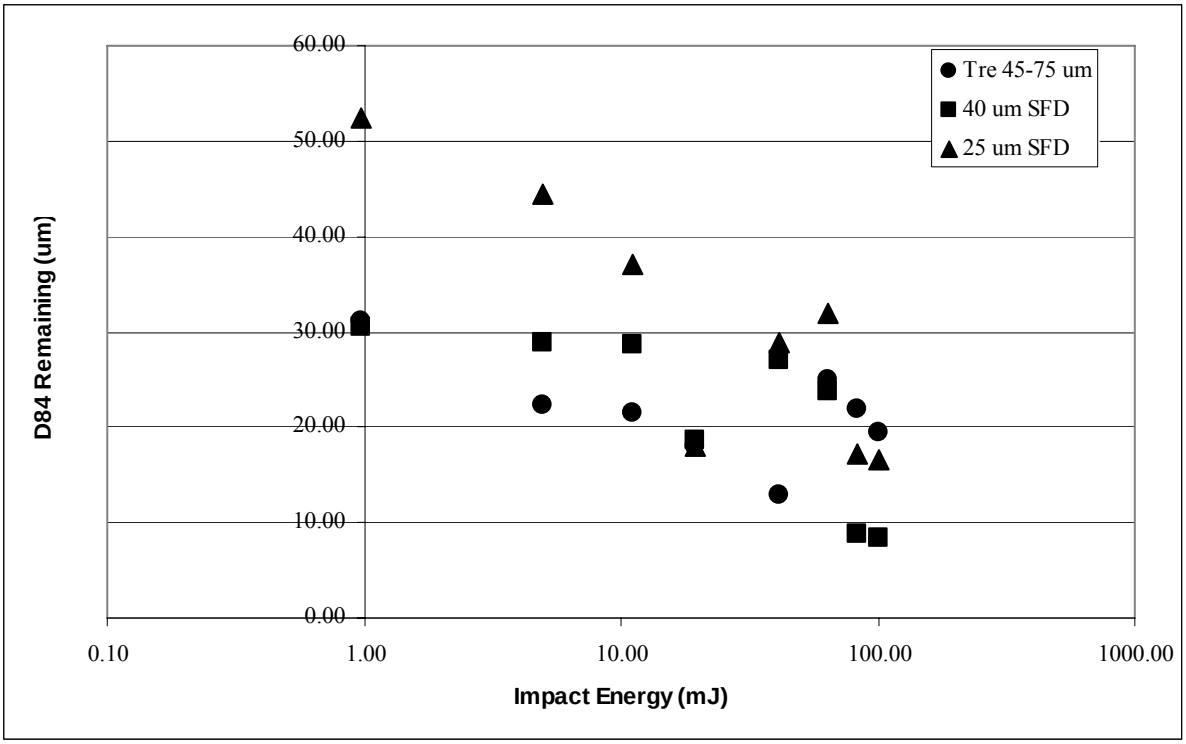

Figure 3.11– The diameter at which 84% of particles are of smaller diameter (D_{84}) for sieved trehalose, 25 µm spray-freeze-dried (SFD), and 40 µm SFD particles remaining on a sapphire disc as a function of impact energy applied by a pendulum (mean, SE).

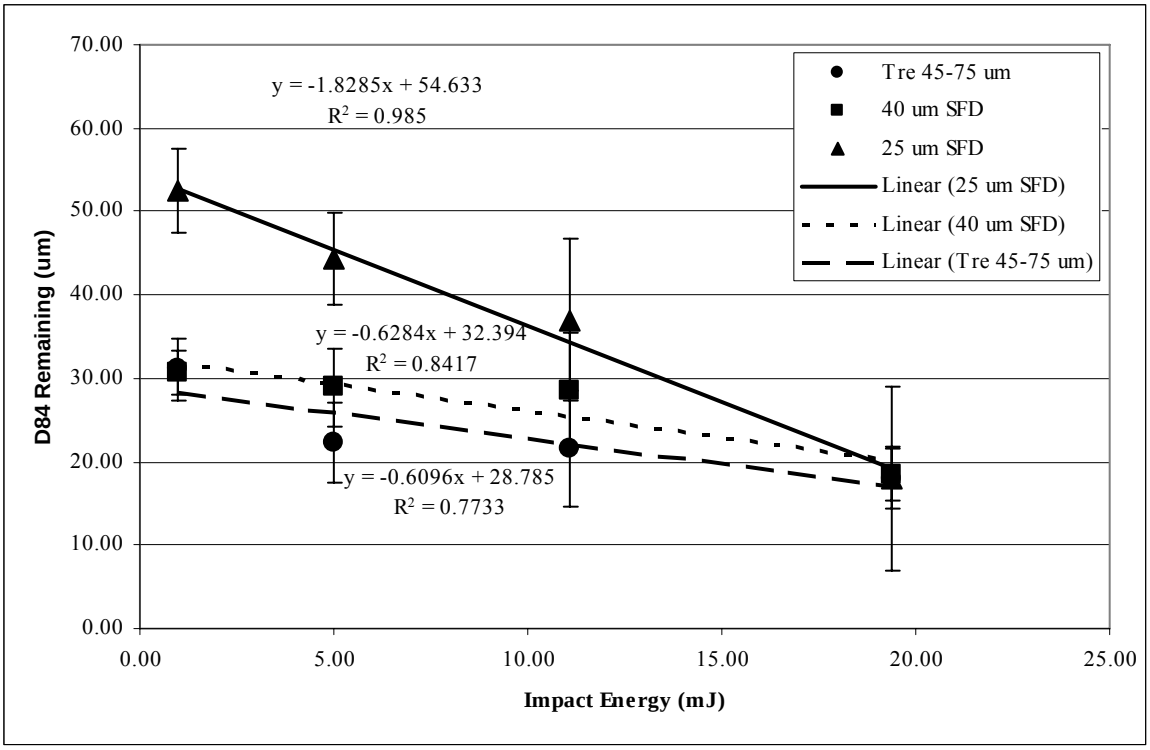

Figure 3.12– The mass fraction of 0.05% fluorescein in SFD human trehalose dispersed from the monodose insufflator (MDS) and the Becton Dickinson Technologies (BDT) device in the modified cascade impactor (mean ± SD, n=5).

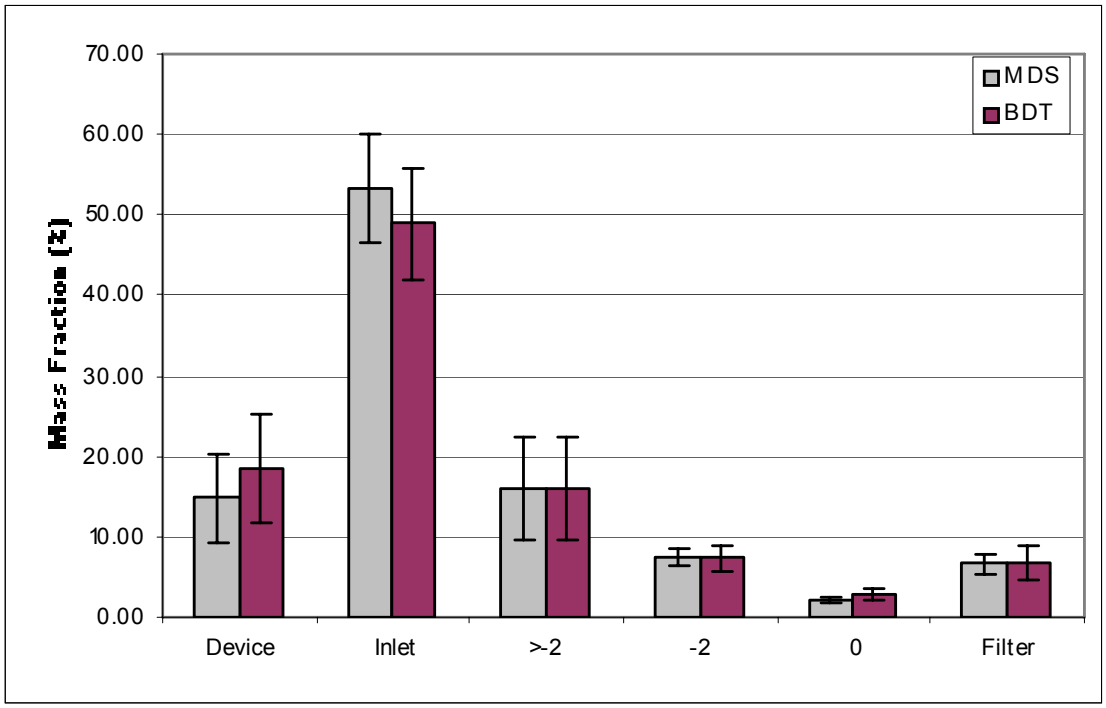

Figure 3.13– The mass fraction of the emitted dose of 0.05% fluorescein in SFD human trehalose dispersed from a monodose insufflator (MDS) and the Becton Dickinson Technologies (BDT) device in the modified cascade impactor (mean ± SD, n=5).

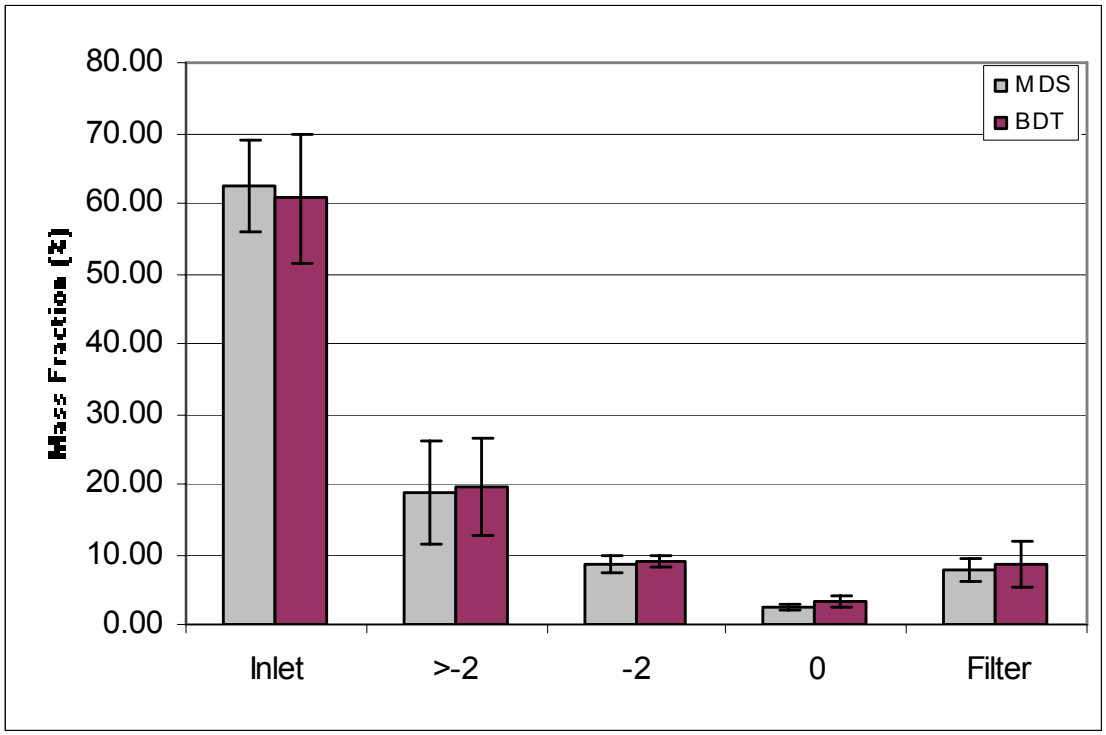

4 EFFECTS OF MUCOADHESIVE COMPOUNDS

4.1 Introduction

Residence time on the nasal mucosa is a determinant of effectiveness of vaccine delivery and response (Bacon, Makin et al. 2000). To afford protection vaccines must present antigen to the target nasal-associated lymphoid tissue (NALT). Mucoadhesive compounds (MA) have been studied to prolong the residence time on a mucosal surface (Aspden, Mason et al. 1997; Soane, Frier et al. 1999; Bacon, Makin et al. 2000; Ugwoke, Agu et al. 2000; Ugwoke, Agu et al. 2000; Illum, Fisher et al. 2001; Soane, Hinchcliffe et al. 2001; Cheng, Dyer et al. 2005). However, most of these systems utilize liquid formulations containing MA in solution. Powder systems require dissolution/hydration to occur for the system to be effective in impeding mucociliary clearance. Release of the active component from a powder to the nasal cavity must take into account wettability, dissolution rate, and the interaction between adjacent MA particles and mucus.

Dissolution rate is an important characteristic of a dry powder for nasal delivery, Particle size and morphology influence wetting and the rate of dissolution (Behl, Pimplaskar et al. 1998). In order for the immersion of a solid in a liquid to occur, the liquid must displace air and spread over the surface of the solid (Gennaro and Remington 1995). The contact angle a liquid droplet makes at the surface of a solid reflects powder wetting. While lyophilized formulations tend to dissolve easily in aqueous solutions, solid MA can induce varying contact angles that may result in delayed or prolonged effect compared to the same compounds in a liquid formulation.

Particle swelling, or hydration, influences mucoadhesion. There are conflicting reports regarding any direct correlation between swelling and mucoadhesion (Ch'ng, Park et al. 1985; Bottenberg, Cleymaet et al. 1991). The rate and extent of swelling may be important for the action of MA (Banker and Rhodes 1989). Polymer swelling is conducted by exposing polymer to a relevant solvent and measuring its uptake as an increase in mass (Gennaro and Remington 1995).

Mucus is a viscoelastic fluid. Its behavior can be described mathematically in terms of viscosity (Newtonian or non-Newtonian) and elasticity (Young's modulus) components. In order to consider the influence of a mucoadhesive powder on mucus displacement, its effects on rheological properties must be considered. MAs are thought to influence the viscous component of mucus behavior. Viscosity, η, is the resistance of a fluid to flow (Martin and Bustamante 1993). Increasing viscosity of a solution increases its resistance to flow. The force per unit area required to induce flow is called the shear stress. The difference in velocity between two planes of liquid is known as the shear rate. Viscosity can be determined from the ratio of shear stress to shear rate.

For systems in which the shear stress is directly proportional to the shear rate, the system is classified as Newtonian. However most pharmaceutical formulations do not exhibit this proportionality and are referred to as non-Newtonian (Martin and Bustamante 1993). There are three types of non-Newtonian systems: plastic, pseudoplastic, and dilatant (Gennaro and Remington 1995). Plastic flow usually occurs in colloidal solutions and emulsions and is characterized by the curve of shear stress versus shear rate intersecting the shear stress axis above the origin. This indicates that a shear stress of a certain value must be exceeded for flow to occur. The stress that needs to be overcome is the value at the point off

intersection with the axis and is known as the yield stress. Below the yield stress, the substance acts as an elastic material. Pseudoplastic flow, which can be seen in liquid dispersions of tragacanth, sodium alginate, methylcellulose, and carboxymethylcellulose sodium, is characterized by a decrease in viscosity with an increasing shear rate (Martin and Bustamante 1993). This is the case because these long-chain macromolecules align, as the shear stress is increased. Therefore, internal resistance decreases (shear-thinning). Dilatant flow, which usually describes suspensions with a high percentage of dispersed solids, is indicated by a volume increase as it is sheared (shear-thickening). The MA used in these experiments have characteristic structures they might be anticipated to exhibit pseudoplastic flow in solution.

There are numerous instruments available for the determination of viscosity of a solution (Gennaro and Remington 1995). They include, but are not limited to the capillary, cone and plate, cup and bob, and falling sphere. However, choice of instrument is dependent on whether the system is Newtonian or non-Newtonian. For an instrument such as the capillary viscometer, a constant shear stress is applied, by gravity, and this allows measurement of the viscosity at a single point. On the other hand, an instrument such as the cone and plate viscometer can vary the shear stress applied and can be used to characterize both Newtonian and non-Newtonian systems. In the present studies two instruments were employed: an Ostwald viscometer to estimate the Newtonian viscosity of dilute solutions and a cone and plate viscometer to estimate non-Newtonian viscosity of more concentrated solutions.

The ultimate measure of the effectiveness of a MA in retarding mucociliary clearance is *in vivo* evaluation by direct imaging or indirect mass balance methods. Both techniques

require marker compounds and sensitive detection systems. The radioisotope, technetium, ^{99m}Tc, may be employed as a marker in scintigraphy studies and is frequently used for this purpose in both animals and man (Newman, Pitcairn et al. 2004). The half life of ^{99m}Tc is 6 hours, which is convenient for use in these types of studies (Gennaro and Remington 1995). The gamma ray energy of ^{99m}Tc is 140 KeV, which may be detected with a gamma camera. The risk of radiation to exposed patients/workers is low because ^{99m}Tc emits few beta-rays. Also, ^{99m}Tc is readily available in hospitals because it is widely used for diagnostic imaging (DiPiro 1997). This marker is usually associated with colloid in order to conduct mucociliary clearance studies to eliminate the potential for another clearance mechanism, absorption, to interfere with measurements (Lay, Berry et al. 1995).

This chapter describes the evaluation of polymer powders for their potential as mucoadhesives. The wettability of these powders was determined by measuring the contact angle. The swelling index of polymer powders was measured. Powder dissolution in phosphate buffer was conducted. Deposition and clearance of a liquid formulation was imaged using a radiolabeled solution in a rat. Finally, the residence time of the formulation in the nasal cavity of rats was measured by conducting nasal lavage mass balance studies using a radolabeled powder and scintillation counting.

4.2 Methods

In Vitro Characterization

4.2.1 Wettability

Compacts of MA alone were manufactured using a single station tablet press (Carver Press, Model C, Wabash, IN) and flat-faced circular punches (Elizabeth Carbide Co,

Elizabeth Township, PA). The contact angle of a 10 μL drop of phosphate buffer (pH 6.0) on their surface was observed by light microscopy (n=3). Images of the droplet were captured by a digital camera (Nikon Coolpix 5000, Sony Corporation, Japan) and the contact angle was measured with image analysis software (Image J, Chapter 2).

4.2.2 Rheology

4.2.2.1 Capillary Viscometry

Fifteen milliliters of phosphate buffer solution (pH 7.4) were equilibrated in a water bath (American Scientific Products, Model BT-23, McGraw Park, IL.) at 37.0 ± 0.5°C. Excipient powder (1.5 g) was poured onto the surface of the buffered solutions. Stirring was achieved by means of a magnetic stir bar placed in the buffer (Flexa Mixer, Fisher Scientific, Pittsburgh, PA). Measurements were taken at 0, 15, 30, 45, and 60 minutes for unstirred systems and at 0, 5, 10, and 15 minutes for stirred systems with each time point performed as an independent sample (n=3). The latter sample periods were adopted in response to the rapid dissolution rates under stirred conditions. After each measurement, solution was removed from the vial, filtered with a 5 μm filter, and stored at 37°C. Solution density was measured by weighing a known volume of sample. Solution viscosity was determined using a capillary viscometer (Ubbelohde Type 1 or 1b, Schott Gerate, Hofheimi a. Ts, Germany) and a Schott Gerate AVS 400 measuring unit coupled with a thermostat (CT 1450). The temperature was maintained at 37 ± 0.2°C (Manufacturers specification for thermostat). The kinetic energy correction term of the viscometer is presumed to be within experimental error attributable to the instrument and was, therefore, neglected, according manufacturer's instructions.

4.2.2.2 Cone and Plate Viscometry

One and a half milliliters of 1% MA in phosphate buffer solution (pH 7.4) were applied evenly on the plate of a cone and plate viscometer (Bohlin Gemini, Malvern Instruments Ltd., Worcestershire, UK) at 37.0 ± 0.1°C. Each solution was analyzed in triplicate.

4.2.3 Polymer Swelling

Compacts (300 ± 15 mg) containing MA alone were manufactured by the single station tablet press and circular, convex punches. Each compact was placed in a USP type I dissolution basket, weighed, submerged in forty milliliters of phosphate buffer solution (pH 6.0) and equilibrated in a water bath (American Scientific Products) at 37.0 ± 0.5°C. The experiments were conducted under unstirred conditions, relevant to the nasal cavity, requiring that the dissolution baskets were not rotated. After a fixed time interval, excess fluid was removed and the sample was weighed. Weights were taken at 0, 5, 10, 15, 30, and 60 minutes (n=3), with each time point representing an independent sample. Additional experiments were carried out to establish maximum swelling. The swelling index (SI) was calculated by dividing the difference between the final and initial weights of the compact by its initial weight.

In Vivo Characterization

Animal Care

Female Brown Norway rats (125–175 g, Charles River, Raleigh, NC) were kept under standard conditions in AAALAC approved facilities under IACUC approved protocol (06-265.0-A). The animals were kept in a controlled temperature room (22 ± 1°C with 12 hour

light and dark cycles and had free access to food and water. Rats were anesthetized by intraperitoneal injection of 40 mg/kg ketamine, 2 mg/kg xylazine and 0.75 mg/kg acepromazine before immunization.

4.2.4 Gamma Scintigraphy

The radiolabeled tracer, ^{99m}technetium-sulfur colloid (^{99m}Tc-SC), was used to gauge deposition of delivered activity and the subsequent course of clearance from the nasal cavity by mucociliary transport with a γ-camera (Picker Dyna Camera 4, Picker, Northford, CT). The camera was set with an 18% window around the peak energy of ^{99m}Tc (140 KeV) and was shielded with a pinhole collimator. Pinhole collimation provided the adequate spatial resolution necessary for distinguishing location and retention of radioactivity within the nasal cavity. The labeled colloid solution was freshly prepared according to the manufacturer's (Cis, Bedford, MA) instructions, and is nonpyrogenic, isotonic, and at a neutral pH. Preparation of ^{99m}Tc-SC from commercial kits with the thiosulfate method is reported to produce polydisperse sub-micrometer particles (Lay, Berry et al. 1995). The particle size of the readiolabeled colloid was measured by dynamic light scattering of the sample suspension (Nicomp Model 370 Particle Sizing Systems, Santa Barbara, CA). An anesthetized, female Brown Norway rat (200g) was imaged in supine position following pipette aspiration delivery to the nostrils of 25 uL saline containing approximately 10 μCi of ^{99m}Tc-SC for 30 minutes, with 120 second frames. The camera was set with an 18% window around the peak energy of ^{99m}Tc and was shielded with a pinhole collimator. Activity levels were adjusted for radioactive decay using the equation:

$$X = X_0 e^{(-kt)} \tag{4.01}$$

where X_0 is the activity at time zero, X is the activity at a given time, t, C_o is the initial activity, and k is the decay constant.

4.2.5 Residence Time Study

Liquid formulations of saline or 1% MA in saline containing insoluble ^{99m}Tc-SC were delivered by placing 25 μL of solution into the right nostril of an anesthetized rat using a 10-100 μL pipette. Several methods were evaluated for radiolabeling powders. To label powder formulations, saline containing insoluble ^{99m}Tc-sulfur colloid were centrifuged at 12000 rpms for 10 minutes. Supernatant was removed and the pellet was washed three times with ethanol. The pellet was allowed to dry before being blended with the rat spray-freeze-dried trehalose with a mortar and pestle. Five milligram quantities were weighed out and placed in gelatin capsules (size 3, Capsugel, Greenwood, SC). An alternative method was thoroughly evaluated and appeared unsuitable for the purposes of the present study (Appendix 3).

Powder formulations were delivered using compressed air at 20 psig through a timed solenoid switch and a 100 μL pipette containing the contents of one dosage capsule in the right nostril of the anesthetized rat. The time points analyzed were 5, 15, and 120 minutes (n=3) and 30, 60, and 180 minutes (n=1). Rats were euthanized following cardiac puncture by CO_2 inhalation and nasal washes were collected by cannulating the trachea and rapidly instilling four aliquots of 1.5 mL of sterile saline. Fluid passed from the trachea through the nostrils was collected and analyzed in a radioisotope calibrator (Model CRC-4, Capintech, Inc. Pittsburgh, PA). All samples quantities were adjusted for radioactive decay.

4.3 Results and Discussions

In Vitro Characterization

4.3.1 Wettability

Contact angles are presented in Table 4.1. The contact angle is a measure of the forces of attraction/repulsion between the liquid and solid phase. On extremely hydrophilic surfaces, a water droplet will completely spread resulting in a contact angle of zero. This occurs for surfaces that have a large affinity for water, including materials that absorb water. On many hydrophilic surfaces, water droplets will exhibit contact angles of 10° to 30°. On highly hydrophobic surfaces, a large contact angle (70° to 90°) is seen. If no wetting occurs, then the contact angle is 180°. The contact angle directly provides information on the interaction energy between the surface and the liquid. The contact angle of the HPMC LMW (~41°) and HPMC HMW (~55°) were significantly greater than the other polymers ($P<0.05$, Figure 4.1). This is expected due to the hydrophobic nature of the HPMC functional groups. CMC, however, has more hydrophilic functional groups, which will interact with the aqueous solution, resulting in a lower contact angle (~29°). Chitosan had the smallest contact angle (~23°) and the portion exposed to the buffer swelled up, taking up the liquid into the compact. The results of these studies show the relative wetting to be HPMC HMW>HPMC LMW>CMC (HMW and LMW)>Chitosan which is consistent with the reverse relative propensity for influencing dissolution rate.

4.3.2 Rheology

The viscosity of the solvent was used as the quantitative measure for the concentration of MA in solution as a function of time in stirred and unstirred systems (Table

4.1). This is based on the assumption that solutions will be dilute and, therefore, will display a linear relationship between relative viscosity and concentration of polymer, according to Einstein equation (Hiemenz 1984). The viscosities of the CMC polymers and SA were significantly greater than the HPMC polymers ($P<0.05$) for both the unstirred and stirred systems. This coincides with the significantly greater contact angle seen in the HPMC polymers. For both the unstirred and stirred systems, the viscosities of the chitosan and 1% trehalose (0.74 ± 0.00 cps) were not significantly different than buffer alone ($P<0.05$). The viscosities of completely dissolved MA solutions were too great to be measured by the capillary viscometer, so the cone and plate viscometer was used. When completely dissolved, the viscosities of HPMC HMW and CMC HMW were orders of magnitude greater than the viscosities of the other solutions.

Beyond the effects of MA on viscosity as estimated in aqueous solutions, the influence of these materials on other mucus rheological properties is also important. The analysis of semisolids, such as mucus, requires a different approach than liquids. A semisolid demonstrates both the viscous properties of a liquid and the elastic properties of a solid. While the viscosity of a solution, as described above is determined by the ratio of shearing force to shearing rate, the elasticity of a solid is determined by the ratio of the stress to the strain. Once the cilia have penetrated the mucus, deforming it, the elasticity of the mucus will act to restore the mucus to its original shape. If the mucus does not have enough elasticity, it will not move like a sheet. On the other hand, if it is too elastic, it will not flow (Silberberg 1983). A viscosity around 15 cps is the optimal for mucociliary clearance (Chen and Dulfano 1978). Mucus samples from rats have been employed to demonstrate that the ratio between viscosity and elasticity is an important determinant of the mucociliary clearance rate.

However, significant variability in mucus transport occurs in response to other factors (Lorenzi, Bohm et al. 1992). These factors include, but are not limited to, disease (infection, cystic fibrosis), lifestyle factors (smoking), and drugs (ipatropium bromide, methacholine, norfloxacin).

4.3.3 Polymer Swelling

Swelling indices are presented in Table 4.2. The SI of the HPMC polymers is significantly lower than the other compounds at all time points ($P<0.05$, Figure 4.2). The SI of the CMC HMW and SA is significantly higher than the CMC LMW and chitosan at 60 min ($P<0.05$). The average time for particles to clear through the nasal cavity is 10-20 minutes in normal health human adults (Liote, Zahm et al. 1989). It has been suggested previously that an increase in the residence time in the nasal cavity can increase the immune response elicited by a dry powder nasal vaccine, but residence time data was not shown (Huang, Garmise et al. 2004). An ideal MA would be able to swell to absorb the excess liquid and increase the viscosity of the mucus, thus decreasing mucociliary clearance. In these experiments, CMC HMW and SA had a large SI consistent with the large effect on viscosity, noted above, at both the 15 and 60 minute time points.

In Vivo Characterization

4.3.4 Gamma Scintigraphy

The particle size characteristics of the 99mTc-SC were an average size of 650 nm, with a standard deviation of 60 nm. These were suitable for labeling the powders for nasal delivery as nanoparticles have been shown to coat the surfaces of large particles (Singh and Gao 1999).

The images illustrating the dynamic clearance of saline containing insoluble ^{99m}Tc-sulfur colloid are shown (Figure 4.2). At 0 (image 1), 2 (image 2), 16 (image 8), and 30 (image 16) minutes, the activities were (after decay correction) 3230, 3072, 2413, and 2078 cts/120sec, respectively. The saline was cleared at a rate of ~1%/min of the initial aspirated dose. One major disadvantage of using radiolabeled preparations was that the formulation is labeled, not the drug entity/biological. Images of the nasal cavity reflected the presence of the formulation, not necessarily the active component. This initial study demonstrated that there were limitations to conducting extended clearance studies from rodents following nasal delivery. Reproducible marker placement, liquid volume, efficiency of powder delivery, sensitivity of the camera, orientation of the head (body prone or supine), potential retrograde clearance, imaging with a parallel hole vs. pin hole were perceived variables that would require assessment (Newman, Pitcairn et al. 2001). The facility costs and camera time to conduct a thorough assessment of these variables were considered prohibitive by the collaborator on these studies.

4.3.5 Residence Time Study

Gamma scintigraphy imaging has proved a useful tool for imaging aerosol deposition but in light of the scope of a validation study an alternative approach was needed to assess the residence time of the formulation in the nasal cavity. A nasal lavage technique was utilized to recover the radioactivity remaining in the nasal cavity as a function of time. Each time point represents one animal. Replicates were completed for only half of the time points in order to conserve animals. The three time points chosen were indicative of the whole curve.

Initial experiments were completed with a novel labeling machine (Appendix A.4). However, this system was unable to remove all of the water content from the nebulized suspension. The remaining moisture caused the SFD- rat powder to collapse and aggregate. When the system was run for short periods of time to prevent the moisture uptake, radioactivity levels were just above than the detectable limit of calibrator, which was not suitable for three hour studies. An alternative admixture technique was adopted. A blend uniformity study was completed by weighing 5 mg of powder, placing the powder in a gelatin capsule, and scintillation counting was conducted. Each capsule was within a relative standard deviation of the target radioactivity.

Comparing the percentage of radioactivity as a function of time, the saline resided longer in the nasal cavity of the Brown Norway rats than the trehalose (Figure 4.3). Liquid and SFD powder formulations containing the MA and saline alone were compared. The curve for liquid HPMC HMW was similar to saline alone at the majority of the time points, but the powder HPMC HMW did not reside as long in the nasal cavity as the liquid formulations (Figure 4.4). The curve for powder CMC HMW was similar to saline alone at almost all of the time points, but the liquid CMC HMW seemed to remain in the nasal cavity longer than the saline and powder formulations (Figure 4.5). The liquid SA was similar to saline alone at almost all of the time points, but the powder SA seemed to initially be cleared faster than the liquid formulations and remain at the same level in the nasal cavity for the rest of the study (Figure 4.6). The powder chitosan was similar to saline alone at almost all of the time points, but lower quantities of radioactivity were detected for the powder chitosan at the 180 minute time point (Figure 4.7).

Regression analysis was performed by mathematically fitting the data to assess residence time differences (see Appendix 3). A two-compartment model was chosen because in most of the curves, there was an initial steep removal of radioactivity from the nasal cavity due to rapid unhindered clearance followed by a more gradual elimination attributable to material that is sequestered in some manner, perhaps adhered to mucus or epithelium. While mechanistically different, from a modeling perspective these phases may be considered equivalent to the distribution phase and the elimination phase after an IV bolus. The particle size of the ^{99m}Tc-SC is too large to be absorbed through the nasal epithelium; the only means of elimination is mucociliary clearance from the nasal cavity and being swallowed. The equation for a two-compartment model with elimination only from the central compartment after an IV bolus is:

$$y = ae^{(-bt)} + ce^{(-dt)} \tag{4.02}$$

where y is the radioactivity remaining and t is the time in minutes. The model was fit to the average value of replicates and each individual point. The correlation coefficient and parameters (a, b, c, and d) determined by the regression analysis are shown (Table 4.3). All of the curves exhibited good fit ($R^2 > 0.94$).

Parameters a and b are representative of initial clearance of the radioactivity from the nasal cavity. They compose the term of a two-compartment IV bolus equation that represents the distribution phase. With the exception of the liquid SA, the distribution constant (b) was larger for the powder formulations than the liquids. This is surprising because run-off and swallowing of the liquid formulations, unhindered clearance, was expected to account for a large, immediate decrease in the radioactivity remaining. However, the viscosity of 1% HPMC HMW and CMC HMW is much greater than 1% SA, which may explain the increase

in residence time. The powders with the least effect on viscosity (trehalose alone and Chitosan with trehalose) were initially cleared much more rapidly than the other formulations.

Parameters c and d are indicative of mucociliary clearance rate. They compose the term of a two-compartment IV bolus equation that represents the elimination phase. The elimination constant (d) was very similar for all of the liquid formulations and powder No MA, CMC HMW, and Chit, while the powder HPMC HMW and SA were significantly lower. These results are expected because HPMC HMW and SA exhibited the greatest viscosity, when fully dissolved, and swelling index, respectively. Based on the *in vitro* results, the powder CMC would be expected to have a lower elimination constant.

The area under the curve (AUC) can be used to determine the total amount of radioactivity in the nasal cavity for the duration of the experiments (Figure 4.8). The AUC of the liquid formulations were greater than all of the powder formulations, with the exception of SA. However, all of the AUCs except trehalose alone and HPMC trehalose were similar (roughly 8000-10000). The rank of the AUC of the liquid formulations (CMC HMW>HPMC HMW, SA>No MA) was consistent with the viscosities of the 1% solutions (HPMC HMW>CMC HMW>SA>No MA). However, it should be noted that larger viscosity does not directly correlate to great increased in residence time (No MA vs HPMC HMW). The rank of the powder formulations (SA>CMC HMW, Chit>HPMC HMW, No MA) was consistent with the contact angle (Chit<CMC HMW<SA<HPMC HMW), viscosity (unstirred at 60 minutes, SA>CMC HMW>HPMC HMW>Chit, No MA), and SI at 60 minutes (CMC HMW, SA>Chit>HPMC HMW>No MA).

4.4 Summary

In vitro experiments were performed to obtain data as potential predictors of the effect that mucoadhesive compounds (MA) may have on the residence time of liquid and powder preparations in the nasal cavity. Wettability of the powders was determined by placing a drop of buffer on a compact of the MA and measuring the angle formed by the droplet on the surface. The dissolution rate of the powders was determined by placing the powder on the buffer and measuring the viscosity of the buffer over time with a capillary or cone and plate viscometer in unstirred and stirred systems. Swelling indices were completed to determine the rate and amount of water uptake of the powders by placing compacts of the powders in buffer and measuring the weight gained by water uptake as a function of time. Gamma scintigraphy and residence time studies were completed to determine the effect of formulation on the residence time in the nasal cavity of Brown Norway rats.

The contact angle of the HPMC HMW and HPMC LMW were significantly greater than the other polymers, indicating a prolonged dissolution time. For both the unstirred and stirred systems, the viscosities of the CMC polymers and SA were significantly greater than the HPMC polymers. The swelling indices of CMC HMW and SA were significantly greater than the other MA. Gamma scintigraphy allowed for the visual imaging of clearance of saline from the nasal cavity of a Brown Norway rat. The residence time studies indicated that increasing the viscosity did not significantly increase the residence time. The serious implications of this observation for the subsequent immunogenicity studies, and for the clinical application of this approach, are taken up in more depth in the Chapter 6. Powder formulations required MA to achieve comparable residence times to liquid formulations with or without mucoadhesive in Brown Norway rats. The rank order of residence time for

powders is SA>CMC HMW, Chit>HPMC HMW, No MA. The *in vitro* and *in vivo* experiments indicate that SA and CMC HMW in powder formulations have the greatest effect on increasing residence time in the nasal cavity of Brown Norway rats. These MA were subsequently prepared in a dry powder influenza vaccine for nasal delivery to rats to determine if residence time in the nasal cavity correlates to the immune response elicited by the vaccine (Chapter 5).

Table 4.1– Contact angle and dissolution as measured by viscosity (unstirred and stirred systems) of hydroxypropyl methylcellulose (HPMC), carboxymethylcellulose sodium (CMC), sodium alginate (SA), and chitosan (Mean (SD), n=3).

Compound	Contact Angle (°)	Dissolution- Unstirred (Viscosity, η (cps))		Dissolution- Stirred (Viscosity, η (cps))		Viscosity, η (cps))
		15 min	60 min	5 min	15 min	1% w/v Solution
HPMC LMW	41.5 (0.9)	0.9 (0.0)	1.1 (0.0)	0.9 (0.0)	1.1 (0.1)	1.6 (0.8)
HPMC HMW	55.2 (2.0)	0.9 (0.1)	0.9 (0.1)	1.1 (0.1)	1.1 (0.1)	13183.1 (2166.5)
CMC LMW	28.6 (0.6)	1.5 (0.1)	3.3 (0.1)	1.4 (0.0)	2.3 (0.1)	3.9 (0.3)
CMC HMW	29.8 (1.5)	1.5 (0.2)	2.5 (0.8)	1.8 (0.4)	2.0 (0.1)	2334.2 (310.2)
SA	34.8 (1.1)	2.0 (0.7)	4.3 (0.6)	2.0 (0.7)	4.4 (2.6)	11.4 (0.6)
Chitosan	22.7 (2.9)	0.8 (0.0)	0.8 (0.0)	0.8 (0.0)	0.8 (0.0)	0.8 (0.0)

Table 4.2– Swelling indices of compacts of hydroxypropyl methylcellulose (HPMC), carboxymethylcellulose sodium (CMC), sodium alginate (SA), and chitosan (Mean (SD), n=3).

Compound	Swelling Index (SI)		
	15 min	60 min	Maximum Swelling
HPMC LMW	0.46 (0.12)	1.14 (0.02)	1.85 (0.29)
HPMC HMW	0.70 (0.02)	1.44 (0.00)	10.26 (0.43)
CMC LMW	1.51 (0.14)	2.37 (0.09)	2.84 (0.03)
CMC HMW	2.05 (0.09)	5.09 (0.24)	29.81 (0.65)
SA	2.02 (0.16)	4.70 (0.26)	8.18 (0.70)
Chitosan	1.90 (0.22)	2.11 (0.16)	2.13 (0.19)

Table 4.3– Correlation coefficient and parameters determined by regression analysis of two-compartment model curves determined by the % radioactivity remaining as a function of time in Brown Norway rats of liquid and powder formulations containing saline (liquid, No MA) and 1% hydroxypropyl methylcellulose (HPMC), carboxymethylcellulose sodium (CMC), or sodium alginate (SA) or trehalose alone (powder, No MA) and 3% HPMC, CMC, SA, and chitosan (Chit).

	Liquid Formulations				Powder Formulations				
	No MA	HPMC HMW	CMC HMW	SA	No MA	HPMC HMW	CMC HMW	SA	Chit
r^2	0.99	0.96	0.97	0.97	0.94	0.99	0.94	0.99	0.95
a	43.06	28.41	34.26	16.82	51.88	72.86	43.80	51.19	34.32
b	0.0631	0.2099	0.094	46.35	4762871.86	0.2272	0.5548	0.2455	12956
c	55.33	72.03	63.95	83.18	48.12	27.34	56.20	48.67	65.68
d	0.0028	0.0043	0.0021	0.0058	0.0057	.0000893	0.0034	0.0002	0.0050

Figure 4.1– Contact angle (θ) of phosphate buffer (pH 6.0) on compacts of hydroxypropyl methylcellulose (HPMC), carboxymethylcellulose sodium (CMC), sodium alginate (SA), and chitosan (Chit).

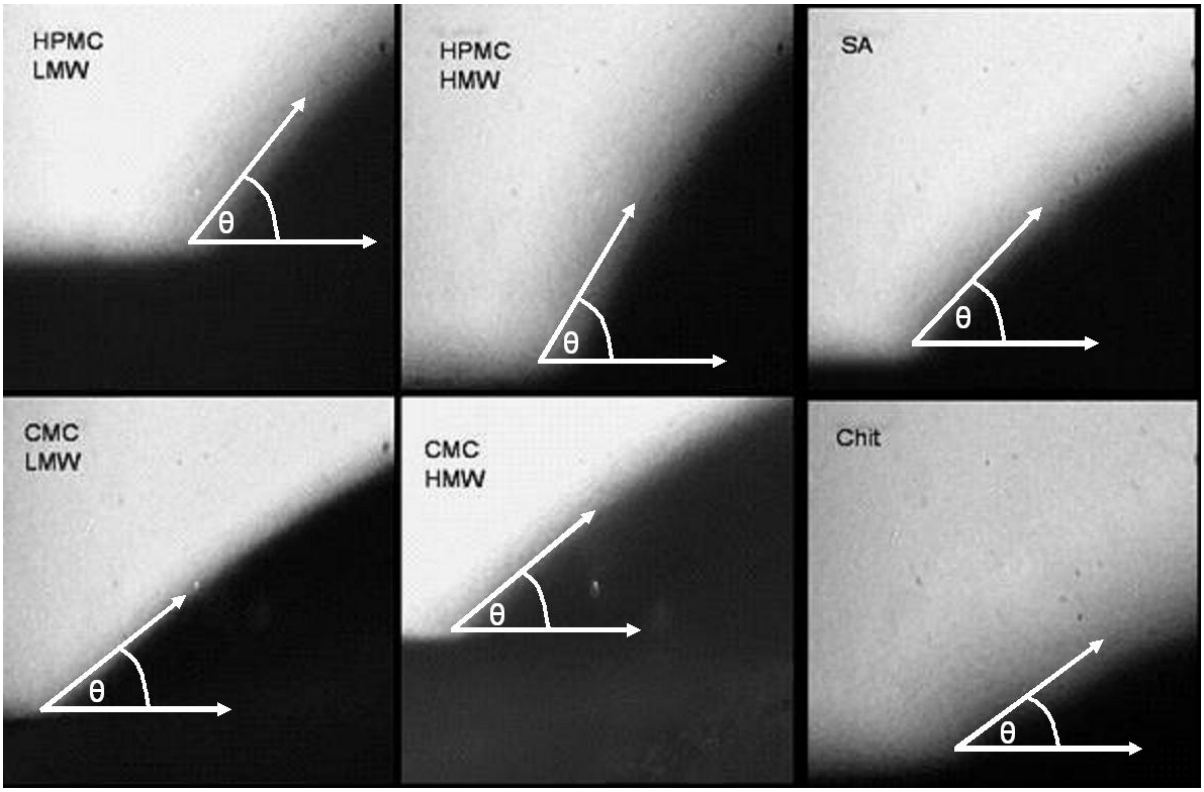

Figure 4.2– The dynamic clearance of 25 uL saline containing insoluble Tc-sulfur colloid delivered to an anesthetized, female Brown Norway rat (200g) in the supine position following pipette aspiration delivery to the nostrils for 30 minutes, with 120 second frames.

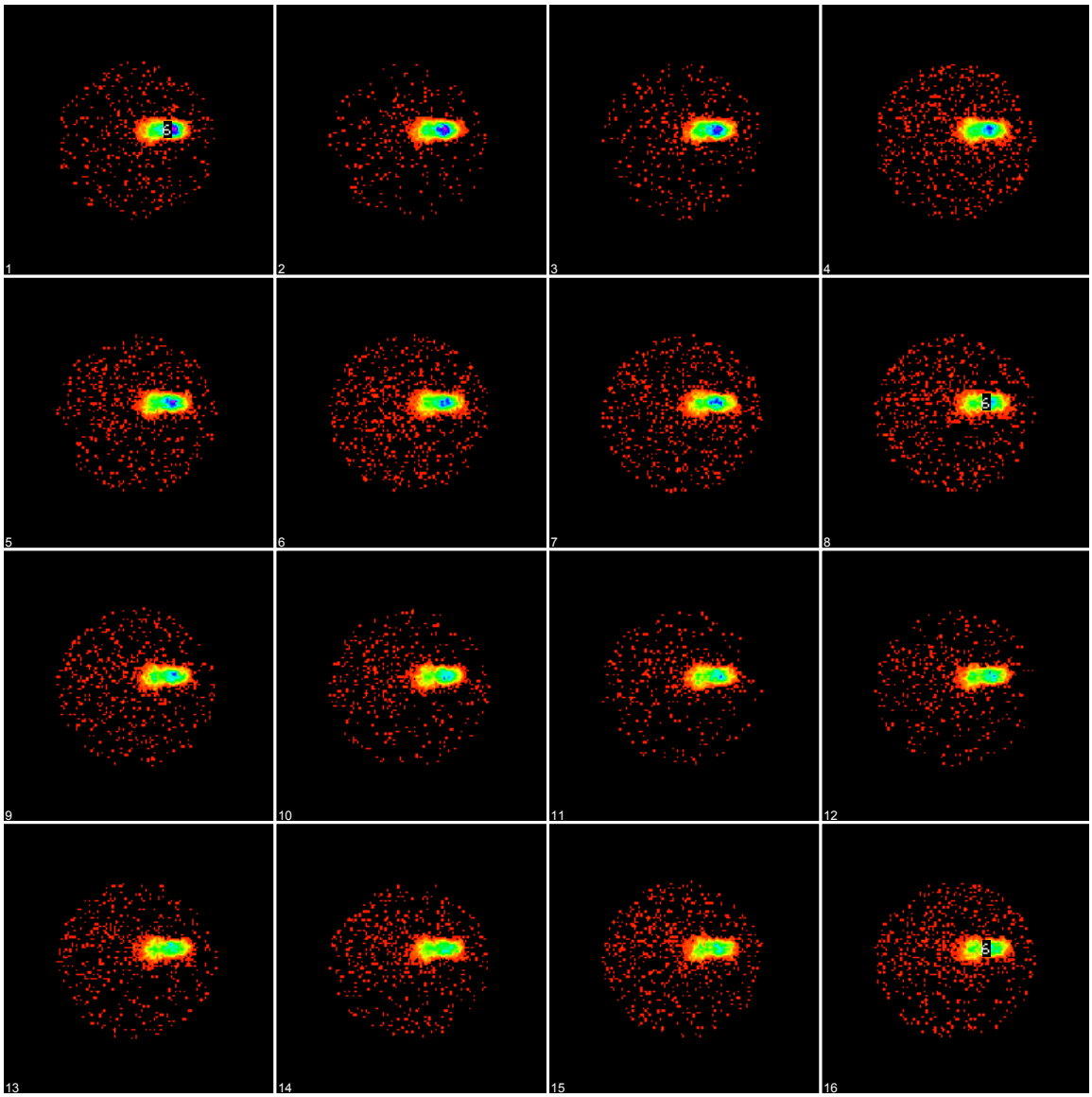

Figure 4.3– The percentage of radioactivity remaining in the nasal cavity of Brown Norway rats as a function of time when radiolabeled saline (Liq- No MA) or trehalose (Pow- No MA) is delivered (error bars represent standard deviations of n=3 at 15, 30, and 120 minute time points).

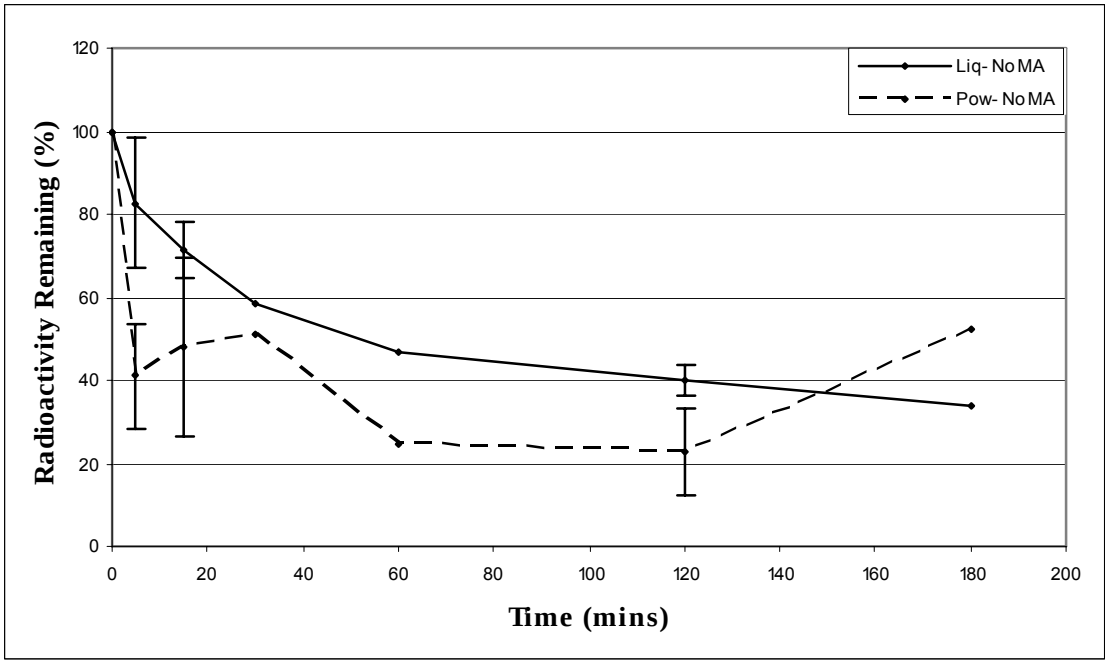

Figure 4.4– The percentage of radioactivity remaining in the nasal cavity of Brown Norway rats as a function of time when radiolabeled saline (Liq- No MA), 1% hydroxypropyl methylcellulose in radiolabeled saline (Liq- HPMC HMW) or 3% hydroxypropyl methylcellulose in radiolabeled trehalose (Pow- HPMC HMW) is delivered (error bars represent standard deviations of n=3 at 15, 30, and 120 minute time points).

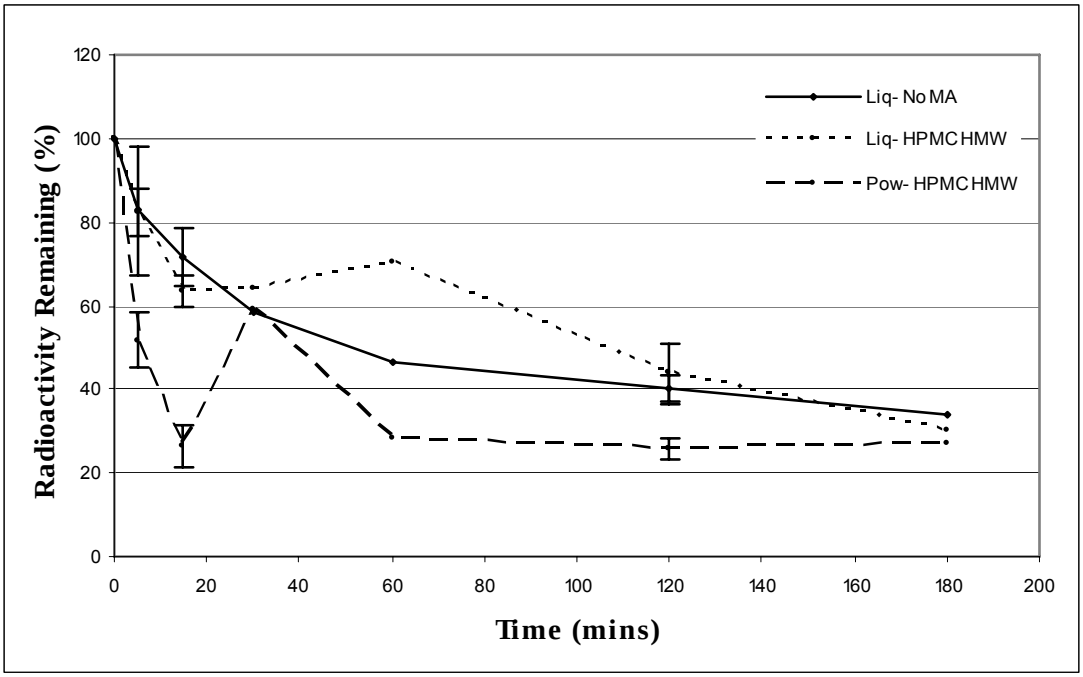

Figure 4.5– The percentage of radioactivity remaining in the nasal cavity of Brown Norway rats as a function of time when radiolabeled saline (Liq- No MA), 1% carboxymethylcellulose sodium in radiolabeled saline (Liq- CMC HMW) or 3% carboxymethylcellulose sodium in radiolabeled trehalose (Pow- CMC HMW) is delivered (error bars represent standard deviations of n=3 at 15, 30, and 120 minute time points).

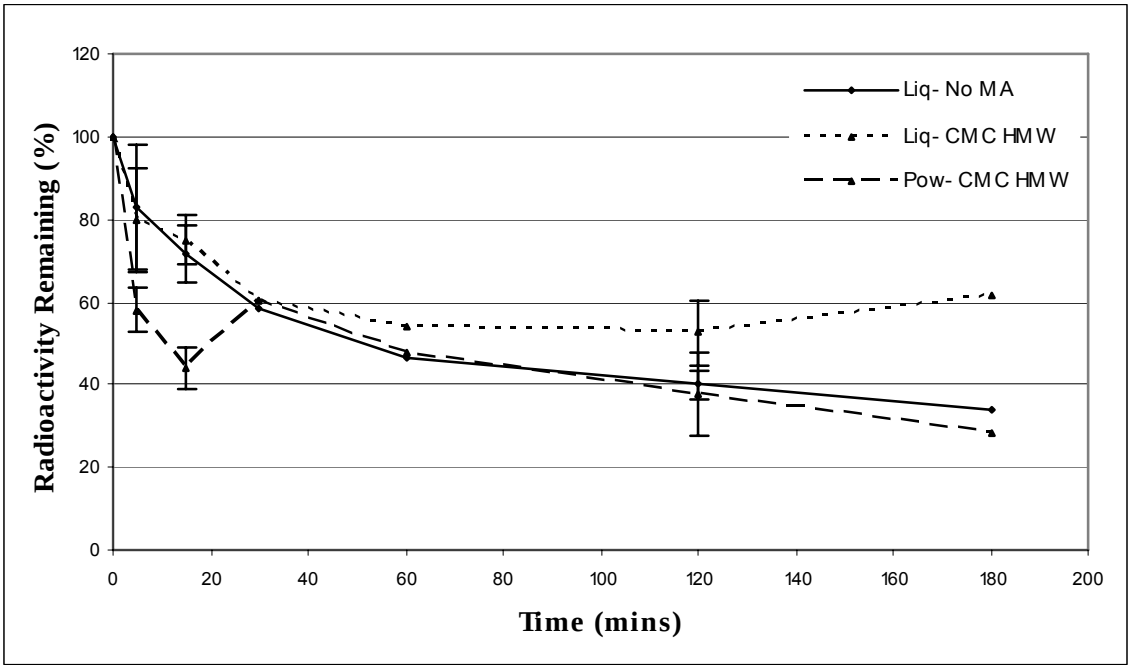

Figure 4.6– The percentage of radioactivity remaining in the nasal cavity of Brown Norway rats as a function of time when radiolabeled saline (Liq- No MA), 1% sodium alginate in radiolabeled saline (Liq- SA) or 3% sodium alginate in radiolabeled trehalose (Pow- SA) is delivered (error bars represent standard deviations of n=3 at 15, 30, and 120 minute time points).

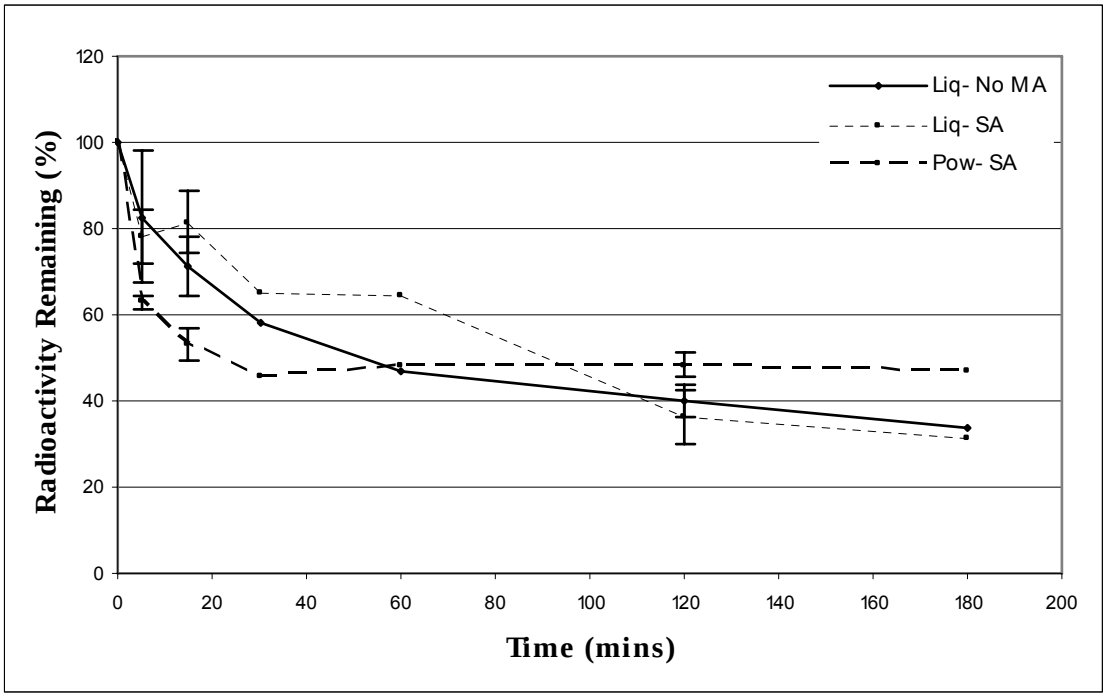

Figure 4.7– The percentage of radioactivity remaining in the nasal cavity of Brown Norway rats as a function of time when radiolabeled saline (Liq- No MA) or 3% Chitosan in radiolabeled trehalose (Pow- Chit) is delivered (mean where error bars represent standard deviations of n=3 at 15, 30, and 120 minute time points).

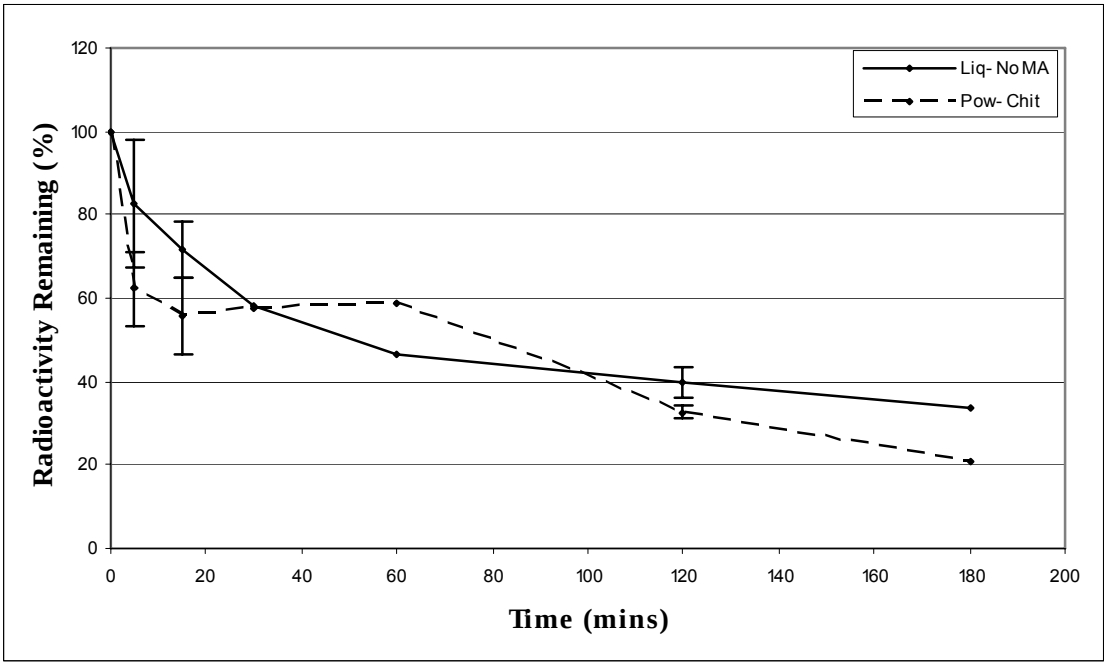

Figure 4.8– The area under the curve of the percentage of radioactivity as a function of time curves for liquid and powder formulations containing no mucoadhesive (No MA), hydroxypropyl methylcellulose (HPMC HMW), sodium alginate (SA), carboxymethylcellulose sodium (CMC HMW), and chitosan (Chit).

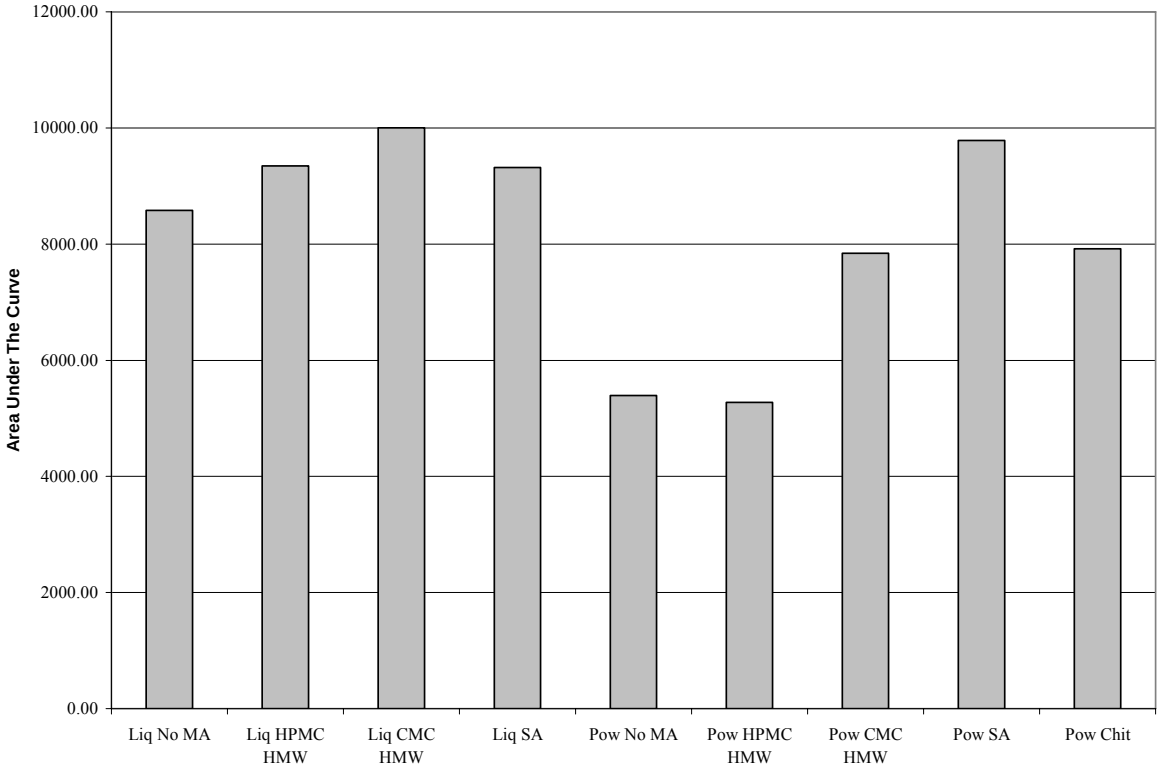

5 IMMUNOGENICITY OF DRY POWDER INTRANASAL INFLUENZA VACCINE WITH A MUCOADHESIVE COMPOUND

5.1 Introduction

Influenza infection results from deposition of influenza virus into the upper respiratory tract (Chapter 1, Section 1.1.6). Therefore, particles intended for the prevention of influenza must be targeted to the nasal-associated lymphoid tissue (NALT). The immune response elicited by the antigen in a host was summarized previously (Chapter 1, Section 1.1.1.5). The humoral immune response generates binding antibodies specific to an antigen. The initiation of the humoral immune response requires: 1) exposure to an antigen (in this case, whole inactivated influenza virus (WIIV)), 2) penetration of the mucosal surface for the antigen to be endocytosed by an M cell or phagocytosed by a dendritic cell, and 3) an interaction between B lymphocytes and the antigen presenting cells (Pier, Lyczak et al. 2004).

Mucosal surfaces are very susceptible to virus entry because of their extensive surface area and their functions require the epithelium to be exposed to the environment. This makes it difficult for the antibodies produced by systemic immune response to sufficiently protect it. The presence of local lymphocytes and the nearby location of local lymphoid tissue (NALT) make mucosal immunization ideal due to its ability to protect locally and systemically. Mucosal immunization promotes formation of both immunoglobulin G (IgG) and immunoglobulin A (IgA). Immunoglobulin M (IgM) has a molecular weight of 900 kD and constitutes 6% of total Ig. IgM is the first antibody of the immune response (Roitt and Delves

2001). Upon first exposure to an antigen, there is an early burst of antigen specific IgM within the first 7 days, while antigen specific IgG synthesis takes longer to reach a maximal rate, usually 2-3 weeks (Figure 7.1). On secondary exposure to the same antigen, again there is an early burst of IgM. The IgG levels, however, rapidly increase within two weeks to a level much higher than first exposure and have a significantly higher binding affinity to the antigen than on first exposure (Gosling and Basso 1994). IgA synthesis resembles the pattern of IgG synthesis. IgG has a molecular weight of 150 kD and accounts for 80% of total Ig (Roitt and Delves 2001). It is the major Ig of general circulation. The site of entry into the host will influence the isotype of antibody produced. There are four isotypes of IgG (IgG1, IgG2, IgG3, IgG4) (Leffell, Donnenberg et al. 1997). IgG1 is the dominant subclass, accounting for 65% of total IgG. IgA is the predominant isotype of antibody in seromucous secretions, specifically in the upper respiratory tract (Roitt and Delves 2001). IgA has a molecular weight of 395 kD and accounts for 13% of total Ig. There are two isotypes of IgA (IgA1, IgA2). IgA constitutes 10% of the total proteins in the upper respiratory tract secretions. IgA1 subclass accounts for two-thirds of the total secretory IgA (sIgA). IgG is present only in trace amounts in the upper respiratory tract secretions.

Viruses are unique in that they can be neutralized by antibodies alone, unlike bacteria that require secondary effectors (Dimmock, Easton et al. 2001). It is possible to determine if antibodies are present for a specific antigen because their interaction is so specific. For this reason, serological tests such as an enzyme-linked immunosorbent assay (ELISA) can be used to quantify antibodies in serum. ELISAs employ a plate coated with the antigen against which antibodies are to be developed for quantification. Serum samples are added to allow the antibody to bind to the antigen. A secondary, conjugated antibody is added that is

covalently linked to an enzyme. Substrate is added and a quantifiable colorimetric assay can be used to determine the amount of antibody present. A classical serological test may also be employed to quantify antibodies by hemagglutination-inhibition assay (HAI). Virus is added to serial dilutions of serum. The presence of antibodies will neutralize the viruses' ability to bind to red blood cells, preventing agglutination which can be detected visually.

Brown Norway rats are considered the strain of choice for conducting humoral response immunogenicity studies (Lebrec and Burleson 1994; Lebrec, Sarlo et al. 1996). The mouse is the most commonly used model for influenza vaccination, but small nostril size prevents reproducible dosing of powders to the nasal cavity. There are limited options for whole organism assessment of influenza vaccines for nasal delivery.

In the following studies here, intranasal vaccination with WIIV was assessed in Brown Norway rats. A dose-response curve of IM injection and IN liquid was established to determine the appropriate dose for a formulation study. Nasal powders with and without MA were compared to IM and IN suspensions. Both serum and mucosal antibodies were quantified.

5.2 Methods

Animal Care

Female Brown Norway rats (125–175 g, Charles River, Raleigh, NC) were kept under standard conditions in AAALAC approved facilities under IACUC approved protocol (06-265.0-A). The animals were kept in a controlled temperature room (22 ± 1°C with 12 hour light and dark cycles and had free access to food and water. Rats were anesthetized by intraperitoneal injection of 40 mg/kg ketamine, 2 mg/kg xylazine and 0.75 mg/kg acepromazine before immunization.

5.2.1 Dose-Response Experiments

WIIV was used as a liquid preparation without addition of adjuvants, as provided by the vendor. Rats were immunized two times IM or IN with the liquid suspension on days 0 and 21. The doses for IM immunization were 0.5, 1, 1.5, 2, 2.5, 5, 10, 20, or 40 μg of HA in 100 μL of sterile normal saline and administered in the muscle of the left hind leg of the animal with a 25-gauge needle (n=3). The same doses of HA for IN immunization were administered in 25 μL of sterile normal saline with a 10-100 μL pipette (n=3).

5.2.1.1 Sample Collection

Blood was obtained, under anesthesia; from the tail artery three weeks post vaccination. Blood was centrifuged at 13201 X g for 10 minutes; serum supernatant was removed and stored at −80°C. Two weeks following the boost immunization, rats were euthanized following cardiac puncture by CO_2 inhalation and nasal washes were collected by cannulating the trachea and rapidly instilling 1ml of sterile saline. Fluid passed from the trachea through the nostrils was collected and stored at −80°C.

5.2.1.2 ELISA

Whole virus-specific antibody titers were determined by ELISA. Plates (96-well, Nalgen Nunc Maxisorb, Rochester, NY) were coated with 100 μL of 1 μg/mL (based on total protein content as above) whole inactivated influenza virus at 4°C overnight, then blocked at 37°C for 1 hour with PBS Tween 20 (PBST; Sigma) containing 5% non-fat dry milk. After washing, serial dilutions of sera or nasal wash (100 μL/well) were added and incubated at 37°C for 1 hour. Plates were washed again, then incubated at 37°C for 45 minutes with horseradish peroxidase (HRP) conjugated secondary antibodies: goat anti-rat Ig (H+L)

(Southern Biotechnology Associates, Inc, Birmingham, AL) or goat anti-rat IgA (Bethyl Laboratories, Montgomery, TX). Plates were developed by incubating for 30 minutes at room temperature with 3,3',5,5'-tetramethyl Benzidine (TMB) substrate (Sigma). After stopping the reaction using 0.5M H_2SO_4, plates were read at 450 nm. The endpoint titers were defined as the highest reciprocal dilution of sera or nasal wash yielding an OD_{450} value at least 3X background obtained using samples obtained prior to immunization. All standards, samples, and controls were analyzed in duplicate.

5.2.3 Formulation evaluation

Rats were immunized IM with the liquid formulation or IN with either the liquid or the powder formulation on days 0 and 21. Each dose contained 2 μg H/100 μL volume for IM injection, 2 μg H/25 μL for IN liquid or 5 μg H/5 mg total powder. IM and IN liquid formulations were administered as described above. Powder formulations were delivered using compressed air at 20 psig through a timed solenoid switch and a 100 μL pipette in the right nostril of the anesthetized rat. The efficiency of dosing resulted in an actual dose delivered to the animal nasal cavity of 2 μg. There were five powder formulation groups. SFD WIIV/trehalose and CMC HMW, SA, chitosan, or HPMC HMW was added at 3% w/w. Each treatment group consisted of six animals.

5.2.3.1 IgG Isotyping

Virus-specific IgG1, IgG2a and IgG2b were measured by ELISA as above, substituting reagents provided in IgG isotyping kits (Bethyl Laboratories). IgG1, IgG2a and IgG2b concentrations were determined using standard curves, as per the manufacturer's

instructions. The sensitivity of isotyping ELISA is in the range of 3–1000 ng/mL. Samples were diluted to fall within the standard curve range.

5.2.3.2 HAI Assay

Test sera were inactivated at 56°C for 10 minutes to destroy complement and HAI inhibitors. Twenty-five milliliter of double serial diluted test sera were then added to wells containing 25 μL of four hemagglutinating units of influenza virus followed by adding 50 μL of 0.5% chicken red blood cells to each well. Plates were then incubated at room temperature for 1 hour. The endpoint HAI titer was defined as the reciprocal of the highest serum dilution that completely inhibited hemagglutination of the chicken red blood cells.

5.2.3.3 Endotoxin Quantification

A commercially available kit (QCL-1000 Chromogenic Limulus Amebocyte Lysate (LAL) Endpoint Assay, Cambrex Corp., East Rutherford, NJ) was purchased for quantification of endotoxin present in MA. Briefly, MA were dissolved in pyrogen-free water and diluted to fall within range of the standard curve.

5.2.3.4 Statistical Analysis

Analysis of variance was performed on the logarithmic transformation of titer values at $\alpha=0.05$ to determine any differences between the dosing groups. A two-tailed t-test assuming unequal variances was used to compare the immune response elicited by IM injection and IN liquid at the same dose for the dose response study. For comparisons of two means, Scheffé's method was used at $\alpha=0.05$.

5.3 Results and Discussion

5.3.1 Dose-Response Experiments

To determine an appropriate dose for use in the formulation experiments, various doses were prepared and inoculated into rats either IM or IN with liquid formulations. The immune responses following inoculation were assessed after an initial vaccination and after a boost dose. IN delivery of liquid vaccine provided equivalent serum antibody titers as those obtained by IM injection at doses ≥2.5 μg after the initial vaccination (Figure 5.2). At doses ≤2 μg, the serum antibody titers elicited by IM injection were significantly greater than that of IN liquid after the first dose ($P<0.05$). After the boost dose, the immune response elicited at doses of 0.5, 1, 2.5, 5, and 10 μg is equivalent for both the IM injection and the IN liquid (Figure 5.3). The serum antibody titers are significantly greater for the IM injection than the IN liquid at 1.5 and 2 μg, while they are greater for the IN liquid than the IM injection at 20 and 40 μg doses.

Nasal lavage fluids were assessed for influenza-specific IgA responses in order to evaluate nasal mucosal immune response following IN delivery vaccine. Positive nasal IgA responses were seen after administration of IN liquid, regardless of dose (Figure 5.4). The local immune response increases with dose until reaching a plateau at ≥5 μg. No detectable IgA responses were observed following IM injection.

The range of doses utilized provided insight into an appropriate dose for use in subsequent experiments. When comparing different formulations, it is important to choose a dose on the steepest slope of the concentration curve to maximize the potential differences in immunogenicity. If too low or too high of a dose is administered, differences in the immune response elicited may not be evident. However, on the upward slope, even subtle differences

in immunogenicity can be detected. A 2 μg dose was chosen as it elicited a significantly greater immune response than doses ≤1.5 μg and significantly less than doses ≥ 5 μg when administered as an IN liquid. There were also significant differences between the IN liquid and IM injection upon administration of the 2 μg dose after the initial vaccination and the boost.

5.3.2 Formulation evaluation

To evaluate the immune responses elicited by a powder influenza vaccine, various formulations were prepared and rats were inoculated IN. The immune responses following inoculation with the powder formulation, with or without MA, and the responses to the liquid formulation administered IN or IM were assessed. IM delivery of liquid vaccine provided equivalent serum antibody titers to those obtained by IN powder without MA, CMC HMW, SA, and HPMC HMW, and significantly greater serum antibody titers than IN liquid and IN powder with chitosan after the initial vaccination (Figure 5.5, $P<0.05$). IM delivery of liquid vaccine provided equivalent serum antibody titers to those obtained by IN liquid and IN powder with No MA, CMC HMW, SA, and HPMC HMW, and significantly greater serum antibody titers than IN powder with chitosan after boosting ($P<0.05$). IN liquid vaccine provided equivalent serum antibody titers to those obtained by IN powder without MA, CMC HMW, SA, chitosan, and HPMC HMW after the initial vaccination. IN liquid provided significantly greater serum antibody titers than IN powder with chitosan after boosting, and was equivalent to all other formulations ($P<0.05$).

Initial studies of the formulation and dosing of a dry powder influenza vaccine for nasal delivery have been described (Huang, Garmise et al. 2004; Garmise, Mar et al. 2006) WIIV and trehalose were freeze-dried, milled, and sieved to produce particles in the 45-125

μm size range. Antibody responses were elicited in rats using a 100 μg powder vaccine and chitosan blend that generated strong nasal mucosal and systemic immune responses. The chitosan mucoadhesive powder formulation generated significantly greater antibody titers compared to IM injection, IN liquid, or IN powder without mucoadhesive formulations at this dosing level after initial vaccination. Similar serum antibody titers were seen in chitosan mucoadhesive powder, IM injection, and IN liquid. Comparable nasal IgA titers were generated in the IN groups containing antigen, while no nasal IgA response was seen in animals dosed IM or with excipients alone intranasally.

In the present experiments, similar serum antibody levels to the previous study were achieved after dosing IN liquid 2 μg H after the initial vaccination and boosting and the IM after boosting to the previous experiment. However, a 10-fold higher response was generated by IM injection after initial vaccination than the previous experiment. The IN powder containing chitosan elicited a 10-fold higher response after the initial vaccination, but a comparable response after boosting. One possible explanation for this could be due to a potential adjuvant effect caused by impurities in the chitosan. In the present studies, highly purified (< 2% impurities) chitosan was blended with the WIIV-SFD particles. This chitosan did not require cryo-milling to produce particles in the desired size range. MA utilized in the present study were assayed to quantify for the presence of endotoxin. There was no more than 0.11 ng of endotoxin present in the MA in any dose of vaccine, an order of magnitude lower than normally administered as an adjuvant (Nelson, Prior et al. 2004). In both the previous and current studies, after initial vaccination and a boost, comparable serum antibody levels were seen when dosed IM, IN liquid, or IN powder with MA.

5.3.3.1 IgG Isotyping

Serum IgG1, IgG2a and IgG2b isotypes were measured as an indirect assessment of T-helper (Th) cell activity (Figure 5.6). In rats, IgG1 and IgG2a antibodies are associated with Th2 activity, while IgG2b antibody is suggestive of a Th1 response (Bazin 1990). All groups generated a mixed and balanced response consisting of IgG1, IgG2a and IgG2b. There was no major shift of the Th1/Th2 response across the different formulations. The data show that all of the formulations and routes of administration elicited a mixed IgG subclass response, which may be important for protection against influenza and other pathogens.

5.3.3.2 HA Inhibition (HAI) Assay

HAI titers also displayed a similar pattern of response as ELISA and IgG isotyping (Figure 5.7).

5.3.3.3 Nasal IgA Titers

Substantial IgA titers were seen in all rats after intranasal immunization (Figure 5.8). All of the nasal IgA titers elicited from nasal formulations were significantly greater than IM injection except for IN powder with chitosan ($P<0.05$). There were no statistically significant differences seen between any of the IN formulations. The production of a mucosal immune response in the form of IgA production demonstrates that intranasal delivery of the WIIV will produce both a local and systemic immune response.

In Chapter 4 one powder, containing SA, was shown to have an increased residence time in the nasal cavity. No statistically significant differences were noted between formulations in eliciting both IgA and IgG responses. However, the trend was that SA

elicited the highest IgA response of all treatments including solution. Even as it elicited one of the higher IgG responses, arguably the trehalose alone and liquid treatments elicited greater responses. While trends in the immune responses may be interpreted to support the original hypothesis, powder preparations containing WIIV were not statistically different in their effect.

5.4 Summary

A dose-response experiment ranging from 0.5 to 40 μg equivalent H was performed using IM and IN liquids to determine an appropriate dose to quantify potential differences in antibody response elicited as a function of formulation in Brown Norway rats. Animals were given an initial dose, followed by a boost dose three weeks later. Serum samples taken three weeks after the initial dose and two weeks after the boost were analyzed by ELISA for the presence of antibodies. Two weeks after the boost dose, the animals were sacrificed and nasal washes were taken to quantify the production of mucosal antibodies. Once a dose was determined, IM injection, IN liquid, and IN powders containing trehalose alone, or 3% SA, CMC HMW, HPMC HMW, and chitosan were dosed as described above. IgG, IgG isotypes, and HAI were quantified using serum, while the IgA was quantified using nasal washings.

IN delivery of liquid vaccine provided equivalent serum antibody titers as those obtained by IM injection at doses ≥2.5 μg after the initial vaccination, but at doses ≤2 μg, the serum antibody titers elicited by IM injection were significantly greater than that of IN liquid after the first dose. After the boost dose, the immune response elicited at doses of 0.5, 1, 2.5, 5, and 10 μg is equivalent for both the IM injection and the IN liquid Positive nasal IgA responses were seen after administration of IN liquid, regardless of dose. No detectable IgA responses were observed following IM injection. A 2 μg dose was chosen to use in the

formulation experiments. In the formulation experiments, IM delivery of liquid vaccine provided equivalent serum antibody titers as those obtained by IN powder with No MA, CMC HMW, SA, and HPMC HMW after the initial dose and equivalent serum antibody titers as those obtained by IN liquid and IN powder with No MA, CMC HMW, SA, and HPMC HMW after the boost. IN liquid vaccine provided equivalent serum antibody titers as those obtained by IN powder with No MA, CMC HMW, SA, chitosan, and HPMC HMW after the initial vaccination. IN liquid provided significantly greater serum antibody titers than IN powder with chitosan after boosting, and was equivalent to all other formulations. IgG isotyping and HAI displayed similar patterns of response as serum antibody levels.

While no significant differences between powder and liquid formulations were observed, trends were consistent with the observations from the residence time studies with respect to the eliciting an immune response. The following chapter will discuss in greater detail the conclusions that may be drawn from these findings with respect to the hypothesis and specific aims and the implications for the potential future studies.

Figure 5.1– The primary and secondary immune response elicited by a vaccine and boost dose as a function of time (Adapted from (Gosling and Basso 1994)).

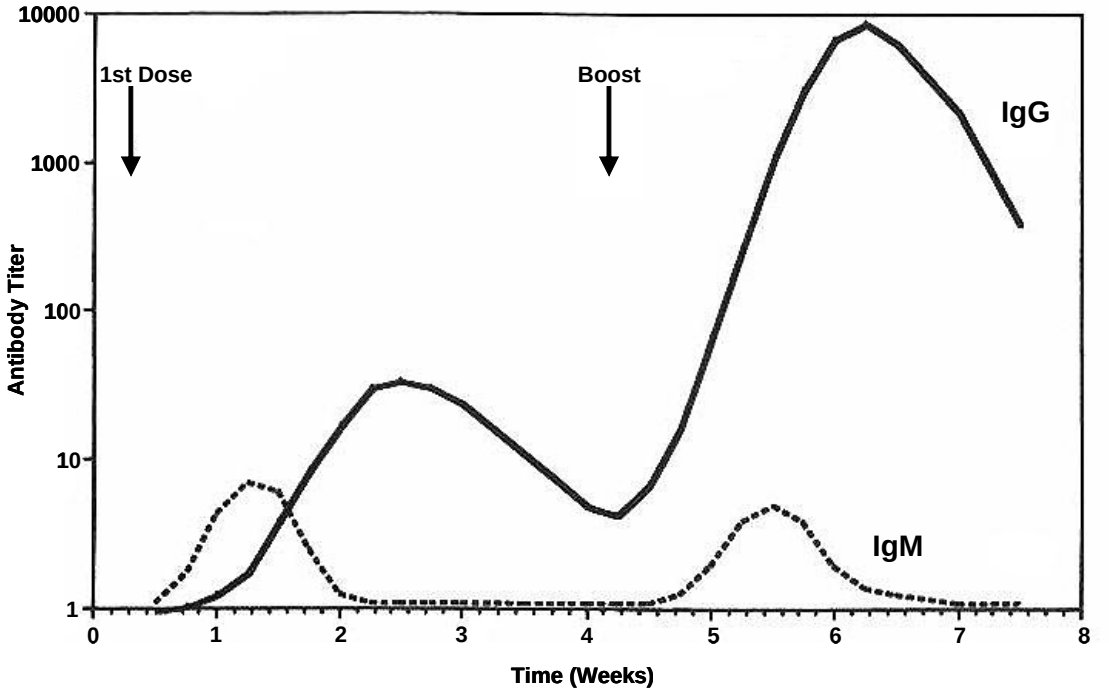

Figure 5.2– Serum antibody titers elicited after primary vaccination in a dose-response study, 3 weeks after dosing of whole inactivated influenza virus in the rat model either intramuscularly (IM) or intranasally (IN) in saline (n=3, error bars represent positive standard deviation).

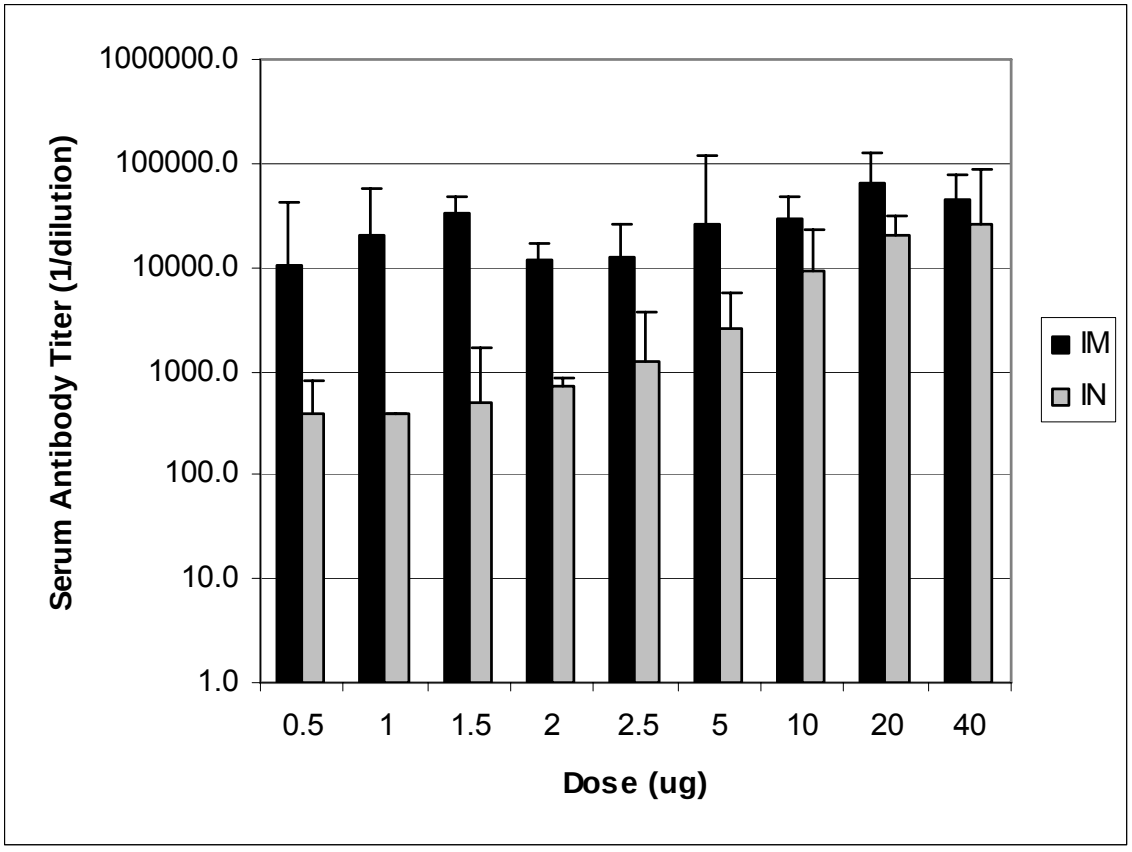

Figure 5.3– Serum antibody titers elicited after boost vaccination in a dose-response study, 2 weeks after dosing of whole inactivated influenza virus in the rat model either intramuscularly (IM) or intranasally (IN) in saline (n=3, error bars represent positive standard deviation).

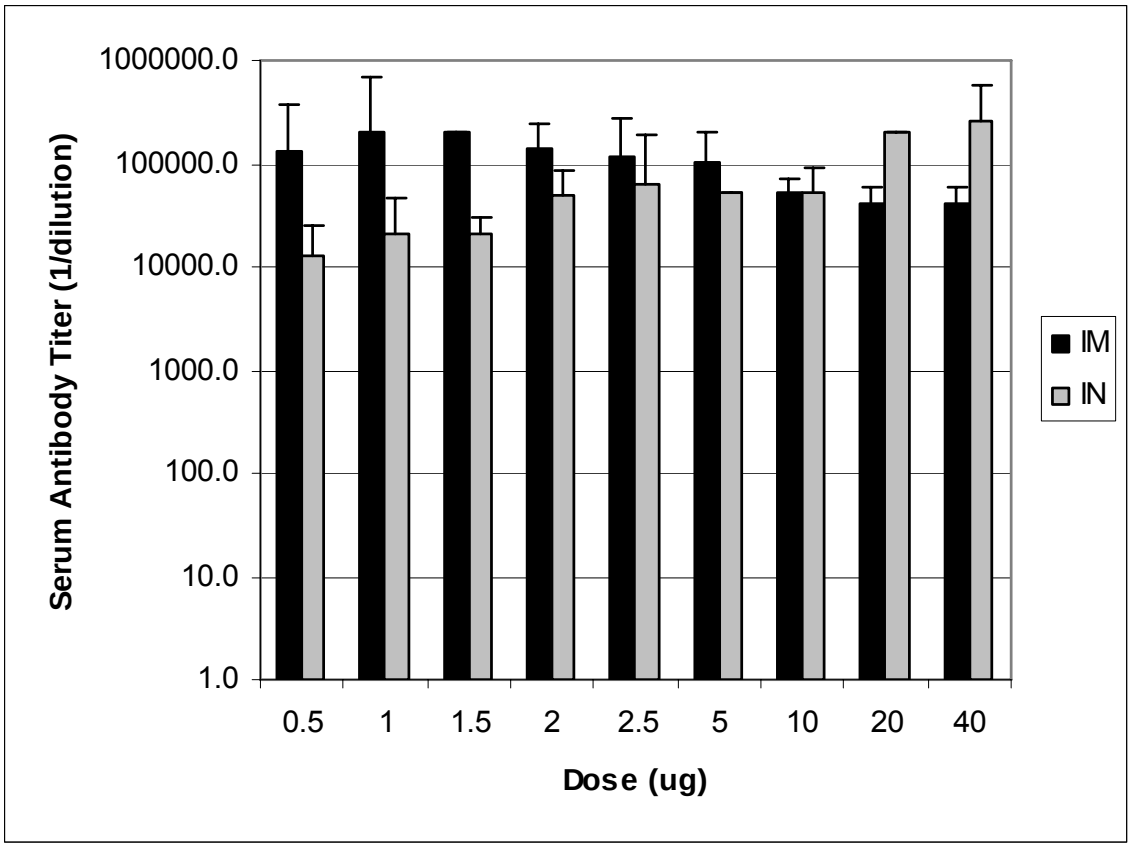

Figure 5.4– Mucosal antibody titers elicited after primary and boost vaccination in a dose-response study, 2 weeks after boost dosing of whole inactivated influenza virus in the rat model intranasally (IN) in saline (n=3, error bars represent positive standard deviation). There was no mucosal immune response elicited in any of the rats dosed intramuscularly (IM).

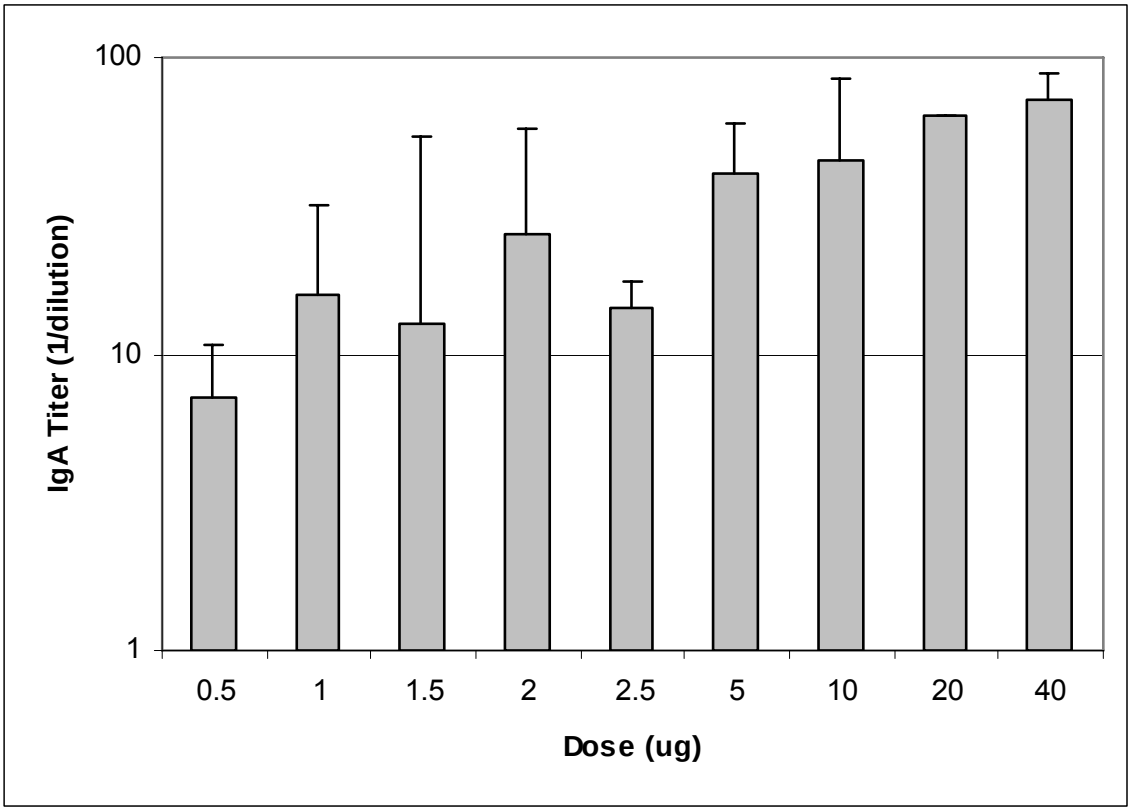

Figure 5.5– Serum antibody titers elicited after primary vaccination in a formulation study, 3 weeks after initial dosing (Bleed 1) and 2 weeks after boost dosing (Bleed 2) of whole inactivated influenza virus in the rat model either intramuscularly (IM) or intranasally (IN) in saline or IN powder with a mucoadhesive compound (n=6, error bars represent positive standard deviation).

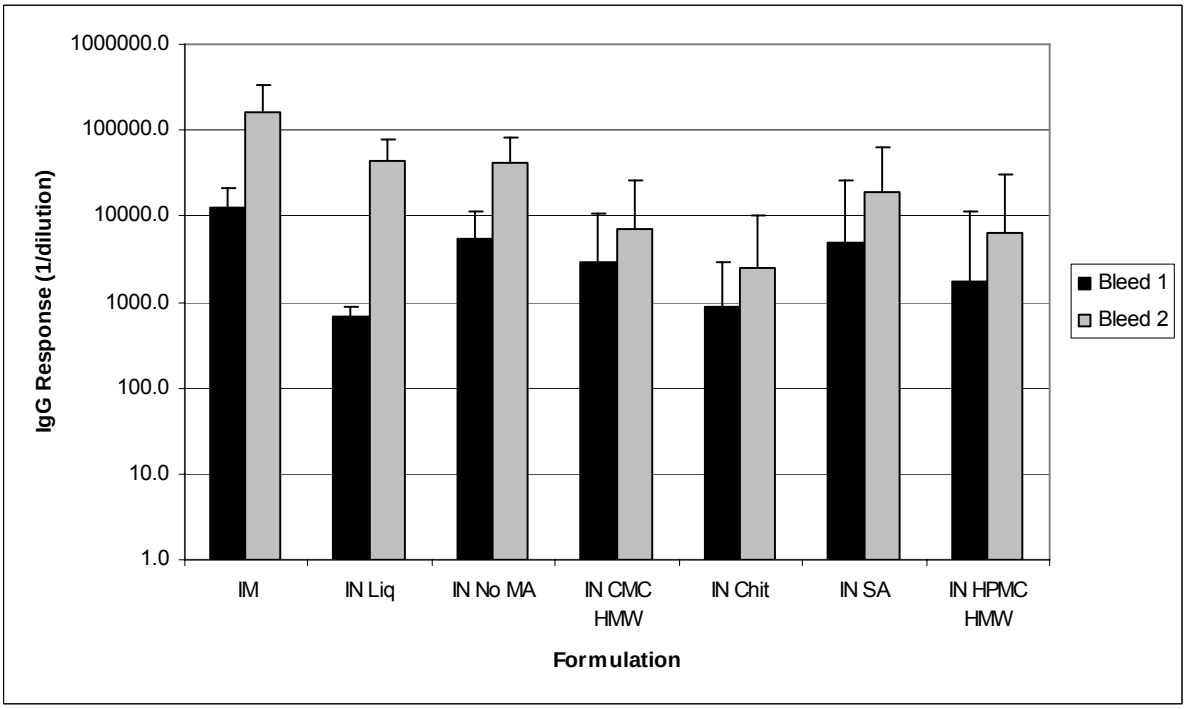

Figure 5.6– Concentration of IgG isotypes elicited after primary and boost vaccination in a formulation study, 2 weeks after boost dosing of whole inactivated influenza virus in the rat model either intramuscularly (IM) or intranasally (IN) in saline or IN powder with a mucoadhesive compound (n=6, error bars represent standard deviation). Naïve, unimmunized rats were used as controls.

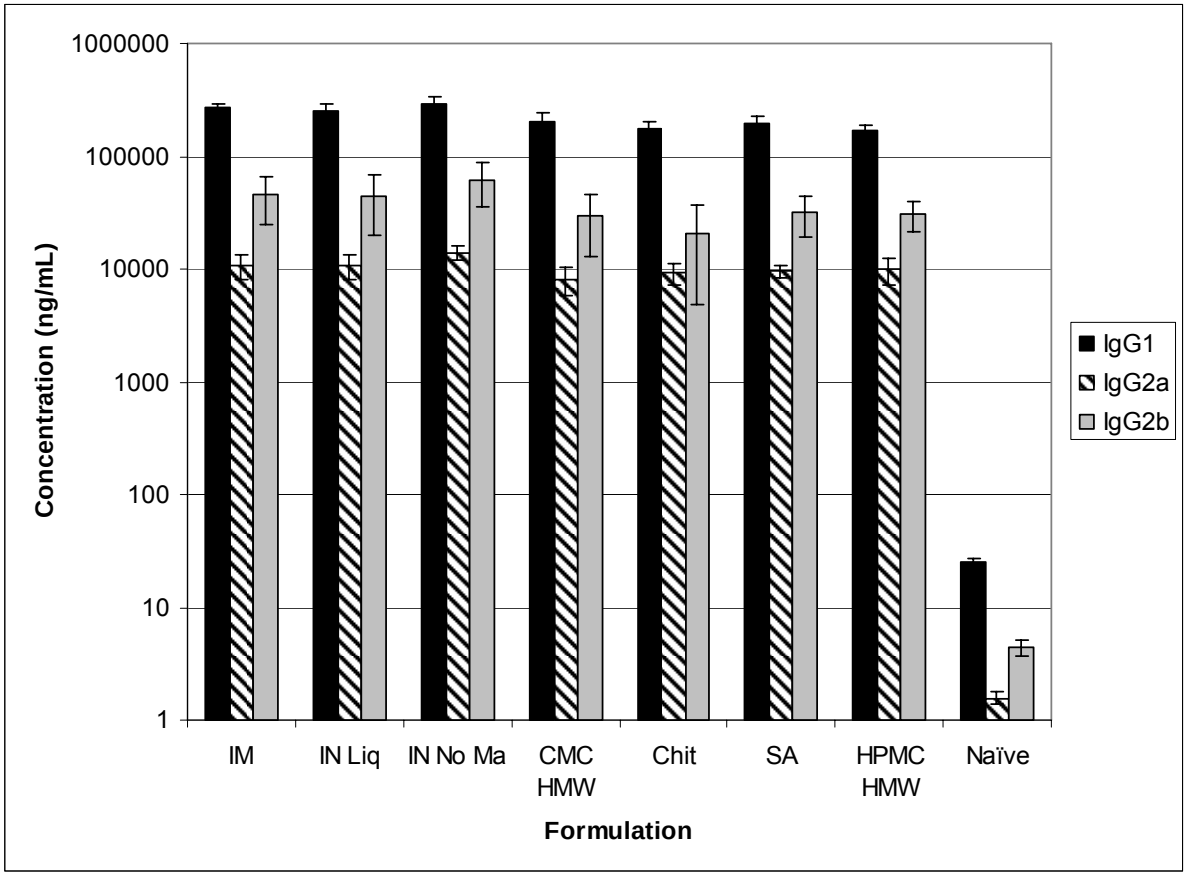

Figure 5.7– Hemagglutin inhibition titers elicited after primary and boost vaccination in a formulation study, 2 weeks after boost dosing of whole inactivated influenza virus in the rat model either intramuscularly (IM) or intranasally (IN) in saline or IN powder with a mucoadhesive compound (n=6, error bars represent standard deviation).

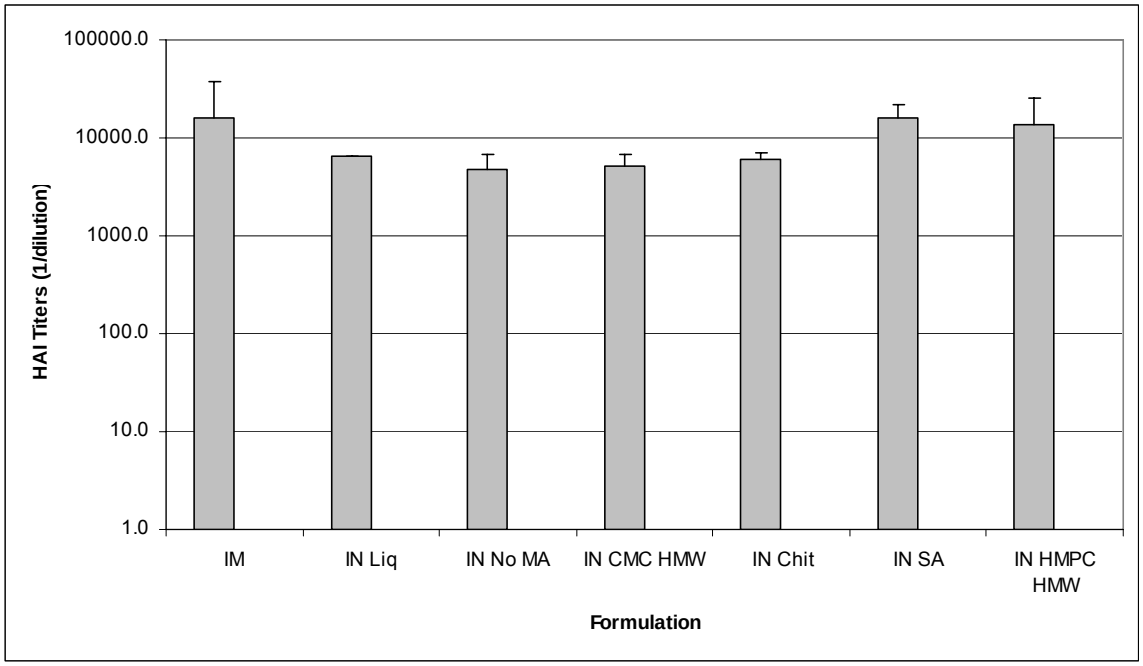

Figure 5.8– Formulation nasal lavage.

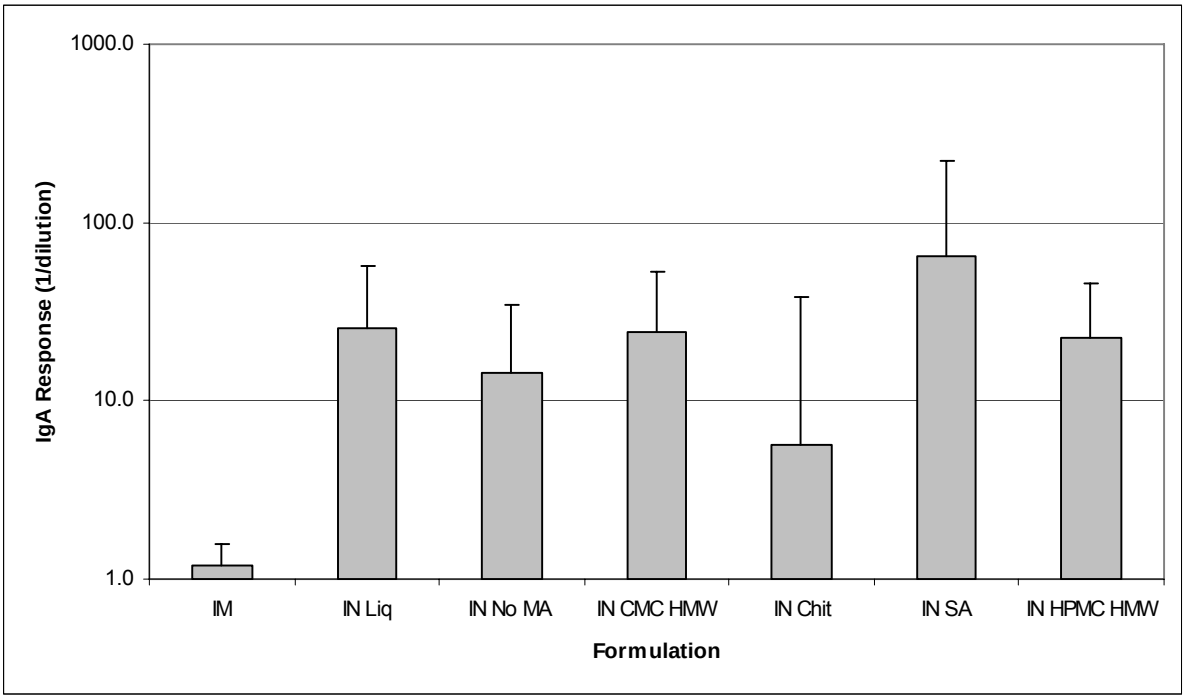

6 CONCLUSIONS AND FUTURE WORK

6.1 Conclusions

Needle-free vaccine delivery is a major current objective with respect to the treatment of global infectious disease (Giudice and Campbel 2006). There would be significant advantages to the development and delivery of dry powder intranasal vaccines designed to overcome a number of the short comings associated with currently marketed intramuscular (IM) and intranasal (IN) liquid influenza vaccines. The limitations, pertaining to IM injection, are based on the requirement for: 1) invasive injections, 2) delivery by trained health care professionals, 3) refrigeration, 4) sterility, and 5) disposal of biological waste. The live, attenuated IN vaccine must be stored frozen and thawed immediately before use and has not been approved for use in select populations such as children, the elderly and the immunocompromised, which are most commonly affected by the virus. The present work involved the manufacture and development of a dry powder, inactivated, heat-stable influenza vaccine for nasal delivery which was intended to overcome these shortcomings. Mucoadhesive compounds (MA), such as chitosan, have been widely used to increase the residence time in the nasal cavity and therefore, increase the immune response elicited by a nasal vaccine. The literature primarily focuses on the use of liquid formulations and there has been no study published comparing *in vitro* characterization of nasal powder formulations to *in vivo* experiments for use in nasal vaccines. It was proposed that maximal mucosal and systemic antibody production would be elicited by a dry powder nasal vaccine formulation

containing whole inactivated influenza virus by increasing the local residence time. This hypothesis was addressed by the following series of specific aims.

1. To prepare particles containing whole inactivated influenza virions and to evaluate the powder properties for nasal delivery.
2. To demonstrate the effectiveness of the powder vaccine delivered intranasally in eliciting a local IgA and systemic IgG immune response *in vivo*.

To prepare particles containing whole inactivated influenza virions and to evaluate the powder properties for nasal delivery.

Two manufacturing methods were employed to produce particles suitable for nasal delivery: freeze-drying (FD) followed by milling and sieving, and spray-freeze-drying (SFD). Designed experiments examining three factors (freezing rate, solute concentration, and annealing for freeze-drying and solution feed rate, atomization airflow rate, and solute concentration for spray-freeze-drying) in a full 2^3 factorial design were used to produce particles suitable for nasal delivery. The primary characteristics (measured by laser diffraction) were: median diameter (D_{50}), 90% diameter (D_{90}), 10% diameter (D_{10}), and span (D_{90}-D_{10}/D_{50}).

Freeze-drying followed by milling and sieving produced particles well below the targeted particle size for human delivery (D_{50}=40 μm). Also, a significant percentage of the powder was in a size range that could potentially deposit in the lower respiratory tract (the lungs). Additionally, heterogeneous shape of the milled particles is unsuitable for blending with MA. Freeze-drying followed by milling and sieving produced particles suitable for nasal delivery to rats (D_{50}=25 μm) under the following conditions: 10% trehalose solution, frozen

at the slow freezing rate, without annealing, lyophilized, milled at 200 rpms for 30 minutes, and sieved in tap mode for 2 hours.

An optimized spray-freeze-drying run of 10% trehalose, a 20 mL/min solution feed rate and an atomization airflow rate of 300 L/hr was employed to successfully produce spherical particles for potential human delivery with a D_{50}=38.5 μm. Also, an optimized spray-freeze-drying run of 10% trehalose, a 10 mL/min solution feed rate and an atomization airflow rate of 500 L/hr successfully produce particles for rat delivery with a D_{50}=26.9 μm. Ultimately, the morphological and size characteristics of the SFD particles were considered superior to the FD particles with respect to the potential for blending reproducibly with MA and minimizing the presence of small particles with potential for deposition in the lower respiratory tract. The SFD particles were selected for use in subsequent vaccine formulations.

SFD and MA powders were characterized for their physico-chemical properties. Based on Carr's Compressibility Index (CCI), 25 μm SFD was the only powder to be considered free-flowing. Bulk and sieved fractions of SA and chitosan were the only MA to be considered free-flowing. The static angle of repose of SFD rat was larger than 25 μm SFD and bulk, sieved trehalose, but all three powders are regarded as free-flowing. All of the MA were considered free-flowing with the exception of sieved CMC HMW, bulk chitosan, and sieved chitosan. Impact energy separation can be a useful tool in characterizing the adhesive and cohesive forces of powders. Trends seen after increasing impact energies were in agreement with the flow properties of the powders.

The surface areas of the SFD formulations were significantly greater than bulk trehalose, while the true densities of the SFD formulations and bulk trehalose were the same, indicating that the SFD process produced porous particles. The moisture content of the SFD

powders was significantly less than the bulk trehalose and the MA. Additionally, the thermal analysis indicated that the SFD powders were amorphous. Results from stability studies performed at different temperatures and relative humidities (4°C and 50% RH, 23°C and 40% RH, and 37°C and 80% RH) demonstrate the improved vaccine storage stability provided by the powder formulation compared to liquid formulation.

A modified cascade impactor (MCI) was developed to characterize the particle size fraction capable of deposition in the lower respiratory tract. This is an important measure of the potential for delivery to a site which is not the route of administration, and which could lead to potential toxicity. Monodisperse aerosols were utilized to calibrate the Stage -2 and Stage -0 of an Andersen Mk II non-viable cascade impactor at 15 liters per minute flow rate. This novel setup extended the ceiling of the range of particle sizes that the cascade impactor can characterize from 8.7 to 16.5 μm. The MCI was used to characterize the dispersion of the SFD human powder from two devices: monodose insufflator and a device developed by Becton Dickinson Technologies (BDT). No significant differences were seen in any of the mass fractions, between devices and both delivered a potential lung dose fraction (LDF) of 10-12%.

In vitro experiments were performed to predict the effect that mucoadhesive compounds (MA) had on the residence time of formulations in the nasal cavity. Wettability, dissolution rate, and swelling indices were completed on MA to characterize hydroxypropyl methylcellulose (HPMC), carboxymethylcellulose sodium (CMC), sodium alginate (SA), and chitosan. The contact angle of the HPMC HMW and HPMC LMW were significantly greater than the other polymers, indicating a prolonged dissolution time. This correlated with the dissolution studies that indicated that CMC HMW and SA dissolved at a faster rate than the

HPMC compounds. The swelling indices of CMC HMW and SA were significantly greater than the other MA. Based on *in vitro* experiments, CMC HMW and SA were identified as two compounds that can increase residence time in the nasal cavity by dissolving in the nasal mucosa, allowing for chain entanglement with mucin, and taking up a substantial amount of fluid, increasing the viscosity of the nasal mucus.

Gamma scintigraphy and residence time studies were completed to determine the effect of formulation on the residence time in the nasal cavity of Brown Norway rats. Gamma scintigraphy allowed for the visual clearance of saline from the nasal cavity of a Brown Norway rat. The residence time studied indicated that increasing the viscosity did not have a great effect on the residence time and powder formulations required MA to have comparable residence times to liquid formulations with or without mucoadhesive in Brown Norway rats. The rank order of residence time for powders is SA>CMC HMW, Chit>HPMC HMW, No MA. The *in vitro* and *in vivo* experiments indicate that SA and CMC HMW in powder formulations have the greatest effect on increasing residence time in the nasal cavity of Brown Norway rats.

To demonstrate the effectiveness of the powder vaccine delivered intranasally in eliciting a local IgA and systemic IgG immune response in vivo.

A dose-response experiment ranging from 0.5 to 40 μg equivalent HA was performed using IM and IN liquids to determine an appropriate dose to quantify potential differences in antibody response elicited as a function of formulation in Brown Norway rats. IN delivery of liquid vaccine provided equivalent serum antibody titers as those obtained by IM injection at doses ≥2.5 μg after the initial vaccination, but at doses ≤2 μg, the serum antibody titers

elicited by IM injection were significantly greater than that of IN liquid after the first dose. After the boost dose, the immune response elicited at doses of 0.5, 1, 2.5, 5, and 10 μg is equivalent for both the IM injection and the IN liquid. Positive nasal IgA responses were seen after administration of IN liquid, regardless of dose. No detectable IgA responses were observed following IM injection. A 2 μg dose was chosen to use in the formulation experiments.

Once a dose was determined, IM injection, IN liquid, and IN powders containing trehalose alone, or 3% SA, CMC HMW, HPMC HMW, and chitosan were dosed. IM delivery of liquid vaccine provided equivalent serum antibody titers as those obtained by IN powder with no MA, CMC HMW, SA, and HPMC HMW after the initial dose and equivalent serum antibody titers as those obtained by IN liquid and IN powder with no MA, CMC HMW, SA, and HPMC HMW after the boost. IN liquid vaccine provided equivalent serum antibody titers as those obtained by IN powder with no MA, CMC HMW, SA, chitosan, and HPMC HMW after the initial vaccination. IgG isotyping and HAI displayed a similar pattern of response as the IgG. While no significant differences between powder and liquid formulations were observed. Trends are consistent with the observations from the residence time studies with respect to the eliciting an immune response.

Preliminary experiments evaluating residence time of various preparations in the nasal cavity of Sprague Dawley rats (350-400 g) were conducted using the same procedure used in Brown Norway rats (Appendix A.5). These studies were completed prior to those in Brown Norway rats; however, it was important to conduct replicate experiments in the strain of rats that would be employed in the immunogenicity studies. In Sprague Dawley rats, all of the liquid formulations with MA and powder formulations had larger areas under the

radiolabeled preparation retention curve (AUC) than the saline (Liq- No MA). Figure 6.1 shows the AUC data for both Brown Norway (Figure 4.8, Chapter 4, Section 4.3.5) and Sprague Dawley (Figure A.5.5, Appendix 5) rats. There is a clear pattern of increased residence time for powder formulations compared with liquid formulations in Sprague Dawley rats which is echoed in the Brown Norway rats, with the exception of the high AUCs for liquids in the latter strain. All of the powders, with the exception of Pow- SA (trehalose and SA) had longer residence times than the liquid formulations with the same MA, in Sprague Dawley rats. The AUC of the Liq- SA and Pow- SA were the same. The rank order of powders was Pow- CMC>Pow- HPMC HMW, Pow- No MA>Pow- SA>Pow- Chit. Compared to the AUC of the Brown Norway rats, the residence time of the liquids in Sprague Dawley rats was significantly lower, while the residence time of the Pow- No MA and Pow- HPMC HMW were significantly greater. This data indicates residence time differences between strains of rats. This may be due to variability from strain to strain or to differences in the size of the animals. The Brown Norway rats are used as an immunological model, but it would be plausible to think that the differences in residence time seen in the Sprague Dawley rats could potentially lead to differences in the immune response elicited if this was a susceptible strain. Moreover, if size of nasal cavity with respect to delivered dose is of significance then other species, such as the rabbit may be a logical selection for further studies (Little, Ivins et al. 2006).

While no significant differences between powder and liquid formulations were observed in Brown Norway rats, there is reason to believe that this will not necessarily be the case in the other species. As previously mentioned, the location of the nasal-associated

lymphoid tissue (NALT) in the rat is in the anterior portion of the nasal cavity. All of the nasal formulations come in contact with this tissue. Differences in residence time may become important if the target tissue is located in the posterior portion of the nasal cavity, as is currently thought to be the case in humans.

The dose response, while apparently sufficient to conduct the study of the antigen, ultimately did not facilitate clear discrimination of effects. At extremely low IM doses the immune response elicited was not significantly different than that at high doses. However, the immune response elicited by IN liquid at a dose of 0.5 μg was significantly lower than that of IM, but was still substantial. Other antigens may be more discriminating based on their dose response profiles.

Mucosal and systemic responses to WIIV were elicited following dry powder nasal vaccine delivery at a level equivalent to IN and IM delivery of solutions. However, it is unclear whether local residence time played a role in the animal model of immunogenicity employed in these studies. Consequently, the hypothesis is not fully supported by the evidence presented. Further work, in a more anatomically relevant animal model, may demonstrate conclusively the influence of mucoadhesive compounds on vaccine residence time at the nasal mucosa with implications for elicited immune response.

These experiments described did address the potential to overcome cold chain requirements (needed for vaccine stability) and to provide single-use, non-refillable delivery technologies that require minimal training. An inactivated, heat-stable, unit-dose vaccine was developed that can elicit both a local and systemic immune response in Brown Norway rats comparable to IM injection, which would be beneficial when used for influenza prevention, since the virus enters the host by this route. Further development of this approach may

ultimately provide a safe and an effective alternative to the currently available influenza vaccines.

6.2 Future Work

A dry powder nasal influenza vaccine was manufactured utilizing HPMC, CMC, SA, or chitosan as MA in Brown Norway rats. These are a small subset of polymers that may be utilized to vary residence time in the nasal cavity. Other compounds include, but should not be limited to: polyacrylic acids, polyvinyl pyrrolidone, polyethylene glycols, and poly(lactic-*co*-glycolic acid). These compounds have been shown, in separate studies, to increase the residence time in the nasal cavity (Ugwoke, Agu et al. 2005). With the characterization approach described here, a large number of compounds can be systematically screened and ranked based on the contact angles, dissolution rates, and swelling indices.

A direct imaging approach to quantify residence time in the nasal cavity is desirable. The sequential lavage method, described here, is time consuming and costly because each data point represents one or more animals. An imaging technique would allow fewer animals to be dosed sequentially in a relatively non-invasive manner and monitored over a period of time. Inter-animal variability would be avoided as each animal would be its own control. Once this method was established it would be an ethically superior approach to the sequential lavage studies, as animals could potentially be rested and used in subsequent experiments.

The immune response experiments should be completed in other susceptible rat strains or species. Comparisons should be made between strains and species to allow extrapolation to man. Unlike rats, rabbits and pigs are relatively small animals with NALT configurations similar to that in humans. Difference in NALT location may help in

determining if the length of residence time in the nasal cavity can affect the immune response elicited. Ultimately, it would be desirable to conduct studies of residence times in humans. However, evidence of safety of the entire formulation and its components would be required prior to the performance of such studies.

The ultimate test of the effectiveness of a vaccine is a challenge study, which involves vaccination of animals and exposure to virulent micro-organism to demonstrate protection from infection. A rat-adapted influenza virus (RAIV) has been previously described (Lebrec and Burleson 1994). Briefly, a human A/Port Chalmers/1/73 (H3N2) influenza virus has been adapted to be infectious in rats as a model of mild pulmonary influenza virus infection. The timeline of events in the rats after infection is known and physical symptoms of the virus, usually seen in the first 48 hours following inoculation include: epithelial lesions of the nose and septum, epithelial erosion, an influx of neutrophils into the respiratory tract. Ninety-six hours after infection, the presence of virus in the tissue is minimal. After vaccination, rats exposed to the RAIV will not show any signs of infection if the vaccination is successful. Use of this method is limited because the RAIV is proprietary. There are few alternative models in mice and ferrets (McLaren, Potter et al. 1974; Alymova, Kodihalli et al. 1998), but better models are required since anatomical and physiological relevance are as important as immunological relevance. Rabbits, non-human primates and pigs are considered anatomically and physiologically relevant (Ivins, Pitt et al. 1998; Macklin, McCabe et al. 1998; Little, Ivins et al. 2006), but their use in influenza challenge studies is as yet unproven.

The scope of the work performed does not have to be limited to the influenza virus. The immune response experiments can be completed utilizing a variety of different antigens.

Differences in the immunogenicity of the antigen could potentially lead to different outcomes of these experiments. It is possible that an increase in residence time in the nasal cavity can increase the immune response elicited by a low potency antigen. This could enable a wide variety of vaccines to be produced without the presence of an adjuvant, while still achieving the same immune response. Current interest in biodefense has increased research with respect to both human (e.g. anthrax, (Jiang, Joshi et al. 2006)) and animal (e.g. Newcastle disease in chickens, (Corbanie, Remon et al. 2006))

This project focused on the use of dry powder nasal vaccines. These principles can be applied to drugs. An extended residence time in the nasal cavity will allow larger quantities of drug to pass through the nasal epithelium into systemic circulation or allow longer activity for locally acting compounds. However, this is a well documented application of both mucoadhesives and nasal delivery. The significance of the present work may be for macromolecules where in addition to enhanced residence time and local delivery to nasal cavity, stable preparations are required. Currently, the only macromolecule delivered nasally is calcitonin for the treatment of osteoporosis (Body 2002). The present observations may be useful for developing stable preparations of other peptides or proteins.

In conclusion, potential future studies may be grouped into several categories: (a) studies of formulation effects on residence time in other anatomically and physiologically relevant species; (b) performance of challenge studies in the rat or mouse or development of models in other species; (c) application to other antigens for vaccination of humans or animals and (d) application to drugs, notably macromolecules, where some features of preparations described in these studies would offer advantages with respect to existing approaches.

Figure 6.1– The area under the curve of the percentage of radioactivity as a function of time curves for liquid and powder formulations containing no mucoadhesive (No MA), hydroxypropyl methylcellulose (HPMC HMW), sodium alginate (SA), carboxymethylcellulose sodium (CMC HMW), and chitosan (Chit) in Brown Norway and Sprague Dawley rats.

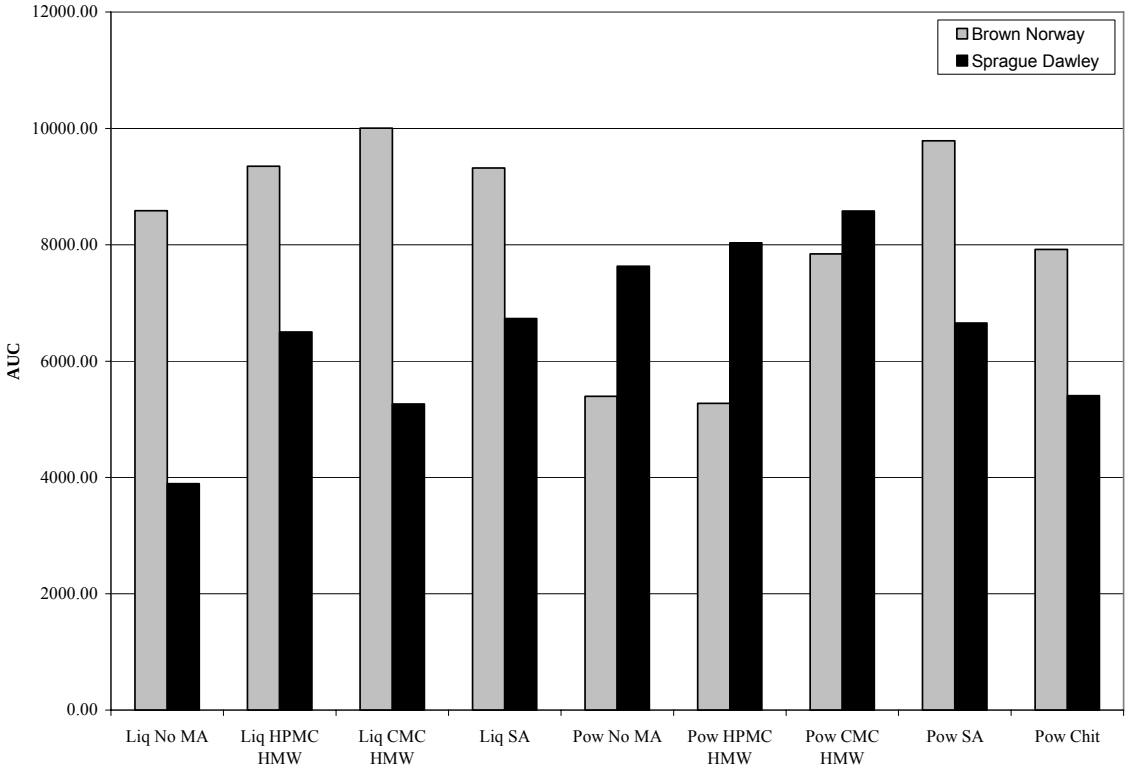

APPENDICES

Appendix A.1- ANALYSIS OF VARIANCE (ANOVA), RESIDUAL PLOTS, AND INTERACTION GRAPHS FOR DESIGNED EXPERIMENTS

FREEZE-DRYING

Design Summary

Study Type	Factorial	**Experiments**	24
Initial Design	2 Level Factorial	**Blocks**	No Blocks
Center Points	0		
Design Model	3FI		

Response	Name	Units	Obs	Minimum	Maximum	Trans	Model
Y1	D50	um	24	10.67	28.65	None	3FI
Y2	D90	um	24	22.97	89.94	None	R2FI
Y3	D10	um	24	0.97	6.95	None	3FI
Y4	Span		24	1.77	3.94	None	3FI

Factor	Name	Units	Type	Low Actual	High Actual	Low Coded	High Coded
A	Freeze Rate		Categorical	Slow	Fast	-1.000	1.000
B	Concentration	g/100 mL	Numeric	1.00	10.00	-1.000	1.000
C	Annealing		Categorical	No	Yes	-1.000	1.000

MEDIAN DIAMETER (D_{50})

Response: D_{50}

Factor	Name	Units	Type	-1 Level	+1 Level
A	Freeze Rate		Categorical	Slow	Fast
B	Conc.	g/100 mL	Numeric	1.00	10.00
C	Annealing		Categorical	No	Yes

ANOVA for Selected Factorial Model

Source	Sum of Squares	DF	Mean Square	F Value	Prob > F
Model	924.34	7	132.05	416.40	< 0.0001
Residual	5.07	16	0.32		
Pure Error	*5.07*	*16*	*0.32*		
Cor Total	929.41	23			

Root MSE	0.56	R-Squared	0.9945	
Dep Mean	18.43	Adj R-Squared	0.9922	
C.V.	3.06	Pred R-Squared	0.9877	
PRESS	11.42	Adeq Precision	54.071	Desire > 4

Factor	Coefficient Estimate	DF	Standard Error	t for H_0Coeff=0	Prob > |t|	VIF
Intercept	18.43	1	0.11			
A-Freeze Rate	0.95	1	0.11	8.26	< 0.0001	1.00
B-Conc.	0.25	1	0.11	2.14	0.0482	1.00
C-Annealing	-4.40	1	0.11	-38.24	< 0.0001	1.00
AB	2.28	1	0.11	19.87	< 0.0001	1.00
AC	2.20	1	0.11	19.15	< 0.0001	1.00
BC	2.79	1	0.11	24.31	< 0.0001	1.00
ABC	0.60	1	0.11	5.23	< 0.0001	1.00

Final Equation in Terms of Coded Factors:

$$D_{50} = 18.43 + 0.95*A + 0.25*B - 4.40*C + 2.28*AB + 2.20*AC + 2.79*BC + 0.60*ABC$$

Diagnostics Case Statistics

Std Order	Actual Value	Predicted Value	Residual	Distance	Student Residual	Cook's Leverage	Outlier t
1	27.78	28.31	-0.53	0.333	-1.145	0.082	-1.158
2	28.49	28.31	0.18	0.333	0.399	0.010	0.388
3	28.65	28.31	0.34	0.333	0.747	0.035	0.736
4	22.29	22.44	-0.15	0.333	-0.319	0.006	-0.310
5	21.67	22.44	-0.77	0.333	-1.667	0.174	-1.776
6	23.35	22.44	0.91	0.333	1.986	0.247	2.216
7	19.92	19.84	0.077	0.333	0.167	0.002	0.162
8	19.69	19.84	-0.15	0.333	-0.333	0.007	-0.324
9	19.92	19.84	0.077	0.333	0.167	0.002	0.162
10	19.84	20.71	-0.87	0.333	-1.885	0.222	-2.069
11	20.49	20.71	-0.22	0.333	-0.471	0.014	-0.459
12	21.79	20.71	1.08	0.333	2.356	0.347	2.823
13	10.81	10.73	0.083	0.333	0.181	0.002	0.176
14	10.70	10.73	-0.027	0.333	-0.058	0.000	-0.056
15	10.67	10.73	-0.057	0.333	-0.123	0.001	-0.119
16	12.06	11.26	0.80	0.333	1.747	0.191	1.881
17	10.97	11.26	-0.29	0.333	-0.623	0.024	-0.611
18	10.74	11.26	-0.52	0.333	-1.124	0.079	-1.134
19	11.06	11.04	0.023	0.333	0.051	0.000	0.049
20	11.01	11.04	-0.027	0.333	-0.058	0.000	-0.056
21	11.04	11.04	0.003	0.333	0.007	0.000	0.007
22	22.91	23.11	-0.20	0.333	-0.428	0.011	-0.417
23	22.95	23.11	-0.16	0.333	-0.341	0.007	-0.331
24	23.46	23.11	0.35	0.333	0.768	0.037	0.758

Figure A.1.1– Residuals plotted versus predicted values for the model describing the effect of various factors on median diameter (D_{50}) of powders manufactured by FD followed by milling and sieving.

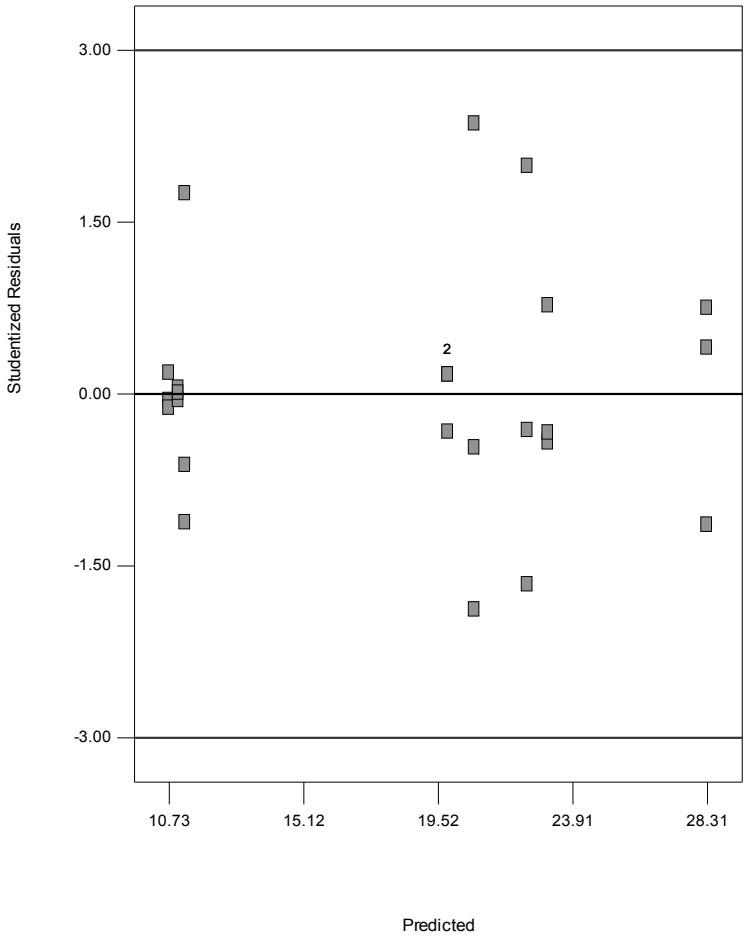

Figure A.1.2– Interaction graphs indicating the effects of a) solute concentration (B-=1%, B+=10%) and freezing rate (A-=Slow, A+=Fast), and b) annealing (C-=No, C+=Yes) and freezing rate (A-=Slow, A+=Fast) on median diameter (D_{50}) of particles produced by FD followed by milling and sieving.

a)

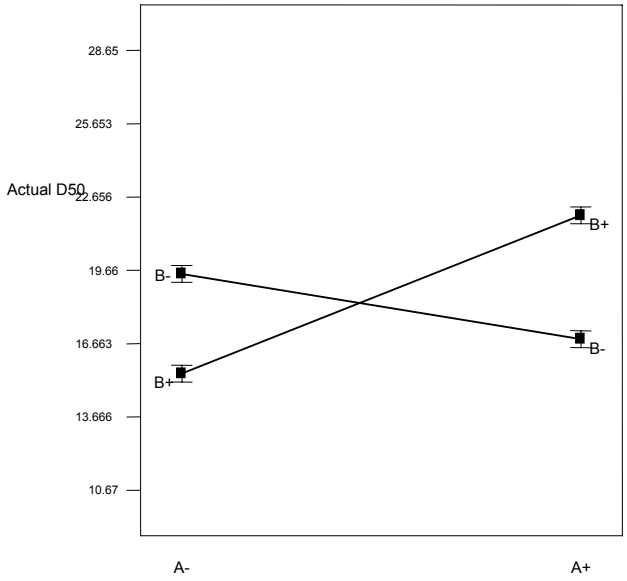

b)

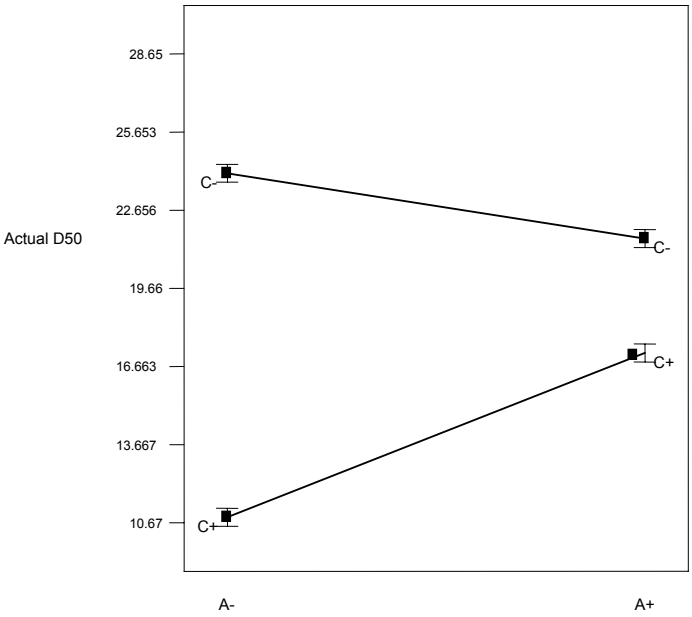

Figure A.1.3– Interaction graphs indicating the effects of annealing (C-=No, C+=Yes) and solute concentration (B-=1%, B+=10%) on median diameter (D_{50}) of particles produced by FD followed by milling and sieving.

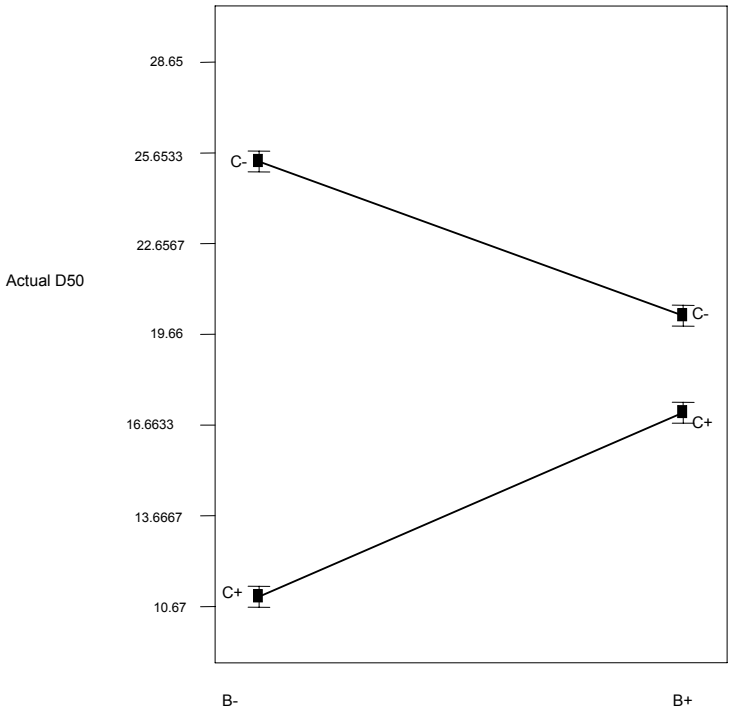

90% DIAMETER (D_{90})

Response: D_{90}

Factor	Name	Units	Type	-1 Level	+1 Level
A	Freeze Rate		Categorical	Slow	Fast
B	Concentration	g/100 mL	Numeric	1.00	10.00
C	Annealing		Categorical	No	Yes

ANOVA for Selected Factorial Model

Source	Sum of Squares	DF	Mean Square	F Value	Prob > F
Model	7380.68	4	1845.17	43.27	< 0.0001
Residual	810.20	19	42.64		
Lack of Fit	*124.32*	*3*	*41.44*	*0.97*	*0.4326*
Pure Error	*685.88*	*16*	*42.87*		
Cor Total	8190.88	23			

Root MSE	6.53	R-Squared	0.9011	
Dep Mean	53.99	Adj R-Squared	0.8803	
C.V.	12.09	Pred R-Squared	0.8422	
PRESS	1292.73	Adeq Precision	20.036	Desire > 4

Factor	Coefficient Estimate	DF	Standard Error	t for H_0Coeff=0	Prob > |t|	VIF
Intercept	53.99	1	1.33			
A-Freeze Rate	10.01	1	1.33	7.51	< 0.0001	1.00
B-Concentration	-0.087	1	1.33	-0.065	0.9486	1.00
C-Annealing	-12.19	1	1.33	-9.15	< 0.0001	1.00
BC	7.65	1	1.33	5.74	< 0.0001	1.00

Final Equation in Terms of Coded Factors:

$$D_{90} = 53.99 + 10.01*A - 0.087*B - 12.19*C + 7.65*BC$$

Diagnostics Case Statistics

Std Order	Actual Value	Predicted Value	Residual	Distance	Student Residual	Cook's Leverage	Outlier t
1	66.74	63.91	2.83	0.208	0.487	0.012	0.477
2	65.57	63.91	1.66	0.208	0.285	0.004	0.278
3	70.28	63.91	6.37	0.208	1.096	0.063	1.102
4	75.13	83.94	-8.81	0.208	-1.516	0.121	-1.574
5	78.41	83.94	-5.53	0.208	-0.951	0.048	-0.949
6	87.42	83.94	3.48	0.208	0.599	0.019	0.589
7	45.89	48.43	-2.54	0.208	-0.438	0.010	-0.428
8	44.89	48.43	-3.54	0.208	-0.610	0.020	-0.600
9	47.00	48.43	-1.43	0.208	-0.247	0.003	-0.241
10	59.73	68.46	-8.73	0.208	-1.502	0.119	-1.558
11	63.23	68.46	-5.23	0.208	-0.900	0.043	-0.895
12	89.94	68.46	21.48	0.208	3.697	0.719	6.793 *
13	23.24	24.22	-0.98	0.208	-0.168	0.001	-0.164
14	22.97	24.22	-1.25	0.208	-0.215	0.002	-0.209
15	22.97	24.22	-1.25	0.208	-0.215	0.002	-0.209
16	48.91	44.24	4.67	0.208	0.803	0.034	0.795
17	42.18	44.24	-2.06	0.208	-0.355	0.007	-0.347
18	45.12	44.24	0.88	0.208	0.151	0.001	0.147
19	40.36	39.35	1.01	0.208	0.174	0.002	0.170
20	38.68	39.35	-0.67	0.208	-0.115	0.001	-0.112
21	39.15	39.35	-0.20	0.208	-0.034	0.000	-0.033
22	62.59	59.37	3.22	0.208	0.553	0.016	0.543
23	59.15	59.37	-0.22	0.208	-0.039	0.000	-0.038
24	56.24	59.37	-3.13	0.208	-0.539	0.015	-0.529

* Case(s) with |Outlier t| > 3.50

Figure A.1.4– Residuals plotted versus predicted values for the model describing the effect of various factors on 90% diameter (D_{90}) of powders manufactured by FD followed by milling and sieving.

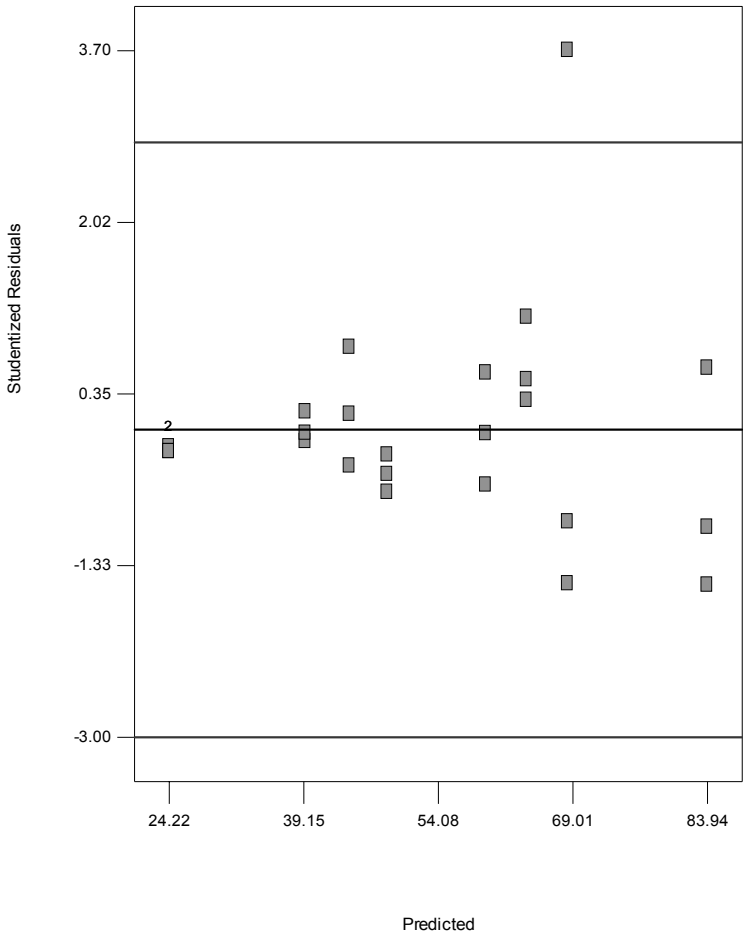

Figure A.1.5– Interaction graphs indicating the effects of annealing (C-=No, C+=Yes) and solute concentration (B-=1%, B+=10%) on 90% diameter (D_{90}) of particles produced by FD followed by milling and sieving.

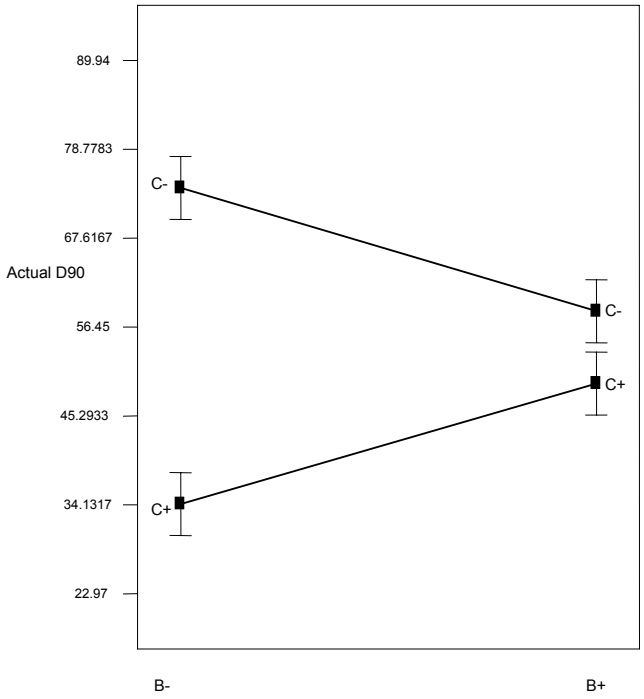

10% DIAMETER (D_{10})

Response: D_{10}

Factor	Name	Units	Type	-1 Level	+1 Level
A	Freeze Rate	Categorical	Slow	Fast	
B	Concentration	g/100 mL	Numeric	1.00	10.00
C	Annealing		Categorical	No	Yes

ANOVA for Selected Factorial Model

Source	Sum of Squares	DF	Mean Square	F Value	Prob > F
Model	60.35	7	8.62	49.11	< 0.0001
Residual	2.81	16	0.18		
Pure Error	*2.81*	*16*	*0.18*		
Cor Total	63.16	23			

Root MSE	0.42	R-Squared	0.9555	
Dep Mean	4.94	Adj R-Squared	0.9361	
C.V.	8.48	Pred R-Squared	0.8999	
PRESS	6.32	Adeq Precision	18.107	Desire > 4

Factor	Coefficient Estimate	DF	Standard Error	t for H0 Coeff=0	Prob > |t|	VIF
Intercept	4.94	1	0.086			
A-Freeze Rate	0.22	1	0.086	2.55	0.0213	1.00
B-Concentration	-0.19	1	0.086	2.19	0.0435	1.00
C-Annealing	-1.06	1	0.086	-12.34	< 0.0001	1.00
AB	0.81	1	0.086	9.44	< 0.0001	1.00
AC	0.52	1	0.086	6.02	< 0.0001	1.00
BC	0.30	1	0.086	3.56	0.0026	1.00
ABC	0.56	1	0.086	6.50	< 0.0001	1.00

Final Equation in Terms of Coded Factors:

D_{10}= 4.94 + 0.22*A + 0.19*B - 1.06*C + 0.81*AB + 0.52*AC + 0.30*BC + 0.56*ABC

Diagnostics Case Statistics

Std Order	Actual Value	Predicted Value	Residual	Distance	Student Residual	Cook's Leverage	Outlier t
1	6.66	6.66	-0.003	0.333	-0.010	0.000	-0.009
2	6.95	6.66	0.29	0.333	0.838	0.044	0.830
3	6.38	6.66	-0.28	0.333	-0.828	0.043	-0.820
4	5.54	5.57	-0.027	0.333	-0.078	0.000	-0.075
5	5.49	5.57	-0.077	0.333	-0.224	0.003	-0.217
6	5.67	5.57	0.10	0.333	0.302	0.006	0.293
7	5.92	5.93	-0.0067	0.333	-0.019	0.000	-0.019
8	5.86	5.93	-0.067	0.333	-0.195	0.002	-0.189
9	6.00	5.93	0.073	0.333	0.214	0.003	0.208
10	5.78	5.84	-0.057	0.333	-0.166	0.002	-0.161
11	5.90	5.84	0.063	0.333	0.185	0.002	0.179
12	5.83	5.84	-0.0067	0.333	-0.019	0.000	-0.019
13	4.05	4.03	0.023	0.333	0.068	0.000	0.066
14	4.06	4.03	0.033	0.333	0.097	0.001	0.094
15	3.97	4.03	-0.057	0.333	-0.166	0.002	-0.161
16	2.81	2.77	0.043	0.333	0.127	0.001	0.123
17	2.73	2.77	-0.037	0.333	-0.107	0.001	-0.104
18	2.76	2.77	-0.0067	0.333	-0.019	0.000	-0.019
19	2.94	2.28	0.66	0.333	1.920	0.230	2.118
20	0.97	2.28	-1.31	0.333	-3.839	0.921	-13.238 *
21	2.94	2.28	0.66	0.333	1.920	0.230	2.118
22	6.56	6.48	0.083	0.333	0.244	0.004	0.236
23	6.49	6.48	0.013	0.333	0.039	0.000	0.038
24	6.38	6.48	-0.097	0.333	-0.283	0.005	-0.274

* Case(s) with |Outlier t| > 3.50

Figure A.1.6– Residuals plotted versus predicted values for the model describing the effect of various factors on 10% diameter (D_{10}) of powders manufactured by FD followed by milling and sieving.

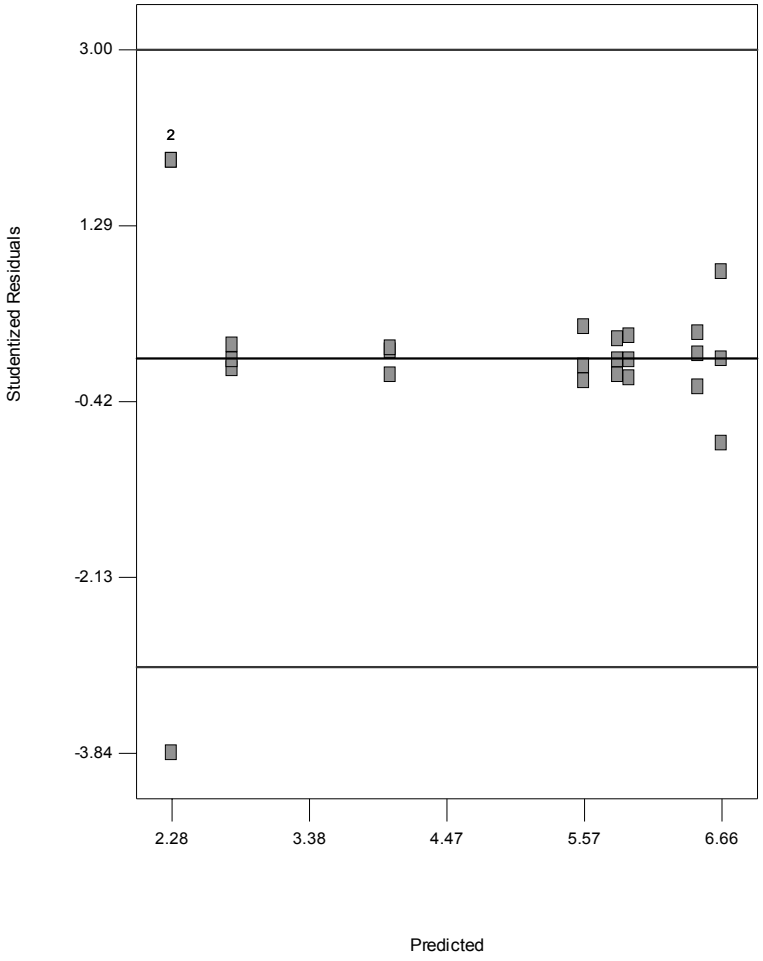

Figure A.1.7– Interaction graphs indicating the effects of a) solute concentration (B-=1%, B+=10%) and freezing rate (A-=Slow, A+=Fast), and b) annealing (C-=No, C+=Yes) and freezing rate (A-=Slow, A+=Fast) on 10% diameter (D_{10}) of particles produced by FD followed by milling and sieving.

a)

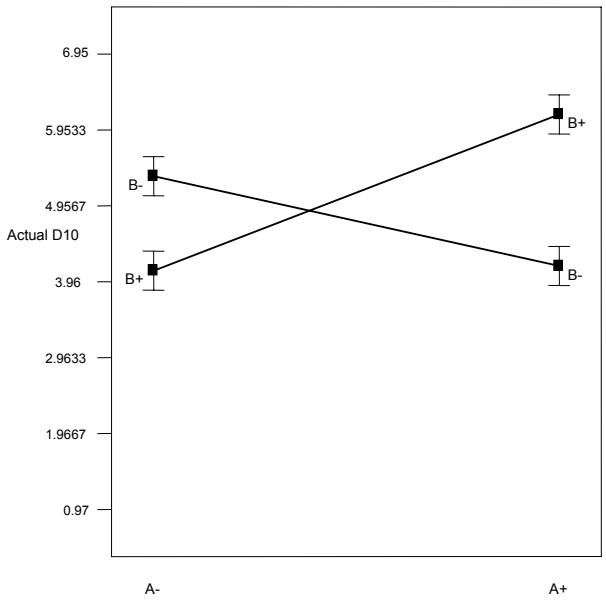

b)

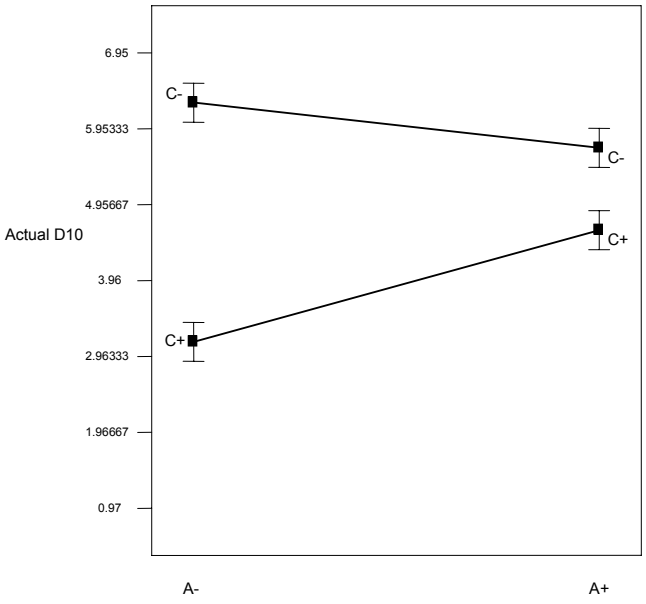

Figure A.1.8– Interaction graphs indicating the effects of annealing (C-=No, C+=Yes) and solute concentration (B-=1%, B+=10%) on 10% diameter (D_{10}) of particles produced by FD followed by milling and sieving.

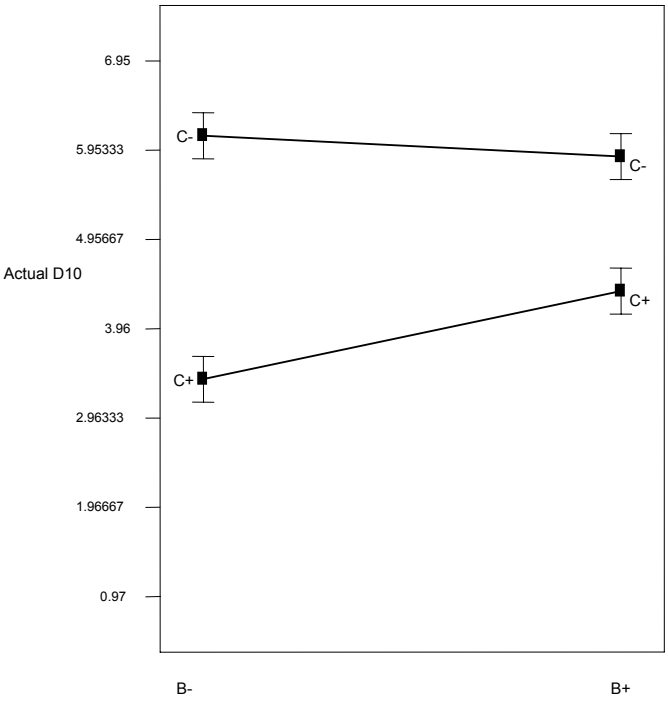

SPAN

Response: Span

Factor	Name	Units	Type	-1 Level	+1 Level
A	Freeze Rate		Categorical	Slow	Fast
B	Concentration	g/100mL	Numeric	1.00	10.00
C	Annealing		Categorical	No	Yes

ANOVA for Selected Factorial Model

Source	Sum of Squares	DF	Mean Square	F Value	Prob > F
Model	11.73	7	1.68	27.75	< 0.0001
Residual	0.97	16	0.060		
Pure Error	*0.97*	*16*	*0.060*		
Cor Total	12.70	23			

Root MSE	0.25	R-Squared	0.9239	
Dep Mean	2.72	Adj R-Squared	0.8906	
C.V.	9.03	Pred R-Squared	0.8288	
PRESS	2.17	Adeq Precision	14.188	Desire > 4

Factor	Coefficient Estimate	DF	Standard Error	t for H0 Coeff=0	Prob > |t|	VIF
Intercept	2.72	1	0.050			
A-FreezeRate	0.41	1	0.050	8.19	< 0.0001	1.00
B-Concen	-0.038	1	0.050	-0.76	0.4560	1.00
C-Annealing	0.066	1	0.050	1.31	0.2080	1.00
AB	-0.39	1	0.050	-7.71	< 0.0001	1.00
AC	-0.16	1	0.050	-3.21	0.0055	1.00
BC	0.045	1	0.050	0.90	0.3831	1.00
ABC	-0.37	1	0.050	-7.37	< 0.0001	1.00

Final Equation in Terms of Coded Factors:

Span= 2.72 + 0.41*A - 0.038*B + 0.066*C - 0.39*AB - 0.16*AC + 0.045*BC - 0.37*ABC

Diagnostics Case Statistics

Std Order	Actual Value	Predicted Value	Residual	Distance	Student Residual	Cook's Leverage	Outlier t
1	2.16	2.15	0.01	0.333	0.050	0.000	0.048
2	2.06	2.15	-0.090	0.333	-0.448	0.013	-0.437
3	2.23	2.15	0.080	0.333	0.399	0.010	0.388
4	3.27	3.33	-0.057	0.333	-0.282	0.005	-0.274
5	3.21	3.33	-0.12	0.333	-0.581	0.021	-0.569
6	3.50	3.33	0.17	0.333	0.864	0.047	0.856
7	2.01	2.02	-0.067	0.333	-0.033	0.000	-0.032
8	1.98	2.02	-0.037	0.333	-0.183	0.002	-0.177
9	2.06	2.02	0.043	0.333	0.216	0.003	0.209
10	2.72	3.13	-0.41	0.333	-2.026	0.257	-2.276
11	3.86	3.13	0.73	0.333	3.654	0.835	8.698 *
12	2.80	3.13	-0.33	0.333	-1.628	0.166	-1.725
13	1.77	1.77	-0.033	0.333	-0.017	0.000	-0.016
14	1.77	1.77	-0.0033	0.333	-0.017	0.000	-0.016
15	1.78	1.77	0.0067	0.333	0.033	0.000	0.032
16	3.82	3.79	0.033	0.333	0.166	0.002	0.161
17	3.60	3.79	-0.19	0.333	-0.930	0.054	-0.926
18	3.94	3.79	0.15	0.333	0.764	0.036	0.754
19	3.28	3.30	-0.020	0.333	-0.100	0.001	-0.097
20	3.24	3.30	-0.060	0.333	-0.299	0.006	-0.290
21	3.38	3.30	0.080	0.333	0.399	0.010	0.388
22	2.18	2.29	-0.11	0.333	-0.532	0.018	-0.519
23	2.29	2.29	0.0033	0.333	0.017	0.000	0.016
24	2.39	2.29	0.10	0.333	0.515	0.017	0.503

* Case(s) with |Outlier t| > 3.50

Figure A.1.9– Residuals plotted versus predicted values for the model describing the effect of various factors on span of powders manufactured by FD followed by milling and sieving.

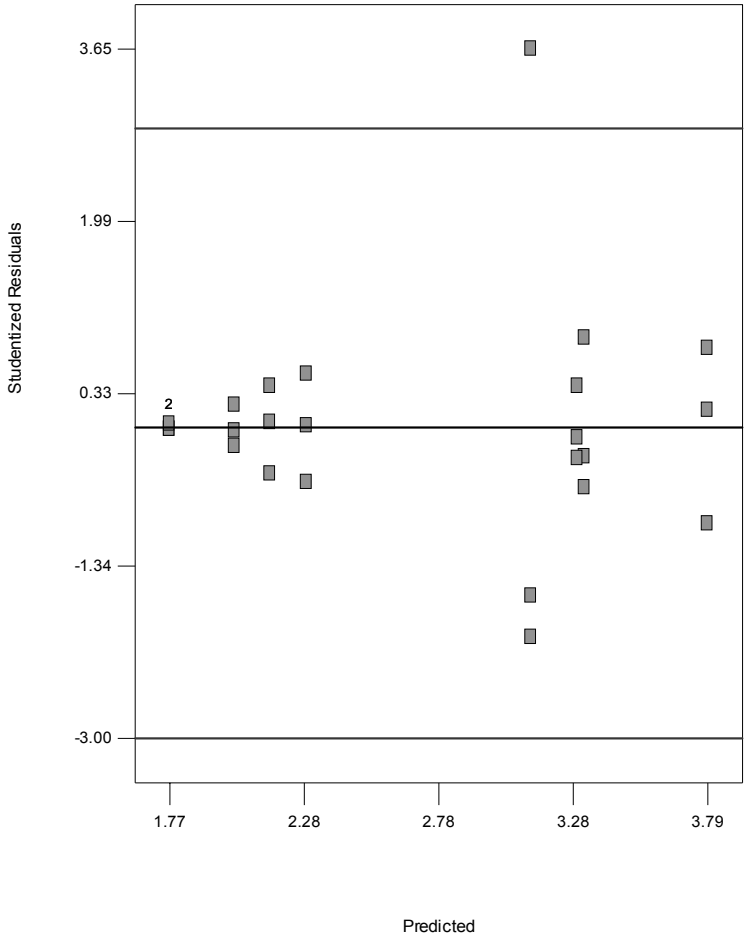

Figure A.1.10– Interaction graphs indicating the effects of a) solute concentration (B-=1%, B+=10%) and freezing rate (A-=Slow, A+=Fast), and b) annealing (C-=No, C+=Yes) and freezing rate (A-=Slow, A+=Fast) on span of particles produced by FD followed by milling and sieving.

a)

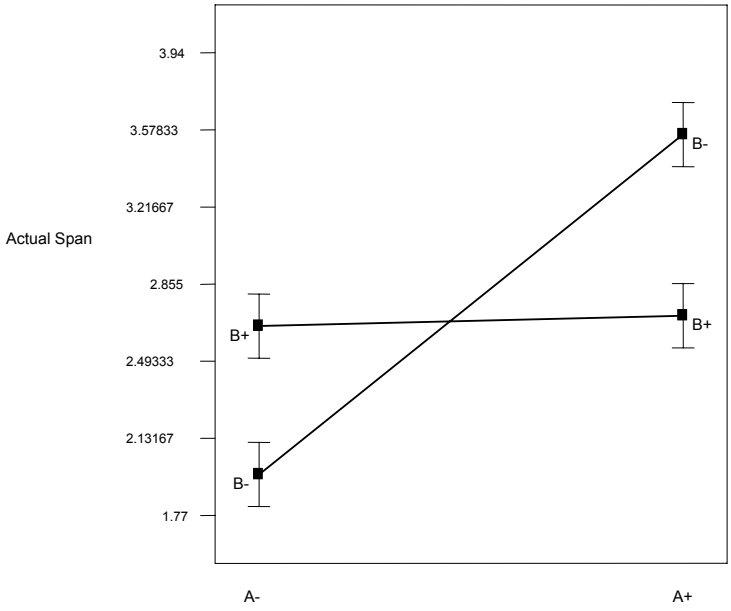

b)

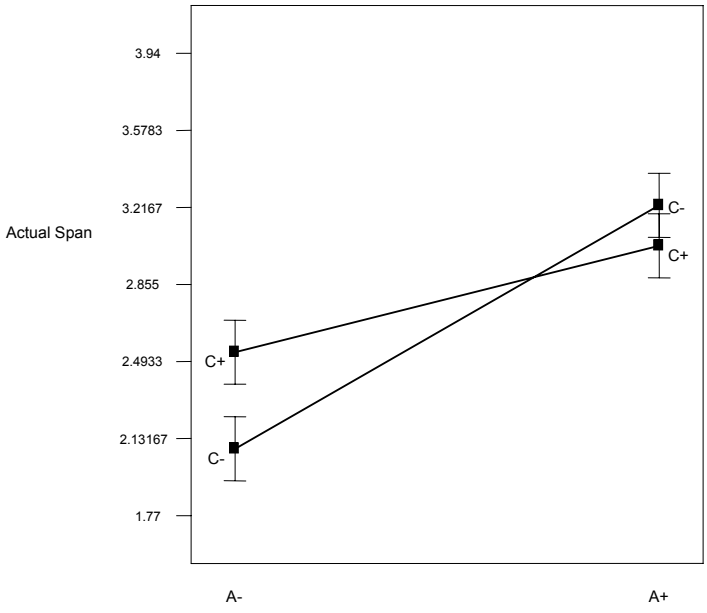

Figure A.1.11– Interaction graphs indicating the effects of annealing (C-=No, C+=Yes) and solute concentration (B-=1%, B+=10%) on span of particles produced by FD followed by milling and sieving.

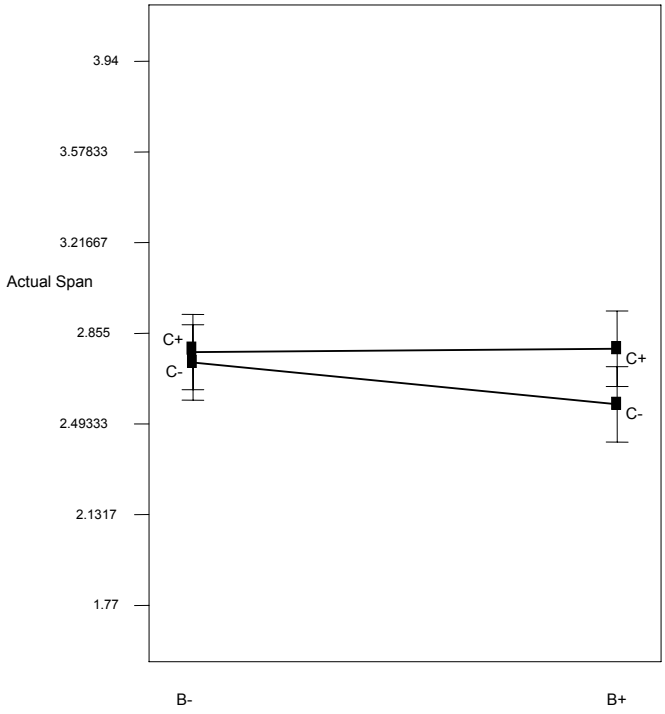

SPRAY-FREEZE DRYING

Design Summary

Study Type	Factorial	**Experiments**	24
Initial Design	2 Level Factorial	**Blocks**	No Blocks
Center Points	0		
Design Model	3FI		

Response	Name	Units	Obs	Minimum	Maximum	Trans	Model
Y1	D50	um	24	15.76	50.92	None	Main effects
Y2	D90	um	24	24.42	181.67	None	Main effects
Y3	D10	um	24	4.13	13.63	None	Main effects
Y4	Span		24	1.28	3.39	None	Main effects

Factor	Name	Units	Type	Low Actual	High Actual	Low Coded	High Coded
A	Sol. Feed	mL/min	Numeric	3.00	25.00	-1.000	1.000
B	Air Flow	L/hr	Numeric	250.00	500.00	-1.000	1.000
C	Sol. Conc.	g/100 mL	Numeric	1.00	10.00	-1.000	1.000

MEDIAN DIAMETER (D_{50})

Response: D_{50}

Factor	Name	Units	Type	-1 Level	+1 Level
A	Sol. Feed	mL/min	Numeric	3.00	25.00
B	Air Flow	L/hr	Numeric	250.00	500.00
C	Sol. Conc.	g/100 mL	Numeric	1.00	10.00

ANOVA for Selected Factorial Model

Source	Sum of Squares	DF	Mean Square	F Value	Prob > F
Model	2582.00	2	1291.00	59.43	< 0.0001
Residual	456.20	21	21.72		
Lack of Fit	*166.13*	*5*	*33.23*	*1.83*	*0.1632*
Pure Error	*290.07*	*16*	*18.13*		
Cor Total	3038.20	23			

Root MSE	4.66	R-Squared	0.8498	
Dep Mean	32.54	Adj R-Squared	0.8355	
C.V.	14.32	Pred R-Squared	0.8039	
PRESS	595.85	Adeq Precision	15.425	Desire > 4

Factor	Coefficient Estimate	DF	Standard Error	t for H_0 Coeff=0	Prob > |t|	VIF
Intercept	32.54	1	0.95			
A-Sol. Feed	10.02	1	0.95	10.53	< 0.0001	1.00
B-Air Flow	-2.69	1	0.95	-2.83	0.0100	1.00

Final Equation in Terms of Coded Factors:

D_{50}= 32.54 + 10.02*A - 2.69*B

Diagnostics Case Statistics

Std Order	Actual Value	Predicted Value	Residual	Distance	Student Residual	Cook's Leverage	Outlier t
1	20.63	25.22	-4.59	0.125	-1.052	0.053	-1.055
2	21.60	25.22	-3.62	0.125	-0.830	0.033	-0.823
3	20.72	25.22	-4.50	0.125	-1.031	0.051	-1.033
4	44.97	45.25	-0.28	0.125	-0.064	0.000	-0.063
5	50.92	45.25	5.67	0.125	1.301	0.081	1.324
6	50.44	45.25	5.19	0.125	1.190	0.067	1.203
7	15.82	19.83	-4.01	0.125	-0.920	0.040	-0.917
8	22.46	19.83	2.63	0.125	0.603	0.017	0.593
9	16.95	19.83	-2.88	0.125	-0.661	0.021	-0.652
10	39.72	39.87	-0.15	0.125	-0.033	0.000	-0.032
11	40.19	39.87	0.32	0.125	0.075	0.000	0.073
12	39.43	39.87	-0.44	0.125	-0.100	0.000	-0.097
13	37.78	25.22	12.56	0.125	2.882	0.395	3.617 *
14	20.80	25.22	-4.42	0.125	-1.013	0.049	-1.014
15	26.39	25.22	1.17	0.125	0.269	0.003	0.263
16	42.79	45.25	-2.46	0.125	-0.564	0.015	-0.555
17	42.22	45.25	-3.03	0.125	-0.695	0.023	-0.686
18	43.54	45.25	-1.71	0.125	-0.392	0.007	-0.384
19	15.76	19.83	-4.07	0.125	-0.934	0.042	-0.931
20	22.12	19.83	2.29	0.125	0.525	0.013	0.516
21	29.26	19.83	9.43	0.125	2.163	0.223	2.394
22	38.63	39.87	-1.23	0.125	-0.283	0.004	-0.277
23	38.62	39.87	-1.25	0.125	-0.286	0.004	-0.279
24	39.22	39.87	-0.65	0.125	-0.148	0.001	-0.144

* Case(s) with |Outlier t| > 3.50

Figure A.1.12– Residuals plotted versus predicted values for the model describing the effect of various factors on median diameter (D_{50}) of powders manufactured by SFD.

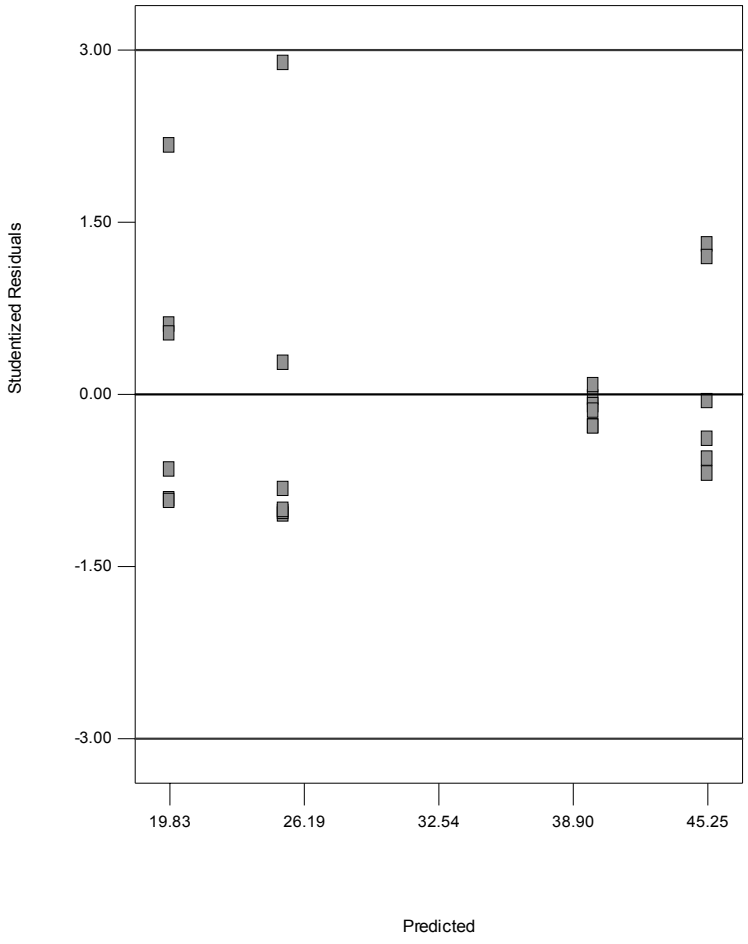

90% DIAMETER (D_{90})

Response: D_{90}

Factor	Name	Units	Type	-1 Level	+1 Level
A	Sol. Feed	mL/min	Numeric	3.00	25.00
B	Air Flow	L/hr	Numeric	250.00	500.00
C	Sol. Conc.	g/100 mL	Numeric	1.00	10.00

ANOVA for Selected Factorial Model

Source	Sum of Squares	DF	Mean Square	F Value	Prob > F
Model	29155.57	2	14577.78	36.66	< 0.0001
Residual	8350.40	21	397.64		
Lack of Fit	*4865.17*	*5*	*973.03*	*4.47*	*0.0097*
Pure Error	*3485.23*	*16*	*217.83*		
Cor Total	37505.97	23			

Root MSE	19.94	R-Squared	0.7774	
Dep Mean	75.40	Adj R-Squared	0.7562	
C.V.	26.45	Pred R-Squared	0.7092	
PRESS	10906.64	Adeq Precision	12.922	Desire > 4

Factor	Coefficient Estimate	DF	Standard Error	t for H_0 Coeff=0	Prob > |t|	VIF
Intercept	75.40	1	4.07			
A-Sol. Feed	32.19	1	4.07	7.91	< 0.0001	1.00
B-Air Flow	-13.36	1	4.07	-3.28	0.0036	1.00

Final Equation in Terms of Coded Factors:

$$D_{90} = 75.40 + 32.19*A - 13.36*B$$

Diagnostics Case Statistics

Std Order	Actual Value	Predicted Value	Residual	Distance	Student Residual	Cook's Leverage	Outlier t
1	44.01	56.57	-12.56	0.125	-0.673	0.022	-0.664
2	46.37	56.57	-10.20	0.125	-0.547	0.014	-0.5373
3	43.44	56.57	-13.13	0.125	-0.704	0.024	-0.695
4	115.37	120.95	-5.58	0.125	-0.299	0.004	-0.293
5	181.67	120.95	60.72	0.125	3.255	0.505	4.513 *
6	158.58	120.95	37.63	0.125	2.017	0.194	2.193
7	33.55	29.85	3.70	0.125	0.199	0.002	0.194
8	40.25	29.85	10.40	0.125	0.558	0.015	0.548
9	34.46	29.85	4.61	0.125	0.247	0.003	0.242
10	90.08	94.23	-4.15	0.125	-0.222	0.002	-0.217
11	89.36	94.23	-4.87	0.125	-0.261	0.003	-0.255
12	90.84	94.23	-3.39	0.125	-0.182	0.002	-0.177
13	72.04	56.57	15.47	0.125	0.829	0.033	0.823
14	37.91	56.57	-18.66	0.125	-1.000	0.048	-1.000
15	48.94	56.57	-7.63	0.125	-0.409	0.008	-0.401
16	102.73	120.95	-18.22	0.125	-0.977	0.045	-0.976
17	98.50	120.95	-22.45	0.125	-1.204	0.069	-1.217
18	115.55	120.95	-5.40	0.125	-0.290	0.004	-0.283
19	24.42	29.85	-5.43	0.125	-0.291	0.004	-0.284
20	39.99	29.85	10.14	0.125	0.544	0.014	0.535
21	53.10	29.85	23.25	0.125	1.247	0.074	1.264
22	85.29	94.23	-8.94	0.125	-0.479	0.011	-0.470
23	80.65	94.23	-13.58	0.125	-0.728	0.025	-0.720
24	82.46	94.23	-11.77	0.125	-0.631	0.019	-0.622

* Case(s) with |Outlier t| > 3.50

Figure A.1.13– Residuals plotted versus predicted values for the model describing the effect of various factors on 90% diameter (D_{90}) of powders manufactured by SFD.

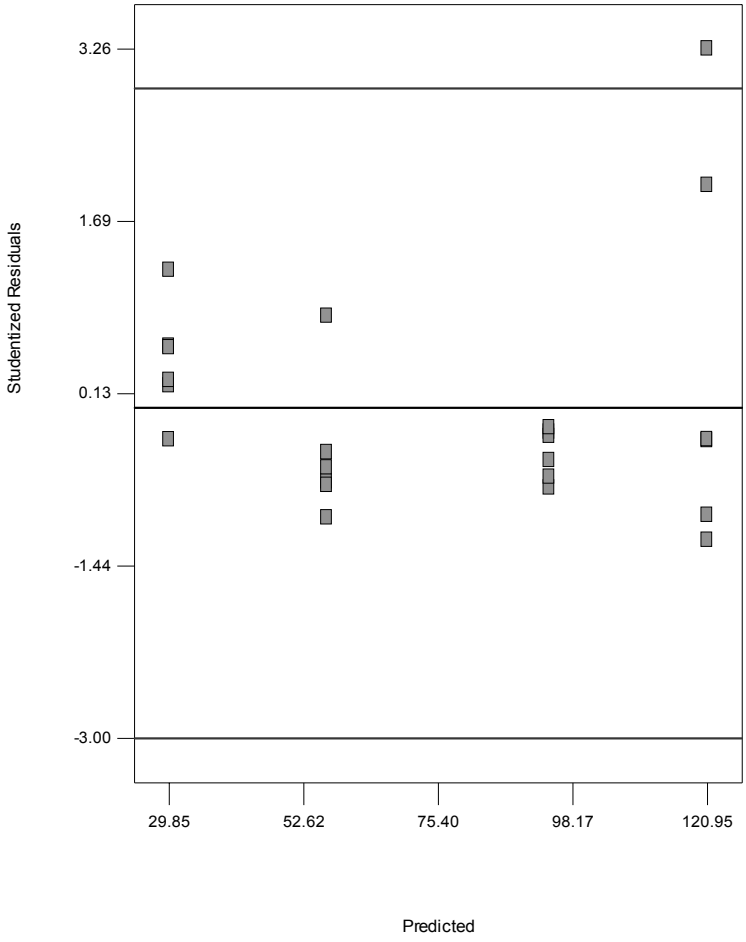

10% DIAMETER (D_{10})

Response: D_{10}

Factor	Name	Units	Type	-1 Level	+1 Level
A	Sol. Feed	mL/min	Numeric	3.00	25.00
B	Air Flow	L/hr	Numeric	250.00	500.00
C	Sol. Conc.	g/100 mL	Numeric	1.00	10.00

ANOVA for Selected Factorial Model

Source	Sum of Squares	DF	Mean Square	F Value	Prob > F
Model	170.36	4	42.59	20.26	< 0.0001
Residual	39.94	19	2.10		
Lack of Fit	*6.62*	*3*	*2.21*	*1.06*	*0.3940*
Pure Error	*33.33*	*16*	*2.08*		
Cor Total	210.31	23			

Root MSE	1.45	R-Squared	0.8101	
Dep Mean	8.52	Adj R-Squared	0.7701	
C.V.	17.02	Pred R-Squared	0.6970	
PRESS	63.73	Adeq Precision	12.458	Desire > 4

Factor	Coefficient Estimate	DF	Standard Error	t for H0 Coeff=0	Prob > |t|	VIF
Intercept	8.52	1	0.30			
A-Sol. Feed	2.14	1	0.30	7.24	< 0.0001	1.00
B-Air Flow	0.69	1	0.30	2.34	0.0304	1.00
C-Sol. Conc.	1.17	1	0.30	3.97	0.0008	1.00
AB	0.81	1	0.30	2.72	0.0136	1.00

Final Equation in Terms of Coded Factors:

$$D_{10} = 8.52 + 2.14*A + 0.69*B + 1.17*C + 0.81*AB$$

Diagnostics Case Statistics

Std Order	Actual Value	Predicted Value	Residual	Distance	Student Residual	Cook's Leverage	Outlier t
1	4.85	5.31	-0.46	0.208	-0.358	0.007	-0.349
2	4.96	5.31	-0.35	0.208	-0.273	0.004	-0.266
3	4.99	5.31	-0.32	0.208	-0.249	0.003	-0.243
4	8.34	7.99	0.35	0.208	0.274	0.004	0.267
5	9.10	7.99	1.11	0.208	0.863	0.039	0.857
6	9.23	7.99	1.24	0.208	0.964	0.049	0.962
7	4.13	5.09	-0.96	0.208	-0.742	0.029	-0.732
8	5.71	5.09	0.62	0.208	0.483	0.012	0.473
9	4.47	5.09	-0.62	0.208	-0.478	0.012	-0.468
10	10.80	10.98	-0.18	0.208	-0.141	0.001	-0.137
11	10.81	10.98	-0.17	0.208	-0.133	0.001	-0.130
12	10.71	10.98	-0.27	0.208	-0.211	0.002	-0.205
13	9.83	7.66	2.17	0.208	1.681	0.149	1.773
14	5.21	7.66	-2.45	0.208	-1.900	0.190	-2.055
15	9.08	7.66	1.42	0.208	1.099	0.064	1.106
16	9.51	10.34	-0.83	0.208	-0.641	0.022	-0.631
17	9.05	10.34	-1.29	0.208	-0.997	0.052	-0.997
18	9.74	10.34	-0.60	0.208	-0.462	0.011	-0.453
19	4.26	7.44	-3.18	0.208	-2.462	0.319	-2.905
20	8.95	7.44	1.51	0.208	1.173	0.072	1.185
21	10.05	7.44	2.61	0.208	2.026	0.216	2.227
22	13.63	13.33	0.30	0.208	0.231	0.003	0.225
23	13.47	13.33	0.14	0.208	0.107	0.001	0.104
24	13.52	13.33	0.19	0.208	0.146	0.001	0.142

Figure A.1.14– Residuals plotted versus predicted values for the model describing the effect of various factors on 10% diameter (D_{10}) of powders manufactured by SFD.

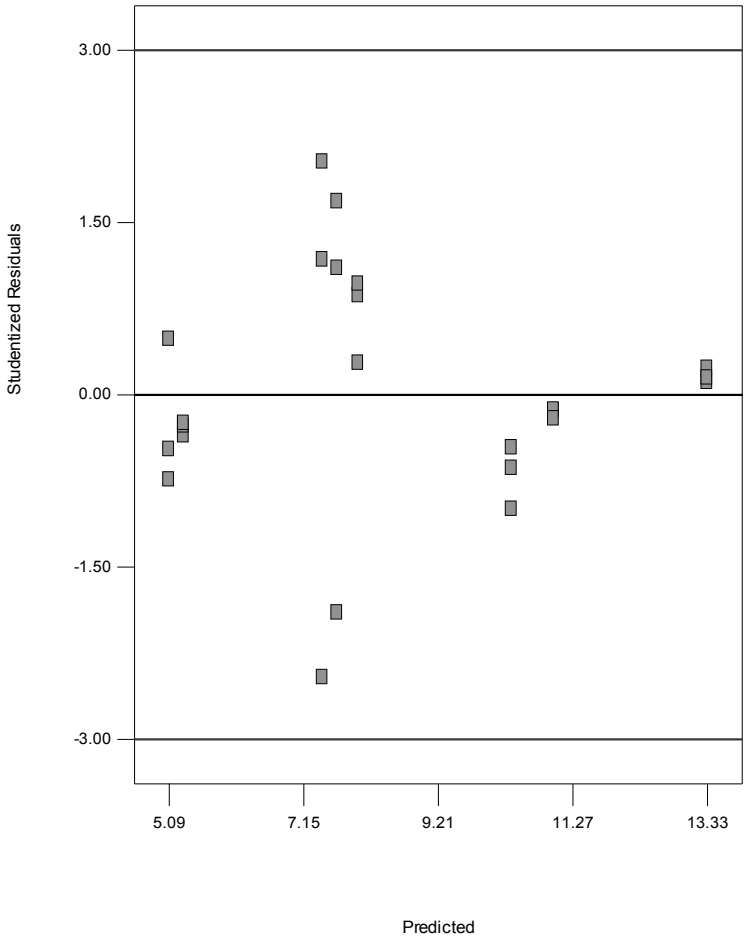

Figure A.1.15– Interaction graphs indicating the effects of airflow rate (B-=1%, B+=10%) and solution feed rate (A-=Slow, A+=Fast) on 10% diameter (D_{10}) of particles produced by SFD.

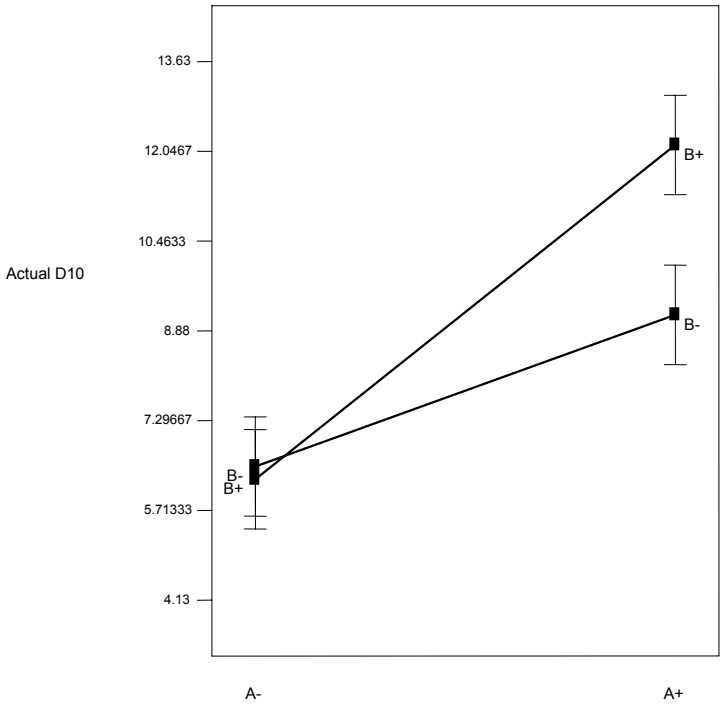

SPAN

Response: Span

Factor	Name	Units	Type	-1 Level	+1 Level
A	Sol. Feed	mL/min	Numeric	3.00	25.00
B	Air Flow	L/hr	Numeric	250.00	500.00
C	Sol. Conc.	g/100 mL	Numeric	1.00	10.00

ANOVA for Selected Factorial Model

Source	Sum of Squares	DF	Mean Square	F Value	Prob > F
Model	4.48	4	1.12	25.55	< 0.0001
Residual	0.83	19	0.044		
Lack of Fit	0.17	3	0.058	1.42	0.2748
Pure Error	0.66	16	0.041		
Cor Total	5.31	23			

Root MSE	0.21	R-Squared	0.8432	
Dep Mean	1.94	Adj R-Squared	0.8102	
C.V.	10.79	Pred R-Squared	0.7499	
PRESS	1.33	Adeq Precision	14.719	Desire > 4

Factor	Coefficient Estimate	DF	Standard Error	t for H0 Coeff=0	Prob > |t|	VIF
Intercept	1.94	1	0.043			
A-Sol. Feed	0.29	1	0.043	6.88	< 0.0001	1.00
B-Air Flow	-0.22	1	0.043	-5.08	< 0.0001	1.00
C-Sol. Conc.	-0.19	1	0.043	-4.50	0.0002	1.00
AB	-0.13	1	0.043	-2.98	0.0078	1.00

Final Equation in Terms of Coded Factors:

Span= 1.94 + 0.29*A - 0.22*B - 0.19*C - 0.13*AB

Diagnostics Case Statistics

Std Order	Actual Value	Predicted Value	Residual	Distance	Student Residual	Cook's Leverage	Outlier t
1	1.90	1.93	-0.027	0.208	-0.145	0.001	-0.142
2	1.92	1.93	-0.007	0.208	-0.038	0.000	-0.037
3	1.86	1.93	-0.067	0.208	-0.360	0.007	-0.352
4	2.38	2.77	-0.39	0.208	-2.088	0.229	-2.315
5	3.39	2.77	0.62	0.208	3.337	0.586	5.047*
6	2.96	2.77	0.19	0.208	1.027	0.056	1.029
7	1.85	1.75	0.10	0.208	0.553	0.016	0.542
8	1.55	1.75	-0.20	0.208	-1.058	0.059	-1.062
9	1.78	1.75	0.033	0.208	0.177	0.002	0.172
10	2.00	2.08	-0.080	0.208	-0.432	0.010	-0.422
11	1.95	2.08	-0.13	0.208	-0.700	0.026	-0.691
12	2.03	2.08	-0.050	0.208	-0.271	0.004	-0.264
13	1.65	1.54	0.11	0.208	0.575	0.017	0.565
14	1.57	1.54	0.027	0.208	0.145	0.001	0.142
15	1.51	1.54	-0.033	0.208	-0.177	0.002	-0.172
16	2.18	2.38	-0.20	0.208	-1.099	0.064	-1.105
17	2.12	2.38	-0.26	0.208	-1.421	0.106	-1.463
18	2.43	2.38	0.045	0.208	0.244	0.003	0.238
19	1.28	1.36	-0.083	0.208	-0.445	0.010	-0.436
20	1.40	1.36	0.037	0.208	0.199	0.002	0.194
21	1.47	1.36	0.11	0.208	0.575	0.017	0.565
22	1.85	1.70	0.15	0.208	0.826	0.036	0.819
23	1.74	1.70	0.044	0.208	0.235	0.003	0.229
24	1.76	1.70	0.064	0.208	0.342	0.006	0.334

* Case(s) with |Outlier t| > 3.50

Figure A.1.16– Residuals plotted versus predicted values for the model describing the effect of various factors on span of powders manufactured by SFD.

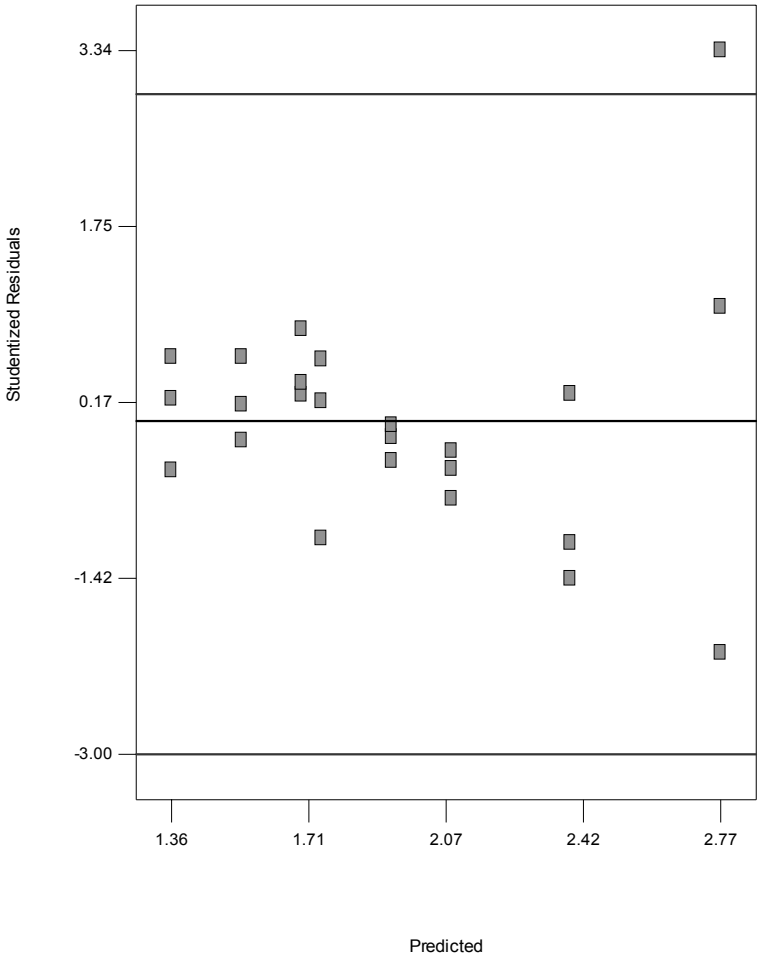

Figure A.1.17– Interaction graphs indicating the effects of solute concentration (B-=1%, B+=10%) and freezing rate (A-=Slow, A+=Fast) on span of particles produced by SFD.

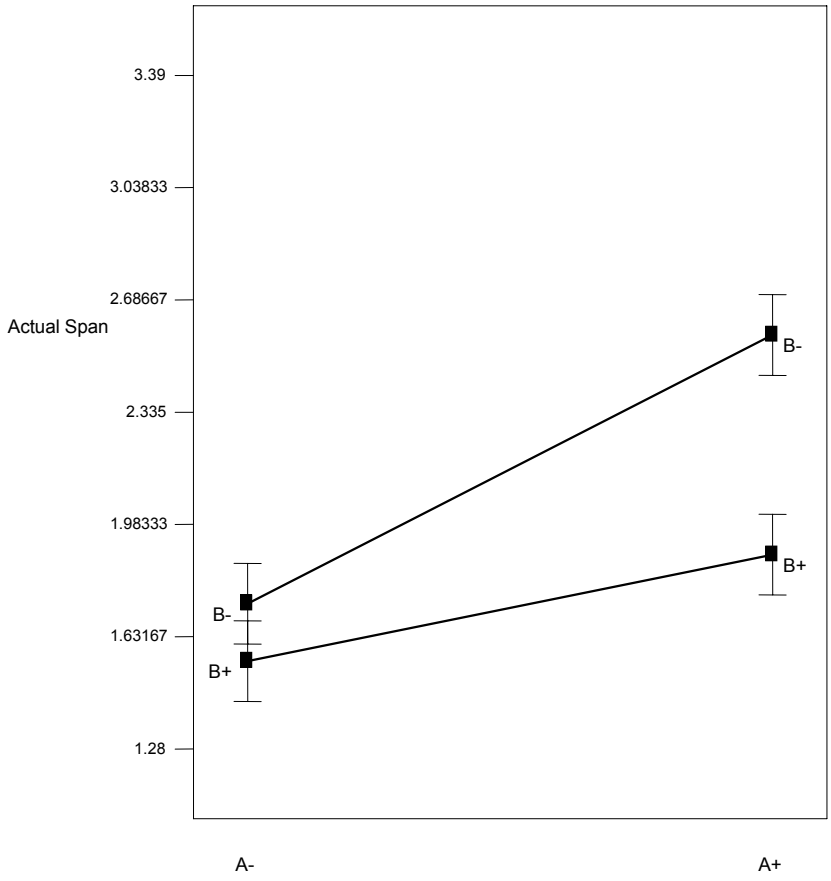

Appendix A.2- CALIBRATION OF THE ANDERSEN CASCADE IMPACTOR FOR THE CHARACTERIZATION OF NASAL PRODUCTS

Theoretical Considerations

The theoretical cut-off diameter of each stage of the impactor can be calculated by the formula:

$$d_{50}\sqrt{C_c} = \left[\frac{9\eta\pi D_j^3 (Stk_{50})}{4\rho_p Q}\right]^{1/2} \quad \text{(A.2.01)}$$

where d_{50} is the cut-off diameter, C_c is the Cunningham correction factor, η is the viscosity, D_j is the diameter of the jet, ρ_p is the density of the particle, and Q is the flow rate of the air (Hinds 1999). To modify the cut-off diameters of the stages of the cascade impactor, the most direct way is to change the flow rate of the air through the system, without changing any of the other factors. However, in order for the cascade impactor stage cut-off diameter to be relevant, the air flow must be turbulent. The Reynolds number (Re) is a dimensionless number that characterizes fluid flow through a pipe or around and obstacle. It is mathematically determined by the equation:

$$\text{Re} = \frac{\rho V d}{\eta} \quad \text{(A.2.02)}$$

where V is the relative velocity and d is the particle diameter. For a cascade impactor, the Re must be between 500 and 3000.

The original Andersen MKII non-viable impactor consisted of eight stages (0-7) operated at a flow rate of 28.3 L/min, with particle size cut-off's, in the respirable range, between 9 and 0.22 μm. If the flow rate is increased (to 60 or 90 L/min) the cut-off diameters for the collection efficiency curves on each stage become smaller and consequently, the

impactor becomes less useful in sizing aerosols in respirable size ranges. Consequently, additional stages (-2, -1 and -0) were designed for insertion at the higher flow rates to enable the respirable size range to be covered. It is fortuitous that if the impactor is operated at a low flow rate (e.g. 15 L/min) these additional stages will have particle size cut-off efficiencies that are higher than those of the conventional impactor. This is a desirable situation for evaluation of nasal products where a fraction of the particles that might deposit in the nose can potentially enter the lungs (in the range 10-20μm). However, the Andersen has not been calibrated at low flow rates with the supplementary stages inserted.

In calibration experiments, the stages, -2, -1, and -0, originally designed for 90 L/min operation of an Andersen MKII non-viable impactor with known cut-off diameters at this flow rate were employed. According to the manufacturer, at 90 L/min, the cut-off diameters for these stages are 8.0, 6.5, and 5.2 μm, respectively. The predicted cut-off diameters at 15 L/min can be calculated from the equation:

$$d_{15\ L/min} = d_{90\ L/min}\,(90/15)^{1/2} \qquad (A.2.03)$$

where d_x is the cut-off diameter of a stage at x L/min (Van Oort, Downey et al. 1996). Using this formula, at 15 L/min, the theoretical cut-off diameters of stages -2, -1, and -0 are 19.6, 17.2, and 12.4 μm, respectively.

Materials and Methods

The Vibrating Orifice Aerosol Generator (VOAG, model 3450, TSI, Inc. Shoreview, MN) was used to produce monodisperse aerosol particles in the 9-22 μm particle size range. Solutions of oleic acid and fluorescein dissolved in methanol flowed through a 35 μm orifice in an inverted apparatus (Figure A.2.1). The aerosol passed a Polonium-210 radioactive source (Nuclespot Static Eliminator, NRD LLC., Grand Island, NY) to reduce the surface

charge on the formed droplets. Due to fluctuations in the fluid pressure seen in the syringe pump provided with the VOAG, a high pressure liquid chromatography (HPLC) pump (Model 510, Waters, Corp. Milford, MA) was used. Droplet sizes were based on the calculations of the operating variables of the VOAG and the volatile and nonvolatile components (Berglund and Liu 1973). The aerodynamic diameter (d_{ae}) was calculated from the equation:

$$d_{ae} = d_p \sqrt{\rho_p} \qquad \text{(A.2.04)}$$

where dp is the diameter of the droplet and ρ_p is the density of the droplet. Prior to and after each measurement of the impactor, the monodispersity of the aerosol was verified using a time-of-flight particle sizing instrument (Aerosizer LD, TSI, In., Shoreview MN) with the geometric standard deviation of the single droplets was <1.2 (Fuchs and Sutugin 1966).

After each measurement, the orifice plate, collection plate, and filter were washed separately with known quantities of 0.001M aqueous solution of sodium hydroxide. The recovered fluorescein content was quantified using fluorometry and the collection efficiency (E) was calculated by dividing the mass of fluorescein on the collection plate by the sum of the mass of fluorescein on the filter and collection plate. All measurements were completed in triplicate.

Results and Discussion

The measured efficiency of each stage as a function of d_{ae} is shown (Table A.2.1). Stage -2 had a collection efficiency ranging from 13 to 83% for d_{ae} 10 to 20 µm. Stage -1 had a collection efficiency ranging from 14 to 84% for d_{ae} 10 to 20 µm. Stage -0 had a collection efficiency ranging from 10 to 75% for d_{ae} 8 to 16 µm.

The efficiency curves of all of the stages of the modified cascade impactor are shown (Figure A.2.2). The efficiency curves for Stages -1 and -2 fall are almost superimposable. Additionally, the efficiency curves for Stages -1 and -2 overlap with the efficiency curve for Stage -0. These deposition characteristics indicate that for the characterization of nasal preparations, only one of the stages, -1 and -2, of the cascade impactor is required; Stage -2 was selected for inclusion.

To determine the cut-off diameter for each stage, two methods were used. The first method used linear regression analysis of a best-fit line through only the linear portion of the data; 9.3808 to 15.0093 µm for Stage -0, 13.1332 to 18.7617 µm for Stage -1, and 13.1332 to 20.6378 µm for Stage -2). The 50% efficiency was then calculated using the equation for the best-fit line. The second method utilized linear regression analysis of a 3-parameter sigmoid fit. This was applied to the entire data set from each impactor stage. The 50% efficiency was then calculated using the equation for the best-fit sigmoidal curve. Results are shown in Table A.2.2. There was no difference in cut-off diameters regardless of the method used to calculate it. However, the geometric standard deviations (GSD) of the curves, determined by dividing the d_{84} by d_{50}, were different for Stages -1 and -0. This is important because the GSD is an indicator of the sharpness of the efficiency curve. Both had higher GSD determined by sigmoidal regression analysis, indicating a flatter curve compared to that determined by linear regression analysis. This indicates that the tails of these curves have a significant effect on the steepness of the efficiency curve. All of the models exhibited good fit on the data.

Based on the calibration of the Andersen Mk II cascade impactor at 15 LPM, the range of particles has been doubled, by extension to larger sizes, to include those that have a

lower but finite probability of penetration to the lungs but are known to exist in nasal products. The modified cascade impactor allows for the collection of particles below 16.5 μm, compared to a calibrated collection efficiency cut-off 8.7 μm using the traditional setup at 28.3 LPM (Dunbar, Hickey et al. 1998). It is a tool that can be utilized as an alternative to imaging in predicting potential deposition in the lower respiratory tract.

Table A.2.1– The efficiency of each stage as a function of aerodynamic diameter (d_{ae}) at 15 liters per minute (Mean (SD), n=3).

d_{ae} (μm)	Stage -2 E (%)	Stage -1 E (%)	Stage -0 E (%)
8.4427	10.55 (0.31)		
9.3808	24.67 (2.28)		
10.3189	30.96 (0.63)	13.86 (0.41)	13.03 (0.60)
11.2570	40.79 (2.42)	16.17 (0.78)	16.22 (0.93)
12.1951	50.14 (2.89)	21.35 (1.56)	19.64 (0.78)
13.1332	56.41 (1.06)	25.81 (2.19)	22.07 (1.61)
14.0712	68.70 (1.65)	33.71 (1.00)	26.77 (3.35)
15.0093	73.95 (0.97)	43.60 (0.70)	37.59 (2.58)
15.9474	75.20 (0.62)	49.71 (0.07)	42.18 (2.74)
16.8855		59.59 (1.48)	53.24 (3.15)
17.8236		67.18 (1.72)	65.71 (1.71)
18.7617		75.62 (1.05)	73.58 (2.15)
19.6997		77.73 (1.27)	78.75 (1.14)
20.6378		84.01 (2.91)	83.58 (1.67)

Table A.2.2– The cut-off diameter, geometric standard deviation (GSD), and correlation coefficient (R^2) determined by linear and sigmoidal regression analysis.

Stage	Linear regression analysis			Sigmoidal regression analysis		
	Cut-off diameter (μm)	GSD	R^2	Cut-off diameter (μm)	GSD	R^2
Stage -2	16.5	1.23	0.9873	16.5	1.24	0.9879
Stage -1	15.9	1.24	0.9985	15.9	1.30	0.9977
Stage -0	12.3	1.30	0.9943	12.2	1.55	0.9925

Figure A.2.1– Experimental setup for the calibration of the cascade impactor (CI) at 15 liters per minute.

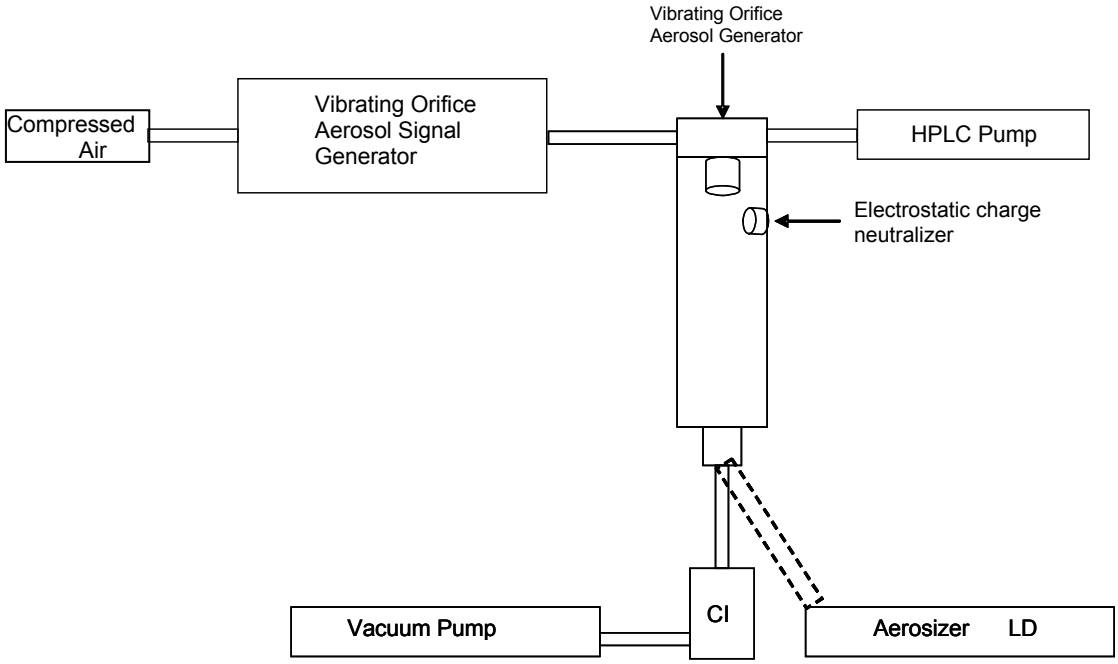

Figure A.2.2– Calibration of the cascade impactor at 15 liters per minute.

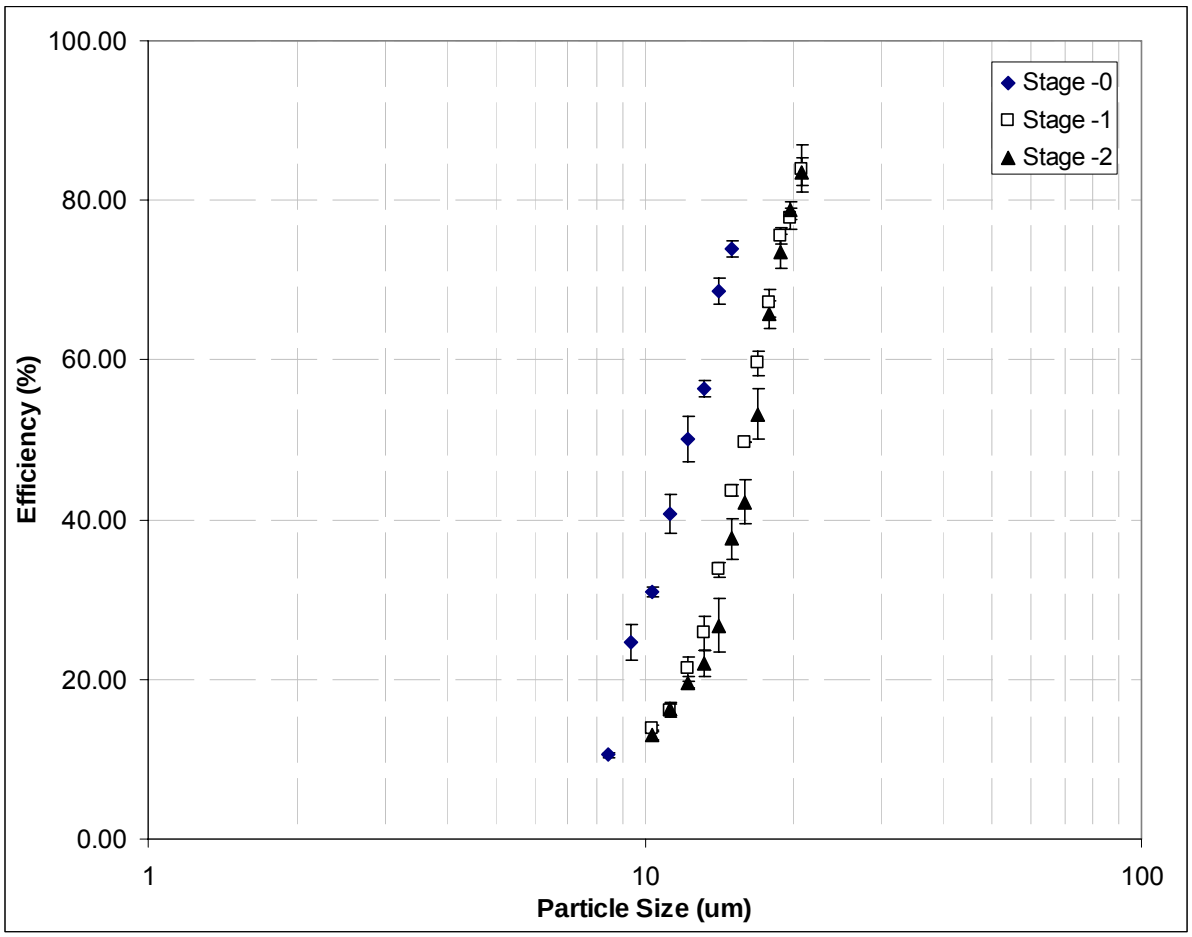

Figure A.2.3– The efficiency curves of Stages -2 and -0 for the modified cascade impactor at 15 liters per minute.

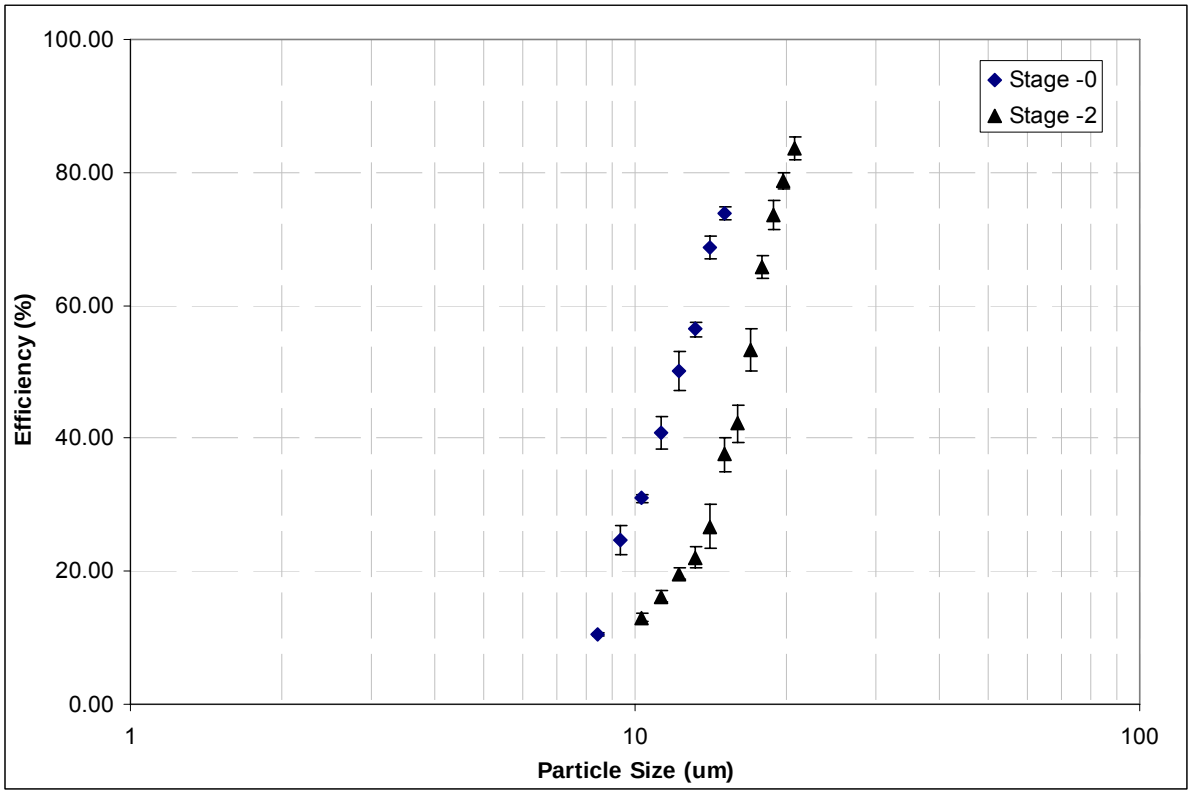

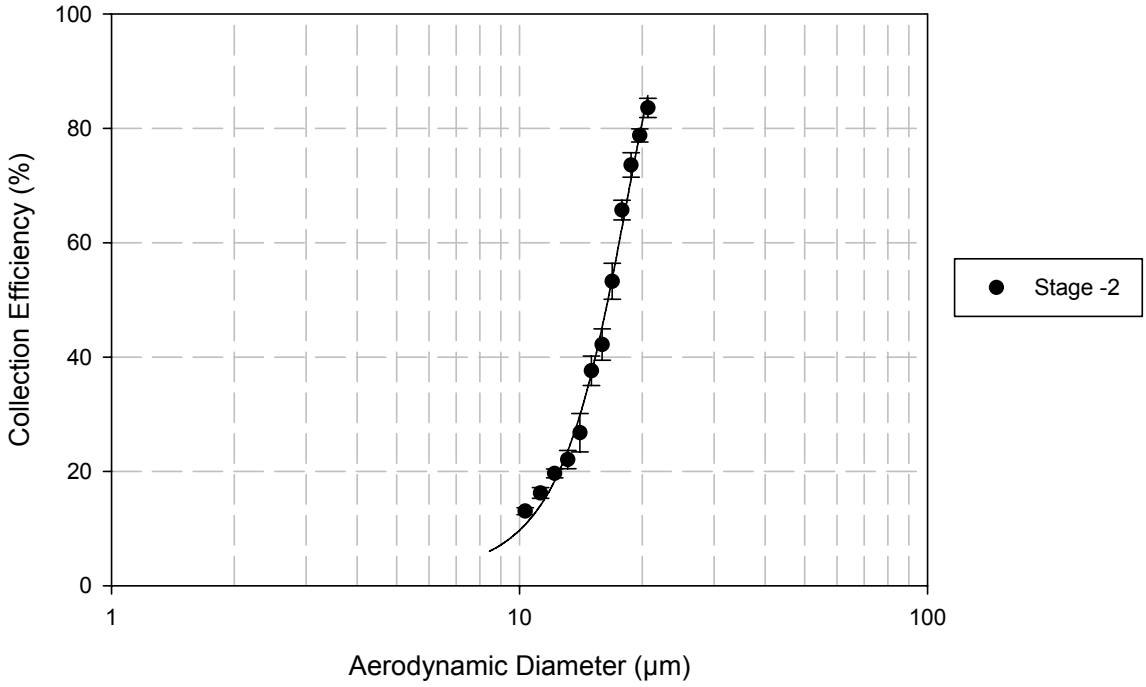

Nonlinear Regression
Equation: Sigmoidal, Sigmoid, 3 Parameter
y= a/(1+exp(-(x-x0)/b))

R	Rsqr	Adj Rsqr	Standard Error of Estimate
0.9962	0.9925	0.9908	2.4728

	Coefficient	Std. Error	t	P	VIF
a	113.1907	9.9821	11.3394	<0.0001	39.4446<
b	3.0342	0.2533	11.9793	<0.0001	5.8004<
x0	17.1853	0.6246	27.5125	<0.0001	41.9096<

Analysis of Variance:
Uncorrected for the mean of the observations:

	DF	SS	MS
Regression	3	30912.9410	10304.3137
Residual	9	55.0332	6.1148
Total	12	30967.9742	2580.6645

Corrected for the mean of the observations:

	DF	SS	MS	F	P
Regression	2	7295.6769	3647.8384	596.5589	<0.0001
Residual	9	55.0332	6.1148		
Total	11	7350.7101	668.2464		

Statistical Tests:

PRESS 110.5894

Durbin-Watson Statistic 1.2334 Failed

Normality Test Passed (P = 0.8554)

K-S Statistic = 0.1678 Significance Level = 0.8554

Constant Variance Test Passed (P = 0.8001)

Power of performed test with alpha = 0.0500: 1.0000

Regression Diagnostics:

Row	Std. Res.	Stud. Res.	Stud. Del. Res.
3	0.9558	1.0429	1.0487
4	0.8770	0.9620	0.9575
5	0.5346	0.5845	0.5619
6	-0.6076	-0.6593	-0.6371
7	-1.2494	-1.3523	-1.4283
8	0.1865	0.2042	0.1930
9	-1.2244	-1.3739	-1.4571
10	-0.2270	-0.2595	-0.2455
11	1.2877	1.4623	1.5789
12	1.0537	1.1809	1.2112
13	-0.0159	-0.0188	-0.0177
14	-0.8644	-1.4296	-1.5331

Influence Diagnostics:

Row	Cook's Dist	Leverage	DFFITS
3	0.0691	0.1601	0.4579
4	0.0626	0.1687	0.4314
5	0.0223	0.1635	0.2484
6	0.0257	0.1507	-0.2684
7	0.1046	0.1464	-0.5916
8	0.0028	0.1660	0.0861
9	0.1630	0.2057	-0.7416
10	0.0069	0.2348	-0.1360
11	0.2063	0.2245	0.8495
12	0.1190	0.2038	0.6128
13	4.7554E-005	0.2875	-0.0113
14	1.1823	0.6344	-2.0197

95% Confidence:

Row	Predicted	95% Conf-L	95% Conf-U	95% Pred-L	95% Pred-U
3	10.6666	8.4281	12.9050	4.6414	16.6917
4	14.0512	11.7534	16.3491	8.0038	20.0987
5	18.3180	16.0562	20.5798	12.2842	24.3518
6	23.5724	21.4005	25.7442	17.5717	29.5731
7	29.8595	27.7190	32.0001	23.8701	35.8490
8	37.1288	34.8494	39.4083	31.0884	43.1693
9	45.2078	42.6704	47.7452	39.0653	51.3503
10	53.8012	51.0906	56.5119	47.5852	60.0173
11	62.5258	59.8752	65.1763	56.3357	68.7159
12	70.9744	68.4489	73.4999	64.8368	77.1119
13	78.7893	75.7900	81.7885	72.4420	85.1365
14	85.7175	81.2619	90.1730	78.5660	92.8690

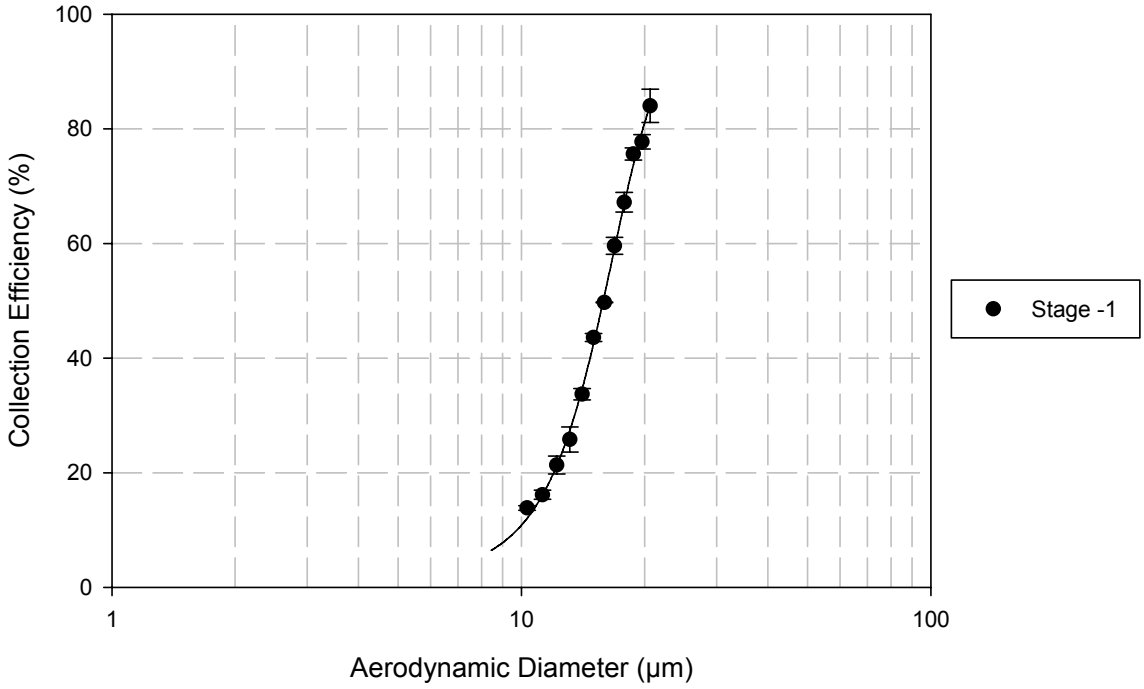

Nonlinear Regression
Equation: Sigmoidal, Sigmoid, 3 Parameter
y= a/(1+exp(-(x-x0)/b))

R	Rsqr	Adj Rsqr	Standard Error of Estimate
0.9988	0.9977	0.9972	1.3466

	Coeff	Std. Error	t	P	VIF
a	98.4556	3.0551	32.2269	<0.0001	18.0898<
b	2.7572	0.1168	23.6100	<0.0001	4.2377<
x0	15.7636	0.2217	71.1153	<0.0001	16.0454<

Analysis of Variance:
Uncorrected for the mean of the observations:

	DF	SS	MS
Regression	3	33949.7723	11316.5908
Residual	9	16.3209	1.8134
Total	12	33966.0932	2830.5078

Corrected for the mean of the observations:

	DF	SS	MS	F	P
Regression	2	7032.2427	3516.1213	1938.9296	<0.0001
Residual	9	16.3209	1.8134		
Total	11	7048.5636	640.7785		

Statistical Tests:

PRESS 25.9563

Durbin-Watson Statistic 2.2381 Passed

Normality Test Passed (P = 0.9661)

K-S Statistic = 0.1373 Significance Level = 0.9661

Constant Variance Test Passed (P = 0.9737)

Power of performed test with alpha = 0.0500: 1.0000

Regression Diagnostics:

Row	Std. Res.	Stud. Res.	Stud. Del. Res.
3	1.3814	1.5210	1.6638
4	0.0748	0.0827	0.0780
5	0.1257	0.1380	0.1303
6	-1.1642	-1.2677	-1.3188
7	-0.6436	-0.7023	-0.6810
8	0.7903	0.8779	0.8656
9	-0.8599	-0.9760	-0.9732
10	0.3586	0.4078	0.3881
11	0.2767	0.3089	0.2928
12	1.4752	1.6414	1.8488
13	-1.2454	-1.4824	-1.6077
14	-0.0665	-0.0999	-0.0942

Influence Diagnostics:

Row	Cook's Dist	Leverage	DFFITS
3	0.1638	0.1752	0.7669
4	0.0005	0.1812	0.0367
5	0.0013	0.1708	0.0591
6	0.0995	0.1566	-0.5682
7	0.0313	0.1600	-0.2972
8	0.0602	0.1897	0.4189
9	0.0916	0.2238	-0.5226
10	0.0163	0.2268	0.2102
11	0.0078	0.1973	0.1452
12	0.2138	0.1923	0.9020
13	0.3054	0.2942	-1.0381
14	0.0042	0.5562	-0.1054

95% Confidence:

Row	Predicted	95% Conf-L	95% Conf-U	95% Pred-L	95% Pred-U
3	11.9998	10.7246	13.2750	8.6974	15.3022
4	16.0693	14.7724	17.3662	12.7584	19.3802
5	21.1808	19.9220	22.4396	17.8846	24.4769
6	27.3778	26.1724	28.5833	24.1017	30.6540
7	34.5767	33.3582	35.7953	31.2958	37.8577
8	42.5358	41.2089	43.8627	39.2130	45.8585
9	50.8680	49.4268	52.3092	47.4980	54.2380
10	59.1072	57.6563	60.5580	55.7330	62.4813
11	66.8073	65.4541	68.1606	63.4740	70.1407
12	73.6335	72.2977	74.9692	70.3072	76.9598
13	79.4071	77.7546	81.0595	75.9415	82.8727
14	84.0996	81.8278	86.3714	80.2994	87.8997

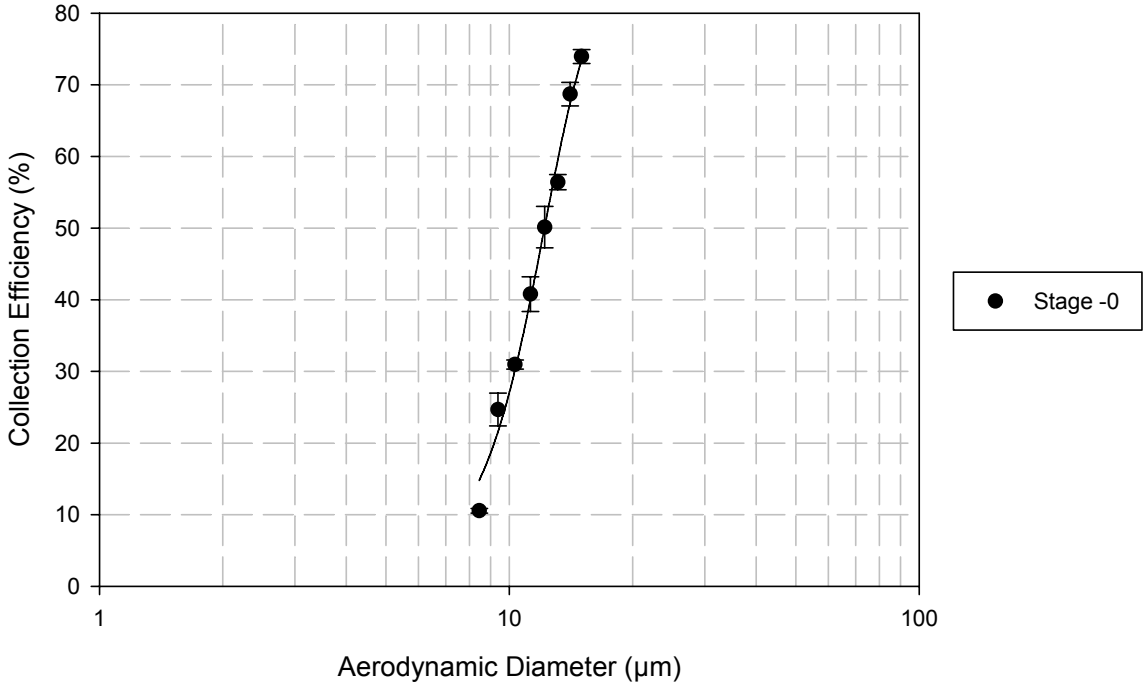

Nonlinear Regression
Equation: Sigmoidal, Sigmoid, 3 Parameter
y= a/(1+exp(-(x-x0)/b))

R	Rsqr	Adj Rsqr	Standard Error of Estimate
0.9939	0.9879	0.9830	2.8589

	Coefficient	Std. Error	t	P	VIF
a	86.0663	8.3950	10.2520	0.0002	22.3333<
b	1.9689	0.3005	6.5511	0.0012	5.1963<
x0	11.5400	0.4861	23.7416	<0.0001	17.5681<

Analysis of Variance:
Uncorrected for the mean of the observations:

	DF	SS	MS
Regression	3	19185.7901	6395.2634
Residual	5	40.8672	8.1734
Total	8	19226.6573	2403.3322

Corrected for the mean of the observations:

	DF	SS	MS	F	P
Regression	2	3328.6565	1664.3283	203.6265	<0.0001
Residual	5	40.8672	8.1734		
Total	7	3369.5237	481.3605		

Statistical Tests:

PRESS 108.8205

Durbin-Watson Statistic 2.2021 Passed

Normality Test Passed (P = 0.6219)

K-S Statistic = 0.2521 Significance Level = 0.6219

Constant Variance Test Passed (P = 0.2067)

Power of performed test with alpha = 0.0500: 1.0000

Regression Diagnostics:

Row	Std. Res.	Stud. Res.	Stud. Del. Res.
1	-1.4811	-1.9733	-3.7529<
2	1.0918	1.3499	1.5144
3	0.3004	0.3475	0.3146
4	0.2951	0.3486	0.3156
5	0.0045	0.0055	0.0049
6	-1.0992	-1.3166	-1.4569
7	0.4459	0.5352	0.4930
8	0.1730	0.3278	0.2964

Influence Diagnostics:

Row	Cook's Dist	Leverage	DFFITS
1	1.0062	0.4367	-3.3042
2	0.3211	0.3458	1.1011
3	0.0136	0.2526	0.1829
4	0.0160	0.2830	0.1983
5	5.5351E-006	0.3517	0.0036
6	0.2511	0.3029	-0.9604
7	0.0421	0.3058	0.3272
8	0.0927	0.7213	0.4768

95% Confidence:

Row	Predicted	95% Conf-L	95% Conf-U	95% Pred-L	95% Pred-U
1	14.7843	9.9279	19.6407	5.9756	23.5930
2	21.5487	17.2269	25.8705	13.0230	30.0744
3	30.1011	26.4073	33.7949	21.8759	38.3263
4	39.9462	36.0364	43.8561	31.6218	48.2707
5	50.1273	45.7687	54.4859	41.5829	58.6716
6	59.5526	55.5078	63.5974	51.1639	67.9412
7	67.4252	63.3610	71.4894	59.0272	75.8233
8	73.4553	67.2137	79.6969	63.8134	83.0972

Appendix A.3- RADIOLABELING APPARATUS

An apparatus was designed to label powder with radioactive tracer for use in the study of deposition of nasal powders in rats. Gamma-camera imaging or time sequence lavaging were employed to follow deposition and clearance from Brown Norway rats. An ideal instrument will allow ultra fine particles to deposit evenly on the surface of nasal powders, labeling the powder uniformly with a radioactive marker. It is imperative that the labeling system does not alter any of the physico-chemical properties (flow properties, thermal properties, moisture content, etc.) of the powders, rendering them substantially different from unlabeled powder. This appendix describes a labeling apparatus that was constructed and evaluated for the purpose of studying nasal powders.

Materials and Methods

A schematic drawing of the label apparatus is shown (Figure A.4.1). A radiolabeled tracer, ^{99m}technetium-labeled sulfur colloid (^{99m}Tc-SC), was used to label 25μm SFD-trehalose. The labeled colloid solution was freshly prepared according to the manufacturer's (Cis, Bedford, MA) instructions. A nebulizer (Pari LC Plus, PARI GmbH, Starnburg, Germany) was filled with 4 mL of ^{99m}Tc-SC and was used to produce droplets approximately 1-3 μm in diameter when operating at 8 L/min. The nebulizer dispersed the droplets through a length of copper tubing, soldered as shown. Copper tubing has a higher thermal conductivity (379 J/s-m-K) than stainless steel (17.3 J/s-m-K) and was selected for this property since heat transfer is the purpose of the apparatus (Hickey and Ganderton 2001). The particles travel through a tube furnace (Type 21100, Barnstead International, Dubuque, IA) which was used to evaporate the water from the nebulized suspension (temperatures of 250-300°C were evaluated). After passing through the copper tubing, the droplets travelled

through a diffusion dryer (Model 3062, TSI, Inc., Shoreview, MN) filled with desiccant (Silica gel, 1 Kg in 3 L) to remove water vapor. The diffusion dryer was set up to flow through in the opposite direction to that suggested by the manufacturer because the right angle bends in the copper tubing function to remove the large droplets. The intended vapor trap of the diffusion drier was used as a repository for the powder to be labeled. The trap was filled up with approximately one quarter volume of glass wool (Fisherbrand, Fisher Scientific, Pittsburgh, PA) to prevent the ^{99m}Tc-SC from exiting the labeling machine and a 40 mesh basket (Hanson Research, Chatsworth, CA) filled with 1-3 g of powder is placed in the water trap. The labeling takes place in a hood approved for the use of radioactive materials.

Results and Discussion

Initial experiments were successfully completed with sieved trehalose as the powder to be labeled. The level of radioactivity measured on 5 mg powder samples was 40 μCi, sufficient to perform residence time studies for a long duration. However, when 25 μm SFD particles were utilized, residual moisture caused the powder to collapse and aggregate. This system was unable to remove all of the water content from the nebulized suspension. While residual water content was not a great concern to the crystalline trehalose, the moisture was quickly absorbed by the amorphous SFD trehalose. When the system was run for short periods of time to prevent the moisture uptake, radioactivity levels were just above than the detectable limit of calibrator, which was not suitable for three hour studies.

This system can still be utilized. Crystalline drug particles of sizes suitable for nasal delivery can be radiolabeled and imaging or residence time studies can be completed. The

label, itself, does not have to be radioactive. Fluorescein or an alternative fluorescent marker can be substituted for the ^{99m}Tc-SC, if exposure to radioactivity is a concern.

Figure A.4.1– A schematic drawing of an apparatus used to label nasal powders with radioactive tracer for use in deposition or residence time studies.

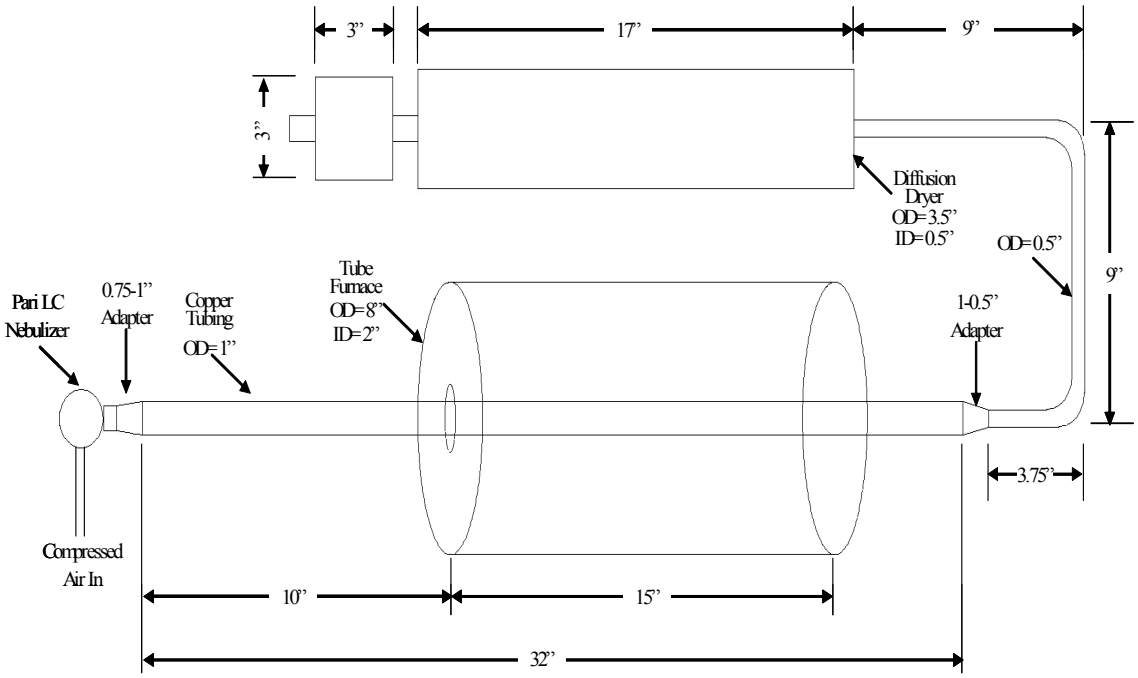

Appendix A.4- REGRESSION ANALYSIS OF RESIDENCE TIME STUDY IN BROWN NORWAY RATS

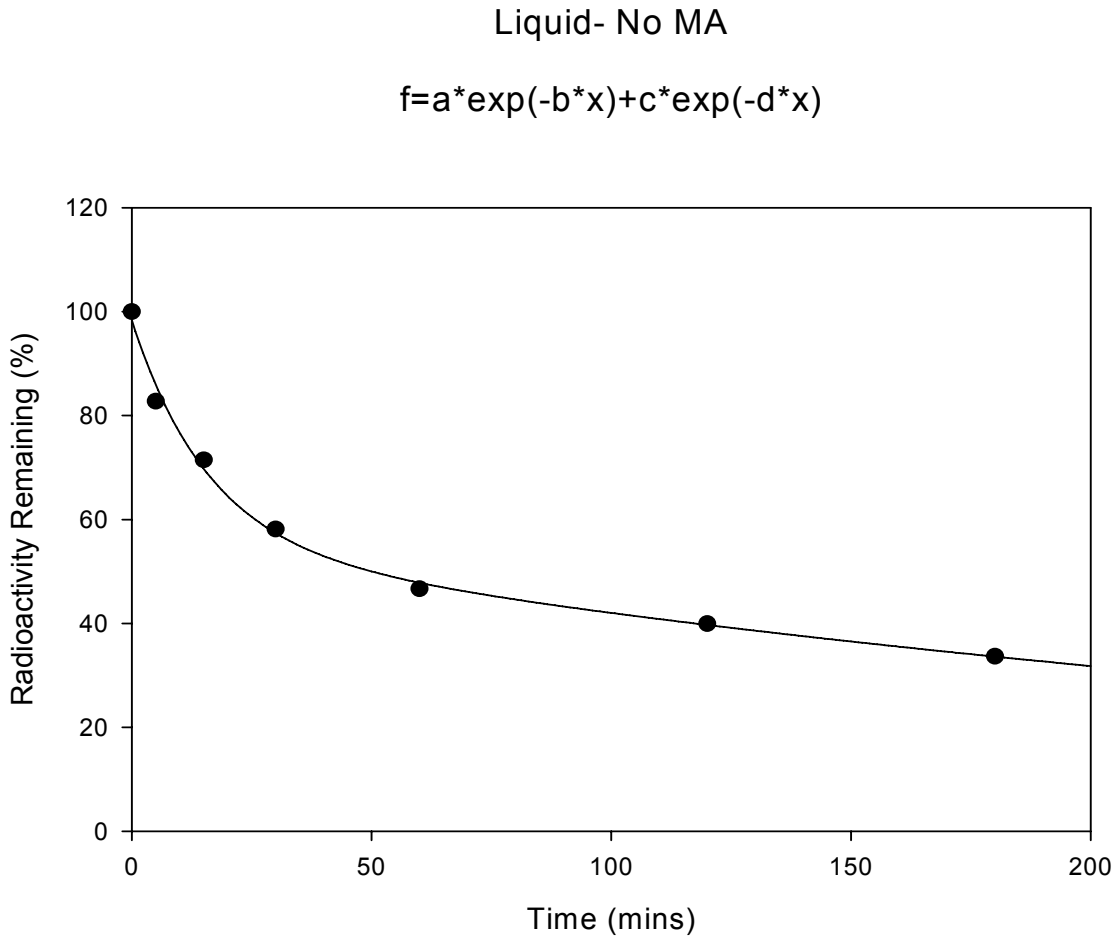

R	Rsqr	Adj Rsqr	Standard Error of Estimate
0.9975	0.9949	0.9898	2.4341

	Coefficient	Std. Error	t	P	VIF
a	43.0648	5.6736	7.5904	0.0047	9.2661<
b	0.0631	0.0159	3.9733	0.0285	5.4829<
c	55.3306	5.7149	9.6818	0.0023	29.4424<
d	0.0028	0.0008	3.3501	0.0441	8.0955<

Analysis of Variance:

Uncorrected for the mean of the observations:

	DF	SS	MS
Regression	4	30234.8992	7558.7248
Residual	3	17.7746	5.9249
Total	7	30252.6738	4321.8105

Corrected for the mean of the observations:

	DF	SS	MS	F	P
Regression	3	3482.9914	1160.9971	195.9536	0.0006
Residual	3	17.7746	5.9249		
Total	6	3500.7660	583.4610		

Liquid- SA

f=a*exp(-b*x)+c*exp(-d*x)

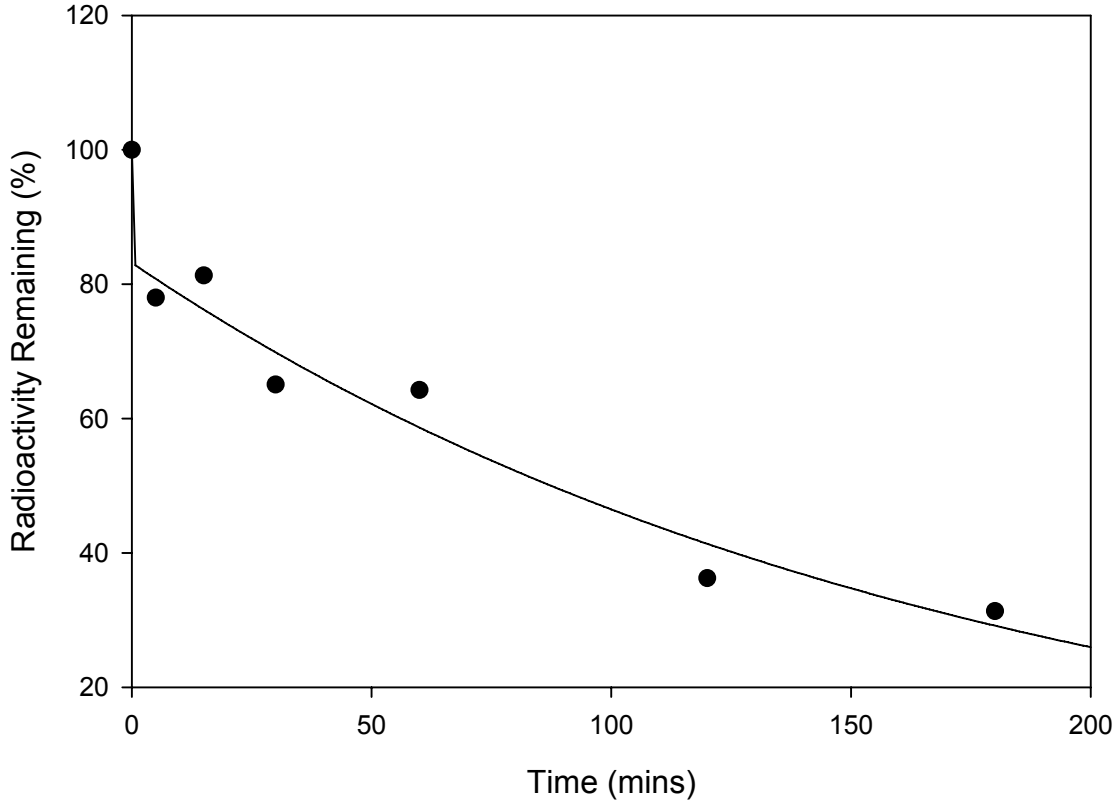

R	Rsqr	Adj Rsqr	Standard Error of Estimate
0.9835	0.9672	0.9344	6.2940

	Coefficient	Std. Error	t	P	VIF
a	16.8167	(NAN)	(+inf)	<0.0001	0.0000
b	46.3546	(NAN)	(+inf)	<0.0001	0.0000
c	83.1833	(NAN)	(+inf)	<0.0001	0.0000
d	0.0058	(NAN)	(+inf)	<0.0001	0.0000

Analysis of Variance:

Uncorrected for the mean of the observations:

	DF	SS	MS
Regression	4	33223.2745	8305.8186
Residual	3	118.8430	39.6143
Total	7	33342.1175	4763.1596

Corrected for the mean of the observations:

	DF	SS	MS	F	P
Regression	3	3502.0666	1167.3555	29.4680	0.0100
Residual	3	118.8430	39.6143		
Total	6	3620.9096	603.4849		

Liquid- CMC HMW

f=a*exp(-b*x)+c*exp(-d*x)

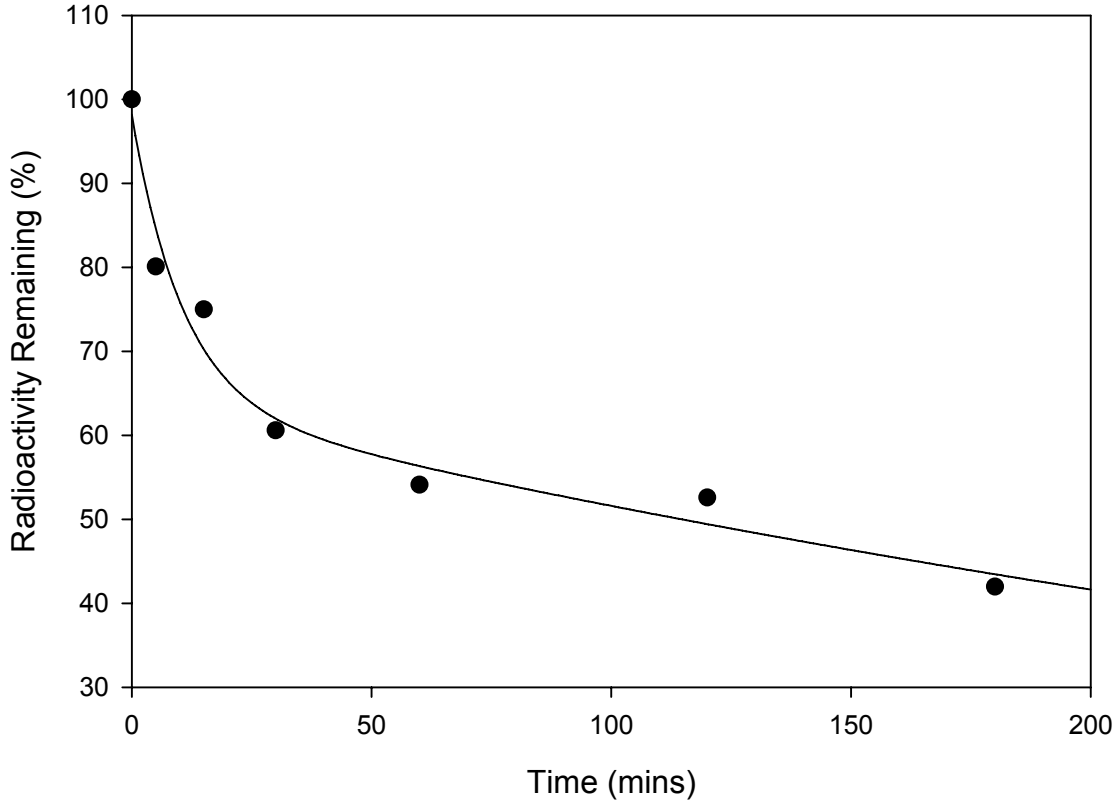

R	Rsqr	Adj Rsqr	Standard Error of Estimate
0.9861	0.9723	0.9446	4.6698

	Coefficient	Std. Error	t	P	VIF
a	34.2577	7.8524	4.3627	0.0223	4.1100<
b	0.0940	0.0491	1.9137	0.1516	3.4297
c	63.9457	7.2234	8.8526	0.0030	13.4677<
d	0.0021	0.0010	2.1582	0.1198	5.0712<

Analysis of Variance:

Uncorrected for the mean of the observations:

	DF	SS	MS
Regression	4	33104.3571	8276.0893
Residual	3	65.4199	21.8066
Total	7	33169.7770	4738.5396

Corrected for the mean of the observations:

	DF	SS	MS	F	P
Regression	3	2296.4308	765.4769	35.1029	0.0078
Residual	3	65.4199	21.8066		
Total	6	2361.8508	393.6418		

Liquid- HPMC HMW

f=a*exp(-b*x)+c*exp(-d*x)

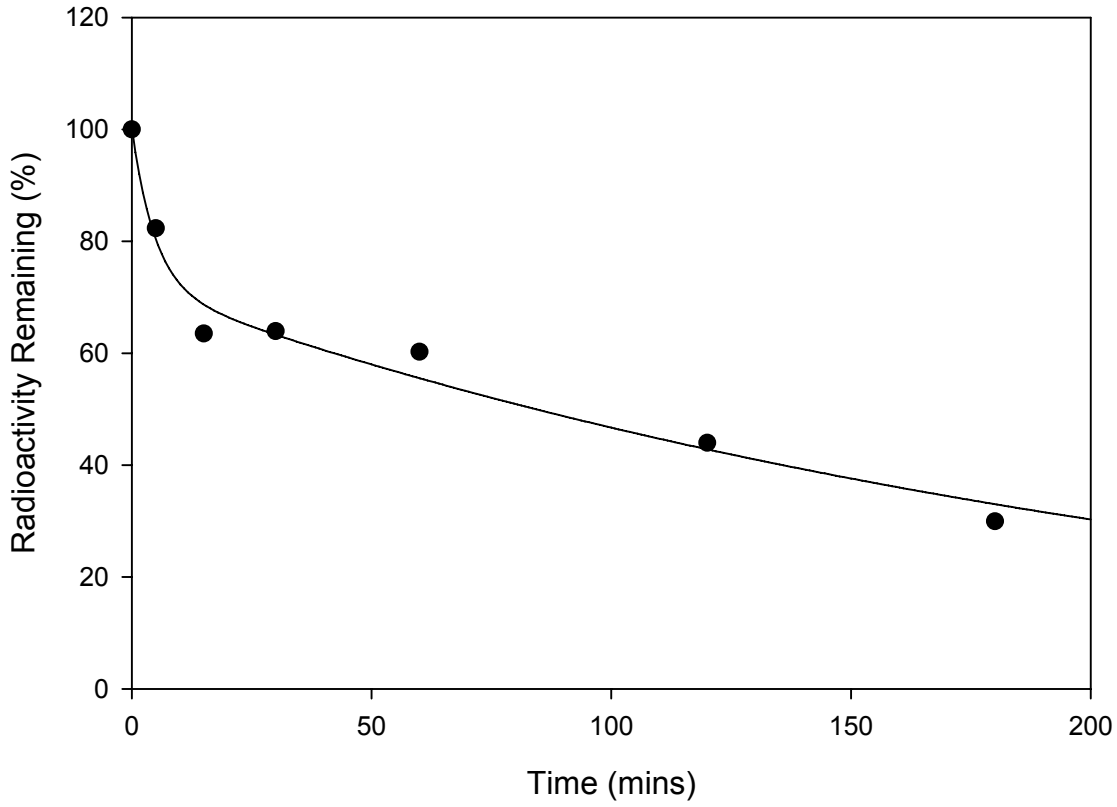

R	Rsqr	Adj Rsqr	Standard Error of Estimate
0.9899	0.9799	0.9599	4.6286

	Coefficient	Std. Error	t	P	VIF
a	28.4088	6.6616	4.2645	0.0237	2.3290
b	0.2099	0.1223	1.7173	0.1844	1.9594
c	72.0323	5.0355	14.3049	0.0007	5.6394<
d	0.0043	0.0009	5.0208	0.0152	2.6979

Analysis of Variance:

Uncorrected for the mean of the observations:

	DF	SS	MS
Regression	4	31296.1077	7824.0269
Residual	3	64.2720	21.4240
Total	7	31360.3797	4480.0542

Corrected for the mean of the observations:

	DF	SS	MS	F	P
Regression	3	3139.6470	1046.5490	48.8494	0.0048
Residual	3	64.2720	21.4240		
Total	6	3203.9190	533.9865		

Powder- No MA

f=a*exp(-b*x)+c*exp(-d*x)

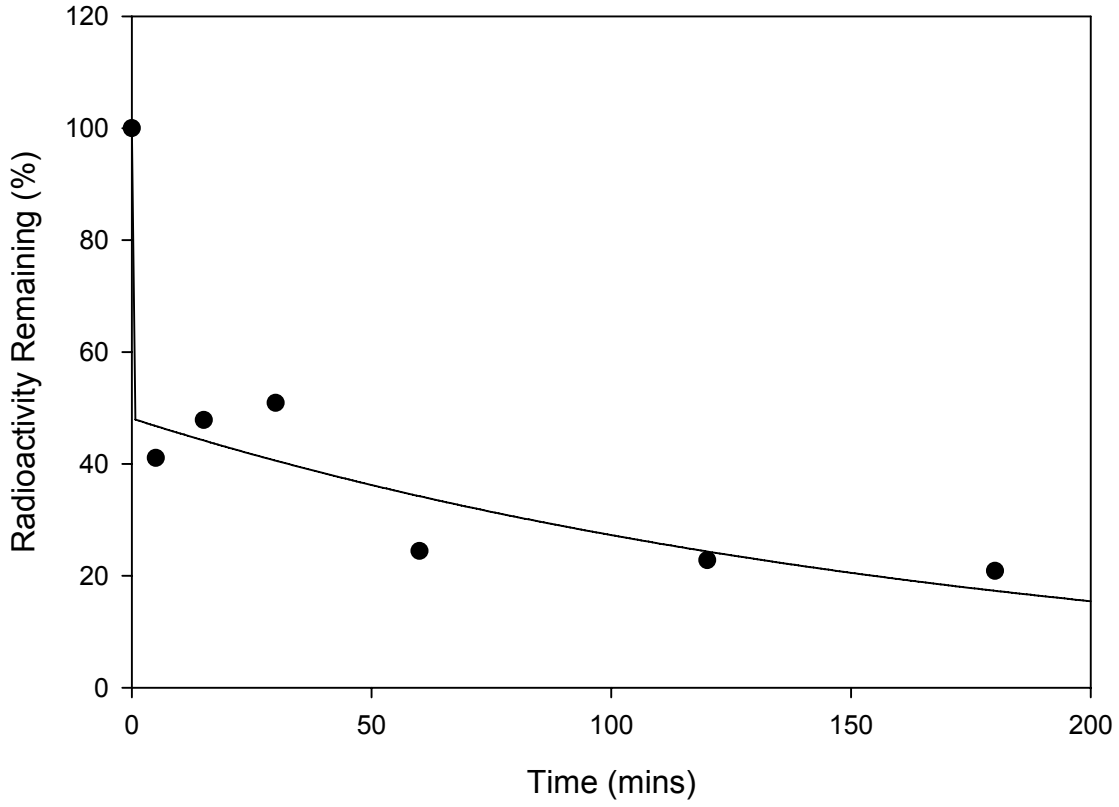

R	Rsqr	Adj Rsqr	Standard Error of Estimate
0.9709	0.9426	0.8852	9.3568

	Coefficient	Std. Error	t	P	VIF
a	51.8757	(NAN)	(+inf)	<0.0001	0.0000
b	4762871.8556	(NAN)	(+inf)	<0.0001	0.0000
c	48.1243	(NAN)	(+inf)	<0.0001	0.0000
d	0.0057	(NAN)	(+inf)	<0.0001	0.0000

Analysis of Variance:

Uncorrected for the mean of the observations:

	DF	SS	MS
Regression	4	17853.0738	4463.2685
Residual	3	262.6506	87.5502
Total	7	18115.7244	2587.9606

Corrected for the mean of the observations:

	DF	SS	MS	F	P
Regression	3	4312.0000	1437.3333	16.4172	0.0229
Residual	3	262.6506	87.5502		
Total	6	4574.6506	762.4418		

Powder- SA

f=a*exp(-b*x)+c*exp(-d*x)

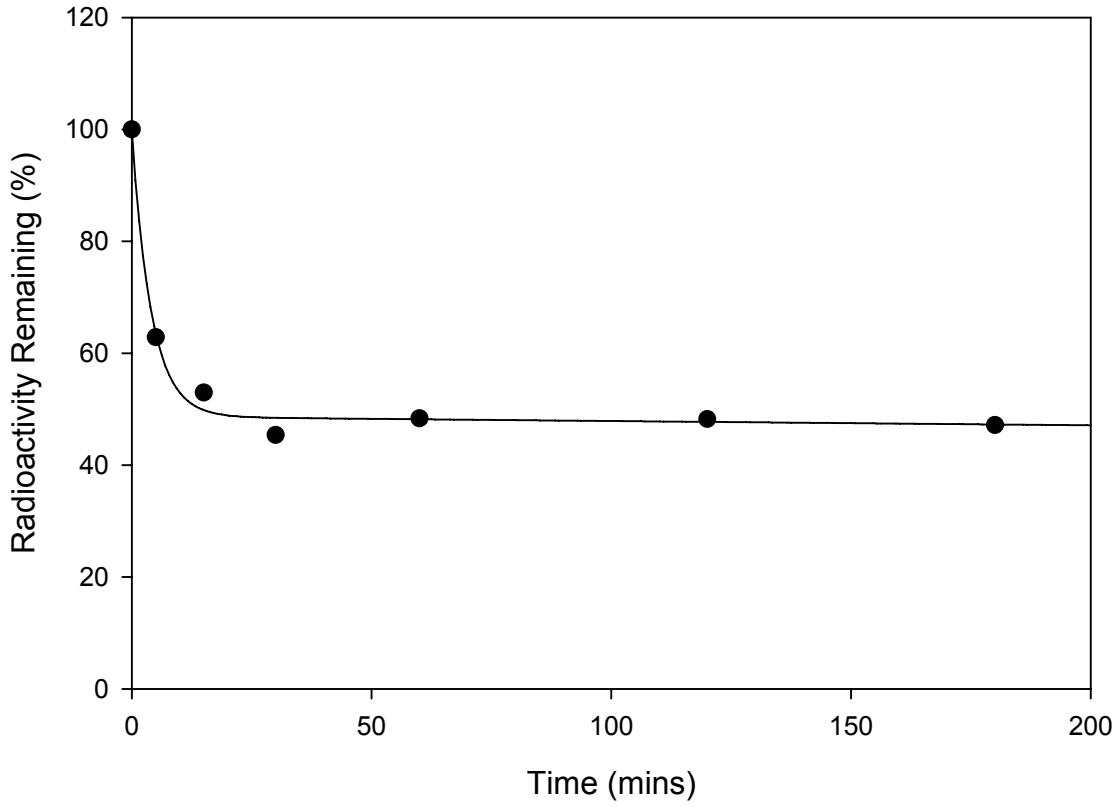

R	Rsqr	Adj Rsqr	Standard Error of Estimate
0.9956	0.9912	0.9823	2.5894

	Coefficient	Std. Error	t	P	VIF
a	51.1864	3.3228	15.4046	0.0006	1.7891
b	0.2455	0.0426	5.7631	0.0104	1.6233
c	48.6658	2.1605	22.5253	0.0002	4.7820<
d	0.0002	0.0004	0.3859	0.7253	3.0930

Analysis of Variance:

Uncorrected for the mean of the observations:

	DF	SS	MS
Regression	4	25683.5302	6420.8826
Residual	3	20.1146	6.7049
Total	7	25703.6448	3671.9493

Corrected for the mean of the observations:

	DF	SS	MS	F	P
Regression	3	2257.9312	752.6437	112.2536	0.0014
Residual	3	20.1146	6.7049		
Total	6	2278.0457	379.6743		

Powder- CMC HMW

f=a*exp(-b*x)+c*exp(-d*x)

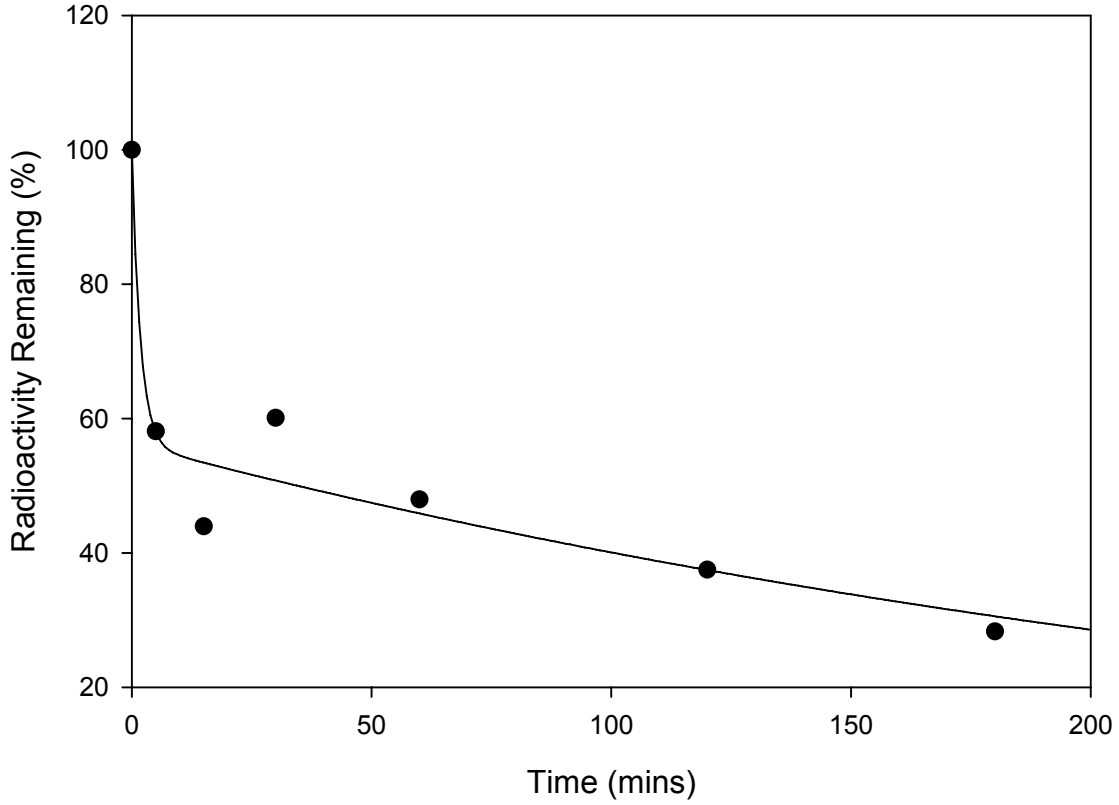

R	Rsqr	Adj Rsqr	Standard Error of Estimate
0.9709	0.9426	0.8851	7.8752

	Coefficient	Std. Error	t	P	VIF
a	43.7997	10.3956	4.2133	0.0244	1.7493
b	0.5548	0.7253	0.7649	0.5000	1.5851
c	56.2049	6.7886	8.2793	0.0037	3.7846
d	0.0034	0.0015	2.2085	0.1143	2.3107

Analysis of Variance:

Uncorrected for the mean of the observations:

	DF	SS	MS
Regression	4	23241.9695	5810.4924
Residual	3	186.0586	62.0195
Total	7	23428.0280	3346.8611

Corrected for the mean of the observations:

	DF	SS	MS	F	P
Regression	3	3053.4095	1017.8032	16.4110	0.0230
Residual	3	186.0586	62.0195		
Total	6	3239.4681	539.9113		

Powder- HPMC HMW

f=a*exp(-b*x)+c*exp(-d*x)

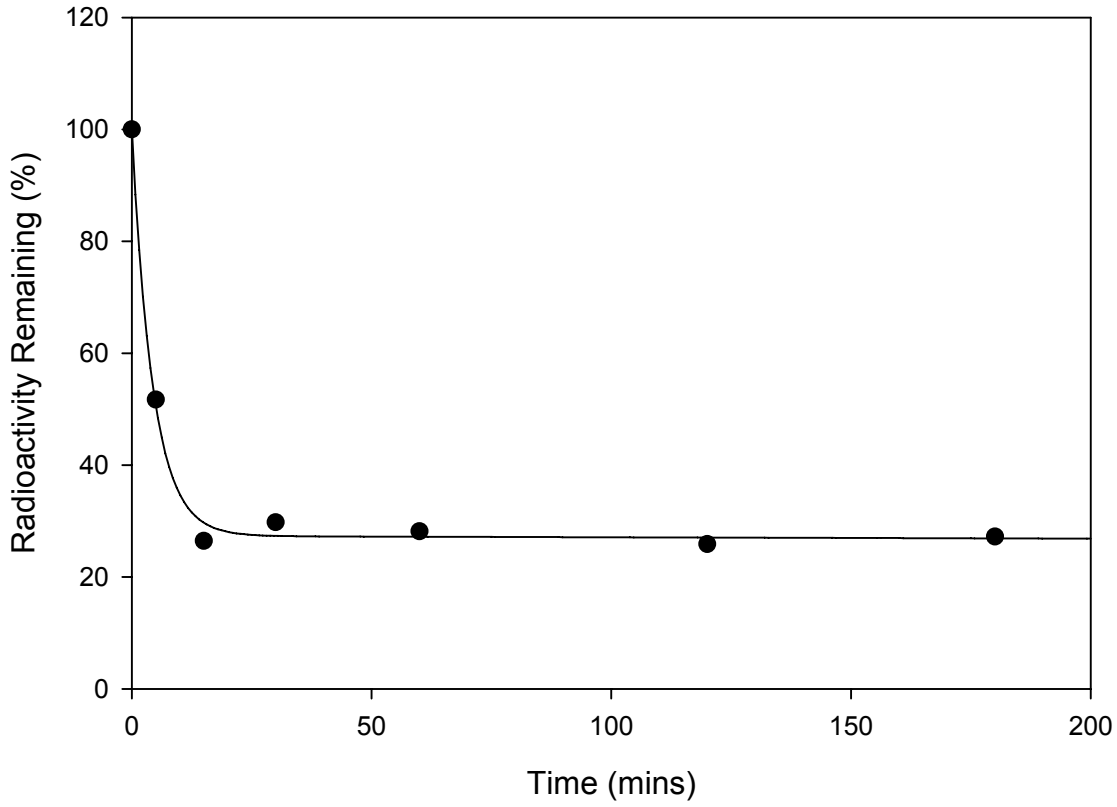

R	Rsqr	Adj Rsqr	Standard Error of Estimate
0.9978	0.9956	0.9912	2.5731

	Coefficient	Std. Error	t	P	VIF
a	72.8644	3.3134	21.9909	0.0002	1.8310
b	0.2272	0.0272	8.3561	0.0036	1.6749
c	27.3384	2.1879	12.4953	0.0011	5.0086<
d	8.9305E-005	0.0008	0.1189	0.9129	3.1954

Analysis of Variance:

Uncorrected for the mean of the observations:

	DF	SS	MS
Regression	4	16438.8060	4109.7015
Residual	3	19.8626	6.6209
Total	7	16458.6686	2351.2384

Corrected for the mean of the observations:

	DF	SS	MS	F	P
Regression	3	4496.7616	1498.9205	226.3928	0.0005
Residual	3	19.8626	6.6209		
Total	6	4516.6243	752.7707		

Powder- Chitosan

f=a*exp(-b*x)+c*exp(-d*x)

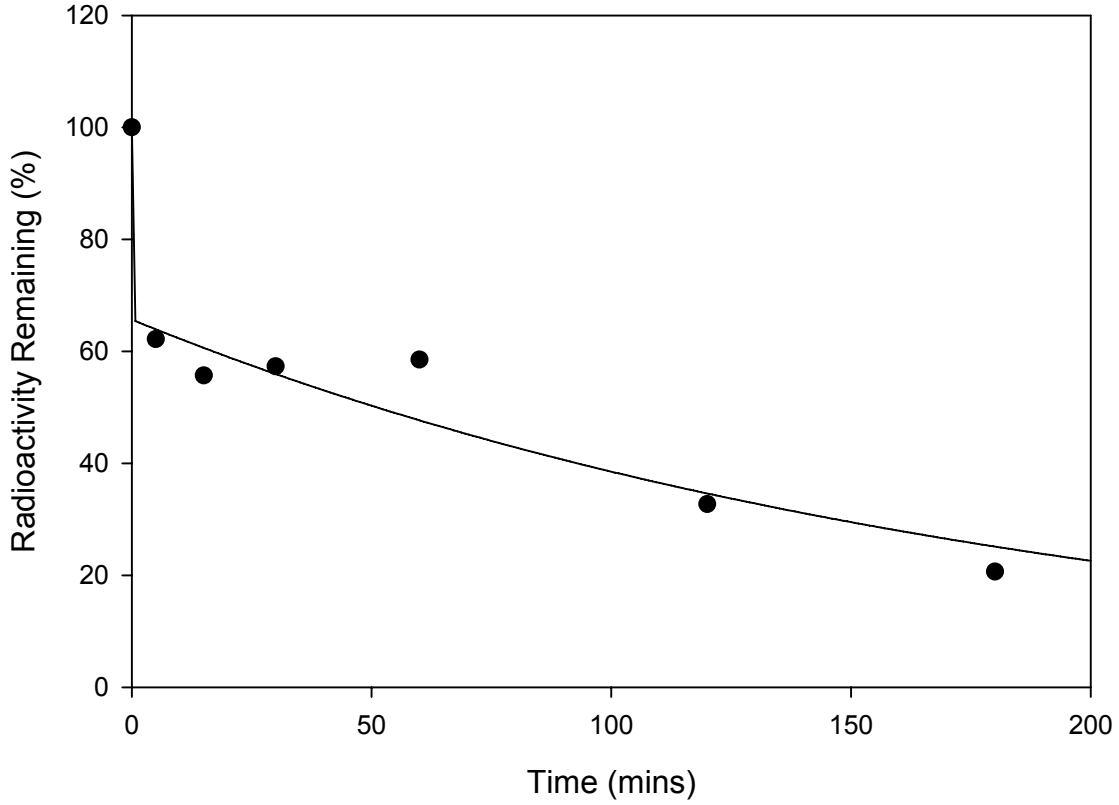

R	Rsqr	Adj Rsqr	Standard Error of Estimate
0.9772	0.9549	0.9099	7.5230

	Coefficient	Std. Error	t	P	VIF
a	34.3223	(NAN)	(+inf)	<0.0001	0.0000
b	129558.4970	(NAN)	(+inf)	<0.0001	0.0000
c	65.6777	(NAN)	(+inf)	<0.0001	0.0000
d	0.0053	(NAN)	(+inf)	<0.0001	0.0000

Analysis of Variance:

Uncorrected for the mean of the observations:

	DF	SS	MS
Regression	4	25002.3906	6250.5977
Residual	3	169.7861	56.5954
Total	7	25172.1767	3596.0252

Corrected for the mean of the observations:

	DF	SS	MS	F	P
Regression	3	3598.9693	1199.6564	21.1971	0.0160
Residual	3	169.7861	56.5954		
Total	6	3768.7554	628.1259		

Appendix A.5- RESIDENCE TIME STUDY IN SPRAGUE DAWLEY RATS

Materials and Methods

Male Sprague Dawley rats (350-400g Charles River, Raleigh, NC) were kept under standard conditions in AAALAC approved facilities under IACUC approved protocol (06-265.0-A). The animals were kept in a controlled temperature room (22 ± 1°C with 12 hour light and dark cycles and had free access to food and water. Rats were anesthetized by intraperitoneal injection of 40 mg/kg ketamine, 2 mg/kg xylazine and 0.75 mg/kg acepromazine before immunization.

Liquid formulations of saline or 1% MA in saline containing insoluble ^{99m}Tc sulfur colloid (^{99m}Tc-SC) were delivered by placing 25 μL of solution into the right nostril of an anesthetized rat using a 10-100 μL pipette. To label powder formulations, saline containing insoluble ^{99m}Tc-SC were centrifuged at 12000 rpms for 10 minutes. Supernatant was removed and the pellet was washed three times with ethanol. The pellet was allowed to dry before being blended with the SFD- rat trehalose with a mortar and pestle. Five milligram quantities were weighed out and placed in gelatin capsules (size 3, Capsugel, Greenwood, SC). Powder formulations were delivered using compressed air at 20 psi through a timed solenoid switch and a 100 μL pipette containing the contents of one dosage capsule in the right nostril of the anesthetized rat. The time points analyzed were 5, 15, and 120 minutes (n=3) and 30, 60, and 180 minutes (n=1). Rats were euthanized following cardiac puncture by CO_2 inhalation and nasal washes were collected by cannulating the trachea and rapidly instilling four aliquots of 1.5 mL of sterile saline. Fluid emerging from the nostrils was collected and analyzed in a radioisotope calibrator (Model CRC-4, Capintech, Inc. Pittsburgh, PA). All samples quantities were adjusted for radioactive decay.

Results and Discussion

Comparing the percentage of radioactivity as a function of time, SFD trehalose powder resided longer in the nasal cavity of the Sprague Dawley rats than saline (Figure A.5.1). Liquid and powder formulations containing the MA and saline alone were compared. The curve for liquid HPMC HMW was similar to powder HPMC HMW, but the saline alone did not reside as long in the nasal cavity as the HPMC HMW formulations (Figure A.5.2). The curve for liquid CMC HMW was similar to saline alone at almost all of the time points, but the powder CMC HMW seemed to remain in the nasal cavity longer than the liquid formulations (Figure A.5.3). The initial removal of saline, liquid SA, and powder SA was similar, but the SA formulations plateaued at a higher percentage of radioactivity remaining than saline (Figure A.5.4). The powder chitosan was similar to saline alone at almost all of the time points, but lower quantities of radioactivity were detected for the saline at the 180 minute time point (Figure A.5.5).

Regression analysis was performed by mathematically fitting the data to assess residence time differences, similar to the Brown Norway rats. The correlation coefficient and parameters (a, b, c, and d) determined by the regression analysis are shown (Table A.5.1). All of the curves exhibited good fit ($R^2 > 0.94$).

Parameters a and b are representative of initial clearance of the radioactivity from the nasal cavity. With the exception of the liquid HPMC, the distribution constant (b) was larger for the powder formulations than the liquids. This is surprising because run-off and swallowing of the liquid formulations, unhindered clearance, was expected to account for a large, immediate decrease in the radioactivity remaining. However, the viscosity of 1%

HPMC HMW is much greater than 1% SA or CMC HMW, which may explain the increase in residence time.

Parameters c and d are indicative of mucociliary clearance rate. The elimination constant (d) was very similar for all of the powder formulations and were larger than liquid HPMC HMW, CMC HMW, and SA, while the liquid NoMA was similar to the powder No MA.

All of the liquid formulations with MA and powder formulations had larger areas under the radiolabeled preparation retention curve (AUC) than the saline (Liq- No MA, Figure A.5.5). All of the powders, with the exception of Pow- SA (trehalose and SA) had longer residence times than the liquid formulations with the same MA. The AUC of the Liq- SA and Pow- SA were the same. The rank order of powders was Pow- CMC>Pow- HPMC HMW, Pow- No MA>Pow- SA>Pow- Chit. Compared to the AUC of the Brown Norway rats, the residence time of the liquids in Sprague Dawley rats was significantly lower, while the residence time of the Pow- No MA and Pow- HPMC HMW were significantly greater.

Table A.5.1– Correlation coefficient and parameters determined by regression analysis of two-compartment model curves determined by the % radioactivity remaining as a function of time in Sprague Dawley rats of liquid and powder formulations containing saline (liquid, No MA) and 1% hydroxypropyl methylcellulose (HPMC), carboxymethylcellulose sodium (CMC), or sodium alginate (SA) or trehalose alone (powder, No MA) and 3% HPMC, CMC, SA, and Chit.

	Liquid Formulations				Powder Formulations				
	No MA	HPMC HMW	CMC HMW	SA	No MA	HPMC HMW	CMC HMW	SA	Chit
r^2	0.9909	0.9914	0.9890	0.9932	0.9435	0.9747	0.9705	0.9773	0.9761
a	73.113	62.3879	70.4395	71.1362	30.3649	40.88	41.7547	48.1498	56.9458
b	0.0788	0.1519	0.0663	0.0697	0.2814	72.9289	0.1189	0.1736	7100.78
c	26.6927	37.1257	25.4678	30.7308	69.6624	59.12	55.7585	51.9502	43.0542
d	0.0074	0.0014	0.0011	1.28E-11	0.0074	0.0036	0.0036	0.0042	0.0048

Figure A.5.1– The percentage of radioactivity remaining in the nasal cavity of Sprague Dawley rats as a function of time when radiolabeled saline (Liq- No MA) or trehalose (Pow- No MA) is delivered (error bars represent standard deviations of n=3 at 15, 30, and 120 minute time points).

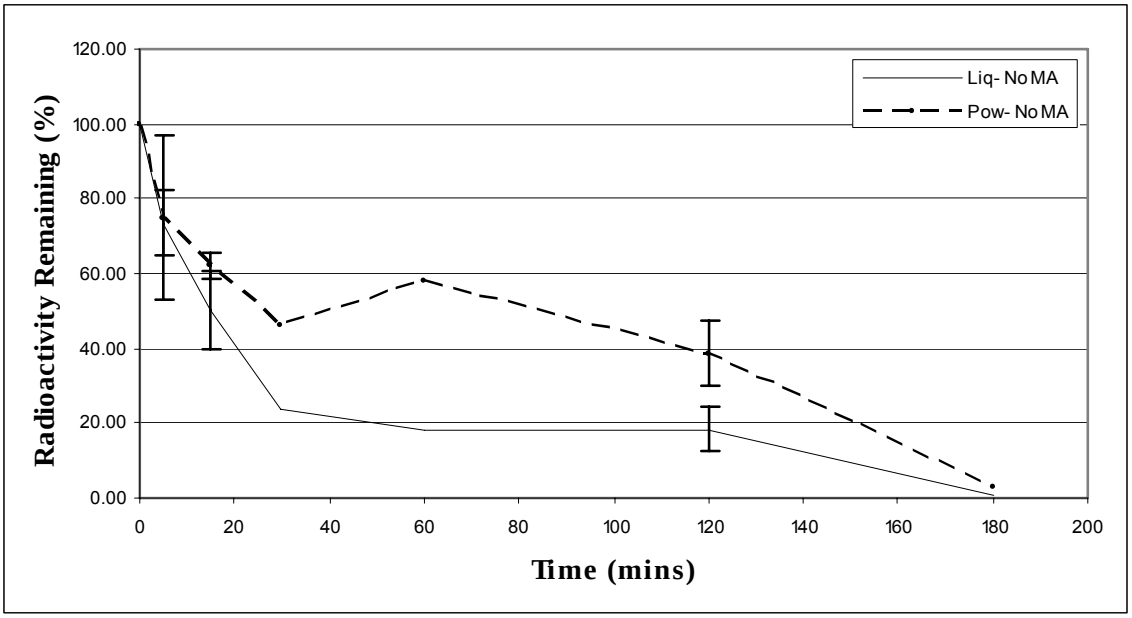

Figure A.5.2– The percentage of radioactivity remaining in the nasal cavity of Sprague Dawley rats as a function of time when radiolabeled saline (Liq- No MA), 1% hydroxypropyl methylcellulose in radiolabeled saline (Liq- HPMC HMW) or 3% hydroxypropyl methylcellulose in radiolabeled trehalose (Pow- HPMC HMW) is delivered (error bars represent standard deviations of n=3 at 15, 30, and 120 minute time points).

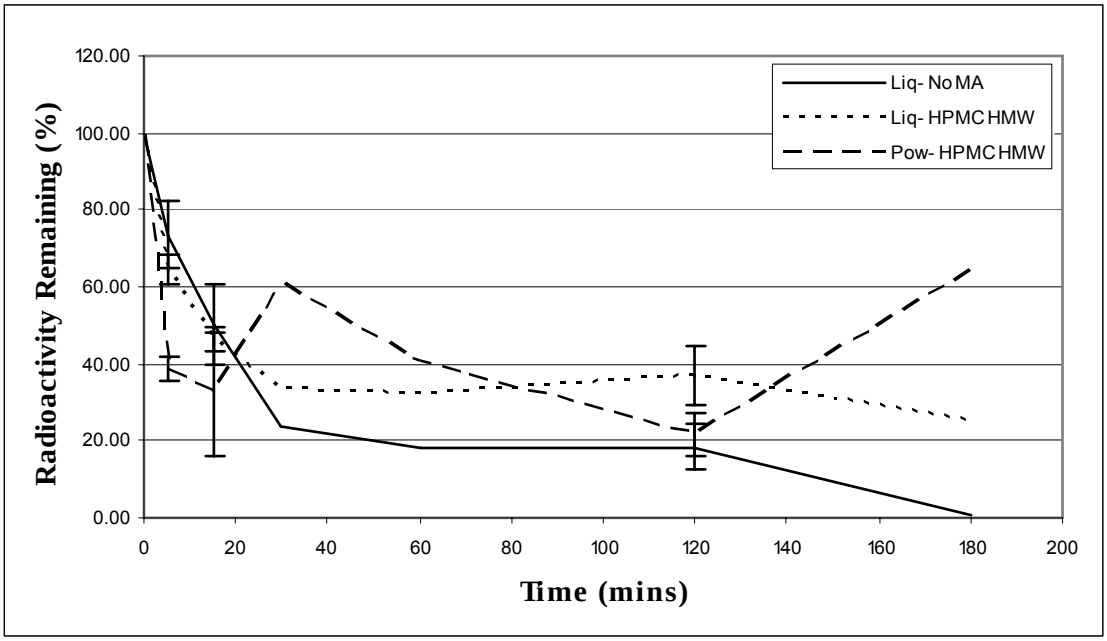

Figure A.5.3– The percentage of radioactivity remaining in the nasal cavity of Sprague Dawley rats as a function of time when radiolabeled saline (Liq- No MA), 1% carboxymethylcellulose sodium in radiolabeled saline (CMC HMW) or 3% carboxymethylcellulose sodium in radiolabeled trehalose (Pow- CMC HMW) is delivered (error bars represent standard deviations of n=3 at 15, 30, and 120 minute time points).

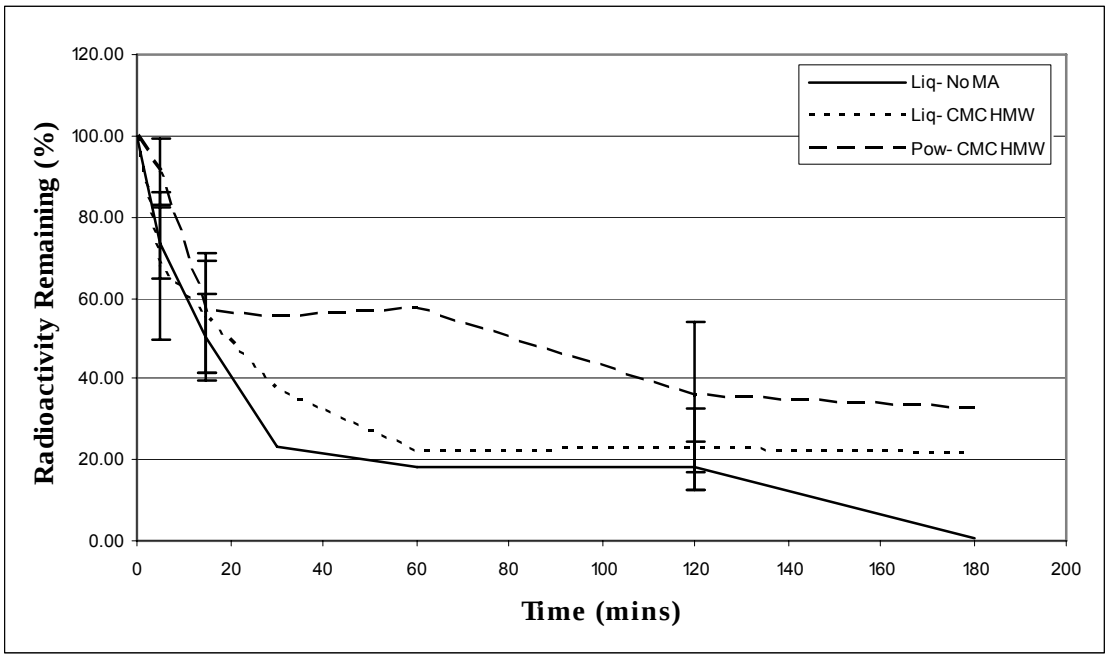

Figure A.5.4– The percentage of radioactivity remaining in the nasal cavity of Sprague Dawley rats as a function of time when radiolabeled saline (Liq- No MA), 1% sodium alginate in radiolabeled saline (Liq- SA) or 3% sodium alginate in radiolabeled trehalose (Pow- SA) is delivered (error bars represent standard deviations of n=3 at 15, 30, and 120 minute time points).

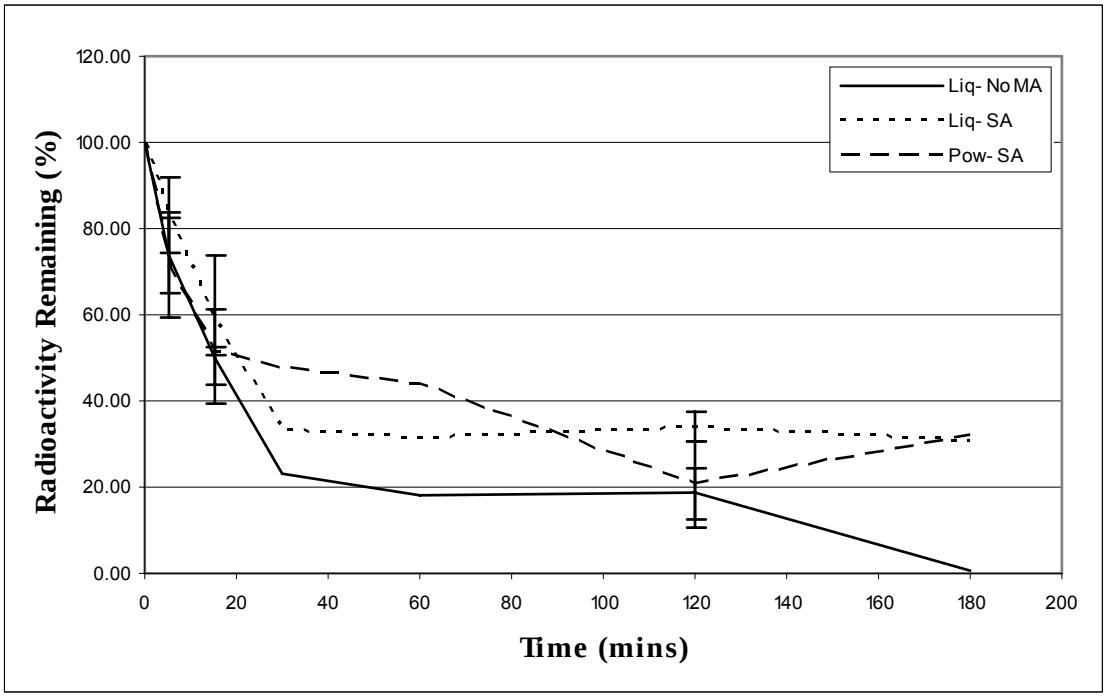

Figure A.5.5– The percentage of radioactivity remaining in the nasal cavity of Sprague Dawley rats as a function of time when radiolabeled saline (Liq- No MA) or 3% Chitosan in radiolabeled trehalose (Pow- Chit) is delivered (error bars represent standard deviations of n=3 at 15, 30, and 120 minute time points).

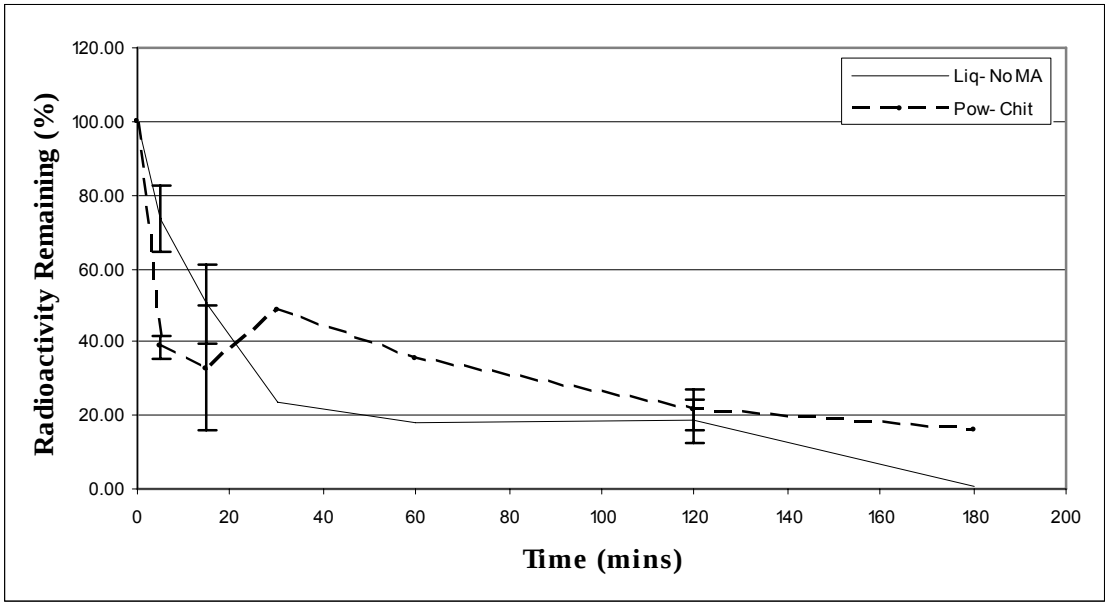

Figure A.5.6– The area under the curve of the percentage of radioactivity as a function of time curves for liquid and powder formulations containing no mucoadhesive (No MA), hydroxypropyl methylcellulose (HPMC HMW), sodium alginate (SA), carboxymethylcellulose sodium (CMC HMW), and chitosan (Chit) in Sprague Dawley rats.

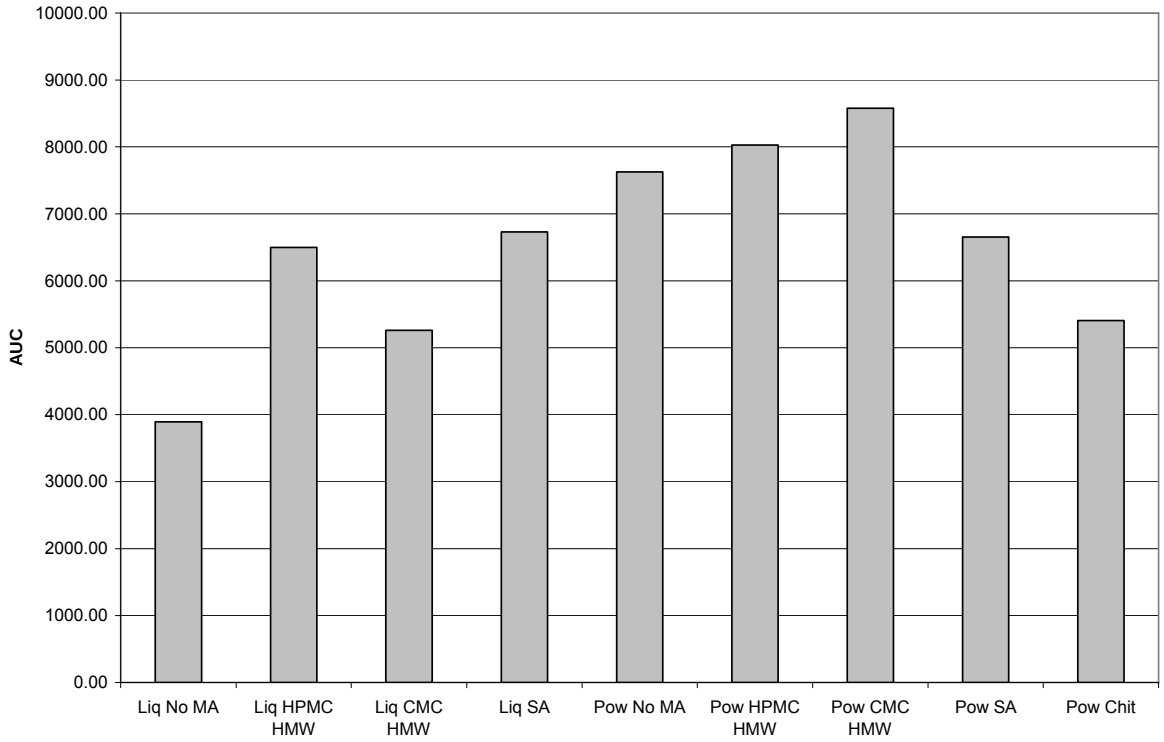

Liquid- No MA

f=a*exp(-b*x)+c*exp(-d*x)

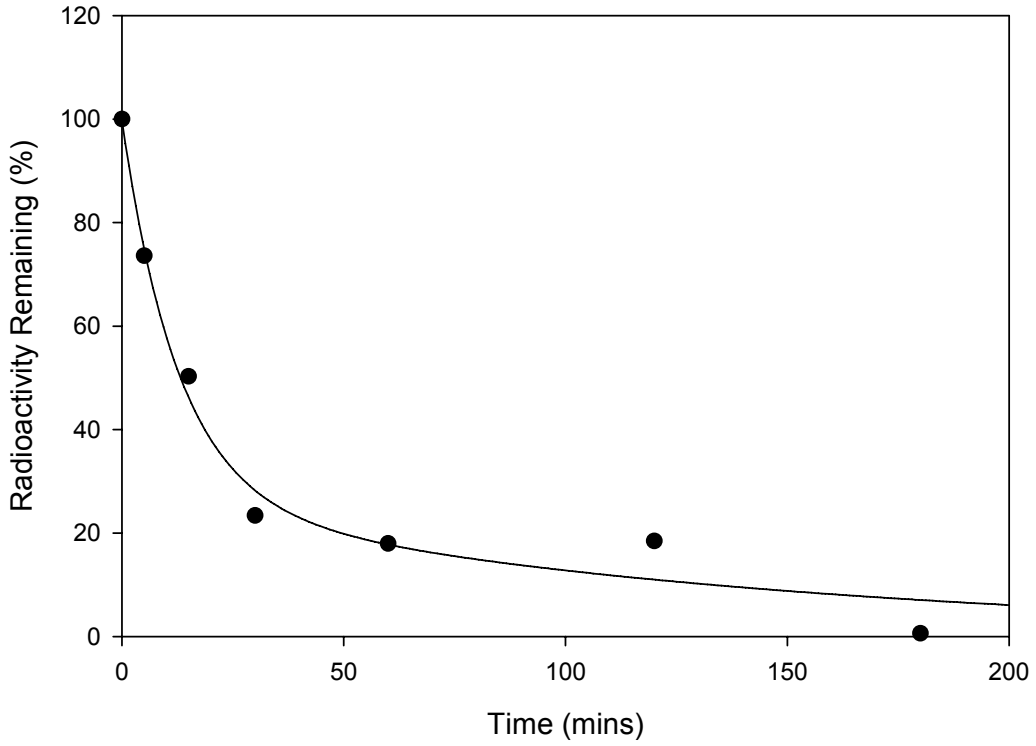

Nonlinear Regression
Equation: Exponential Decay, Double, 4 Parameter
f=a*exp(-b*x)+c*exp(-d*x)

R	Rsqr	Adj Rsqr	Standard Error of Estimate
0.9909	0.9818	0.9636	6.7951

	Coefficient	Std. Error	t	P	VIF
a	73.1130	19.0864	3.8306	0.0313	12.2889<
b	0.0788	0.0353	2.2297	0.1120	5.8949<
c	26.6927	19.3078	1.3825	0.2608	32.4989<
d	0.0074	0.0075	0.9890	0.3956	6.0055<

Analysis of Variance:
Uncorrected for the mean of the observations:

	DF	SS	MS
Regression	4	19021.7030	4755.4257
Residual	3	138.5216	46.1739
Total	7	19160.2245	2737.1749

Corrected for the mean of the observations:

	DF	SS	MS	F	P
Regression	3	7466.1258	2488.7086	53.8987	0.0042
Residual	3	138.5216	46.1739		
Total	6	7604.6474	1267.4412		

Liquid- HPMC HMW

f=a*exp(-b*x)+c*exp(-d*x)

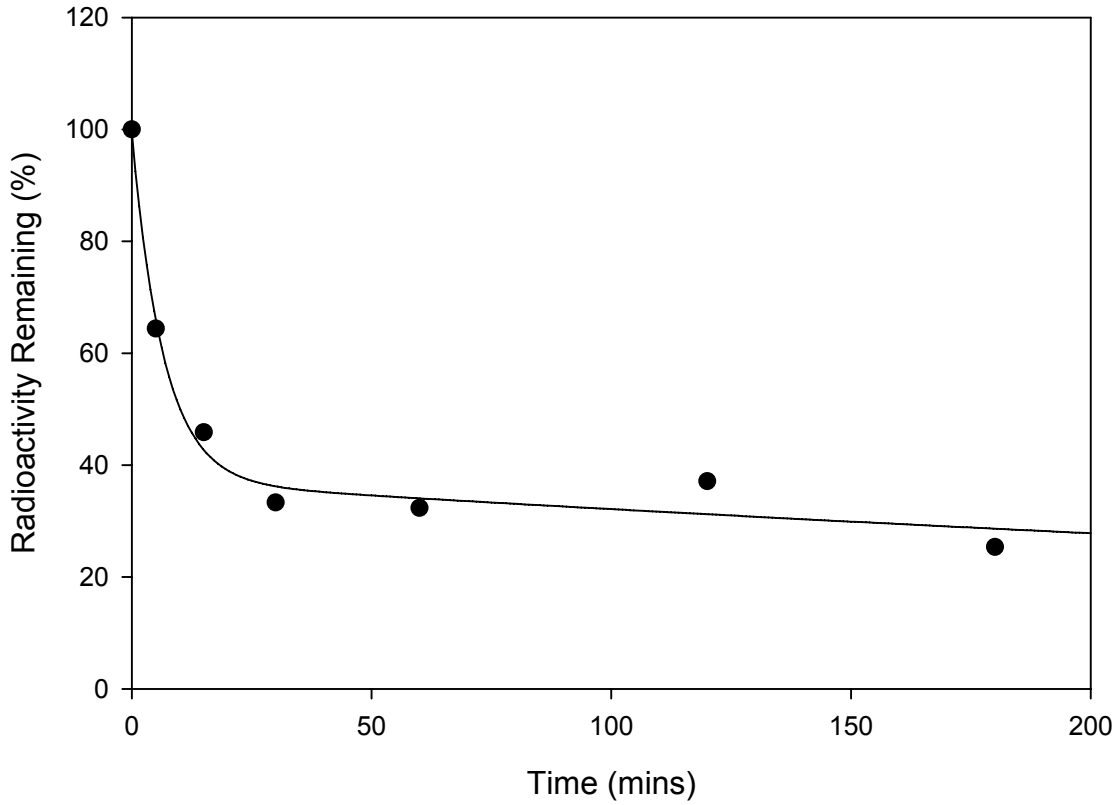

Nonlinear Regression
Equation: Exponential Decay, Double, 4 Parameter
f=a*exp(-b*x)+c*exp(-d*x)

R	Rsqr	Adj Rsqr	Standard Error of Estimate
0.9914	0.9830	0.9659	4.8065

	Coefficient	Std. Error	t	P	VIF
a	62.3879	6.7113	9.2960	0.0026	2.3973
b	0.1519	0.0408	3.7239	0.0337	2.2241
c	37.1257	5.1996	7.1401	0.0057	7.0252<
d	0.0014	0.0013	1.0812	0.3588	3.5679

Analysis of Variance:
Uncorrected for the mean of the observations:

	DF	SS	MS
Regression	4	20356.2365	5089.0591
Residual	3	69.3067	23.1022
Total	7	20425.5432	2917.9347

Corrected for the mean of the observations:

	DF	SS	MS	F	P
Regression	3	3999.1647	1333.0549	57.7024	0.0038
Residual	3	69.3067	23.1022		
Total	6	4068.4714	678.0786		

Liquid- CMC HMW

f=a*exp(-b*x)+c*exp(-d*x)

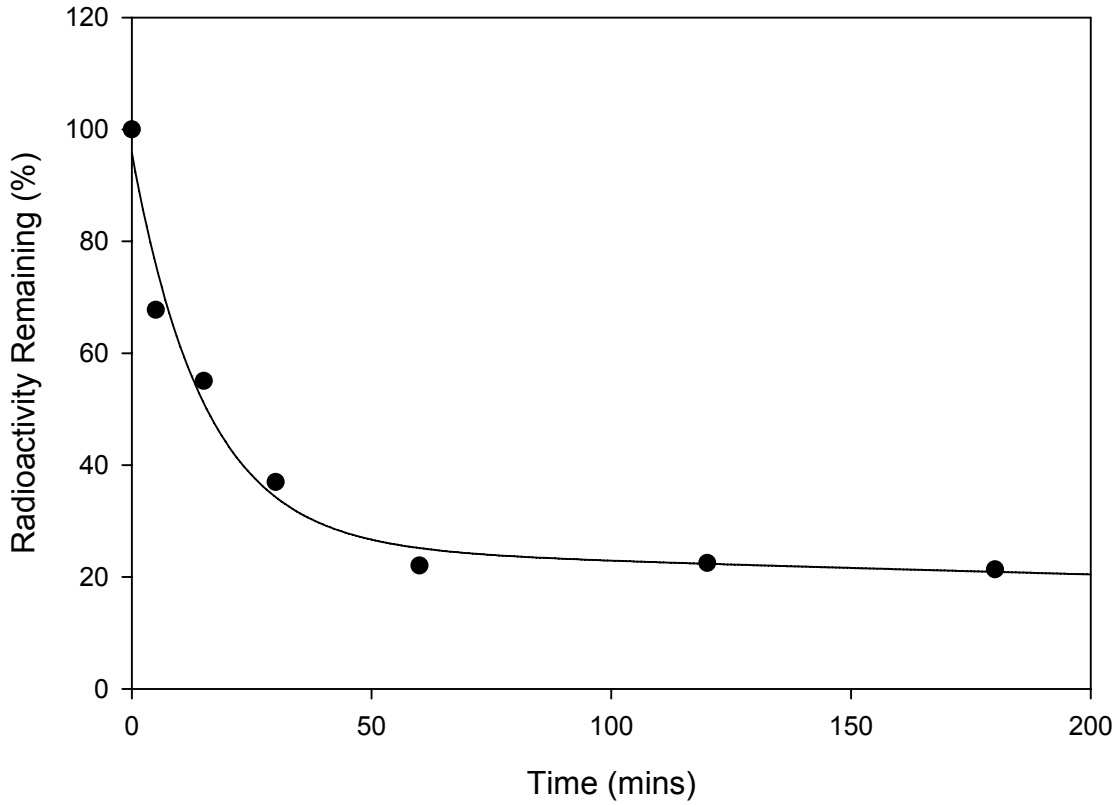

Nonlinear Regression
Equation: Exponential Decay, Double, 4 Parameter
f=a*exp(-b*x)+c*exp(-d*x)

R	Rsqr	Adj Rsqr	Standard Error of Estimate
0.9890	0.9781	0.9562	6.2130

	Coefficient	Std. Error	t	P	VIF
a	70.4395	12.0693	5.8363	0.0100	6.3075<
b	0.0663	0.0239	2.7677	0.0697	4.5578<
c	25.4678	11.8380	2.1514	0.1206	22.5579<
d	0.0011	0.0036	0.3055	0.7799	8.0096<

Analysis of Variance:
Uncorrected for the mean of the observations:

	DF	SS	MS
Regression	4	20319.2690	5079.8173
Residual	3	115.8056	38.6019
Total	7	20435.0746	2919.2964

Corrected for the mean of the observations:

	DF	SS	MS	F	P
Regression	3	5167.8418	1722.6139	44.6252	0.0055
Residual	3	115.8056	38.6019		
Total	6	5283.6474	880.6079		

Liquid- SA

f=a*exp(-b*x)+c*exp(-d*x)

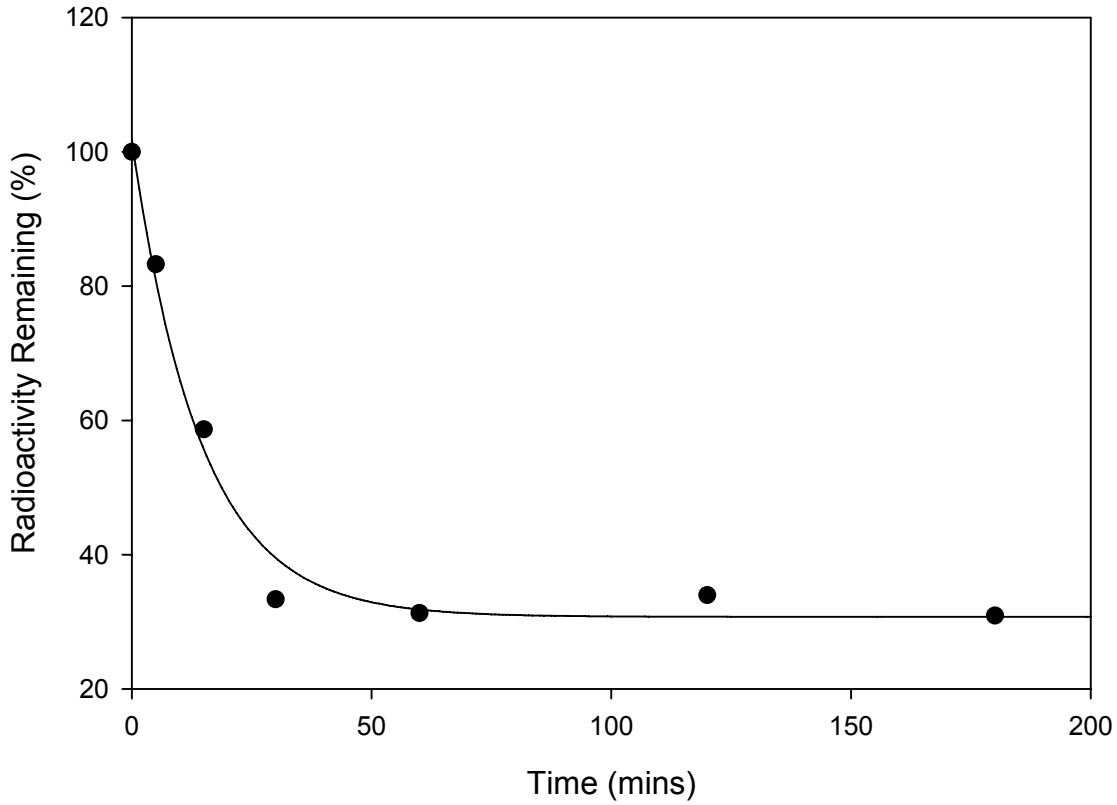

Nonlinear Regression
Equation: Exponential Decay, Double, 4 Parameter
f=a*exp(-b*x)+c*exp(-d*x)

R	Rsqr	Adj Rsqr	Standard Error of Estimate
0.9932	0.9864	0.9728	4.6980

	Coefficient	Std. Error	t	P	VIF
a	71.1362	8.1286	8.7514	0.0031	4.9011<
b	0.0697	0.0179	3.9020	0.0299	4.0114<
c	30.7308	7.7394	3.9707	0.0286	18.9967<
d	1.2833E-011	0.0019	6.7564E-009	1.0000	7.9468<

Analysis of Variance:
Uncorrected for the mean of the observations:

	DF	SS	MS
Regression	4	24498.4286	6124.6071
Residual	3	66.2149	22.0716
Total	7	24564.6434	3509.2348

Corrected for the mean of the observations:

	DF	SS	MS	F	P
Regression	3	4797.3457	1599.1152	72.4512	0.0027
Residual	3	66.2149	22.0716		
Total	6	4863.5605	810.5934		

Powder- No MA

f=a*exp(-b*x)+c*exp(-d*x)

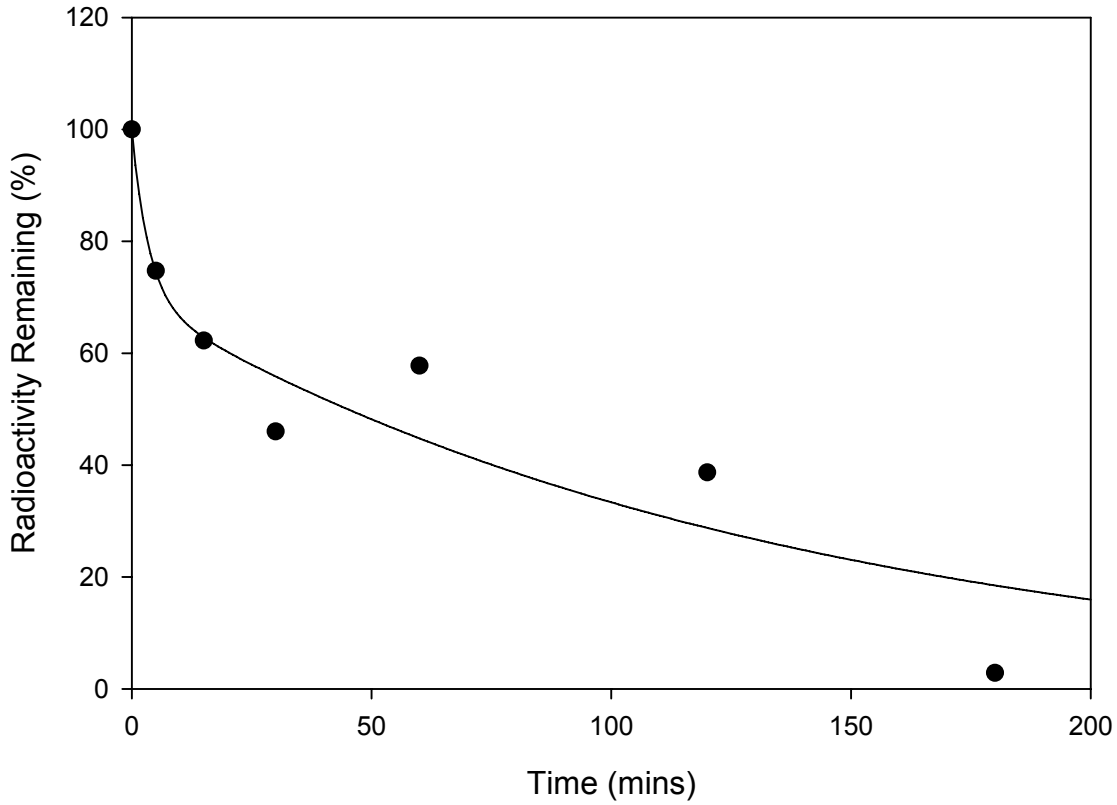

Nonlinear Regression
Equation: Exponential Decay, Double, 4 Parameter
f=a*exp(-b*x)+c*exp(-d*x)

R	Rsqr	Adj Rsqr	Standard Error of Estimate
0.9435	0.8901	0.7802	14.2452

	Coefficient	Std. Error	t	P	VIF
a	30.3649	21.4030	1.4187	0.2510	2.3932
b	0.2814	0.5150	0.5465	0.6228	1.8643
c	69.6624	16.2627	4.2836	0.0234	5.2493<
d	0.0074	0.0038	1.9428	0.1473	2.4108

Analysis of Variance:
Uncorrected for the mean of the observations:

	DF	SS	MS
Regression	4	25808.1903	6452.0476
Residual	3	608.7762	202.9254
Total	7	26416.9665	3773.8524

Corrected for the mean of the observations:

	DF	SS	MS	F	P
Regression	3	4931.7780	1643.9260	8.1011	0.0598
Residual	3	608.7762	202.9254		
Total	6	5540.5542	923.4257		

Powder- HPMC HMW

f=a*exp(-b*x)+c*exp(-d*x)

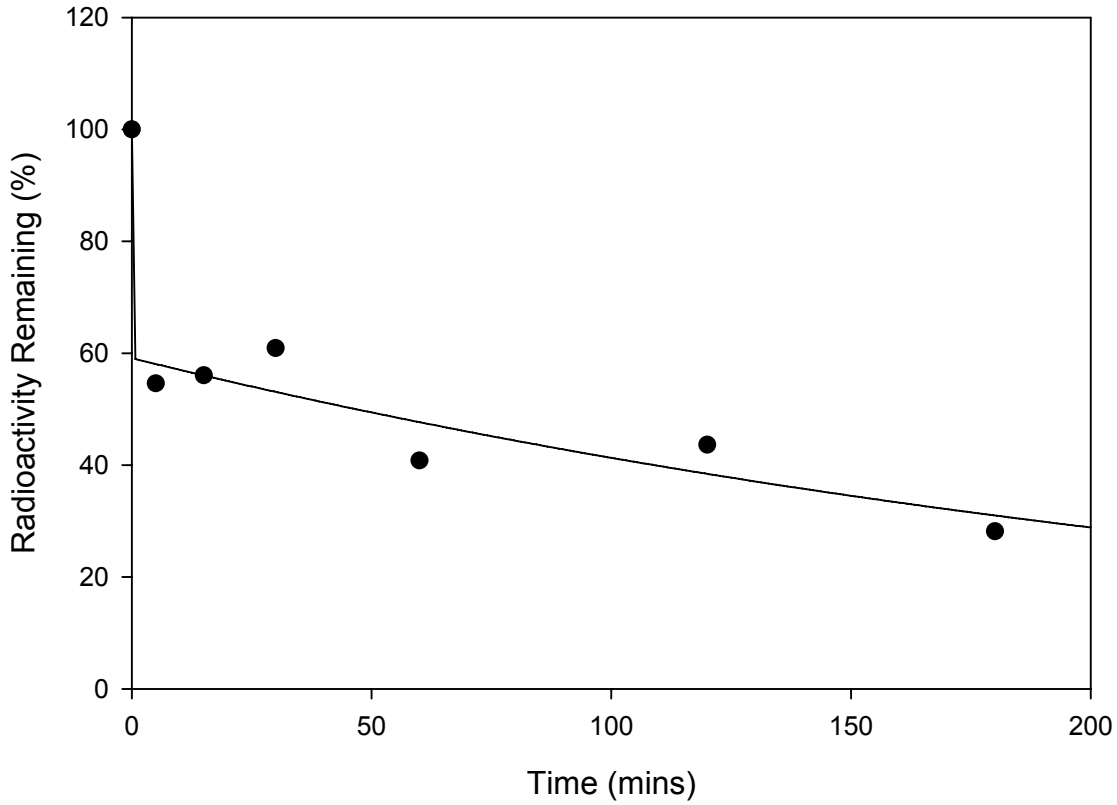

Nonlinear Regression
Equation: Exponential Decay, Double, 4 Parameter
f=a*exp(-b*x)+c*exp(-d*x)

R	Rsqr	Adj Rsqr	Standard Error of Estimate
0.9747	0.9501	0.9002	7.1955

	Coefficient	Std. Error	t	P	VIF
a	40.8800	(NAN)	(+inf)	<0.0001	0.0000
b	72.9289	(NAN)	(+inf)	<0.0001	0.0000
c	59.1200	(NAN)	(+inf)	<0.0001	0.0000
d	0.0036	(NAN)	(+inf)	<0.0001	0.0000

Analysis of Variance:
Uncorrected for the mean of the observations:

	DF	SS	MS
Regression	4	24039.9717	6009.9929
Residual	3	155.3264	51.7755
Total	7	24195.2981	3456.4712

Corrected for the mean of the observations:

	DF	SS	MS	F	P
Regression	3	2956.4931	985.4977	19.0341	0.0186
Residual	3	155.3264	51.7755		
Total	6	3111.8195	518.6366		

Powder- CMC HMW

f=a*exp(-b*x)+c*exp(-d*x)

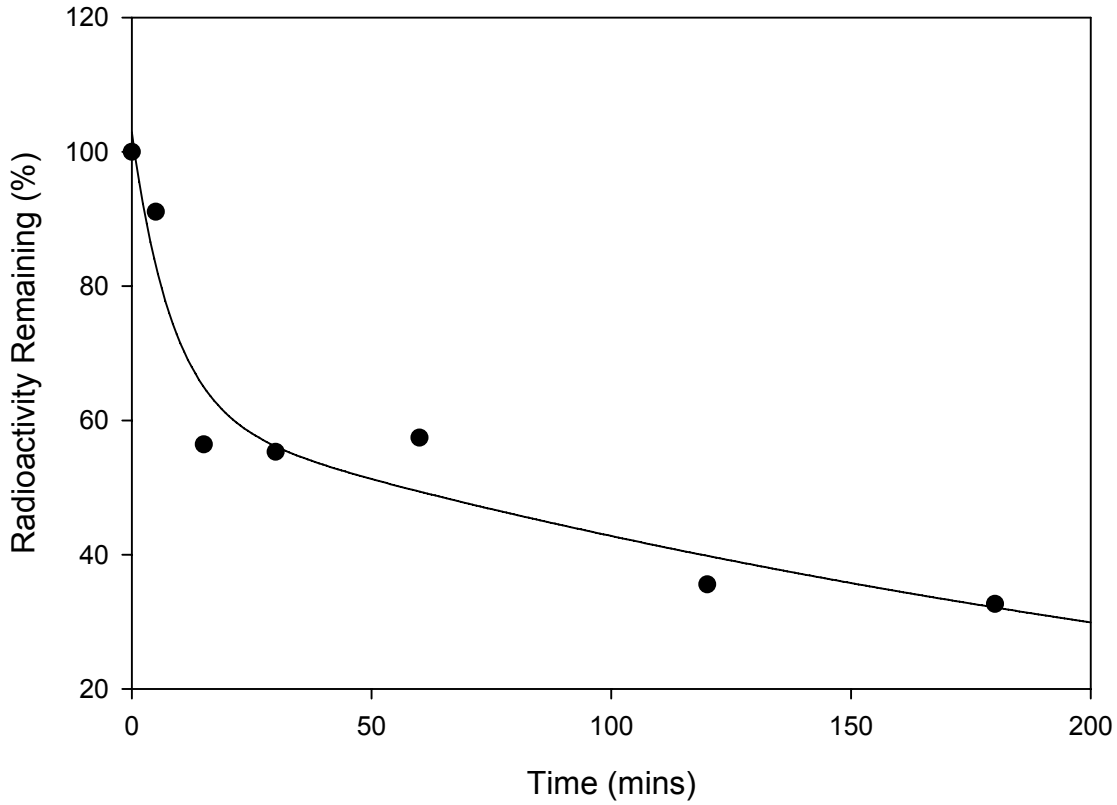

Nonlinear Regression
Equation: Exponential Decay, Double, 4 Parameter
f=a*exp(-b*x)+c*exp(-d*x)

R	Rsqr	Adj Rsqr	Standard Error of Estimate
0.9705	0.9419	0.8839	8.7349

	Coefficient	Std. Error	t	P	VIF
a	41.7547	14.2332	2.9336	0.0608	3.5410
b	0.1189	0.0941	1.2636	0.2956	2.9717
c	61.1717	12.6041	4.8533	0.0167	10.4534<
d	0.0036	0.0021	1.7183	0.1842	3.8976

Analysis of Variance:
Uncorrected for the mean of the observations:

	DF	SS	MS
Regression	4	29936.6071	7484.1518
Residual	3	228.8972	76.2991
Total	7	30165.5042	4309.3577

Corrected for the mean of the observations:

	DF	SS	MS	F	P
Regression	3	3713.7041	1237.9014	16.2243	0.0233
Residual	3	228.8972	76.2991		
Total	6	3942.6013	657.1002		

Powder- SA

f=a*exp(-b*x)+c*exp(-d*x)

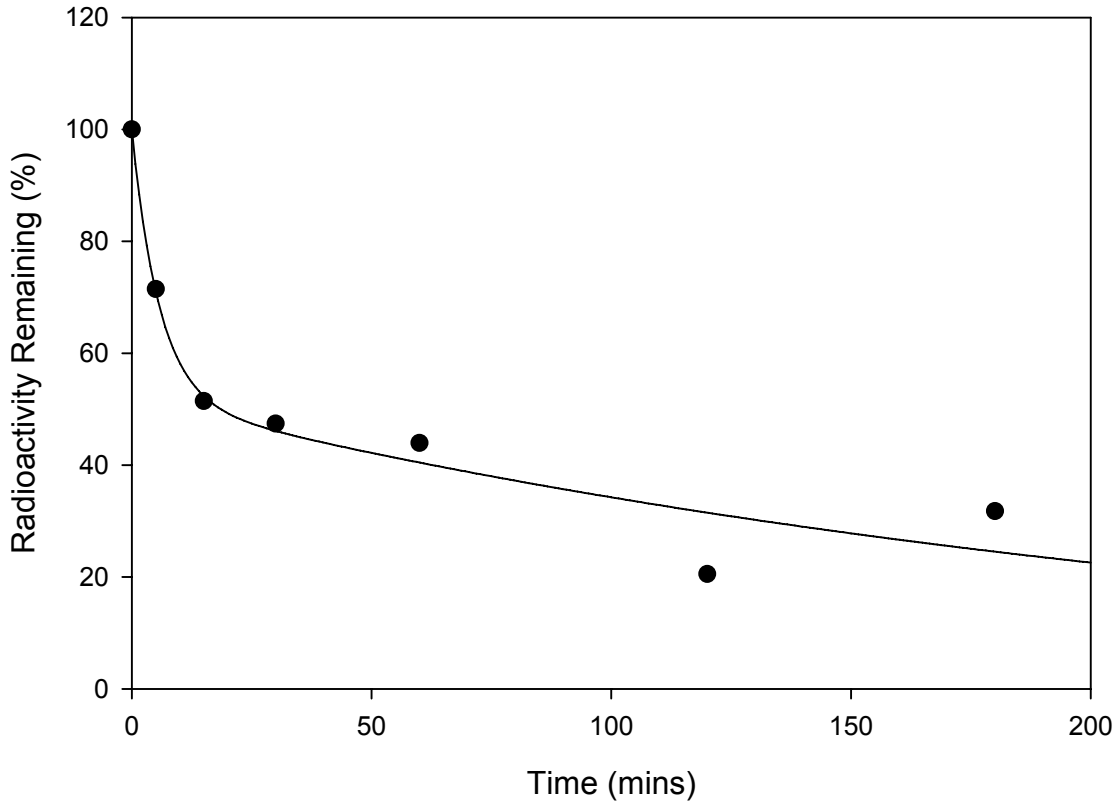

Nonlinear Regression
Equation: Exponential Decay, Double, 4 Parameter
f=a*exp(-b*x)+c*exp(-d*x)

R	Rsqr	Adj Rsqr	Standard Error of Estimate
0.9773	0.9551	0.9102	7.8972

	Coefficient	Std. Error	t	P	VIF
a	48.1498	11.7209	4.1080	0.0261	2.6030
b	0.1736	0.1026	1.6929	0.1891	2.2141
c	51.9502	9.3291	5.5686	0.0114	6.7230<
d	0.0042	0.0021	1.9899	0.1407	2.9670

Analysis of Variance:
Uncorrected for the mean of the observations:

	DF	SS	MS
Regression	4	23172.8914	5793.2229
Residual	3	187.0968	62.3656
Total	7	23359.9882	3337.1412

Corrected for the mean of the observations:

	DF	SS	MS	F	P
Regression	3	3982.0843	1327.3614	21.2836	0.0159
Residual	3	187.0968	62.3656		
Total	6	4169.1811	694.8635		

Powder- Chitosan

f=a*exp(-b*x)+c*exp(-d*x)

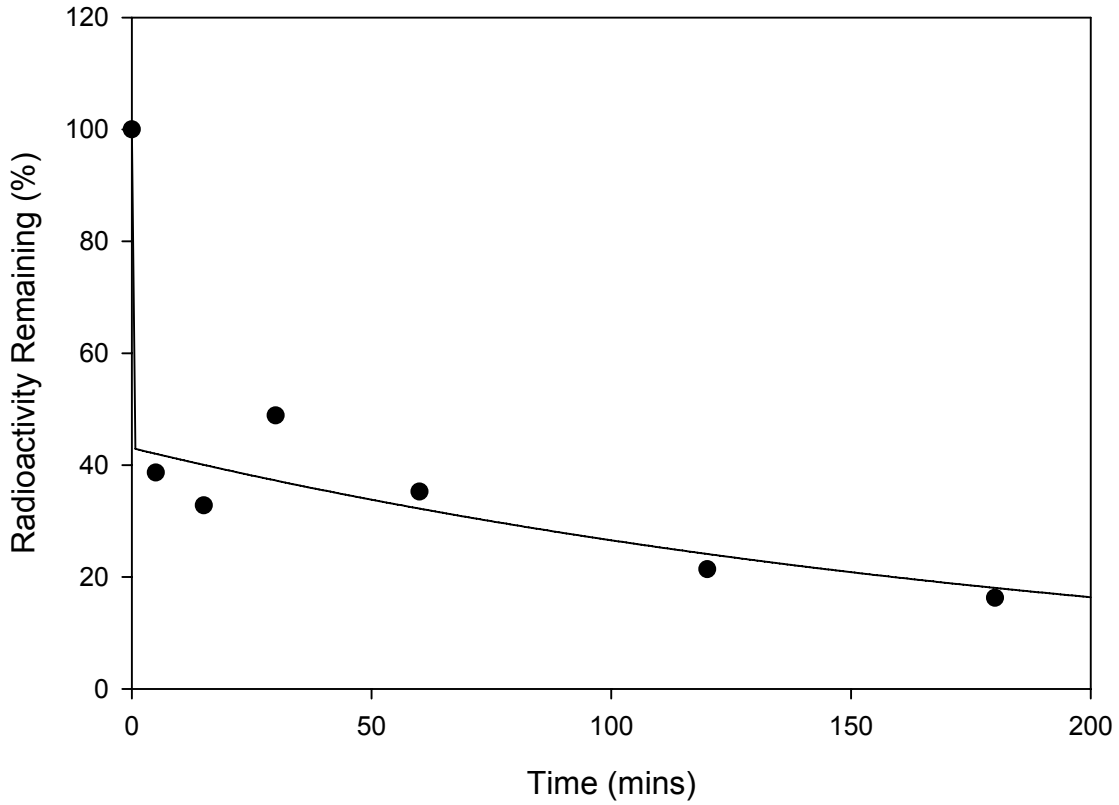

Nonlinear Regression
Equation: Exponential Decay, Double, 4 Parameter
f=a*exp(-b*x)+c*exp(-d*x)

R	Rsqr	Adj Rsqr	Standard Error of Estimate
0.9761	0.9527	0.9054	8.5549

	Coefficient	Std. Error	t	P	VIF
a	56.9458	(NAN)	(+inf)	<0.0001	0.0000
b	7100.7776	(NAN)	(+inf)	<0.0001	0.0000
c	43.0542	(NAN)	(+inf)	<0.0001	0.0000
d	0.0048	(NAN)	(+inf)	<0.0001	0.0000

Analysis of Variance:
Uncorrected for the mean of the observations:

	DF	SS	MS
Regression	4	16703.0326	4175.7582
Residual	3	219.5567	73.1856
Total	7	16922.5894	2417.5128

Corrected for the mean of the observations:

	DF	SS	MS	F	P
Regression	3	4422.0123	1474.0041	20.1406	0.0172
Residual	3	219.5567	73.1856		
Total	6	4641.5691	773.5948		

Appendix A.6- ANIMAL PROTOCOLS

Application to Use Live Vertebrate Animals

PI: Anthony J Hickey
CB: CB# 7360 1310 Kerr Hall
IACUC ID: 05-329.0 Web ID: 5838

Title: Development of a Dry Powder Influenza Vaccine for Nasal Delivery
Species: Rat ( )
Application Type: Amendment
Multiple Species No
Total Animal Number: 78

IACUC Use Only

IACUC ID:	05-329.0-A
Renewal Date:	11/2006

No	1.1: Are there confidential or potentially patentable issues?
No	1.2: Will collaborator(s), other than the PI, Co-PI or approved personnel within the PI's laboratory, perform any procedures on animals in this animal use application?
Yes	3.1: Will animals be housed or used in any DLAM, investigator laboratory, or other space?
No	3.2: Are you requesting that DLAM conduct animal procedures?
No	3.3: Will animals be housed outside DLAM-managed area for >12 hours? (Satellite Facility Form)
No	3.4: Are study animals free-ranging wildlife?
Yes	4.1: Will animals experience potential pain and/or distress as a result of the study or phenotype?
No	5.1: Will animals be bred as part of this study?
No	5.2: Will animals be used in a terminal surgical procedure (non-survival surgery)?
No	5.3: Will animals undergo a surgical procedure from which they recover (survival surgery)?
No	5.4: Will tumors be induced in study animals or may they form spontaneously?
No	5.5: Will behavioral and/or conditioning experiments be conducted?
No	5.6: Will conscious animals be physically restrained?
No	5.7: Will animals experience weight loss as a result of this study?
No	5.8: Will tissues be collected from live or dead animals?
Yes	5.9: Will blood or body fluids be collected from live or dead animals?
No	6.1: Will animals be given food and/or fluids other than that provided by DLAM in regular husbandry? Will food and/or fluids be restricted?
No	8: Are you requesting an exception to established regulation or IACUC policy?
No	9: Will animal be used for monoclonal antibody production or mouse ascites production?
No	10: Will animals be immunized or used for polyclonal anitbody (non-ascites) production?
No	11: Will animals be treated with chemical, pharmacologic, toxicologic or radioactive agents (not anesthetics/analgesics)?
No	Schedule G: Are transgenic animals, recombinant DNA, viral vectors used or produced during this study? Requires Institutional Biosafety Committee approval.
No	Are Chemical Hazards used?
No	Are Radioactive Hazards used?
Yes	Are Biological Hazards used? (includes use of biological agents, human blood, tissue, body fluids, infectious agents etc.)
No	Will cell lines or other agents be passaged in animals? If yes, contact DLAM to have your cell lines tested.

Submission History:

04/05/2006 - Complete
04/05/2006 - In Process
03/23/2006 - Under Review
03/21/2006 - Revised
03/21/2006 - Reopened
03/20/2006 - Submitted

Date Approved: 4/05/2006

1. Personnel Information:	Role(s):	
Anthony J Hickey **PID:** 704280014 **Dept:** 004501 - School Of Pharmacy **Campus Box:** CB# 7360 1310 Kerr Hall **Phone:** 919 962-0223 **Email:** ahickey@unc.edu	Principal Investigator	
Robert J Garmise **PID:** 709285854 **Dept:** 004501 - School Of Pharmacy **Campus Box:** CB# 7360 Beard Hall **Phone:** 966-0484 **Email:** garmise@email.unc.edu	24-Hour Contact Animal Handler Animal Ordering	**Technique(s)** / **Certified** Anesthesia - Administering: Yes Anesthesia - Monitoring: Yes Cardiac Puncture: Yes Ear Notch: Yes Exsanguination: N/A Handling and Restraint: Yes Intramuscular Injection: Yes Intraperitoneal Injection: Yes Sexing: N/A Tail Artery Bleed (Syringe): Yes Weighing and Measuring: N/A
Lucila Garcia-Contreras **PID:** 706193792 **Dept:** 004501 - School Of Pharmacy **Campus Box:** CB# 7360 1311 Kerr Hall **Phone:** 919 966-0484 **Email:** lgarciac@email.unc.edu	Laboratory Coordinator Official Contact Animal Handler Animal Ordering	**Technique(s)** / **Certified** Anesthesia - Administering: Yes Anesthesia - Monitoring: Yes Aseptic Technique: Yes Cardiac Puncture: Yes Ear Notch: No Exsanguination: N/A Handling and Restraint: Yes Intramuscular Injection: Yes Intraperitoneal Injection: Yes Laboratory Coordinator Lecture: Yes Tail Artery Bleed (Syringe): Yes Weighing and Measuring: N/A

2. Funding Source :	Agency Deadline:	Funding Period:	Grant Number:
University Trust Account			

3. Scientific Justification for Animal Species

Justify the species to be used by indicating

1. **No** This is a new model. (DLAM veterinarians available for consultation on new model development.)
   No The results will be directly applicable to the health, care or welfare of this species
   Yes Other -

   Rats have been employed to study the nasal disposition of drugs and vaccines. Although mice are commonly used to test novel influenza vaccines, it is intended to study the disposition of intramuscular vaccine formulations and its impact on immunity, as opposed to intranasal vaccination which requires a larger animal model. The size of the rat will facilitate the collection of nasal lavage fluid and the administration of powder formulation.

2. **No** Will the PI conduct the same experiment in multiple species?

3. Features of the species (e.g. anatomic, physiologic, genetic, etc.) that make it desirable for this model.

   MEDLINE and other computer database searches have been performed to identify alternative methods. Cell models would not offer the systemic response necessary to evaluate the effect of the vaccine in this study or allow the evaluation of mucociliary transport on induced immunity. Larger species, such as the rabbit, have been employed for similar studies, but offer no advantage for the performance of the present studies.

3.1 Building - Room Number:	Housing Type :
Kerr Hall - B244	DLAM
Kerr Hall - 1311	Investigator Laboratory

3.2 Procedures in Laboratory, DLAM/Satellite Housing & Confinement

1. **Yes** Will animals be removed from DLAM or approved satellite facility?
   Maximum time length living animals remain outside DLAM:
   6 hrs.
2. If animals will be removed from DLAM, approved Satellite Facility or taken to Investigator Laboratory, indicate the procedures to be performed, and the contact information:

   » **Procedure(s) to be performed:** Vaccination, blood sampling, nasal lavage
   » **Contact Person:** Robert J Garmise

4. Reduction, Refinement, Replacement, and Animal Numbers

1. Animal Number Reduction

a. Replacing vertebrate animals:
Are there computer simulation, non-living, or in vitro alternatives to the proposed use of animals described in your application? **No**
If yes, state why these alternatives are not appropriate:

b. Refining experimental procedures to minimize pain or distress:
Did you consider the use of pain-relieving drugs, or procedures that avoid or minimize discomfort, distress and pain, and humane endpoints in the design of the experiment? **Yes**

If not considered, state why the alternative was not applicable:

c. Reduction in the number of animals:

Yes Rational selection of group size (e.g., pilot studies to estimate variability, power analysis)

Yes Careful experimental design (e.g., appropriate choice of control groups)

Yes Maximizing use of animals (e.g., selecting the minimal number of animals per group required for statistical verification, sharing tissues with other investigators)

Yes Minimizing loss of animals (e.g., good post-operative care, avoidance of unintended breeding)

If you selected none of the above choices, state why they are not appropriate:

2. Using the specifics of your experimental plan, justify the number of animals requested and list the number of animals used for each pain category (B, C, D, E):

Animals will be dosed whole inactivated influenza virus (WIIV) either intramuscularly (IM) or intranasally (IN). A number of mucoadhesive compounds (MA) will be screened prior to the study for increasing residence time on the nasal mucosa. These compounds (ie. hydroxypropylmethyl cellulose, carboxymethyl cellulose, sodium alginate, etc.) are all categorized the Food and Drug Administration as generally regarded as safe (GRAS).

Group #	Dose Equivalent of WIIV (ug)	Route	Vehicle/Excipient	Animals
1	TBD	IM	Saline	6
2	TBD	IN	Saline	6
3	TBD	IN	Trehalose (Control)	6
4	TBD	IN	Trehalose	6
5	TBD	IN	Trehalose/MA High Clearance Rate	6
6	TBD	IN	Trehalose/MA Intermediate Clearance Rate	6
7	TBD	IN	Trehalose/MA Low Clearance Rate	6
8	1	IM	Saline	3
9	4	IM	Saline	3
10	6	IM	Saline	3
11	8	IM	Saline	3
12	10	IM	Saline	3
13	12	IM	Saline	3
14	14	IM	Saline	3
15	16	IM	Saline	3

16	18	IM	Saline	3
17	20	IM	Saline	3
18	30	IM	Saline	3
19	40	IM	Saline	3
				78 Total

Groups 8-19 will be utilized as a dose ranging study to determine the appropriate dose for the animals in Groups 1-7. Each group in the dose ranging study will require 3 animals because the dose response curve generated is known to be a step function and the curve will be defined by the twelve groups. Each group in the formulation study will require 6 animals for statistical validity and to control as much as possible for inter-and intra-animal variability.

3. Estimate the following animal number totals required for this study during the three-year approval period>

Pain Category	Unweaned	Breeders	Adults
B	0	0	0
C	0	0	78
D	0	0	0
E	0	0	0

Total Animal Number = **78**

4. Category E Justification:

5. Transfer of Existing Animals: No

4.1 Alternatives to Animals Classified in USDA Pain Categories D or E

1. Details About Alternatives Search

a. Literature search conducted:

Pub Med: 10/25/2005

b. Keywords used in database searches

mucoadhesive

rat

intranasal

influenza

vaccine

influenza animal model

brown norway rats

c. Years Search: 1994-2005

d. » Information Services and other Literature Sources:

No Animal Welfare Information Center
No Lab Animal Welfare Bibliography (NLM)
No Laboratory Animal Science Journal
No Alternatives to Laboratory Animals Journal (FRAME, U.K.)
No Quick Bibliography Series (AGRICOLA)
No Peer Review -
No Other -

» Knowledge of Field/Consultants:

» Other Methods or Sources Used:

5. Details of Animal Use:

1. Goals and objective(s) of your research.

In light of the recent crisis of the availability of influenza vaccine and the inability of the pharmaceutical industry to produce room-temperature stable needle-free options, it is imperative that the scientific and technological foundation for the development of such systems is addressed. It is proposed that maximal mucosal and systemic antibody production will be elicited by a dry powder nasal vaccine formulation containing whole-inactivated influenza virus (WIIV) with optimized local residence time in the nose. Dry powders of suitable size for nasal delivery will be prepared by freeze-drying (FD) followed by milling or spray-freeze-drying (SFD). Desirable properties include aerodynamic diameter >20μm with a median diameter of 45-125μm; suitable for dispersion; exhibiting a range of viscosity modification and charge characteristics consistent with retention on the nasal mucosa. Each manufactured powder will be characterized for particle size distribution, morphology, thermal properties, moisture content, flow properties, surface area, and electrostatic properties. A novel delivery device will be employed and the dispersion properties of the formulation will be examined. Functional stability of the dry powder preparation will be determined using an ELISA assay. The impact of charge and viscosity on mucoadhesive compounds will be evaluated by determining the rheological properties of mucus. Site of deposition will be evaluated using scintigraphic imaging. Selected mucoadhesive (MA) compounds will be used to modify the residence time on the nasal mucosa and will be blended with the trehalose powder. A modified Andersen cascade impactor will allow for characterization of particles in the 0.22-20μm size range. Impact force detachment will be used to evaluate the dispersion properties of heterogeneous particles. Dry powder vaccine will be evaluated in rats to determine the magnitude of the immune response and compared to positive and negative controls, nasal solution and intramuscular injection. Production of local and systemic antibodies in a rat model will be measured by nasal lavage and blood samples. It is anticipated that the dose of antigen, formulation characteristics (particle size, distribution, composition, use of mucoadhesive) will elicit a quantifiable immune response that will provide protection against the virus upon future contact.

2. If this application is a continuation of an ongoing project, state concisely how these goals differ from those in the original application and what was accomplished during the prior approval period. If this is a new project, please indicate so.

Experiments carried out from the previous protocol (ID# 00-207.0.A) were to determine feasibility of nasal delivery of a whole inactivated influenza vaccine (WIIV) and to determine quantity of WIIV required to elicit a sufficient immune response. The previous experiments successfully resulted in the production of systemic and local antibodies by the animal. Current studies will examine the use of excipients which have been proven to increase the residence time of the WIIV in the nasal cavity. These excipients could potentially lead to greater production of systemic and local antibodies and/or allow for smaller doses to elicit a comparable immune response to higher doses. Studies conducted in collaboration with Dr. Mike Foster, Duke University, will establish mucociliary clearance rate for different formulations from which properties for the proposed groups in this study can be selected.

3. Describe the specific experimental manipulations and treatments of the animals in terms that are intelligible to a non-scientist.

Female Brown Norway rats will receive an IP injection of anesthesia. Blood samples will be drawn from the tail artery. Animals will be dosed with a vaccine by either intramuscularly or intranasally. After dosing, animals will be returned to their cages without bedding (to avoid possible choking), placed on a heating pad (30-35°C) to avoid hypothermia, and monitored every 15 minutes for 3 hours. Even though a reversing agent could be used to decrease the time that the animal is under anesthesia (because acepromazine increases recovery time by ~30%),we would prefer to avoid the use of another pharmaceutical compound, reducing the possibility of adverse effects, and we will increase the monitoring of the recovery time from the suggested 2 hours to 3 hours. During the recovery period, the patient will be monitored for basic biological functions (ie. breathing rate (70-115/minute), intake, and elimination) and return of motor skills.

Three weeks after immunization, animals will again receive anaesthesia, blood samples will be drawn from the tail artery, and animals will be dosed again via the same route of administration. Two weeks after this second dose, animals will receive anaesthesia, nasal lavage samples will be taken by washing the nasal cavity with 1 mL of PBS containing 20 ug/mL of aprotinin, and the animal will be sacrificed by cardiac puncture followed by carbon dioxide overdose.

5.9 Collection of blood or body fluids from live or dead vertebrate animals

1. Will fluid be collected from dead animals? Yes

Collected Fluid: blood

2. Describe the purpose for collecting blood or other body fluids from live animals (other than ascites):

The purpose of the study is to elicit an immune response in the animals from the vaccine formulation. Blood samples will be drawn to determine antibody production in the animal to the virus.

3. Fluid withdrawn, frequency, volume, method and site:

Fluid Collected : Blood
Frequency: Once every 3 weeks
Volume: 300 uL
Method: Tail vein/artery withdrawal
Site: Laboratory

Fluid Collected : Blood
Frequency: On Termination
Volume: 10 mL
Method: Cardiac puncture
Site: Laboratory

If any of the above methods are Retro-orbital, please justify

If any of the above methods are Cardiac-Puncture, please indicate that required criteria are met

These criteria are met.

If any of the above methods are Other, please specify collection method:

4. Fluid and/or blood collection

Anesthetic Agent: Ketamine HCL
Dosage: 40 mg/kg
Route: IP

Schedule:	Every 3 weeks
Anesthetic Agent:	Xylazine HCL
Dosage:	2 mg/kg
Route:	IP
Schedule:	Every 3 weeks
Anesthetic Agent:	Acepromazine maleate
Dosage:	0.75 mg/kg
Route:	IP
Schedule:	Every 3 weeks

6. Animal Care

1. Animal ID Method:

No Ear Tag
Yes Ear Punch
No Microchip
No Tattoo
No Toe Clip
No Not Applicable
No Other
Other Explanation -

2. How will animals be monitored?

Animals will be monitored by housing staff.

If special monitoring has been arranged with DLAM facility supervisor, provide DLAM contact name:

3. Should DLAM contact PI/emergency contact if animal(s) found dead? Yes

4. Indicate requests for special handling of sick and dead animals:

5. Special Housing (DLAM):

Will any special housing or care be necessary? **No**

Deviations from standard DLAM husbandry procedures, Guide recommendations or special animal care needs:

6. Special Diets (DLAM)

Are special diets, additives to food and/or water (e.g. colyte) and/or antibiotics administered? **No**

7. Endpoints (time points, tumor sizes etc.) and/or the maximum time length of study:

The study will end 2 weeks after boost immunization, for a total length of study of 5 weeks (6 weeks including 1 week acclimation period.)

8. Will animals be euthanized as part of the study? Yes

Animals will be euthanized at the end of the study 2 weeks after the boost immunization.

» Euthanasia Methods

Yes CO_2-compressed carbon dioxide gas in cylinders

No Barbituate overdose
Dosage and route:

No Cervical Dislocation
If no anesthesia, scientific justification:

No Decapitation
If no anesthesia, scientific justification:

No Overdose of gas anesthetic
Specify Agent:

No Anesthesia - followed by physical euthanasia
Agent, Dose and Route:

Yes Other Method of Euthanasia
Exanguination by cardiac puncture while under anaesthesia.

9. Would the PI be willing to share, donate or make available extra animal tissues or organs to other PI's? Yes

7. Anticipated Animal Pain & Distress

1. Are there any clinical, behavioral, or physiological manifestations expected to result from experimental manipulation such as surgery, diet, tumor, chronic disease, radiation sickness or toxicity, or potential health problems due to animal phenotype?Yes

a. Expected clinical and/or behavioral signs of pain and distress in animals

No Decreased weight
No Changes in food/water consumption
No Decreased ambulation
No Ruffled fur
No Skin abnormality
No Urinary problems
No Hunched posture
No Paw guarding
No Porphyrin Staining
No Lethargy
No Diarrhea
Yes Other
Other Explanation - Extremely unlikely event of nose bleed after dosing animals with dry powder vaccine.

b. Methods of dealing with the above complications:

No Analgesics
No Anesthetics
No Sedation or tranquilization
No Increased bedding
Yes Other
Other Explanation - Call veterinary services.

1b. continued...

b. Agents used in dealing with complications

2. Animals experiencing unrelieved pain or distress prior to the endpoint, as defined by institutional policy, must be humanely euthanized, unless an exception to policy is requested and approved. Is exception required? No

a. Criteria for euthanasia that will used for this exception:

b. Scientific justification for not using an earlier endpoint:

Application to Use Live Vertebrate Animals

PI: Anthony J Hickey
CB: CB# 7360 1310 Kerr Hall
IACUC ID: 05-329.0 Web ID: 5838

Application Certification

I agree to the following statements. Signify your agreement by signing at the bottom

- I certify that I am familiar with and assure compliance in this Project with the legal standards of animal care and use established under the Federal and State laws and the policies on animal welfare of the National Institutes of Health and the University of North Carolina.
- I assume responsibility for ensuring that all persons working with animals on this project are familiar with and are trained in relevant animal procedures and that they will comply with established laws and policies regarding animal care and use. Applications will not be approved for investigators that have taken the IACUC orientation but have not completed required Laboratory Animal Coordinator certification. Contact the IACUC office to arrange training.
- I will appoint a Laboratory Coordinator to manage all animal use in the lab. I will ensure that the Coordinator receives required training and certification. I will ensure that after being certified, the Coordinator or IACUC representative will train and certify all individuals working with animals in the lab.
- I certify that all individuals working with animals on this project will register with the University Employee Occupational Health Clinic (UEOHC) by completing and submitting the "Research Animal Handlers & Animal Caretakers" medical history questionnaire (each individual who works with animals must complete the questionnaire during online orientation - UEOHC will assess the PI a processing fee).
- I certify the following: the research proposed herein is not unnecessarily duplicative of previously reported research; appropriate non-animal alternatives for this research do not exist; no alternatives to the potentially painful and/or distressful procedures conducted in this project exist. I have indicated methods used to make these determinations in the appropriate section of this animal use application.
- I will secure IACUC approval before changing procedures or personnel associated with this study (including adding personnel)
- I assure that I and personnel under by direct supervision will use the animals acquired for the activity described herein solely for said purpose. I also certify that if live animals are shared with other PIs or are used in any procedure other than those described in this application, I will provide the details in the form of a written amendment to the original application prior to their use.
- I acknowledge that veterinary care will be administered to moribund animals or animals experiencing more than momentary or slight pain or distress. Division of Laboratory Animal Medicine (DLAM) veterinary staff will attempt to contact me regarding the care of treatment of a moribund animal, but will institute treatment or euthanasia, as needed, if PI cannot be reached.
- I assure the IACUC and the University of North Carolina at Chapel Hill that the general procedures involving animals described in my grant application have been described in the animal use application and submitted to the IACUC for review.
- I assure that I have read "Notes on Euthanasia" of animals used in research and understand how it applies to animals in this animal use application.

NOTE: Consultation of a DLAM veterinarian regarding space allocation is recommended prior to submission of application. IACUC approval of application does not assure DLAM space availability. Please contact DLAM for pre-study strategy meeting prior to ordering animals to dicuss availability of housing.

NOTE: Cell lines that have been passaged in animals or maintained using animal serum may contain murine viruses that can alter the outcome of the study and may cause an outbreak of disease among other mice. ATTCC does not screen cell lines for murine pathogens. Cell lines that have been passaged in animals or grown in media containing rodent serum should be tested for murine pathogens prior to use in animals. Please contact DLAM for more information on testing of your cell lines.

PI Signature Date

Co-PI Signature Date

Date Approved: 4/05/2006

Application to Use Live Vertebrate Animals

PI: Anthony J Hickey
CB: CB:7360 1310 Kerr Hall
IACUC ID: 06-265.0 Web ID: 8088

Title: Effect of Residence Time on Immune Response Elicited from a Dry Powder Nasal Vaccine
Species: Rat ( )
Application Type: New Application
Multiple Species No
Total Animal Number: 342

IACUC Use Only

IACUC ID:	06-265.0-A
Renewal Date:	10/2007

No	1.1: Are there confidential or potentially patentable issues?
No	1.2: Will collaborator(s), other than the PI, Co-PI or approved personnel within the PI's laboratory, perform any procedures on animals in this animal use application?
Yes	3.1: Will animals be housed or used in any DLAM, investigator laboratory, or other space?
No	3.2: Are you requesting that DLAM conduct animal procedures?
No	3.3: Will animals be housed outside DLAM-managed area for >12 hours? (Satellite Facility Form)
No	3.4: Are study animals free-ranging wildlife?
Yes	4.1: Will animals experience potential pain and/or distress as a result of the study or phenotype?
No	5.1: Will animals be bred as part of this study?
No	5.2: Will animals be used in a terminal surgical procedure (non-survival surgery)?
No	5.3: Will animals undergo a surgical procedure from which they recover (survival surgery)?
No	5.4: Will tumors be induced in study animals or may they form spontaneously?
No	5.5: Will behavioral and/or conditioning experiments be conducted?
No	5.6: Will conscious animals be physically restrained?

No	5.7: Will animals experience weight loss as a result of this study?
No	5.8: Will tissues be collected from live or dead animals?
Yes	5.9: Will blood or body fluids be collected from live or dead animals?
No	6.1: Will animals be given food and/or fluids other than that provided by DLAM in regular husbandry? Will food and/or fluids be restricted?
No	8: Are you requesting an exception to established regulation or IACUC policy?
No	9: Will animal be used for monoclonal antibody production or mouse ascites production?
No	10: Will animals be immunized or used for polyclonal anitbody (non-ascites) production?
Yes	11: Will animals be treated with chemical, pharmacologic, toxicologic or radioactive agents (not anesthetics/analgesics)?
No	Schedule G: Are transgenic animals, recombinant DNA, viral vectors used or produced during this study? Requires Institutional Biosafety Committee approval.
No	Are Chemical Hazards used?
Yes	Are Radioactive Hazards used?
No	Are Biological Hazards used? (includes use of biological agents, human blood, tissue, body fluids, infectious agents etc.)
No	Will cell lines or other agents be passaged in animals? If yes, contact DLAM to have your cell lines tested.

Submission History:

10/26/2006 - Complete	10/19/2006 - In Process	10/17/2006 - Revised	10/16/2006 - Reopened
09/27/2006 - Under Review	09/26/2006 - Revised	09/26/2006 - Reopened	09/15/2006 - Submitted

Date Approved: 10/26/2006

1. Personnel Information:

Robert J Garmise

PID: 709285854
Dept: 4501 - School Of Pharmacy
Campus Box: CB: 7360
Phone: 6-484
Email: garmise@email.unc.edu

Role(s):
Animal Ordering
24-Hour Contact
Animal Handler
Email Contact

Technique(s)	Certified
Anesthesia - Administering	Yes
Anesthesia - Monitoring	Yes
Cardiac Puncture	Yes
CO2 Euthanasia	Yes
Ear Notch	Yes
Handling and Restraint	Yes
Intramuscular Injection	Yes
Intraperitoneal Injection	Yes
Tail Artery Bleed (Syringe)	Yes

Lucila Garcia-Contreras

PID: 706193792
Dept: 4501 - School Of Pharmacy
Campus Box: CB:7360 1311 Kerr Hall
Phone: (919) 966-0484
Email: lgarciac@email.unc.edu

Laboratory Coordinator
Official Contact
Animal Handler

Technique(s)	Certified
Anesthesia - Administering	Yes
Anesthesia - Monitoring	Yes
Cardiac Puncture	Yes
CO2 Euthanasia	Yes
Handling and Restraint	Yes
Intramuscular Injection	Yes
Intraperitoneal Injection	Yes
Tail Artery Bleed (Syringe)	Yes

Anthony J Hickey

PID: 704280014
Dept: 4501 - School Of Pharmacy
Campus Box: CB:7360 1310 Kerr Hall
Phone: (919) 962-0223
Email: ahickey@unc.edu

Principal Investigator

2. Funding Source :

Agency Deadline:	Funding Period:	Grant Number:
University of North Carolina at Chapel Hill		6-68394

3. Scientific Justification for Animal Species

Date Approved: 10/26/2006

Justify the species to be used by indicating

1. **No** This is a new model. (DLAM veterinarians available for consultation on new model development.)
   No The results will be directly applicable to the health, care or welfare of this species
   Yes Other -

   Rats have been employed to study the nasal disposition of drugs and vaccines. Although mice are commonly used to test novel influenza vaccines, it is intended to study the disposition of intramuscular vaccine formulations and their impact on immunity, in comparison to intranasal vaccination which requires a larger animal model. The size of the rat will facilitate the collection of nasal lavage fluid and the administration of powder formulation.

2. **No** Will the PI conduct the same experiment in multiple species?

3. Features of the species (e.g. anatomic, physiologic, genetic, etc.) that make it desirable for this model.

   MEDLINE and other computer database searches have been performed to identify alternative methods. Cell models would not offer the systemic response necessary to evaluate the effect of the vaccine in this study or allow the evaluation of mucociliary transport on induced immunity. Larger species, such as the rabbit, have been employed for similar studies, but offer no advantage for the performance of the present studies.

3.1 Building - Room Number:	Housing Type :
Kerr Hall - B242	DLAM
Kerr Hall - 1311	Investigator Laboratory

3.2 Procedures in Laboratory, DLAM/Satellite Housing & Confinement

1. **Yes** Will animals be removed from DLAM or approved satellite facility?
   Maximum time length living animals remain outside DLAM:
   8 hrs.
2. If animals will be removed from DLAM, approved Satellite Facility or taken to Investigator Laboratory, indicate the procedures to be performed, and the contact information:

   » **Procedure(s) to be performed:** Vaccination, dosing, blood draw, nasal lavage
   » **Contact Person:** Robert J Garmise

4. Reduction, Refinement, Replacement, and Animal Numbers

1. Animal Number Reduction

a. Replacing vertebrate animals:
Are there computer simulation, non-living, or in vitro alternatives to the proposed use of animals described in your application? **No**
If yes, state why these alternatives are not appropriate:

b. Refining experimental procedures to minimize pain or distress:
Did you consider the use of pain-relieving drugs, or procedures that avoid or minimize discomfort, distress and pain, and humane endpoints in the design of the experiment? **Yes**
If not considered, state why the alternative was not applicable:

c. Reduction in the number of animals:
Yes Rational selection of group size (e.g., pilot studies to estimate variability, power analysis)
Yes Careful experimental design (e.g., appropriate choice of control groups)

Yes Maximizing use of animals (e.g., selecting the minimal number of animals per group required for statistical verification, sharing tissues with other investigators)

Yes Minimizing loss of animals (e.g., good post-operative care, avoidance of unintended breeding)

If you selected none of the above choices, state why they are not appropriate:

2. Using the specifics of your experimental plan, justify the number of animals requested and list the number of animals used for each pain category (B, C, D, E):

Animals will be dosed intranasally (IN) or intramuscularly (IM) with a radiolabeled liquid or powder formulation. A number of mucoadhesive compounds (MA) will be screened for increasing residence time on the nasal mucosa. These compounds (eg. hydroxypropylmethyl cellulose (HPMC), carboxymethyl cellulose (CMC), sodium alginate (SA), chitosan, gelatin) are all generally regarded as safe (GRAS) as defined by the Food and Drug Administration. Preliminary experiments carried out in our lab (data not published) examined the effect of MA on mucociliary clearance rate. Rats were dosed with either saline, 1% CMC in saline, or 3% CMC in trehalose powder, labeled with technetium 99. At either 5, 15, 30, 60, 120, or 180 minutes, an animal was sacrificed and nasal lavage was performed. The nasal lavage fluid was quantified for percent of activity remaining. At most of the time points, the relative clearance rate occurred as follows: CMC powders>CMC liquid>saline. However, in the study, an n of 1 was used, so it isn't possible to determine if the differences were statistically significant.

STUDY 1- RESIDENCE TIME STUDY

In the first part of the proposed study, three time points have been chosen, which best defines the curve previously generated. There will be 7 MA, 2 formulations (liquid and powder), 3 time points (5, 15, and 120 min) with 5 animals per group. There will also be 2 control groups: saline and trehalose powder alone. The total number of animals required for this portion of the study is 210 (7X2X3X5).

STUDY 2- IMMUNE RESPONSE

Upon determination of the residence time in the nasal cavity in the first part of the study, the immune response to a virus will attempt to be correlated to theresidence time in the nasal cavity of different animals. Animals will be dosed whole inactivated influenza virus (WIIV) either IM or IN.

Group #	Dose Equivalent of WIIV (ug)	Route	Vehicle/Excipient	Animals
1	0.5	IN	Trehalose	3
2	1	IN	Trehalose	3
3	1.5	IN	Trehalose	3
4	2	IN	Trehalose	3
5	2.5	IN	Trehalose	3
6	3	IN	Trehalose	3
7	3.5	IN	Trehalose	3
8	4	IN	Trehalose	3
9	4.5	IN	Trehalose	3

10	5	IN	Trehalose	3
11	0.5	IN	Saline	3
12	1	IN	Saline	3
13	1.5	IN	Saline	3
14	2	IN	Saline	3
15	2.5	IN	Saline	3
16	3	IN	Saline	3
17	3.5	IN	Saline	3
18	4	IN	Saline	3
19	4.5	IN	Saline	3
20	5	IN	Saline	3
21	TBD	IM	Saline	6
22	TBD	IN	Saline	6
23	TBD	IN	CMC/Trehalose	6
24	TBD	IN	SA/Trehalose	6
25	TBD	IN	Chitosan/Trehalose	6
26	TBD	IN	HPMC/Trehalose	6
27	TBD	IN	Gelatin/Trehalose	6
28	TBD	IN	CMC/Saline	6
29	TBD	IN	SA/Saline	6
30	TBD	IN	Chitosan/Saline	6
31	TBD	IN	HPMC/Saline	6
32	TBD	IN	Gelatin/Saline	6
			Total	132

Each group in the dose ranging study will require 3 animals because the dose response curve generated is known to be a step function and the curve will be defined by the twelve groups. Each group in the formulation study will require 6 animals for statistical validity and to control as much as possible for inter-and intra-animal variability.

3. Estimate the following animal number totals required for this study during the three-year approval period>

Pain Category	Unweaned	Breeders	Adults
B	0	0	0
C	0	0	0
D	0	0	342
E	0	0	0

Total Animal Number = **342**

4. Category E Justification:

5. Transfer of Existing Animals: No

4.1 Alternatives to Animals Classified in USDA Pain Categories D or E

1. Details About Alternatives Search

a. Literature search conducted:

Medline: 9/12/2006

b. Keywords used in database searches

mucoadhesive

rat

intranasal

influenza

vaccine

influenza animal model

c. Years Search: 1996-2006

d. » Information Services and other Literature Sources:

No Animal Welfare Information Center
No Lab Animal Welfare Bibliography (NLM)
No Laboratory Animal Science Journal
No Alternatives to Laboratory Animals Journal (FRAME, U.K.)
No Quick Bibliography Series (AGRICOLA)
No Peer Review -
No Other -

» Knowledge of Field/Consultants:

» Other Methods or Sources Used:

5. Details of Animal Use:

1. Goals and objective(s) of your research.

In light of the recent crisis of the availability of influenza vaccine and the inability of the pharmaceutical industry to produce room-temperature stable needle-free options, it is imperative that the scientific and technological foundation for the development of such systems is addressed. It is proposed that maximal mucosal and systemic antibody production will be elicited by a dry powder nasal vaccine formulation containing whole-inactivated influenza virus (WIIV) with optimized local residence time in the nose. Dry powders of suitable size for nasal delivery were prepared by freeze-drying (FD) followed by milling or spray-freeze-drying (SFD). Desirable properties included aerodynamic diameter >20μm with a median diameter of 45-125μm; suitable for dispersion; exhibiting a range of viscosity modification and charge characteristics consistent with retention on the nasal mucosa. Each manufactured powder was characterized for particle size distribution, morphology, thermal properties, moisture content, flow properties, surface area, and electrostatic properties. A novel delivery device was employed and the dispersion properties of the formulation was examined. Functional stability of the dry powder preparation was determined using a hemagglutinin inhibition assay. The impact of charge and viscosity on mucoadhesive compounds will be evaluated by determining the rheological properties of mucus. Selected mucoadhesive (MA) compounds will be used to modify the residence time on the nasal mucosa and will be blended with the trehalose powder.

A modified Andersen cascade impactor will allow for characterization of particles in the 0.22-20µm size range. Dry powder vaccine will be evaluated in rats to determine the magnitude of the immune response and compared to positive and negative controls, nasal solution and intramuscular injection. Production of local and systemic antibodies in a rat model will be measured by nasal lavage and blood samples. It is anticipated that the dose of antigen, formulation characteristics (particle size, distribution, composition, use of mucoadhesive) will elicit a quantifiable immune response that will provide protection against the virus upon future contact.

2. If this application is a continuation of an ongoing project, state concisely how these goals differ from those in the original application and what was accomplished during the prior approval period. If this is a new project, please indicate so.

Experiments carried out from a previous protocol (ID# 00-207.0.A) were to determine feasibility of nasal delivery of a whole inactivated influenza vaccine (WIIV). They successfully resulted in the production of systemic and local antibodies by the animal. These experiments were followed by another protocol (ID# 05-329.0) which established a dose-response curve for the delivery of WIIV intramuscularly. However, although the dose for IM was optimized, the immune response elicited by intranasal delivery of powders was significantly less than IM. For this reason, a dose-response curve will be necessary for the IN formulations.

Current studies will examine the use of excipients which have been proven to increase the residence time of the WIIV in the nasal cavity. These excipients could potentially lead to greater production of systemic and local antibodies and/or allow for smaller doses to elicit a comparable immune response to higher doses. Studies to be conducted will establish mucociliary clearance rate for different formulations from which properties for the proposed groups in this study can be selected.

3. Describe the specific experimental manipulations and treatments of the animals in terms that are intelligible to a non-scientist.

For residence time studies, rats will receive an IP injection of anesthesia. Animals will be dosed by liquid or powder formulation intranasally. After dosing, animals will be returned to their cages without bedding (to avoid possible choking), placed on a heating pad (30-35 °C) to avoid hypothermia, and monitored every 15 minutes for 3 hours. For the 5 and 15 minute time points, the animal will still be under anesthesia and will be sacrificed by cardiac puncture followed by CO2 overdose. For the 120 minute time point, a majority of the animals were still under anesthesia. However, if they respond to the hind paw pinch test, they will receive a boost dose of anesthesia prior to performing the cardiac puncture followed by CO2 overdose. Nasal lavage will be performed to recover any of the radioactivity remaining in the nasal cavity.

Female Brown Norway rats will receive an IP injection of anesthesia. Blood samples will be drawn from the tail artery. Animals will be dosed with a vaccine either intramuscularly or intranasally. After dosing, animals will be returned to their cages without bedding (to avoid possible choking), placed on a heating pad (30-35°C) to avoid hypothermia, and monitored every 15 minutes for 3 hours. Even though a reversing agent could be used to decrease the time that the animal is under anesthesia (because acepromazine increases recovery time by ~30%),we would prefer to avoid the use of another pharmaceutical compound, reducing the possibility of adverse effects, and we will increase the monitoring of the recovery time from the suggested 2 hours to 3 hours. During the recovery period, the animal will be monitored for basic biological functions (ie. breathing rate (70-115/minute), intake, and elimination) and return of motor skills. Three weeks after immunization, animals will again receive anaesthesia, blood samples will be drawn from the tail artery, and animals will be dosed again via the same route of administration. Two weeks after this second dose, animals will receive anaesthesia, nasal lavage samples will be taken by washing the nasal cavity with 1 mL of PBS containing 20 ug/mL of aprotinin, and the animal will be sacrificed by cardiac puncture followed by carbon dioxide overdose.

5.9 Collection of blood or body fluids from live or dead vertebrate animals

1. Will fluid be collected from dead animals? Yes
Collected Fluid: Blood

2. Describe the purpose for collecting blood or other body fluids from live animals (other than ascites):

The purpose of the study is to elicit an immune response in the animals from the vaccine formulation. Blood samples will be drawn to determine antibody production in the animal to the virus.

3. Fluid withdrawn, frequency, volume, method and site:

Fluid Collected : Blood
Frequency: Once every 3 weeks
Volume: 300 uL
Method: Tail vein/artery withdrawal
Site: Laboratory

Fluid Collected : Blood
Frequency: On Termination
Volume: 10 mL
Method: Cardiac puncture
Site: Laboratory

If any of the above methods are Retro-orbital, please justify

If any of the above methods are Cardiac-Puncture, please indicate that required criteria are met
These criteria are met.

If any of the above methods are Other, please specify collection method:

4. Fluid and/or blood collection

Anesthetic Agent: Ketamine HCL
Dosage: 40 mg/kg
Route: IP
Schedule: Once every 3 weeks

Anesthetic Agent: Xylazine HCL
Dosage: 2 mg/kg
Route: IP
Schedule: Once every 3 weeks

Anesthetic Agent: Acepromazine
Dosage: 0.75 mg/kg
Route: IP
Schedule: Once every 3 weeks

6. Animal Care

1. Animal ID Method:

No Ear Tag
Yes Ear Punch
No Microchip
No Tattoo

No Toe Clip
No Not Applicable
No Other
Other Explanation -

2. How will animals be monitored?
Animals will be monitored by the housing staff.
If special monitoring has been arranged with DLAM facility supervisor, provide DLAM contact name:

3. Should DLAM contact PI/emergency contact if animal(s) found dead? Yes

4. Indicate requests for special handling of sick and dead animals:

5. Special Housing (DLAM):
Will any special housing or care be necessary? **No**
Deviations from standard DLAM husbandry procedures, Guide recommendations or special animal care needs:

6. Special Diets (DLAM)
Are special diets, additives to food and/or water (e.g. colyte) and/or antibiotics administered? **No**

7. Endpoints (time points, tumor sizes etc.) and/or the maximum time length of study:
The residence time study will end at the designated time point (5, 15, or 120 minutes).

The immune response study will end 2 weeks after the boost immunization, for a total length of 5 weeks (6 weeks including 1 week acclimation period).

8. Will animals be euthanized as part of the study? Yes
Animals will be euthanized at the end of the study, 2 weeks after the boost immunization.

» **Euthanasia Methods**

Yes CO_2-compressed carbon dioxide gas in cylinders
No Barbituate overdose
Dosage and route:

No Cervical Dislocation
If no anesthesia, scientific justification:

No Decapitation
If no anesthesia, scientific justification:

No Overdose of gas anesthetic
Specify Agent:

No Anesthesia - followed by physical euthanasia
Agent, Dose and Route:

Yes Other Method of Euthanasia
Exanguination by cardiac puncture while under anesthesia followed by CO_2 gas until rigor mortis sets in.

9. Would the PI be willing to share, donate or make available extra animal tissues or organs to other PI's? Yes

7. Anticipated Animal Pain & Distress

1. Are there any clinical, behavioral, or physiological manifestations expected to result from experimental manipulation such as surgery, diet, tumor, chronic disease, radiation sickness or toxicity, or potential health problems due to animal phenotype? Yes

a. Expected clinical and/or behavioral signs of pain and distress in animals

- No Decreased weight
- No Changes in food/water consumption
- No Decreased ambulation
- No Ruffled fur
- No Skin abnormality
- No Urinary problems
- No Hunched posture
- No Paw guarding
- No Porphyrin Staining
- No Lethargy
- No Diarrhea
- Yes Other

Other Explanation - Extremely unlikely event of nose bleed after dosing animals with dry powder vaccine.

b. Methods of dealing with the above complications:

- No Analgesics
- No Anesthetics
- No Sedation or tranquilization
- No Increased bedding
- Yes Other

Other Explanation - Call veterinary services.

1b. continued...

b. Agents used in dealing with complications

2. Animals experiencing unrelieved pain or distress prior to the endpoint, as defined by institutional policy, must be humanely euthanized, unless an exception to policy is requested and approved. Is exception required? No

a. Criteria for euthanasia that will used for this exception:

b. Scientific justification for not using an earlier endpoint:

11. Chemical, Pharmacological, Toxicological and Radioactive Compounds/Agents

1. Chemical compounds, pharmacological, toxicological and radioactive agents that will be administered to animals as part of the experimental procedures.

Agent:	Technetium 99
Dosage/Volume:	100 millicuries per 25 uL saline or 5 mg powder
Route:	Other
Schedule:	Once

If using more than three compounds, please list name, dosage/volume, route and schedule here:

If route is other, explain here: Intranasal

2. Will it be necessary to test compounds not described to the left? No

3. Are any of the listed agents to the left hazardous?: Yes

No Chemical Hazard
No Biological Hazard
Yes Radiological Hazard

12. Items not covered in other parts of the application

The animals will be housed in DLAM for the entire course of the study. They will only be in our lab for dosing, blood sampling, and nasal lavage. I

Application to Use Live Vertebrate Animals

PI: Anthony J Hickey
CB: CB:7360 1310 Kerr Hall
IACUC ID: 06-265.0 Web ID: 8088

Application Certification

I agree to the following statements. Signify your agreement by signing at the bottom

- I certify that I am familiar with and assure compliance in this Project with the legal standards of animal care and use established under the Federal and State laws and the policies on animal welfare of the National Institutes of Health and the University of North Carolina.
- I assume responsibility for ensuring that all persons working with animals on this project are familiar with and are trained in relevant animal procedures and that they will comply with established laws and policies regarding animal care and use. Applications will not be approved for investigators that have taken the IACUC orientation but have not completed required Laboratory Animal Coordinator certification. Contact the IACUC office to arrange training.
- I will appoint a Laboratory Coordinator to manage all animal use in the lab. I will ensure that the Coordinator receives required training and certification. I will ensure that after being certified, the Coordinator or IACUC representative will train and certify all individuals working with animals in the lab.
- I certify that all individuals working with animals on this project will register with the University Employee Occupational Health Clinic (UEOHC) by completing and submitting the "Research Animal Handlers & Animal Caretakers" medical history questionnaire (each individual who works with animals must complete the questionnaire during online orientation - UEOHC will assess the PI a processing fee).
- I certify the following: the research proposed herein is not unnecessarily duplicative of previously reported research; appropriate non-animal alternatives for this research do not exist; no alternatives to the potentially painful and/or distressful procedures conducted in this project exist. I have indicated methods used to make these determinations in the appropriate section of this animal use application.
- I will secure IACUC approval before changing procedures or personnel associated with this study (including adding personnel)
- I assure that I and personnel under by direct supervision will use the animals acquired for the activity described herein solely for said purpose. I also certify that if live animals are shared with other PIs or are used in any procedure other than those described in this application, I will provide the details in the form of a written amendment to the original application prior to their use.
- I acknowledge that veterinary care will be administered to moribund animals or animals experiencing more than momentary or slight pain or distress. Division of Laboratory Animal Medicine (DLAM) veterinary staff will attempt to contact me regarding the care of treatment of a moribund animal, but will institute treatment or euthanasia, as needed, if PI cannot be reached.
- I assure the IACUC and the University of North Carolina at Chapel Hill that the general procedures involving animals described in my grant application have been described in the animal use application and submitted to the IACUC for review.
- I assure that I have read "Notes on Euthanasia" of animals used in research and understand how it applies to animals in this animal use application.

NOTE: Consultation of a DLAM veterinarian regarding space allocation is recommended prior to submission of application. IACUC approval of application does not assure DLAM space availability. Please contact DLAM for pre-study strategy meeting prior to ordering animals to dicuss availability of housing.

NOTE: Cell lines that have been passaged in animals or maintained using animal serum may contain murine viruses that can alter the outcome of the study and may cause an outbreak of disease among other mice. ATTCC does not screen cell lines for murine pathogens. Cell lines that have been passaged in animals or grown in media containing rodent serum should be tested for murine pathogens prior to use in animals. Please contact DLAM for more information on testing of your cell lines.

PI Signature Date

Co-PI Signature Date

Date Approved: 10/26/2006

REFERENCES

Aldhous, P. and S. Tomlin (2005). "Avian flu special Avian flu: Are we ready?" Nature **435**(7041): 399.

Alymova, I. V., S. Kodihalli, et al. (1998). "Immunogenicity and Protective Efficacy in Mice of Influenza B Virus Vaccines Grown in Mammalian Cells or Embryonated Chicken Eggs." J. Virol. **72**(5): 4472-4477.

Anderson, J., E. Fishbourne, et al. (2000). "Protection of cattle against rinderpest by intranasal immunisation with a dry powder tissue culture vaccine." Vaccine **19**(7-8): 840-3.

Artursson, P., T. Lindmark, et al. (1994). "Effect of chitosan on the permeability of monolayers of intestinal epithelial cells (Caco-2)." Pharm Res **11**(9): 1358-61.

Aspden, T. J., J. D. Mason, et al. (1997). "Chitosan as a nasal delivery system: the effect of chitosan solutions on in vitro and in vivo mucociliary transport rates in human turbinates and volunteers." J Pharm Sci **86**(4): 509-13.

Audsley, J. and G. Tannock (2004). "The role of cell culture vaccines in the control of the next influenza." Expert Opin Biol Ther **4**(5): 709-17.

Bacon, A., J. Makin, et al. (2000). "Carbohydrate biopolymers enhance antibody responses to mucosally delivered vaccine antigens." Infect Immun **68**(10): 5764-70.

Banker, G. S. and C. T. Rhodes (1989). Modern pharmaceutics. New York, N.Y., M. Dekker.

Baron, P. A. and K. Willeke (2001). Aerosol measurement: principles, techniques, and applications. New York, Wiley.

Bates, D. V., B. R. Fish, et al. (1966). "Deposition and retention models for internal dosimetry of the human respiratory tract. Task group on lung dynamics." Health Phys **12**(2): 173-207.

Bazin, H. (1990). Rat immunoglobulins. Rat hybridomas and rat monoclonal antibodies. H. Bazin. Boca Raton, FL, CRC Press**:** 5-42.

Behl, C. R., H. K. Pimplaskar, et al. (1998). "Effects of physicochemical properties and other factors on systemic nasal drug delivery." Adv Drug Del Rev **29**(1-2): 89-116.

Belshe, R. B., P. M. Mendelman, et al. (1998). "The efficacy of live attenuated, cold-adapted, trivalent, intranasal influenzavirus vaccine in children." N Engl J Med **338**(20): 1405-12.

Berglund, R. N. and B. Y. H. Liu (1973). "Generation of monodisperse aerosol standards." Environmental Science and Technology **7**: 147-153.

Bergquist, C., E. L. Johansson, et al. (1997). "Intranasal vaccination of humans with recombinant cholera toxin B subunit induces systemic and local antibody responses in the upper respiratory tract and the vagina." Infect Immun **65**(7): 2676-84.

Body, J. J. (2002). "Calcitonin for the long-term prevention and treatment of postmenopausal osteoporosis." Bone **30**(5 Suppl): 75S-79S.

Bottenberg, P., R. Cleymaet, et al. (1991). "Development and testing of bioadhesive fluoride-containing slow-release tablets for oral use." J Pharm Pharmacol **43**: 457-464.

Box, G. E. P., W. G. Hunter, et al. (2005). Statistics for Experimenters. New York, NY, John Wiley and Sons.

Boyaka, P. N., A. Tafaro, et al. (2003). "Effective mucosal immunity to anthrax: neutralizing antibodies and Th cell responses following nasal immunization with protective antigen." J Immunol **170**(11): 5636-43.

Bright, R. A., D. K. Shay, et al. (2006). "Adamantane resistance among influenza A viruses isolated early during the 2005-2006 influenza season in the United States." JAMA **295**(8): 891-4.

Brittain, H. G. (1995). Physical characterization of pharmaceutical solids. New York, M. Dekker.

Brunauer, S., P. H. Emmett, et al. (1938). "Adsorption of Gases in Multimolecular Layers." J. Am. Chem. Soc. **60**(2): 309-319.

Burke, P. A., L. A. Klumb, et al. (2004). "Poly(lactide-co-glycolide) microsphere formulations of darbepoetin alfa: spray drying is an alternative to encapsulation by spray-freeze drying." Pharm Res **21**(3): 500-6.

Callens, C. and J. P. Remon (2000). "Evaluation of starch-maltodextrin-Carbopol 974 P mixtures for the nasal delivery of insulin in rabbits." J Control Release **66**(2-3): 215-20.

Carpenter, J. F., T. Arakawa, et al. (1992). "Interactions of stabilizing additives with proteins during freeze-thawing and freeze-drying." Dev Biol Stand **74**: 225-38; discussion 238-9.

Carpenter, J. F. and B. S. Chang (1996). Lyophilization of protein pharmaceuticals. Biotechnology and Biopharmaceutical Manufacturing, Processing, and Preservation. K. E. Avis and V. L. Wu. Buffalo Grove, IL, Interpharm Press**:** 199-264.

Carpenter, J. F., M. J. Pikal, et al. (1997). "Rational design of stable lyophilized protein formulations: some practical advice." Pharm Res **14**(8): 969-975.

Carr, R. L., Jr. (1965). "Classifying flow properties of solids." Chem. Eng. **72**(3): 69-72.

Carr, R. L., Jr. (1965). "Evaluating flow properties of solids." Chem. Eng. **72**(2): 163-8.

Carrasquillo, K. G., J. C. Carro, et al. (2001). "Reduction of structural perturbations in bovine serum albumin by non-aqueous microencapsulation." J Pharm Pharmacol **53**(1): 115-20.

Carrasquillo, K. G., A. M. Stanley, et al. (2001). "Non-aqueous encapsulation of excipient-stabilized spray-freeze dried BSA into poly(lactide-co-glycolide) microspheres results in release of native protein." J Control Release **76**(3): 199-208.

Carstensen, J. T. (1993). Pharmaceutical principles of solid dosage forms. Lancaster, Pa., Technomic Pub.

Chang, B., G. Reeder, et al. (1996). "Development of a stable freeze-dried formulation of recombinant human interleukin-1 receptor antagonist." Pharm Res **13**(2): 243-9.

Chen, T. M. and M. J. Dulfano (1978). "Mucus viscoelasticity and mucociliary transport rate." J Lab Clin Med **91**(3): 423-31.

Cheng, Y.-H., A. M. Dyer, et al. (2005). "Intranasal delivery of recombinant human growth hormone (somatropin) in sheep using chitosan-based powder formulations." Eur J Pharm Sci **26**(1): 9-15.

Ch'ng, H. S., H. Park, et al. (1985). "Bioadhesive polymers as platforms for oral controlled drug delivey II: synthesis and evaluation of some swelling water insoluble bioadhesive polymers." J Pharm Sci **74**: 399-405.

Clarke, M. J., J. Peart, et al. (2002). "Adhesion of powders for inhalation: an evaluation of drug detachment from surfaces following deposition from aerosol streams." Pharm Res **19**(3): 322-9.

Concessio, N. M. (1997). Dynamic Properties of Pharmaceutical Powders and Their Impact on Aerosol Dispersion. School of Pharmacy. Chapel Hill, University of North Carolina at Chapel Hill**:** 379.

Concessio, N. M., M. M. Van Oort, et al. (1998). Impact force measurements- Their relevance in powder aerosol formulation. Respiratory Drug Delivery VI, Interpharm Press.

Corbanie, E., J. Remon, et al. (2006). Spray drying of an attenuated vaccine virus for dry powder aerosol vaccination in poultry. American Association of Pharmaceutical Scientists Annual Meeting, San Antonio, TX.

Costantino, H. R., L. Firouzabadian, et al. (2000). "Protein spray-freeze drying. Effect of atomization conditions on particle size and stability." Pharm Res **17**(11): 1374-83.

Costantino, H. R., L. Firouzabadian, et al. (2002). "Protein spray freeze drying. 2. Effect of formulation variables on particle size and stability." J Pharm Sci **91**(2): 388-95.

Costantino, H. R., O. L. Johnson, et al. (2004). "Relationship between encapsulated drug particle size and initial release of recombinant human growth hormone from biodegradable microspheres." J Pharm Sci **93**(10): 2624-34.

Craig, D. Q. M., P. G. Royall, et al. (1999). "The relevance of the amorphous state to pharmaceutical dosage forms: glassy drugs and freeze dried systems." Int J Pharm **179**(2): 179-207.

Crowder, T. M. (2003). A Guide to Pharmaceutical Particulate Science. Boca Raton, Fla., Interpharm Press/CRC.

Davis, S. S. (2001). "Nasal vaccines." Adv Drug Deliv Rev **51**(1-3): 21-42.

Dawson, P. J. and D. J. Hockley (1992). "Scanning electron microscopy of freeze-dried preparations: relationship of morphology to freeze-drying parameters." Dev Biol Stand **74**: 185-92.

Deaton, A. T., L. D. Jones, et al. (2002). "Generation of Gelatin Aerosol Particles from Nebulized Solutions as Model Drug Carrier Systems." Pharmaceutical Development & Technology **7**(2): 147.

Debertin, A. S., T. Tschernig, et al. (2003). "Nasal-associated lymphoid tissue (NALT): frequency and localization in young children." Clin Exp Immunol **134**(3): 503-7.

Debin, A., R. Kravtzoff, et al. (2002). "Intranasal immunization with recombinant antigens associated with new cationic particles induces strong mucosal as well as systemic antibody and CTL responses." Vaccine **20**(21-22): 2752-63.

Dimmock, N. J., A. J. Easton, et al. (2001). Introduction to modern virology. Malden, MA, Blackwell Science.

DiPiro, J. T. (1997). Pharmacotherapy : a pathophysiologic approach. Stanford, Conn., Appleton & Lange.

Dunbar, C. A., A. J. Hickey, et al. (1998). "Dispersion and characterization of pharmaceutical dry powder aerosols." KONA **16**: 7-44.

FDA (2003). U.S. FDA Draft Guidance for Industry. Bioavailability and Bioequivalence Studies for Nasal Aerosols and Nasal Sprays for Local Action. FDA. Bethesda, MD.

FDA (2003). U.S. FDA Draft Guidance for Industry. Q1A(R2) Stability Testing of New Drug Substances and Products. FDA. Bethesda, MD.

FluMist Package Insert (2003). Gaithersburg, MD, MedImmune.

Fonner, J., DE, G. Banker, et al. (1966). "Micromeritics of granular pharmaceutical solids. I. Physical properties of particles prepared by five different granulation methods." J Pharm Sci **55**(2): 181-6.

Foy, J. W.-D. and R. A. Schatz (2004). "Inhibition of Rat Respiratory-Tract Cytochrome P-450 Activity After Acute Low-Level m -Xylene Inhalation: Role in 1-Nitronaphthalene Toxicity." Inhal Tox **16**(3): 125-132.

Fuchs, N. A. and A. G. Sutugin (1966). Generation and use of monodisperse aerosols. Aerosol Science. C. N. Davies. New York, Academic Press**:** 1-30.

Garmise, R. J., K. Mar, et al. (2006). "Formulation of a dry powder influenza vaccine for nasal delivery." AAPS Pharm Sci Tech **7**(1): Article 19.

Gatlin, L. A. (1992). "Kinetics of a phase transition in a frozen solution." Dev Biol Stand **74**: 93-103; discussion 104.

Gennaro, A. R. and J. P. Remington (1995). Remington, the science and practice of pharmacy. Easton, Pa., Mack Pub. Co.

Giudice, E. L. and l. J. D. Campbel (2006). "Needle-free vaccine delivery." Adv Drug Deliv Rev **58**(1): 68-89.

Glueck, R. (2001). "Review of intranasal influenza immunization." Adv Drug Del Rev **51**: 203-211.

Gohel, M. C. and A. F. Amin (1998). "Formulation optimization of controlled release diclofenac sodium microspheres using factorial design." J Control Release **51**(2-3): 115-22.

Gombotz, W. R., M. S. Healy, et al. (1990). Process for producing small particles of biologically active molecules, Alkermes Controlled Therapeutics, Inc.

Gonda, I. (2000). "The ascent of pulmonary drug delivery." J Pharm Sci **89**(7): 940-5.

Gosling, J. P. and L. V. Basso (1994). Immunoassay : laboratory analysis and clinical applications. Boston, Butterworth-Heinemann.

Groneberg, D. A., C. Witt, et al. (2003). "Fundamentals of pulmonary drug delivery." Respir Med **97**(4): 382-7.

Gross, E. A., J. A. Swenberg, et al. (1982). "Comparative morphometry of the nasal cavity in rats and mice." J Anat **135**(Pt 1): 83-8.

Gu, J. M., J. R. Robinson, et al. (1988). "Binding of acrylic polymers to mucin/epithelial surfaces: structure-property relationships." Crit Rev Ther Drug Carrier Syst **5**(1): 21-67.

Guyton, A. C. and J. E. Hall (1996). Textbook of Medical Physiology. Philadelphia, W.B. Saunders.

Hageman, M. (1992). Water sorption and solid state stability of proteins. Stability of protein pharmaceuticals. T. J. Ahern and M. C. Manning. New York, Plenum Press**:** 273-309.

Hayden, F. G. (2006). "Antiviral Resistance in Influenza Viruses -- Implications for Management and Pandemic Response." N Engl J Med **354**(8): 785-788.

Heller, M. C., J. F. Carpenter, et al. (1999). "Protein formulation and lyophilization cycle design: prevention of damage due to freeze-concentration induced phase separation." Biotechnol Bioeng **63**(2): 166-74.

Hickey, A. J. (2003). "Pharmaceutical Inhalation Aerosol Powder Dispersion - An Unbalancing Act." Am Pharm Rev **6**(4): 106-110.

Hickey, A. J. and D. Ganderton (2001). Pharmaceutical Process Engineering. New York, NY, Marcel Dekker.

Hiemenz, P. C. (1984). Polymer chemistry : the basic concepts. New York, M. Dekker.

Hinds, W. C. (1999). Aerosol technology : properties, behavior, and measurement of airborne particles. New York, NY, J. Wiley.

Hirabayashi, Y., H. Kurata, et al. (1990). "Comparison of intranasal inoculation of influenza HA vaccine combined with cholera toxin B subunit with oral or parenteral vaccination." Vaccine **8**(3): 243-8.

Huang, J., R. J. Garmise, et al. (2004). "A novel dry powder influenza vaccine and intranasal delivery technology: induction of systemic and mucosal immune responses in rats." Vaccine **23**(6): 794-801.

Hunter, S. K., M. E. Andracki, et al. (2001). "Biodegradable microspheres containing group B Streptococcus vaccine: immune response in mice." Am J Obstet Gynecol **185**(5): 1174-9.

Ikechukwu Ugwoke, M., E. Sam, et al. (1999). "Nasal mucoadhesive delivery systems of the anti-parkinsonian drug, apomorphine: influence of drug-loading on in vitro and in vivo release in rabbits." Int J Pharm **181**(1): 125-38.

Illum, L. (1999). Bioadhesive formulations for nasal peptide delivery. Bioadhesive drug delivery systems: fundamentals, novel approaches, and development. E. Mathiowitz, D. E. Chickering and C.-M. Lehr. New York, Marcel Dekker**:** 507-539.

Illum, L. (2002). "Nasal drug delivery: new developments and strategies." Drug Discov Today **7**(23): 1184-9.

Illum, L. (2006). "Nasal clearance in health and disease." Journal of Aerosol Medicine **19**(1): 92-99.

Illum, L., A. N. Fisher, et al. (2001). "Bioadhesive starch microspheres and absorption enhancing agents act synergistically to enhance the nasal absorption of polypeptides." Int J Pharm **222**(1): 109-119.

Illum, L., I. Jabbal-Gill, et al. (2001). "Chitosan as a novel nasal delivery system for vaccines." Adv Drug Deliv Rev **51**(1-3): 81-96.

Illum, L., P. Jenkins, et al. (1999). "New developments in nasal vaccine delivery." Pharmaceutical Science & Technology Today **2**(4): 129-131.

Ivins, B. E., M. L. M. Pitt, et al. (1998). "Comparative efficacy of experimental anthrax vaccine candidates against inhalation anthrax in rhesus macaques." Vaccine **16**(11-12): 1141-1148.

Jabbal-Gill, I., A. N. Fisher, et al. (1998). "Stimulation of mucosal and systemic antibody responses against Bordetella pertussis filamentous haemagglutinin and recombinant pertussis toxin after nasal administration with chitosan in mice." Vaccine **16**(20): 2039-46.

Jiang, G., S. B. Joshi, et al. (2006). "Anthrax vaccine powder formulations for nasal mucosal delivery." J Pharm Sci **95**(1): 80-96.

Jones, N. (2001). "The nose and paranasal sinuses: physiology and anatomy." Adv Drug Del Rev **51**(1-3): 5-19.

Keitel, W. A. and P. A. Piedra (1998). Live cold-adapted, reassortant influenza vaccines. Textbook of influenza. K. Nicholson, R. G. Webster and A. J. Hay. Oxford, UK ; Malden, Mass., Blackwell Science.

Kelly, J. T., C. M. Bobbitt, et al. (2001). "In Vivo Measurement of Fine and Coarse Aerosol Deposition in the Nasal Airways of Female Long-Evans Rats." Toxicol. Sci. **64**(2): 253-258.

Kendall, J. and V. Latter (2003). "Intranasal diamorphine as an alternative to intramuscular morphine: pharmacokinetic and pharmacodynamic aspects." Clin Pharmacokinet **42**(6): 501-13.

Krinke, G. (2000). The laboratory rat. San Diego, Calif., Academic Press.

Kulvanich, P. and P. J. Stewart (1987). "The effect of particle size and concentration on the adhesive characteristics of a model drug-carrier interactive system." J Pharm Pharmacol **39**(9): 673-8.

Kulvanich, P. and P. J. Stewart (1988). "Influence of relative humidity on the adhesive properties of a model interactive system." J Pharm Pharmacol **40**(7): 453-8.

Kuper, C. F., D. M. Hameleers, et al. (1990). "Lymphoid and non-lymphoid cells in nasal-associated lymphoid tissue (NALT) in the rat. An immuno- and enzyme-histochemical study." Cell Tissue Res **259**(2): 371-7.

Kuper, C. F., P. J. Koornstra, et al. (1992). "The role of nasopharyngeal lymphoid tissue." Immunol Today **13**(6): 219-24.

Lam, X. M., E. T. Duenas, et al. (2001). "Encapsulation and stabilization of nerve growth factor into poly(lactic-co-glycolic) acid microspheres." J Pharm Sci **90**(9): 1356-65.

Lamb, R. and R. Krug (1996). Orthomyxoviridae: The viruses and their replication. Virology. B. Field, D. Knipe, P. M. Howley and D. E. Griffin. Philadelphia, Lippincott-Raven Publishers.

Lay, J. C., C. R. Berry, et al. (1995). "Retention of insoluble particles after local intrabronchial deposition in dogs." J Appl Physiol **79**(6): 1921-1929.

Lebrec, H. and G. R. Burleson (1994). "Influenza virus host resistance models in mice and rats: utilization for immune function assessment and immunotoxicology." Toxicology **91**(2): 179-88.

Lebrec, H., K. Sarlo, et al. (1996). "Effect of influenza virus infection on ovalbumin-specific IgE responses to inhaled antigen in the rat." J Toxicol Environ Health **49**(6): 619-30.

Leffell, M. S., A. D. Donnenberg, et al. (1997). Handbook of Human Immunology. Boca Raton, CRC Press.

Li, Q., V. Rudolph, et al. (2004). "Interparticle van der Waals force in powder flowability and compactibility." Int J Pharm **280**(1-2): 77-93.

LiCalsi, C., T. Christensen, et al. (1999). "Dry powder inhalation as a potential delivery method for vaccines." Vaccine **17**(13-14): 1796-803.

LiCalsi, C., M. J. Maniaci, et al. (2001). "A powder formulation of measles vaccine for aerosol delivery." Vaccine **19**(17-19): 2629-36.

Liote, H., J. Zahm, et al. (1989). "Role of mucus and cilia in nasal mucociliary clearance in healthy subjects." Am Rev Respir Dis **140**(1): 132-6.

Little, S. F., B. E. Ivins, et al. (2006). "Duration of protection of rabbits after vaccination with Bacillus anthracis recombinant protective antigen vaccine." Vaccine **24**(14): 2530-2536.

Liversidge, G. G., C. G. Wilson, et al. (1988). "Nasal delivery of a vasopressin antagonist in dogs." J Appl Physiol **64**(1): 377-383.

Lodge, J. P. and T. L. Chan (1986). Cascade impactor : sampling & data analysis. Akron, OH, American Industrial Hygiene Association.

Lorenzi, G., G. M. Bohm, et al. (1992). "Correlation between rheologic properties and in vitro ciliary transport of rat nasal mucus." Biorheology **29**(4): 433-40.

Maa, Y. F., M. Ameri, et al. (2004). "Influenza vaccine powder formulation development: spray-freeze-drying and stability evaluation." J Pharm Sci **93**(7): 1912-1923.

Maa, Y. F., P. A. Nguyen, et al. (1999). "Protein inhalation powders: spray drying vs spray freeze drying." Pharm Res **16**(2): 249-54.

Maa, Y. F., L. Zhao, et al. (2003). "Stabilization of alum-adjuvanted vaccine dry powder formulations: mechanism and application." J Pharm Sci **92**(2): 319-32.

Macklin, M. D., D. McCabe, et al. (1998). "Immunization of Pigs with a Particle-Mediated DNA Vaccine to Influenza A Virus Protects against Challenge with Homologous Virus." J. Virol. **72**(2): 1491-1496.

Mariotti, S., R. Teloni, et al. (2002). "Immunogenicity of anti-Haemophilus influenzae type b CRM197 conjugate following mucosal vaccination with oligodeoxynucleotide containing immunostimulatory sequences as adjuvant." Vaccine **20**(17-18): 2229-39.

Martin, A. N. and P. Bustamante (1993). Physical pharmacy: physical chemical principles in the pharmaceutical sciences. Philadelphia, Lea & Febiger.

Masters, K. (1976). Spray drying: an introduction to principles, operational practice, and applications. London, Wiley.

McLaren, C., C. W. Potter, et al. (1974). "Immunity to influenza in ferrets." Medical Microbiology and Immunology **V160**(1): 33-45.

Medi, B. M., L. Tian, et al. (2006). A Stable Dry Powder Vaccine Formulation (GelVacTM) for Nasal Delivery. American Association of Pharmaceutical Scientists, San Antonio, TX.

Mercer, T. T. (1963). "On the calibration of cascade impactors." Ann Occup Hyg **6**: 1-14.

Mestecky, J., Z. Moldoveanu, et al. (1997). "Current options for vaccine delivery systems by mucosal routes." J Control Release **48**(2-3): 243-257.

Morgan, K. T., D. L. Patterson, et al. (1986). Toxicology of the nasal passages. C. S. Barrow. Washington, Hemisphere Pub. Corp.**:** xvi, 317 p.

Mullins, M. E., L. P. Michaels, et al. (1992). "Effect of geometry on particle adhesion." Aerosol Science and Technology **17**: 105-118.

Muszkat, M., G. Friedman, et al. (2000). "Local SIgA response following administration of a novel intranasal inactivated influenza virus vaccine in community residing elderly." Vaccine **18**(16): 1696-9.

Mygind, N. and R. Dahl (1998). "Anatomy, physiology and function of the nasal cavities in health and disease." Adv Drug Del Rev **29**(1-2): 3-12.

Nelson, M., J. L. Prior, et al. (2004). "Evaluation of lipopolysaccharide and capsular polysaccharide as subunit vaccines against experimental melioidosis." J Med Microbiol **53**(12): 1177-1182.

Newman, S. P., G. R. Pitcairn, et al. (2004). "Drug delivery to the nasal cavity: in vitro and in vivo assessment." Crit Rev Ther Drug Carrier Syst **21**(1): 21-66.

Newman, S. P., G. R. Pitcairn, et al. (2001). "A brief history of gamma scintigraphy." J Aerosol Med **14**(2): 139-145.

Newman, S. P., K. P. Steed, et al. (1995). "Scintigraphic assessment of the oropharyngeal and nasal depositions of fusafungine from a pressurized inhaler and from a novel pump spray device." J Pharm Pharmacol **47**(10): 818-21.

Nguyen, X. C., J. D. Herberger, et al. (2004). "Protein powders for encapsulation: a comparison of spray-freeze drying and spray drying of darbepoetin alfa." Pharm Res **21**(3): 507-14.

Ni, Y., L. Tian, et al. (2005). Induction of Protective Immunity Against Influenza Virus with a Nasal Powder Vaccine Delivery System (GelVac™). 45th ICAAC Meeting, Washington, DC.

Ni, Y. and K. M. Yates (2004). In-situ gel formation of pectin, Carrington Laboratories, Inc.

Nichol, K. L., P. M. Mendelman, et al. (1999). "Effectiveness of live, attenuated intranasal influenza virus vaccine in healthy, working adults: a randomized controlled trial." JAMA **282**(2): 137-44.

Nicholson, K., R. G. Webster, et al. (1998). Textbook of influenza. Oxford, UK ; Malden, Mass., Blackwell Science.

Nordqvist, C. (2006). "FluMist more effective than injections for small children and babies." Medical News Today.

Oetjen, G.-W. and P. Haseley (2004). Freeze-drying. Weinheim ; New York, Wiley-VCH.

Otsuka, A., K. Iida, et al. (1983). "Measurements of the adhesive force between particles of powdered organic substances and a glass substrate by means of the impact separation method. I. Effect of temperature." Chem Pharm Bull (Tokyo) **31**(12): 4483-8.

Partidos, C. D. (2000). "Intranasal vaccines: forthcoming challenges." Pharm. Sci. Technol. Today **3**(8): 273-281.

Pier, G. B., J. B. Lyczak, et al. (2004). Immunology, infection, and immunity. Washington, D.C., ASM Press.

Pikal, M. J. (1994). Freeze-drying of proteins. Formulation and Delivery of Proteins and Peptides. J. L. Cleland and R. Langer, ACS Symposium Series. **5567:** 120-133.

Podczeck, F., J. M. Newton, et al. (1997). "Influence of relative humidity of storage air on the adhesion and autoadhesion of micronized particles to particulate and compacted powder surfaces." J Colloid Interface Sci **187**(2): 484-91.

Proctor, D. F. and I. H. P. Andersen (1982). The nose, upper airway physiology and the atmospheric environment. New York, Elsevier Biomedical Press.

Proctor, D. F. and G. Lundqvist (1973). "Clearance of inhaled particles from the human nose." Arch Intern Med **131**(1): 132-9.

Puchelle, E., F. Aug, et al. (1981). "Comparison of three methods for measuring nasal mucociliary clearance in man." Acta Otolaryngol **91**(3-4): 297-303.

Quraishi, M. S., N. S. Jones, et al. (1998). "The rheology of nasal mucus: a review." Clin Otolaryngol Allied Sci **23**(5): 403-13.

Ranucci, J. (1992). "Dynamic plume-particle size analysis using laser diffraction." Pharmaceutical Technology **16**(10): 109-114.

Rey, L. and J. C. May (2004). Freeze-drying/lyophilization of pharmaceutical and biological products. New York, Marcel Dekker.

Rharbaoui, F., B. Drabner, et al. (2002). "The Mycoplasma-derived lipopeptide MALP-2 is a potent mucosal adjuvant." Eur J Immunol **32**(10): 2857-65.

Ridgway, K. and R. Rupp (1969). "The effect of particle shape on powder properties." J Pharm Pharmacol **21**: Suppl:30S+.

Roitt, I. M. and P. J. Delves (2001). Roitt's essential immunology. Oxford ; Malden, MA, USA, Blackwell Science.

Roth, Y., J. S. Chapnik, et al. (2003). "Feasibility of aerosol vaccination in humans." Ann Otol Rhinol Laryngol **112**(3): 264-70.

Russell, M. W., Z. Moldoveanu, et al. (1996). "Salivary, nasal, genital, and systemic antibody responses in monkeys immunized intranasally with a bacterial protein antigen and the Cholera toxin B subunit." Infect Immun **64**(4): 1272-83.

Schreider, J. P. and O. G. Raabe (1981). "Anatomy of the nasal-pharyngeal airway of experimental animals." Anat Rec **200**(2): 195-205.

Silberberg, A. (1983). "Biorheological matching: mucociliary interaction and epithelial clearance." Biorheology **20**(2): 215-22.

Singh, M., M. Briones, et al. (2001). "A novel bioadhesive intranasal delivery system for inactivated influenza vaccines." J Control Release **70**(3): 267-76.

Singh, R. K. and H. Gao (1999). "Nanometric dry powder coatings using a novel process." KONA **17**.

Smith, D. J., S. Bot, et al. (2003). "Evaluation of novel aerosol formulations designed for mucosal vaccination against influenza virus." Vaccine **21**(21-22): 2805-12.

Smith, N. M., J. S. Bresee, et al. (2006). "Prevention and control of influenza. Recommendations of the Advisory Committee on Immunization Practices (ACIP)." MMWR Recomm Rep **55**(RR10): 1-42.

Smyth, H., G. Brace, et al. (2006). "Spray Pattern Analysis for Metered Dose Inhalers: Effect of Actuator Design." Pharm Res **V23**(7): 1591-1596.

Soane, R. J., M. Frier, et al. (1999). "Evaluation of the clearance characteristics of bioadhesive systems in humans." Int J Pharm **178**(1): 55-65.

Soane, R. J., M. Hinchcliffe, et al. (2001). "Clearance characteristics of chitosan based formulations in the sheep nasal cavity." Int J Pharm **217**(1-2): 183-91.

Sonner, C., Y. F. Maa, et al. (2002). "Spray-freeze-drying for protein powder preparation: particle characterization and a case study with trypsinogen stability." J Pharm Sci **91**(10): 2122-39.

Spit, B. J., E. G. Hendriksen, et al. (1989). "Nasal lymphoid tissue in the rat." Cell Tissue Res **255**(1): 193-8.

Staats, H. F., C. P. Bradney, et al. (2001). "Cytokine requirements for induction of systemic and mucosal CTL after nasal immunization." J Immunol **167**(9): 5386-94.

Staniforth, J. N. (1994). The importance of electrostatic measurements in aerosol formulation and preformulation. Respiratory Drug Delivery IV, Interpharm Press, Deerfield, IL.

Staniforth, J. N. (2002). Powder Flow. Pharmaceutics : the science of dosage form design. M. E. Aulton. Edinburgh ; New York, Churchill Livingstone**:** 197-210.

Stannard, W. and C. O'Callaghan (2006). "Ciliary function and the role of cilia in clearance." Journal of Aerosol Medicine **19**(1): 110-115.

Sullivan, V. J., J. A. Mikszta, et al. (2006). "Noninvasive delivery technologies: respiratory delivery of vaccines." Expert Opin. Drug Deliv. **3**(1): 87-95.

Suman, J. D., B. L. Laube, et al. (2002). "Validity of in vitro tests on aqueous spray pumps as surrogates for nasal deposition." Pharm Res **19**(1): 1-6.

Surana, R., A. Pyne, et al. (2004). "Effect of preparation method on physical properties of amorphous trehalose." Pharm Res **21**(7): 1167-1176.

Taber, C. W. and C. L. Thomas (2001). Taber's cyclopedic medical dictionary. Philadelphia, F.A. Davis Co.

Tamura, S. and T. Kurata (2004). "Defense mechanisms against influenza viruse infection in the respiratory tract mucosa." Japanese Journal of Infectious Disease **57**: 236-247.

Tang, X. C. and M. J. Pikal (2004). "Design of freeze-drying processes for pharmaceuticals: practical advice." Pharm Res **21**(2): 191-200.

Thijssen, H. A. C. (1969). "Freeze concentration of food liquids." Food Manufacture **44**(7): 49-54.

Treanor, J. J., K. Kotloff, et al. (1999). "Evaluation of trivalent, live, cold-adapted (CAIV-T) and inactivated (TIV) influenza vaccines in prevention of virus infection and illness following challenge of adults with wild-type influenza A (H1N1), A (H3N2), and B viruses." Vaccine **18**(9-10): 899-906.

Tsurudome, M., R. Glueck, et al. (1992). "Lipid interactions of the hemagglutinin HA2 amino-terminal segment during influenza virus-induced membrane fusion." J Bio Chem **267**(28): 20225-32.

Ugwoke, M. I., R. U. Agu, et al. (2000). "Nasal toxicological investigations of Carbopol 971P formulation of apomorphine: effects on ciliary beat frequency of human nasal primary cell culture and in vivo on rabbit nasal mucosa." Eur J Pharm Sci **9**(4): 387-96.

Ugwoke, M. I., R. U. Agu, et al. (2000). "Scintigraphic evaluation in rabbits of nasal drug delivery systems based on carbopol 971p((R)) and carboxymethylcellulose." J Control Release **68**(2): 207-14.

Ugwoke, M. I., R. U. Agu, et al. (2005). "Nasal mucoadhesive drug delivery: Background, applications, trends and future perspectives." Adv Drug Del Rev **57**(11): 1640-1665.

Ugwoke, M. I., S. Exaud, et al. (1999). "Bioavailability of apomorphine following intranasal administration of mucoadhesive drug delivery systems in rabbits." Eur J Pharm Sci **9**(2): 213-9.

Ugwoke, M. I., N. Verbeke, et al. (2001). "The biopharmaceutical aspects of nasal mucoadhesive drug delivery." J Pharm Pharmacol **53**(1): 3-21.

USP (2006). <601> Aerosols, Metered-Dose Inhalers, and Dry Powder Inhalers. United States Pharmacopoeia. Rockville, MD. **30**.

van der Lubben, I. M., G. Kersten, et al. (2003). "Chitosan microparticles for mucosal vaccination against diphtheria: oral and nasal efficacy studies in mice." Vaccine **21**(13-14): 1400-8.

van der Lubben, I. M., J. C. Verhoef, et al. (2001). "Chitosan for mucosal vaccination." Adv Drug Deliv Rev **52**(2): 139-44.

Van Oort, M., B. Downey, et al. (1996). "Verification of operating the Andersen cascade impactor at different flow rates." Pharm Forum **22**(2): 2211-2215.

Vaughn, N. P. (1989). "The Andersen impactor: Calibration, wall losses and numerical simulation." J Aer Sci **20**(1): 67-90.

Visser, J. (1970). "Measurement of the force of adhesion between submicron carbon-black particles and a cellulose film in aqueous solution." Journal of Colloid and Interface Science **34**(1): 26-31.

Voltaire (1961). Philosophical letters. Indianapolis,, Bobbs-Merrill.

Wang, J., K. M. Chua, et al. (2004). "Stabilization and encapsulation of human immunoglobulin G into biodegradable microspheres." Journal of Colloid and Interface Science **271**(1): 92-101.

Westerink, M. A., S. L. Smithson, et al. (2001). "ProJuvant (Pluronic F127/chitosan) enhances the immune response to intranasally administered tetanus toxoid." Vaccine **20**(5-6): 711-23.

WHO (2006). "Epidemiology of WHO-confirmed human cases of avian influenza A(H5N1) infection." Weekly Epidemiological Record **81**(26): 249-260.

WHO (2006). "WHO Fact Sheet." **Avian influenza (" bird flu")**.

Wilfong, E. and R. Dey (2005). "The Release of Nerve Growth Factor from the Nasal Mucosa Following Toluene Diisocyanate." Journal of Toxicology and Environmental Health Part A **68**(15): 1337-1348.

Wu, C.-F. and M. Hamada (2000). Experiments : planning, analysis, and parameter design optimization. New York, Wiley.

Yates, K. (2006). A Novel Inactivated Nasal Influenza Vaccine. World Vaccine Congress, Washington, DC.

Yu, Z., K. P. Johnston, et al. (2006). "Spray freezing into liquid versus spray-freeze drying: Influence of atomization on protein aggregation and biological activity." Eur J Pharm Sci **27**(1): 9-18.

Zijlstra, G. S., W. L. Hinrichs, et al. (2004). "The role of particle engineering in relation to formulation and de-agglomeration principle in the development of a dry powder formulation for inhalation of cetrorelix." Eur J Pharm Sci **23**(2): 139-49.